TECHNISCHE UNIVERSITÄT MÜNCHEN
Lehrstuhl für Brau- und Getränketechnologie

Development of an Ultrasonic Based Pattern Recognition Algorithm for Detecting Fouling in Bioprocesses

Eva Wallhäußer

Vollständiger Abdruck der von der Fakultät Wissenschaftszentrum Weihenstephan für Ernährung, Landnutzung und Umwelt der Technischen Universität München zur Erlangung des akademischen Grades eines

Doktors der Naturwissenschaften

genehmigten Dissertation.

Vorsitzender:		Univ.-Prof. Dr. H.-Ch. Langowski
Prüfer der Dissertation:	1.	Univ.-Prof. Dr. Th. Becker
	2.	Univ.-Prof. Dr. J. Hinrichs (Universität Hohenheim)

Die Dissertation wurde am 11.04.2014 bei der Technischen Universität München eingereicht und durch die Fakultät Wissenschaftszentrum Weihenstephan für Ernährung, Landnutzung und Umwelt am 25.09.2014 angenommen.

"We are not always what we seem and hardly ever what we dream." - Peter S. Beagle, *The Last Unicorn*

Contents

List of Figures

List of Tables

1. Preface

I want to thank Prof. Thomas Becker for the possibility to do an interesting PhD starting 2008 at the University of Hohenheim, Stuttgart, and finishing 2012 at the Technische Universität München, Freising.
I want to thank Prof. Hinrichs for building a setup in the University of Hohenheim, Stuttgart, and for undertaking the co-examination of my PhD. Thanks to Stefan Noebel for supervising the runs in Hohenheim and to Mattias Sprunk who did most of the experiments in Hohenheim.
I want to thank my supervisor, Dr. Mohamed Hussein, for his looking over, his support, and our intriguing as well as appealing discussions.
I want to thank all Bachelor and Diploma students who worked for me and did quite a lot of the background tasks. Thanks to Marco, Uli, Anja, and Manuela!
I also want to thank all my fellow students which I got to know over the years. In particular I want to thank Walid Hussein and Ahmed Sayed for their assistance in writing the used codes in Matlab and C++, Roland Novy for sharing my candies with me, and Stephan Birle for the yummy cherries. Susie, I want to thank you for having a lot of fun. I am honoured to call you my friend.
Micha, without you this thesis may not have been finished. You supported and helped me whenever and whereever you could. I am blessed to know you.
My family (and my friends) made it possible for me to study Physics and to do my PhD. You backed me when necessary and have always been there for me. Thank you!

2. Abstract

Fouling is unwanted deposit which develops during product processing on heat transfer walls. Fouling is a severe issue in many industries and plays an important role because it leads to cleaning varying from once a year (crude oil processing) up to at least once a day (food processing like brewing and dairy industry). This thesis focuses on dairy industry and its applications.

In dairy industry, milk and milk products are exposed at least once to thermal treatment for improving shelf life and reducing microbiological risks. During heating fouling develops because proteins denaturate and agglomerate and salts precipitate. This decreases heat exchanger performance by reduced heat transfer, equipment may be damaged by high pressure drop, and product quality losses occur like burned particles and changed sensorical impression. As a result, unsupervised cleaning is undertaken using fixed cleaning cycles which leads to plant downtime and high costs see e.g. [8] [10] [51] [153].

Many different research approaches were undertaken concerning fouling to get fouling and cleaning under control. One approach is studying fouling and cleaning kinetics to understand both parts better see [59] [111]. Another approach is to improve anti-fouling strategies like coating of heat exchangers [7] [142] or improving cleaning efficiency by adapting cleaning cycles [43] [52]. Monitoring fouling will help to reduce plant downtime and cleaning costs. To do so, several methods were developed all having different advantages and drawbacks (for an overview see [127] [165] [167]). Most of the developed methods are applicable for fouling detection but not for monitoring cleaning success and adapt cleaning to fouling. Here, a gap opens because monitoring cleaning and adapting it to need will reduce production costs strongly. Thus, a method is preferable which can be used both for fouling and cleaning monitoring.

Ultrasonic methods are a good choice to monitor fouling and cleaning online because ultrasound is very sensitive to material changes at interfaces. Material change are e.g. fouling development (liquid milk –> solid fouling) or cleaning (solid fouling –> liquid water). Also, ultrasound can be used for time of flight measurements but this was not preferable in the work underdone here. A reason is that fouling layers during cleaning end are very thin and high errors may occur with time of flight measurements making measurements not as accurate as necessary. Analysis and evaluation of measured ultrasonic signals can be done using classification systems like artificial neural networks (ANN) or support vector machines (SVM). These systems are based on pattern recognition methods dividing between fouled and clean surfaces. They are advantageous because different features can be combined which improves detection stability as well as accuracy. Also, simulations can be introduced for comparison and improvement.

In this work, a detection system based on the combination of ultrasonic measurements and intelligent classification systems (ANN, SVM) was developed.

The developed system can be used to detect presence and absence of dairy protein fouling and to monitor and to improve cleaning cycles. Ultrasonic measurements were made using a self-developed ultrasonic measuring unit attached to a planar heat exchanger. Ultrasonic signals were read in automatically and analysed giving seven features which were sensitive to fouling: characteristic acoustic impedance Z, short time energy STE, temporal/spectral crest factor TCF/SCF, spectral smoothness $SSMOOTH$, temporal decrease $TSLOPE$, and descent time $TDESCENT$. These features were fed together with temperature T and mass flow rate $\dot{m}$ in an ANN and a SVM, respectively. Using several features, detection accuracy and stability was improved. The classification systems were trained offline using data of clean and fouled heat exchanger and of cleaning cycles.

A multilayer perceptron was used for ANN architecture with LOGSIG, TANSIG, and PURELIN transfer functions between input, one hidden, and output layer. For classification, one-class classification was chosen where input and output layer were compared. Offline accuracy was 80 % when output was weighted using a nonlinear neuron.

For SVM, binary classification was chosen where fouling and no fouling samples were divided. Data was not linear separable in input space, thus, a radial basis function (rbf) kernel was chosen for transformation in higher dimensional feature space. Offline accuracy was 94 % and much better than ANN accuracy. This is explained by the fact that SVM finds an absolute extremum when looking for the separating hyper plane and is less influenced by data variation.

The classification systems were compared by monitoring ultrasonically measured cleaning cycles. Here, SVM showed considerably better results than ANN. A third method showed a clean heat exchanger after 22 ± 3 min. This method was based on slope change of the seven used features. The determined features showed constant values when surface was either fouled or clean but changed when cleaning was conducted. This was used for monitoring cleaning: when the features showed a change in slope (thus, in value) cleaning was underdone. As soon as no change of the features was found surface was considered clean. The developed ultrasonic system can be used for online monitoring of cleaning cycles in a planar heat exchanger. Cleaning cycles are adaptable to fouling while cleaning success is validated.

Different classification methods were chosen for comparison to determine if one method is preferable above others. It has been found that all three different methods have their

advantages and drawbacks. For the developed system all three classification methods can be used while SVM and the third method based on slope change are most promising. In future, the method dependent on the conditions has to be chosen or a combination of several methods can be used. Using redundancy the system will be more fault-tolerant.
This work is divided in different parts. First, a brief introduction to ultrasound and hydrodynamical considerations as well as fouling and cleaning is given. Then, the work is summarised and presented in publications. In the end, a conclusion and outlook is given. Detailed derivation of equations, pseudo code, and more detailled information concerning β-lactoglobulin and error analysis can be found in the Appendix.

3. Zusammenfassung

Fouling sind unerwünschte Ablagerungen, die während der Produktion auf wärmeübertragenden Wänden auftreten. Es ist ein globales Problem in verschiedenen Industriezweigen und führt zu notwendigen Reinigungen. Diese werden von einmal im Jahr (ölverarbeitende Industrie) bis zu mindestens einmal am Tag (Brau- und Milchindustrie) durchgeführt. Diese Arbeit setzt den Fokus auf die Milchindustrie.

In der Milchindustrie werden Milch und Milchprodukte mindestens einmal thermisch behandelt, um die Haltbarkeit zu erhöhen und mikrobielle Risiken zu minimieren. Während des Erhitzungsprozesses bildet sich Fouling, da Proteine denaturieren und agglomerieren und Salze ausfallen. Dabei wird die Leistung von Wärmetauschern aufgrund des geringeren Wärmeübertrags verringert. Zudem kann es zu Beschädigungen an Wärmetauschern aufgrund erhöhten Druckverlusts und verminderter Produktqualität (angebrannte Partikel, veränderte Sensorik) kommen. Daraus resultierend werden nicht überwachte Reinigungen mit festen Reinigungszyklen durchgeführt. Das führt zu niedrigen Standzeiten der Anlage und hohen Kosten, z.B. [8] [10] [51] [153].

Verschiedene Vorgehensweisen wurden in der Forschung durchgeführt, um Fouling und dessen Reinigung besser zu kontrollieren. Ein Ansatz ist dabei die Kinetiken der Foulingbildung und Reinigungen besser zu verstehen, z.B. [59] [111]. Ein weiterer Ansatz befasst sich mit Antifoulingstrategien wie das Beschichten von Wärmetauschern [7] [142] oder die Verbesserung der Reinigungseffizienz [43] [52]. Die Detektion und Überwachung von Fouling soll dabei helfen, die Standzeiten von Anlagen und Reinigungskosten zu verringern. Dafür wurden unterschiedliche Methoden entwickeln, die verschiedene Vorteile und Mankos aufweisen (für eine Übersicht siehe z.B. [127] [165] [167]). Die meisten dieser Methoden sind zwar für die Detektion von Fouling, aber nicht für die Überwachung der Reinigung und des Reinigungserfolgs geeignet. Somit tritt eine Lücke auf, bei der die Überwachung des Reinigungserfolgs und die Anpassung der Reinigung an Fouling die Produktionskosten stark reduzieren kann. Daraus folgt, dass eine Methode benötigt wird, die gleichzeitig Fouling und Reinigung überwachen kann.

Ultraschallbasierte Methoden sind eine gute Wahl, Fouling und dessen Reinigung online zu überwachen, da Ultraschall sehr empfindlich auf Zustandsänderung von Materialien an Grenzflächen reagiert. Derartige Zustandsänderungen sind z.B. der Foulingaufbau (flüssige Milch –> festes Fouling) oder eine Reinigung (festes Fouling –> flüssiges Wasser). Ultraschall kann außerdem für Laufzeitmessungen verwendet werden. Dieses Messprinzip wurde in der hier durchgeführten Arbeit nicht verwendet, da die Foulingschichten insbesondere am Ende der Reinigung sehr dünn sind. Dadurch können bei Laufzeitmessungen hohe Fehler auftreten und exakte Messungen erschwert werden. Auswertung und Bewertung der aufgenommenen Ultraschallsignale kann über Klassifizierzungsmethoden wie künstliche neuronale Netzwerke (KNN) oder Stützvektormaschinen (support vector machine, SVM) durchgeführt werden. Diese Methoden basieren auf Mustererkennung und unterscheiden zwischen Oberflächen mit und ohne Fouling. Klassifizierungsmethoden sind aus verschiedenen Gründen vorteilhaft. Zum Einen können verschiedene Feature bzw. Merkmale einfach kombiniert werden, was sowohl die Erkennungsstabilität als auch die Genauigkeit stark erhöht. Zudem können Simulationen einfach für Abgleiche und Verbesserungen eingefügt werden.

In dieser Arbeit wurde eine Detektionssystem entwickelt, das auf der Kombination auf Ultraschallmessungen und intelligenten Klassifizierungmethoden (KNN, SVM) basiert.

Das entwickelte System kann dafür verwendet werden, die An- und Abwesenheit von Proteinfouling zu detektieren und Reinigungszyklen zu überwachen bzw. zu verbessern. Ultraschallmessungen wurden mit einer selbstentwickelten Ultraschallmesseinheit durchgeführt, die an einem planaren Wärmetauscher angebracht wurde. Ultraschallsignale wurden automatisch eingelesen und sieben Merkmale wurden extrahiert, die alle auf Fouling empfindlich waren: charakteristische akustische Impedanz Z, Kurzzeitenergie (short time energy) STE, temporaler bzw. spektraler Scheitelfaktor (temporal/spectral crest factor) TCF/SCF, spektrale Glattheit (spectral smoothnes) $SSMOOTH$, temporaler Abfall (temporal decrease) $TSLOPE$ und die überstrichene Zeit (descent time) $TDESCENT$. Diese Merkmale wurden zusammen mit der Temperatur T und dem Massendurchfluss $\dot{m}$ in ein KNN bzw. eine SVM eingelesen. Mit der Kombination der Merkmale konnte die Erkennungstabilität sowie die Detektionsgenauigkeit verbessert werden. KNN und SVM wurden offline mit Daten von einem sauberen Wärmetauscher, Fouling und Reinigungszyklen trainiert.

Ein Mehrschichten-Perzeptron wurde für das KNN verwendet mit den Transferfunktionen LOGSIG, TANSIG und PURELIN zwischen der Eingangs-, einer versteckten und der Ausgangsschicht. Eine-Klasse-Klassifikation (one-class classification) wurde verwendet, wobei die Eingangs- mit der Ausgangsschicht verglichen wurd. Die Offline-Genauigkeit betrug nach Gewichtung mit einem nichtlinearen Neuron 80 %.

Für die SVM wurde die binäre Klassifizierung verwendet und zwischen Fouling und Nicht-Fouling (sauber) unterschieden. Die Daten waren im Eingangsraum nicht linear separierbar, daher wurde eine Gaußfunktion (radial basis function) als Kernel für die Transformation in den höherdimensionalen Merkmalsraum gewählt. Die Offline-Genauigkeit betrug 94 % und war höher als für das KNN, da die SVM ein globales Extremum bei der

Suche nach der Hyperebene findet und weniger von Datenvariationen beeinflusst wird.
Die Klassifizierungsmethoden wurden mit Reinigungen verglichen, die mit Ultraschall aufgenommen worden waren. Dabei zeigte die SVM bessere Ergebnisse als das KNN. Eine dritte Methoden zeigte einen sauberen Wärmetauscher nach 22 ± 3 min. Diese Methode basierte auf der Änderung der Steigung der sieben aufgenommenen Merkmale. Sie war konstant bei Fouling bzw. einem sauberen Wärmetauscher (konstanter Wert), änderte sich allerdings während einer Reinigung (variierender Wert). Sobald die Steigung wieder konstant war, wurde der Wärmetauscher als sauber betrachtet. Das entwickelte System kann für die Online-Überwachung von Reinigungen in einem planaren Wärmetauscher verwendet werden. Reinigungen können an das vorhandene Fouling angepasst und gleichzeitig kann der Reinigungserfolg validiert werden.
Verschiedene Klasifizierungsmethoden wurden miteinander verglichen, um die beste Methode für die Überwachung der Reinigung zu bestimmen. Dabei zeigte sich, dass die Methode abhängig von den Voraussetzungen gewählt werden muss, da alle untersuchten Methoden verwendet werden können. Eine Kombination zweier oder aller drei Methoden ist ebenfalls möglich. Durch diese Redundanz wird das Gesamtsystem fehlertolerant.
Die Arbeit ist in mehrere Teile geteilt. Nach einer kurzen Einführung werden die Ergebnisse resümiert und in den wissenschaftlichen Artikeln präsentiert. Dann wird die Arbeit zusammengefasst und ein Ausblick auf künftige Arbeitsfelder gegeben. Herleitungen, Pseudocode und detaillierte Informationen finden sich im Anhang.

4. Fundamental Framework

4.1. Fouling and Cleaning

Understanding Fouling

Fouling is unwanted deposit on heat transfer walls playing an important role particularly in food processing and pharmaceutical industry but is also present in crude oil processing. Fouling is divided in macro and micro fouling where the first includes foulants like mussels which are present on ship hulls and the latter contains proteins and colloids. Macro fouling will not be considered further because it was not relevant in this thesis. Micro fouling is divided into five different kinds (corrosion, precipitation, chemical reaction, biofilm, solidification) which are compared in table 4.1.

Table 4.1.: Comparison between different fouling types with their description and occurrence (after [20])

Fouling type	**Description**	**Occurrence**	**Example**
Corrosion	Corrosion product on a surface	Water treatment	Rust
Precipitation	Precipitation of salts	(Dairy) heat exchangers, crude oil processing	Diary fouling type B, crude oil fouling
Chemical reaction	Deposition due to chemical reactions	Heat exchangers in food processing	Dairy fouling type A
Biofilm	Formation of bacteria, algae on surfaces	Food processing, water treatment	Membranes, contact lenses
Solidification	Freezing on a surface	Water treatment	Paraffin wax, ice

Dairy fouling made from (skim) milk solutions is investigated where precipitation and chemical reaction fouling plays the most important role. Milk is a complex biological fluid composed inter alia of proteins, salts, and fat. In dairy industry, milk is heated mainly due to microbiological and shelf life increasing reasons. Above specific temperatures proteins start to denaturate and salts start to precipitate leading to deposits on heat transfer walls. Fouling is a problem because it reduces heat transfer to the product (thorough product heating is only ensured if heating medium temperature is increased with time) and leads to necessary cleaning [49] [53]. Burton divided dairy fouling in two types dependent on main composition and temperature at which it occurs calling them type A (protein fouling) and type B (mineral fouling) [22] [23] (compare with Table 4.2). Protein fouling will be explained in detail because mineral fouling did not play a major role in this thesis.

Table 4.2.: Comparison between type A (protein) and type B (mineral) fouling

Fouling type	**Protein amount**	**Mineral amount**	**Fat**	**Temperature range**	**Description**
Type A (Protein fouling)	50 - 70 %, mainly β-lg, casein	30 - 40 %	4 - 6 %	pasteurisation temperature, 72 °C - 90 °C	white, soft, spongy
Type B (mineral fouling)	15 - 20 %	70 - 80 %, mainly calcium phosphate	4 - 6 %	UHT-temperature, above 110 °C	greyish, brittle, hard, compact

Protein Fouling (Type A Fouling)

Protein fouling is chemical reaction fouling and consists mostly of proteins, fat, and salts [10] [22] [23]. The most present protein in the fouling layer is β-lactoglobulin (β-lg) which makes only 0.3 % of proteins in raw milk but accounts for 50 % of whey proteins present. β-lg is an eight stranded β-sheet and α-helix globular protein with 162 amino acids, one thiol, and two disulfide bonds for stabilising the globular conformation, a diameter of ca. 3 nm, and a molecular weight of 18.3 kDa [82] [102] [119]. Its isoelectric point (IEP) is around 5.13, at pH 7 it shows amphoteric behaviour, and at this pH and ambient temperature its electrical charge is calculated to be -8 [44]. Unlike caseins which make up 50 % of all proteins in milk β-lg is not heat stable with its denaturation temperature at about 72 - 75 °C [116]. Exact denaturation temperature depends on heating process, amount of protein, and salts.

When heated at different pH values β-lg aggregates as particulates as well as amyloid fibrils [83] [108] [137]. At IEP or at low/screened charge, β-lg forms particulate gels with spherical aggregates. Far away from IEP or at high charge, β-lg forms amyloid fibres which can assemble into suprafibrillar structures. At the pH of milk (around 6.4), usually amyloid fibres are present in the fouling layer. Heat denaturation of β-lg is thought to follow a multistage process via dissociation, denaturation, and aggregation steps [145] [158]. The denaturation kinetics of β-lg was investigated in detail together with the influence of calcium [125] and dependent on pH and charge screening due to salts [68] [151] [160] [174]. Recently Raman spectroscopy analysis revealed that fouling seems to be mainly controlled by denaturated protein at the interface stainless steel-deposit [16]. The adhesion of fouling is not only goverened by mechanical forces but also by molecular interactions like DLVO (Derjagiun, Landau, Verwey, and Overbeek) forces including van der Waals and electrostatic double layer forces [47] [115] [117].

The following fouling process is agreed to be followed (Fig. 4.1): First, an induction period at room temperature takes place where a very thin layer of fouling is conducted on heat transfer surface [117]. This layer has negligible influence on heat transfer resistance but increases surface roughness and heat transfer to the fluid. Then, fouling grows as more proteins denaturate, agglomerate, and adsorb [10] [27] [45]. When flow is present fouling growth is restricted by fluid removal. It remains unclear if the induction layer is made of proteins or salts [25] [30] even though salt is found after some time as undermost layer. This may be explained by first precipitation of salts or after adsorption of proteins salts diffuse through the spongy layer.

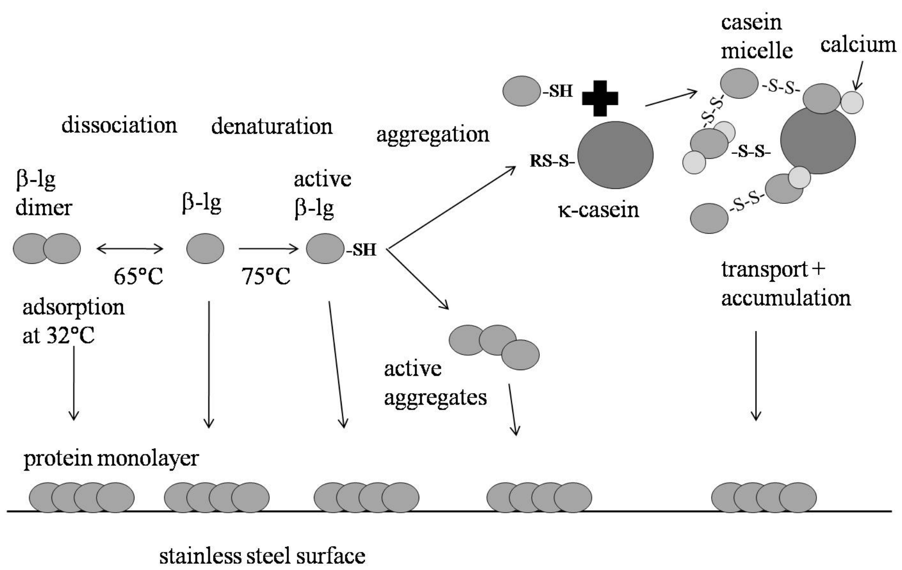

Figure 4.1.: Fouling deposition at pH 7 (after [164]). At 32 °C first adsorption layers occur. β-lg dissociates around 65 °C and denaturates at ca. 75 °C (reversible) becoming active, aggregating with β-lgs and caseins (irreversible), and accumulating on the surface.

For negligible amount of β-lg in raw milk, the following set of rate equations with reaction rates r of monomer B, activated monomer B^*, protein aggregates t, and deposition f and reaction rate constant K are valid (reaction rates after [34] [35])

$$r_B = -K_{denat}[B],\ r_{B^*} = K_{denat}[B] - K_{agg}[B^*]^2,\ r_t = K_{agg}[B^*]^2, ,\ r_F = K_{ads}[B^*]^{1.2}. \quad (4.1)$$

An overall reaction of different steps takes place in the adsorption process (r_F) due to its broken reaction order of 1.2. This reaction rate can be used to directly obtain concentration of β-lg [124]. The reaction rate constant follows the Arrhenius relationship and is related to absolute temperature with activation energy E_A, gas constant R, and wall temperature T.

$$K = K_0 \cdot exp(-E_A/(R \cdot T_{surface})) \tag{4.2}$$

It remains unclear which order the overall denaturation, aggregation, and adsorption process actually has. Some groups report second order reactions, while others find first order reaction and others determine a reaction order of 1.5.
Discussion remains if fouling process is mainly due to bulk and surface reactions [14] [147], reaction controlled [35] [62], or mass transfer controlled [11] [54]. While some results point to protein denaturation as governing reaction [78] and some favour protein aggregation [36] [59]. A lot of work is done concerning fouling, fouling models, and its governing reactions to understand and model fouling better [10] [76] [164].
A lot of work concerning fouling was done to prevent or mitigate fouling in heat exchangers and to understand fouling adhesion in more detail. Mitigation strategies mostly focuses on surface treatments e.g. changing surface finish and bulk composition [77] [88] [139], change of surface energy due to coating [2] or using different materials as heat transfer walls [7]. Also, interaction between stainless steel and foulants [128] [141] and adhesion of fouling was investigated [117] for better understanding. Open questions remain concerning interactions between surfaces and fouling where answering these questions may help in cleaning fouling layers.

Cleaning

Fouling decreases heat transfer from heating medium to product, product quality, leads to possible damage of heat exchanger equipment due to increased pressure drop, and increases production costs due to necessary cleaning [49] [53] [51]. Cleaning of fouling depends on many different parameters like soaking and dissolving of the layer, shear stress, composition and temperature of cleaning agent, amount of protein, and others [3] [27] [46]. Different attempts were made to reduce cleaning costs e.g. by choice of cleaning in place (CIP) cycle used [43], developing a cleaning map for different fouling types [53] and using it to improve cleaning [51] [52]. Another way for cleaning improvement is determination of influencing factors [27] [72], influence of surface [77] [97] [169], effect of surface coating/treatment [7] [131] [140], and mathematical description of cleaning models [111] [170]. Cleaning is considered as one of the most important operations in dairy processing due to its costs and daily occurance. E.g., Xin et al. developed a cleaning model to predict removal of protein fouling using NaOH as cleaning agent [169]. Usually fixed CIP cycles are conducted in industry which are designed to cover the worst case. These CIP cycles are not adaptable to actual fouling which remains unknown. Sometimes changes between different CIP cycles are possible but cleaning success cannot be verified if shorter cycles are used due to missing monitoring possibilites. Cleaning is conducted usually at least once a day conducted following the steps below.

- Prerinse with water until discharge is clear
- Rinse with an alkaline solution (most often sodium hydroxide (NaOH) or comparable) to remove proteinaceous residues
- Second washing with water until pH is that of water
- Rinse with acid, e.g. nitric acid (HNO_3) for removing mineral residues
- Third washing with water whereas cleaning agents are washed out
- Sanitise if necessary
- Fourth washing with water to remove sanitising agent

Sometimes chelates or enzymes are used for cleaning even though they may be not environmental friendly [43]. In general, CIP cycles are performed in the temperature range of 65° - 75° C and last between one and two hours. The used concentration and cleaning agents depend on fouling type present following thumb rules. Whereas protein fouling needs alkaline cleaning agents, acid-based cleaning is necessary for precipitated salts which may also occur during protein fouling. For all fouling types holds: rinsing and cleaning time affects efficiency [50] [110] [111]. Usage of pulsed cleaning despite constant flow showed an improvement in some cases [19] [57]. Also, different approaches were made to determine cleaning kinetics in heat exchangers [40] [41] [48] [170].
Monitoring of CIP cycles is a challenging task because heat exchangers cannot be easily opened or equipped with windows for visual inspection. Thus, CIP cycles are too long for most fouling cases which adds up costs together with oversized heat exchangers. Until now no online cleaning monitoring method is present on the market which helps to reduce cleaning time and ensures a clean heat exchanger. Different approaches for CIP monitoring were developed e.g. usage of ultrasonic methods in membranes [92] [101] [171], usage

of intelligent systems like artificial neural networks [138] [156], physical modelling [64], nano-vibrations [121] [122], or monitoring of electrical or thermal properties [28] [159]. All investigated methods show different advantages and disadvantages depending on requirements and fields of application.

4.2. Ultrasonic Background

Ultrasound is a pressure wave and is sensitive to materials and material changes at interfaces. Ultrasound is high frequency sound (20 kHz - 2 GHz) and commonly used in non-destrucitive testing (NDT) e.g. [100] [157], in investigation of aircrafts [21] [146] or metal parts [175] and in medical applications like [12] [114]. Thus ultrasound is a suitable method to detect viscoelastic fouling and to monitor cleaning success when material changes at an interface take place. Equations are shown in three dimensional descriptions but are simplified to one dimension when necessary.
Different kinds of sound waves can be excited dependent on medium present: in liquids and gases usually only longitudinal and surface waves are stimulated while solids also show transversal and shear waves. Conversion from one kind to another at an interface influences the ultrasonic wave and can be used for detection. Only longitudinal waves were considered.

Continuum Mechanical Basics

Ultrasound is displacement of particles out of their position of rest resulting in pressure wandering through material. In continuum mechanics, ultrasound can be described with the deformation tensor $\underline{\epsilon}$ which depends on material and is influenced by materials (e.g. fouling presence) which in turn influences an ultrasonic wave. For small deformations, only volume change takes place, $\underline{\epsilon}$ gets symmetrical, and the continuity equation is valid.

$$\epsilon_{11} + \epsilon_{22} + \epsilon_{33} = \nabla \boldsymbol{u} \tag{4.3}$$

where $\mathbf{u}$ is the displacement vector.
Stress occurs additional to deformation and changes with material. When only stress is present at the surface the stress tensor $\underline{\sigma}$ with elements σ_{ij} is symmetric and independent of time and space. The change of $\underline{\sigma}$ is linear for a small force perpendicular to the x-axis and materials like fouling influence $\underline{\sigma}$. With Newton's second law, the equation of motion with particles displacement in direction of x is

$$\frac{\partial \sigma_{ik}}{\partial x_k} = \frac{\partial v_i}{dt} = \rho \frac{\partial^2 u_i}{\partial t^2} \tag{4.4}$$

with medium density $\rho = \rho_0 + \Delta\rho$ and density at rest ρ_0. If both deformation and stress occurs, $\sigma_{ik} = \sigma_{ik}(\epsilon_{ij})$, Hooke's law is valid at small deformations with Young's modulus E_{nm} (symmetric tensor of forth order):

$$\sigma_n = E_{nm}\epsilon_m \text{ , with } n, m = 1...6. \tag{4.5}$$

Both $\underline{\sigma}$ and $\underline{\epsilon}$ are influenced by material state and influence ultrasonic waves. This can be used for detection of fouling presence and absence. Different moduli are present in different material states, e.g. Young's modulus E, shear modulus σ, compression modulus K in solids. These moduli define the velocity of propagation (sound velocity) of the sound wave which is got from the wave equation. Changes in moduli due to material changes can be seen in changes in different ultrasonic features and used for detection. Acoustic feature calculation is based on wave propagation described by the wave equation.

The Linear Lossless Wave Equation and Important Features

The ideal lossless wave equation is independent on material state and derived by starting from the hydrodynamical equations. The wave equation can be used to determine features dependent on material state which in turn can be used for measuring materials. In an ideal fluid, no shearing takes place and pressure is perpendicular to the surface, $\nabla \times \mathbf{v} = 0$.The equation of motion

$$-\nabla p = \rho \frac{d\mathbf{v}}{dt} = \rho \frac{\partial v}{\partial t} + (v\nabla)v = \rho_0 \frac{\partial v}{\partial t} \tag{4.6}$$

with velocity potential φ and pressure $\nabla p = \rho_0 \partial\varphi/\partial t$, and the continuity equation

$$-1/\rho = div\ v \ \Rightarrow\ \partial\rho/\partial t = \rho_0 \triangle\varphi \tag{4.7}$$

are used to derive the ultrasonic wave equation. Pressure depends on density from which it follows that a travelling pressure wave influences medium density and vice versa

$$p \approx p_0 \left(\frac{dp}{d\rho}\right)_{\rho=\rho_0} \Rightarrow \frac{p - p_0}{\rho - \rho_0} \approx \left(\frac{dp}{d\rho}\right)_{\rho=\rho_0}. \tag{4.8}$$

Density and pressure changes due to a travelling sound wave are reversible and overall pressure and density are considered constant if power of an ultrasonic wave is low (adiabatic movement). Thus, changed material density can be used for e.g. detection of fouling presenc or absence.

To derive the plane linear wave equation which describes the behaviour of an ultrasonic wave in a medium, continuity equation (Eq. 4.7) and equation of motion (Eq. 4.6) are evolved with respect to time t, rearranged, and result in the wave equation

$$\triangle\varphi = \frac{1}{c_0^2}\frac{\partial^2\varphi}{\partial t^2} \text{ with } c_0^2 = (dp/d\rho)_{\rho=0} \Rightarrow c_0 = \sqrt{\frac{K}{\rho_0}}. \tag{4.9}$$

$\triangle\varphi$ is the change of volume compression and c_0 is medium sound velocity. Sound velocity depends on temperature T, pressure p, density ρ, and, in a fluid, on compression modulus K. Influences due to refraction and particles on the wave equation can be included using secondary sources [118] [135].

One homogeneous solution of the plane linear wave equation (4.9) describes an one dimensional plane wave which is divided into two waves: one incoming and one outgoing (in x-direction). The result can be written as linear combination of cosine or exponential functions

$$\varphi = Ccos(\omega t + \underline{kx}) + Dsin(\omega t + \underline{kx}) = Ae^{i\omega t+\underline{kx}} + Be^{-i\omega t+\underline{kx}} \tag{4.10}$$

which is valid in far field, and can only be applied for the ideal case. In presence of external forces a linear combination of the solution of the homogeneous wave equation and a generic one has to be found. Introduction of losses e.g. by damping materials like viscoelastic fouling leads to inclusion of loss terms which consider different types of losses like thermal and visco-elastic losses. Kobryn and Hirata for example derived a statistical-mechanical theory of ultrasonic absorption in molecular liquids including losses [80].

Another way to determine the ideal lossless wave equation is to start from an inhomogeneous lossy wave formula (4.11 after [79]):

$$(1+\tau\cdot\frac{\partial}{\partial t})\Delta p - \frac{1}{c^2}\cdot\frac{\partial^2 p}{\partial t^2} - \nabla(\rho_0\cdot g) - \frac{\partial G}{\partial t} - \nabla F - \frac{\partial^2(\rho u_i uj)}{\partial x_i \partial x_j} = 0 \text{with } \tau = \frac{4/3\cdot\eta + \eta_B}{\rho - 0\cdot c^2}. \tag{4.11}$$

Detailed explanation of derivation and symbols is found in Appendix A.

Sound velocity is often used for determination of e.g. changed material properties but also characteristic acoustic impedance Z is used for material inspection. Z describes the resistance a medium opposes to a traveling sound wave. Z is defined in the far field by medium density and sound velocity

$$Z = \rho \cdot c. \tag{4.12}$$

High Z stands for solids whereas low Z is characteristic for gases. At an interface, the impedances of different media determine how much of a sound wave is transmitted and reflected (Fig. 4.2). This can be applied to determine fouling presence at an interface.

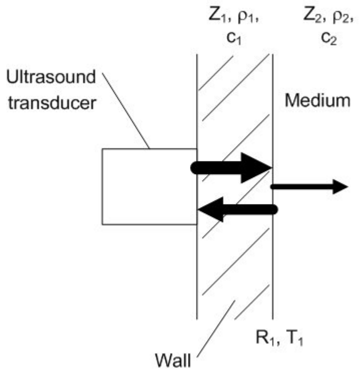

Figure 4.2.: Dependent on characteristic acoustic impedances at an interface reflection and transmission at an interface changes.

Fouling and Ultrasound

The interaction between an adhered fouling layer and an ultrasonic wave was not extensively investigated. Because low power ultrasound is used in this thesis, cavitational effects of air bubbles embedded in fouling layer are negligible. The fouling layer damps the ultrasonic signal due to viscoelasticity but this is important mainly for thick layers and transmission measurements. Solid-like fouling also influences the way reflections at the interface wall-medium takes place because interactions between wall and medium changes. The overall spring constant of the wall-medium part is influenced and this influences the oscillation of particles at these interface which emits the reflected wave. Cleaning leads also to changes of characteristic acoustic impedance and changed reflection coefficients at the investigated interface which can be monitored for cleaning supervision. These considerations show that fouling influences an ultrasonic wave strongly enough to be measured. Thus, appropriate acoustic features have to be found to determine fouling presence and absence.

4.3. Piezoelectricity

The piezoelectric effect can be used to emit and receive ultrasonic waves due to thickness variations caused by electric potential and vice versa and to determine materials like fouling presence and absence. The piezoeffect is linear and related to the microscopic structure of the material. The measurable electric potential is due to macroscopic charge displacement in crystal structure. From these conditions, it follows that such a material must not have a centre of inversion and shows charge separation when exposed to pressure or an electric field (direct/indirect piezoelectric effect, Fig. 4.3). Piezoelectric materials belong to one of the 21 point groups without inversion centres and are often also ferroelectric [6] [113]. Piezoelectricity was described by the Curie brothers in 1880 in quartz, tourmaline, and Rochelle salt [32] [33] while Lippmann first described inverse piezoelectric effect [96]. This effect was later experimentally confirmed by the Curie brothers.

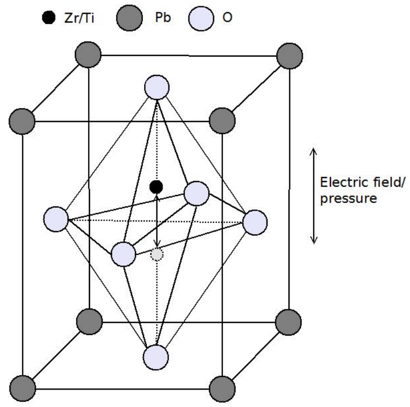

Figure 4.3.: PZT crystal in Perowskit structure. When pressure or an electric field is applied, the Zr/Ti atom is displaced and a measurable charge separation takes place.

Beginning of the 20th century a macroscopic description of the piezoelectric effect was developed and in 1972 Martin established a microscopic description showing that piezoelectricity is a bulk effect [103]. Today, lead zirconate titanate (PZT) is one of the most used materials crystallising in Perowskit structure (ABO_3), being ferroelectric, and showing a dipole momentum below Curie temperature T_C. Heating to T_C and applying a high D.C. field Weiss domains are organised and a polarisation direction is imposed. When used in thickness mode, the resonance frequency ν_{res} depends on ceramic thickness d, $\nu_{res} \propto d$ [155]. PZT ceramics can be manufactured in a wide range of forms dependent on application and can be used in many different applications like detection of fouling.

Generation of Ultrasound

Changes of an ultrasonic wave due to travelling through material and beeing reflected at interfaces can be determined using piezoceramic sensors because a mechanical deformation is transformed into electrical changes and vice versa. Production of ultrasound in a piezoelectric material like PZT is described macroscopical using a combination of continuum mechanics and electrical engineering while non-linear effects are neglected. Knowledge about the interaction between the electrical and the mechanical part of an ultrasonic transducer is crucial to understand how an ultrasonic wave is measured.

A piezoplate includes mechanical and electrical parts with piezoelectric constitutive equations between stress T, strain S, electric field E, and dielectric displacement D

$$D = d \cdot T + \varepsilon^T \cdot E \tag{4.13}$$

$$S = s^E \cdot T + d \cdot E \tag{4.14}$$

with piezoelectric constants e and d, permittivity at constant stress ε^T, and elasticity constant at constant electric field s^E. The mechanical deformation of a piezoplate follows the classical wave equation with plane wave solution for wave function Ψ:

$$\Psi(t) = \Psi_0 \cdot exp(-i\omega t). \tag{4.15}$$

The electrical part of a piezoactive material can be described by telegrapher equations with voltage V, current I, resistance R, inductance L, conductance G, and capacity C:

$$-\frac{\partial V(x,t)}{\partial x} = R \cdot I(x,t) + L \cdot \frac{\partial I(x,t)}{\partial t} \tag{4.16}$$

$$-\frac{\partial I(x,t)}{\partial x} = G \cdot V(x,t) + C \cdot \frac{\partial V(x,t)}{\partial t}. \tag{4.17}$$

With Gauß law, $\nabla D = 0$, and Kirchhoff's rules it is found

$$V(x,t) = Re(V(x) \cdot e^{i\omega t}) \rightarrow -\frac{dV}{dx} = (R + i\omega L) \cdot I(x) \tag{4.18}$$

$$I(x,t) = Re(I(x) \cdot e^{i\omega t}) \rightarrow -\frac{dI}{dx} = (G + i\omega C) \cdot V(x). \tag{4.19}$$

With propagation constant γ the equation is rewritten for V and I, respectively, and resembles the wave equation (4.9).

$$\frac{d^2V(x)}{dx} - \gamma^2 \cdot V(x) = 0 \tag{4.20}$$

with $\gamma = \alpha + i\beta = \sqrt{(T + i\omega L) \cdot (G + i\omega C)}$ a classical solution follows

$$V(x,t) = A \cdot e^{-\alpha x} \cdot e^{i(\omega t - \beta x)} + B \cdot e^{-\alpha x} \cdot exp^{i(\omega t + \beta x)}. \tag{4.21}$$

Derivation for the linear case is given in more detail for example in [161] [109] [73]. Parenthoine also derived the equations for the non-linear case [120] where Wang et al. derived the solution for an ultrasonic wave in composite materials (solid with liquid) [166]. Redwood showed that the wave equation of a planar compression wave in a piezoelectric plate resembles the same as in a non-piezoeletric material [136]. Latter is of great importance for piezoceramic sensors because analysis of measured signals is simplified.

The link between mechanical pressure waves and their electrical counterpart in a piezoceramic was shown. This link is crucial for understanding generation and measuring of ultrasonic waves and how to build a sensor fitting for different applications. These influence can be determined by a piezoceramic which transforms mechanical to electrical measurable quantities where the electrical quantities show influences due to material changes like cleaning of fouling layers. This makes piezoceramics a reliable tool for both generation and measurement of ultrasonic waves to determine fouling. For understanding ultrasonic generation and propagation lumped circuit description can help besides other modelling tools.

Lumped Circuits and Other Models for Ultrasonic Generation

To model generation and reception of ultrasound different models can be used. One-dimensional models based on lumped circuits are briefly presented which can be applied for sensitivity analysis or implemented in SPICE (Simulation Program with Integrated Circuit Emphasis). Including diffraction effects and losses this approach can be extended to overcome some challenges concerning one-dimensionality [4] [148] [150].

First models were built 1914 by Butterworth [24] and 1928 by van Dyke [162]. van Dyke's model is basic but still in use today for estimations close to resonance frequency (Fig. 4.4). The drawback is that far away from resonance frequency behaviour is not interpreted correctly.

In 1935, Mason developed a more complex model which includes transformers to describe the piezoelectric behaviour in detail (Fig. 4.5) [105]. The transformer transforms the

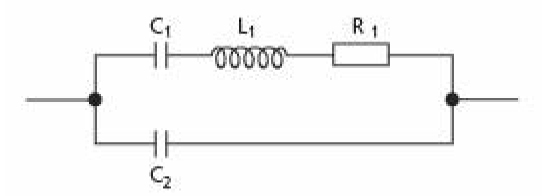

Figure 4.4.: van Dyke model with capacities C_1 and C_2, inductance L_1, and resistance R_1.

electric signal into a mechanical one and vice versa. This model was revised several times (e.g. by Redwood [136]) and criticised due to its negative capacitance. Still, it is one of the most used lumped circuit models giving good results.

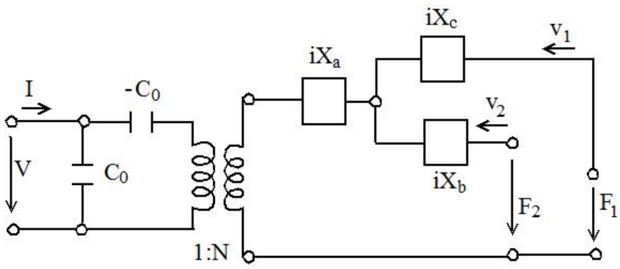

Figure 4.5.: Mason's model with voltage V, current I, capacity C_0, transformer (1:N), compliances X_a, X_b, X_c, forces F_1, F_2, and velocites v_1 and v_2.

Krimholtz, Leedom, and Mattaei extended Mason's model in 1970 (KLM model [84]) (Fig. 4.6). Besides Mason's model, it is popular to model ultrasonic transducers with lumped circuits. Comparison of Mason's and KLM model show similar behaviour despite different circuits [149] even when losses are introduced. The biggest difference between Mason's and KLM model is the exclusion of the negative resistance and a better applicability of KLM model concerning frequency analysis. Both models are often used to describe and model the behaviour of a piezoelectric ceramic because they combine the mechanical and electrical part of a piezoelectric material via transformers.
Leach developed a model including controlled sources to overcome problems of negative resistance and frequency dependent transformers of Mason's and KLM model [87]. This model is quite complex and can be used to model in two dimensions in contrast to the other presented models. Püttmer et al. [129] and Deventer et al. [161] included and investigated losses while Johansson and Martinsson [75] and Aouzale et al. [5] included and investigated diffraction effects using Leach's model.
Network theory can be used to make sensitivity analysis and to determine influences on ultrasonic signals. An ultrasonic transducer (piezoceramic and backing) together with its

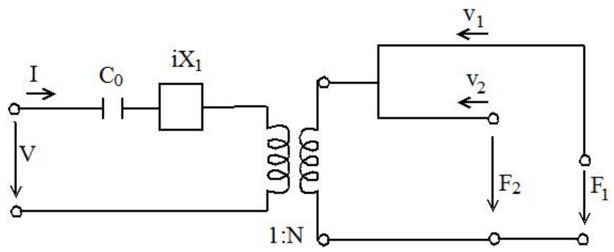

Figure 4.6.: Model of Krimholtz, Leedom, and Mattei with voltage V, current I, capacity C_0, transformer (1:N), compliance X_1, forces F_1, F_2, and velocites v_1 and v_2.

excitation electronic can be described using a port model [74] [132]. In a three port model one port stands for the transformation of the electrical part to the mechanical part of the ultrasonic transducer and vice versa. The remaining two ports describe the mechanical oscillation of the piezoceramic. When the backing of the ultrasonic transducer is sheer resistance the three port reduces to a two port corresponding to a piezoceramic which is described by lumped circuits.

An ultrasonic setup (in reflection and transmission) consisting of an ultrasonic transducer together with the experimental setup can then be described as combination of two ports with (an) electromechanical two port(s) for the transducer(s) and purely mechanical two ports for all other setup parts. The resulting transfer function is got by multiplying the two port matrices of all single two ports. The transfer function can be used to describe and improve ultrasonic measurements and to make sensitivity analysis [98] [99]. This helps to determine the influence of fouling and other quantities on ultrasonic measurements.

It has to be kept in mind that adsorption, reflection, and refraction are present in material. Including those via secondary sources the complexity of the equations increases and may also increase computational time as well as capability to solve the equations. To overcome this problem, finite elements (FE) may be used for modeling [1] [168] [172]. This approach has the advantage that detailed knowledge of the investigated problem together with its equation is not necessary for solving the equations. Comparisons between SPICE and FE show limitations and advantages of both methods [55].

4.4. Upscaling and Fluid Dynamics

Upscaling

Upscaling is done to compare a setup developed in laboratory scale with an industrial setup to determine similarities and differences and overcome challenges. For comparison, fluid dynamic quantities were used: blockage factor, Reynolds number, friction coefficient, and pressure drop together with self-developed π-parameters were included. All chosen quantities are presented in table 4.3 together with their equations and a brief explanation.

Table 4.3.: Fluid dynamic characteristics to compare lab and industry scale

Fluid dynamic quantity	**Equation**	**Description**
Blockage factor B	A/A_B	Ratio between free and blocked channel
Pressure drop Δp	$\Delta p = (\lambda\ \rho v^2)/(2 \cdot d_h)$	Ratio between pressure drop and heat exchanger length
Reynolds number Re	$Re = (vL\rho)/\eta$	Ratio of interior forces to viscous forces in the medium
π_1 (Biot number)	$\pi_1 = R_f\alpha$	Ratio of the heat transfer resistance inside and outside (at the surface) of a body
π_2	$\pi_2 = (\dot{Q}\rho)/(p\dot{m})$	Ratio between heat flux and mass flow rate
Friction factor λ (after [17])	$\lambda = 0.3164/Re^{0.25}$	Ratio of friction losses related to Reynolds number

With A as unblocked area, A_B as blocked area, v as mean velocity, L as length of heat exchanger, ρ as fluid density, η as fluid viscosity, d_h as hydraulic diameter, R_f as fouling resistance, α as heat transfer, $\dot{Q}$ as heat flow, p as pressure, and $\dot{m}$ as mass flow rate.

Comparison of the characteristics helps to find out where a lab-scale setup and a heat exchanger used in industry behave similarly and where further considerations and calculations have to be done. These characteristics give an overview and a first impression about comparability of lab and industrial scale e.g. fouling production to determine if similar fouling can be expected. Most parameters are known explicitly only for ideal cases like the used friction factor which is valid for $Re < 10^5$ and have to be assumed for other cases.

Fouling and Fluid Dynamics

For fouling, the interaction between surface and fouling layer plays an important role. Also, interaction between flow field and fouling layer is important and flow velocity plays a role particularly in cleaning. Transport from detergent to fouling layer and removal of particles as well as shear stress between fouling and flow field determines growth velocity of a layer and cleaning, respectively. Following Bott ([20]), the generalised fouling process with deposited mass over time dm/dt is described with flux of deposition Φ_D and flux of removal Φ_R:

$$\frac{dm}{dt} = \Phi_D - \Phi_R. \tag{4.22}$$

With high shear stress and high removal flux Φ_R, growth of fouling is restricted and fouling may even decrease. This effect can be used when pulsed flow is applied for cleaning where non-uniform flow with very high shear stresses is present. For pulsed flow, laminar flow fields are superimposed with low frequency pulsed flow [18] [56]. Flow field and shear stress varies strongly when pulsed flow is applied and can lead to diminished deposition rate and improved cleaning [57] [173]. This may help to clean a fouled heat exchanger faster but it is sophisticated to obtain an evenly pulsed flow throughout an industrial heat exchanger. To improve cleaning it is important to determine shear stress inside an heat exchanger. Celnik et al. developed a method to calculate shear stress and flow rates of incompressible Newtonian fluids under laminar flow [26]. This may help to improve cleaning but usually in industry turbulent flow is used and also non-Newtonian fluids like yoghurt are processed.

Besides flow field influence the strength with which a fouling layer is attached to a surface is important for cleaning. Strength and fouling composition can be investigated using a technique called fluid dynamic gauging (e.g. [29] [58]). Shear stress to detach a fouling layer can be determined by determining a dimensionless shear stress τ^* derived from Navier-Stokes and continuity equation.

$$\tau^* \equiv \frac{\tau_{wall}}{4\rho v_c^2} = \frac{\omega^*_{wall}}{Re_{tube}} \tag{4.23}$$

where τ_{wall} as shear stress at the wall, ω^*_{wall} as dimensionless vorticity at the wall, ρ as density, Re_{tube} as Reynolds number in the siphon tube, and v_c as characteristic velocity. Detailed investigation of forces present between fouling and surfaces can be found in Appendix C.

When fouling is investigated under flow conditions interactions between flow field, surface and fouling layer have to be considered. When laminar flow is present influence on fouling growth is much lower than with turbulent flow. Also, cleaning will change and an ultrasonic signal may be influenced differently. For ultrasonic measurements the following question is of importance: how strongly is the measured ultrasonic signal influenced by present flow field? Is this influence higher than changed reflection behaviour at the investigated interface or not? Ultrasound used in reflection may help to reduce flow field influence, still, it cannot be ruled out completely.

5. Summary of Results (Thesis Publications)

5.1. Paper Summary

"Detection methods of fouling in heat exchangers in the food industry", E. Wallhäußer, M.A. Hussein, T. Becker; Food Control 27 (2012), 1-10

Fouling is unwanted deposit and occurs in food processing industry where most foodstuff is heated to extend shelf life and reduce microbiological hazard. When fouling occurs it decreases product temperature, product quality, and product safety by introducing an extra heat transfer resistance. Also, cleaning of heat exchangers is necessary leading to increased costs and plant downtime. Cleaning is usually not monitored but based on experience and cleaning success cannot be evaluated without opening the equipment. It is thus of great importance for food industry to monitor cleaning success. In particular dairy industry has a great need because unsupervised cleaning is done at least once a day. Monitoring fouling and cleaning requires high demands for measuring and analysing systems due to the complexity of fouling and cleaning. This paper gives an overview over different methods which can be used in heat exchangers to monitor fouling/cleaning. The focus lies on detection of dairy protein fouling but most described methods can easily be applied in other food or non-food areas. The described methods are divided in experimental, numerical, and computational methods. These include, e.g., measurements of temperature, heat transfer parameters, electrical and acoustic variables as well as usage of decision machines like artificial neural networks and modelling approaches. All methods are presented and compared with each other. Main influences on which method could be used are the process where fouling should be monitored and user demands. It seems preferable to combine different methods and not only rely on experimental data but combining experimental and numerical methods to adapt easier to changing process parameters, enhance product quality, and reduce error proneness.

"On the usage of acoustic properties combined with an artificial neural network - A new approach of determining presence of dairy fouling", E. Wallhäußer, W.B. Hussein, M.A. Hussein, J. Hinrichs, T. Becker; Journal of Food Engineering 103 (2011), 449-456

Fouling is a severe challenge in dairy industry. It influences product quality, decreases heat transfer, and increases production costs due to unsupervised cleaning. Monitoring cleaning success and adapting cleaning cycles would help to reduce costs. To do this, dairy fouling type A was monitored in a small static setup using an ultrasonic transducer. Dairy protein fouling (type A fouling) mainly consists of β-lactoglobulin (β-lg) and usually occurs at temperatures above 71 °C (pasteurisation temperature). Here, in a small static setup dairy protein fouling was produced using reconstituted milk with protein content of ca. 6 w%. Milk was heated to 92±1 °C for 90±5 min. Then, superfluous milk was poured and water was filled into the setup. Measurements were done at room temperature (20±2 °C) using an ultrasonic transducer with a center frequency of 2.1±0.2 MHz. The transducer was excited using an in-house electronics with 20 V and measured with Virtual Expert. As reference, water (clean surface) was measured. Five acoustic parameters were extracted from the ultrasonic signal and analysed offline using Matlab. The acoustic parameters were characteristic acoustic impedance (Z), energy of echo 1 (*E1*) and echo 2 (*E2*), and logarithmic decrement of echo 1. Results were fed into an artificial neural network (ANN) which was a multilayer perceptron based on back-propagation algorithm. The ANN had five neurons in input layer, two neurons in one hidden layer, and one neuron in output layer which displayed 1 for fouling and 0 for no fouling. As transfer functions LOGSIG, LOGSIG, and TANSIG were chosen. The ANN was trained with 75 % of the data and tested with the remaining 25 % displaying a detection accuracy of 98.6 %. It has been shown in this paper that it is possible to determine fouling presence and absence offline in a static setup using an ultrasonic based measuring method together with a pattern recognition method like an ANN. In future, measurements under flow shall be done and mineral fouling shall be included.

"Detection of dairy fouling: Combining ultrasonic measurements and classification methods", E. Wallhäußer, W.B. Hussein, M.A. Hussein, J. Hinrichs, T. Becker; Engineering in Life Science (2013), 292-301

In the same static setup as described in the above paper protein and mineral fouling was produced. Protein fouling was made as previously desribed. Mineral fouling consists mainly of precipitated salts and was made from reconstituted permeate powder which was heated to 92±2 °C for ca. 5 h. Using an ultrasonic transducer fouling layer presence and absence was measured. Five acoustic and signal parameters were extracted using Matlab. These features were characteristic acoustic impedance Z, short time energy STE, temporal crest factor TCF, spectral crest factor SCF, and spectral smoothness SSMOOTH. The results from protein and mineral fouling were investigated using artificial neural networks (ANN) and support vector machines (SVM). An ANN is an emulation of a network like a brain which can establish different connections between in- and output. Here, a feedforward multilayer perceptron was used with five neurons in input layer, two neurons in one hidden layer, and one neuron in output layer which displayed 1 for fouling and 0 for no fouling. As transfer function between the layers for all ANNs TANSIG was used. For only protein fouling, ANN showed an accuracy of 100 %, for only mineral fouling the detection precision was 93.49 %. When both fouling types were combined as may happen under real conditions the accuracy dropped to 71.86 %. This may be due to highly varying fouling layers and high variations in the data. A SVM classifies data into different groups and divides them using a hyperplane built on support vectors from this group. If no linear division is possible the kernel trick is applied which transfers data in feature space where a linear division is possible. The SVM built for protein fouling showed a precision of 100 % using 30 support vectors. For mineral fouling, 80 support vectors were used and 98.19 % were identified correctly. For combined fouling the SVM needed 116 support vectors and showed an accuracy of 97.57 %. This is better than the ANN because SVM was less dependent on fouling type and managed high variations in data better. It was shown that offline detection of protein and mineral fouling can be done using ultrasonic measurements combined with a classification method.

"Investigating and understanding fouling in a planar setup using ultrasonic methods", E. Wallhäußer, M.A. Hussein, T. Becker; Review of Scientific Instruments 83 (2012), 094904-1-10

Fouling in food processes usually occurs when foodstuff is heated. Its detection is a challenging task and different methods were already applied. In this paper, a setup is described with which it is possible to produce fouling under controlled conditions and to measure its presence and absence under flow using an ultrasonic measuring method. The theoretical and experimental description of the planar setup and the ultrasonic measuring system is given. Electrical and mechanical lumped circuits were applied for theoretical description of the system. Sensitivity analysis (SA) was done to determine the influence of different quantities on the ultrasonic signal and to see feasibility of fouling detection using ultrasound. SA was performed using central difference equation and high weights were found for characteristic acoustic impedance Z, thickness θ, and real and imaginary part of the elastic modulus E and η of delay line, stainless steel wall, material behind the fouling, and piezoplate. During measurements, these features are nearly constant and can thus be regarded as stable showing only a small influence on measured signal. Fouling also showed high weights and does change during fouling and cleaning. It thus can be considered as measurable quantity. Experiments confirmed the already theoretically found influence of delay line and showed an influence of solid coupling material between delay line and stainless steel wall. Solid coupling has to be included in further sensitivity analysis. First tests to produce dairy protein fouling showed the possibility to produce it reproducible.

Determination of influencing quantities on the ultrasonic signal can help to improve the developed setup better. Also, experiments can be planned and experimental results can be explained better. Because fouling does have a high weight it is possible to measure cleaning success and fouling absence and so to adapt cleaning cycles to necessity.

"Determination of cleaning end of protein fouling using an online system combining ultrasonic and classification methods", E. Wallhäußer, A. Sayed, S. Nöbel, M.A. Hussein, J. Hinrichs, T. Becker; Food and Bioprocess Technology 6 (1) (2013), 1-10

One of the highest cost factors in dairy protein fouling is cleaning a fouled heat exchanger. Cleaning is usually done using a fixed cleaning in place (CIP) cycle which handles the worst case. Even if there are shorter CIP cycles it remains unkown if they are sufficient. The crux is that until now no online monitoring method for cleaning cycles exists. There are several possibilities to determine fouling presence (pressure drop, temperatures, heat transfer parameters and others) but no measuring method which is easily applied to determine the end of a CIP cycle showing a clean surface. Here, an online monitoring method of dairy protein fouling using ultrasound in a planar test section is described.

A planar test section was used to build up dairy protein fouling in a reproducible way. Fouling made was comparable to the one usually present in dairy industry. After detailed investigation of different temperature effects ultrasonic measurements of fouling presence and absence (clean surface) were made. Based on these measurements an artificial neural network (ANN) and a support vector machine (SVM), respectively, was developed and tested offline using Matlab. ANN used 1-class classification and existed of one input layer with nine neurons corresponding to nine inputs characteristic acoustic impedance Z, short time energy STE, temporal and spectral crest factor TCF, SCF, spectral smoothness $SSMOOTH$, temporal decrease $Tdescend$, temporal slope $Tslope$, mass flow rate $\dot{m}$, and temperature in the measuring section T, one hidden layer with fourteen neurons, and one output layer with nine neurons stating if output and input layer were the same or not. As transfer functions, TANSIG, LOGSIG, and PURELIN were chosen. ANN training was done using clean heat exchanger while fouled surface data was used for testing resulting

in a detection accuracy of more than 80 %. SVM used same input as ANN but used both fouled and clean surfaces for training and testing (50/50). As kernel function, a radial basis function was found to represent the hyplerplane best and detection accuracy was 94 %. Both ANN and SVM were implemented in C++ to establish an online monitoring method for cleaning of protein fouling where different challenges were encountered. To overcome them angle based outlier detection (ABOD) and exceptional handling were implemented in the online monitoring code. ABOD is based on the fact that outliers have small angles between them and points of a group and can be easily identified by variance. This method is stable in x- and y-direction and more reliable than simple regression. Exceptional handling is based on windows tendency check. Here, a window size of 10 signals were chosen. Inside the window signals were compared with each other and dependent on the majority ($n \geq windowsize/2$) all signals are transferred either to fouling or no fouling. This makes the decision process much more stable but introduces a time delay of *window size/2* between measured and displayed signal.
A third method to monitor cleaning success, monitored the slope of the above chosen features with cleaning success. Temperature and mass flow rate were excluded because they did not vary strongly. Here, slope of all features was monitored over time because it changed during cleaning and stayed constant before and after a while. When a fouled heat exchanger was present slope of e.g. TCF stayed nearly constant ($m \approx 0$), as soon as cleaning was started slope changed ($m \neq 0$), and after a while slope was nearly constant ($m \approx 0$) again. With this method the time for cleaning could directly determined to be 22 ± 3 min.
The methods seem to be applicable in determination of fouling presence and absence and in monitoring cleaning success of a planar fouled heat exchanger. This may help industry a lot to save money due to oversized cleaning cycles and cleaning can be adapted to reduce amount of water, detergent, and time needed.

5.2. Paper Copies

5.2.1. "Detection methods of fouling in heat exchangers in the food industry - a review", E. Wallhäußer, M.A. Hussein, T. Becker; Food Control 27 (2012), 1-10

(This is a sample cover image for this issue. The actual cover is not yet available at this time.)

Food Control 27 (2012) 1–10

Contents lists available at SciVerse ScienceDirect

Food Control

journal homepage: www.elsevier.com/locate/foodcont

Review

Detection methods of fouling in heat exchangers in the food industry

E. Wallhäußer*, M.A. Hussein, T. Becker

(Bio-)Process Technology and Process Analysis, Life Science Engineering, Technische Universitaet Muenchen, Weihenstephaner Steig 20, 85354 Freising, Germany

A R T I C L E I N F O

Article history:
Received 14 September 2011
Received in revised form
23 February 2012
Accepted 28 February 2012

Keywords:
Fouling
Heat exchanger
Detection method
Fouling sensor

A B S T R A C T

Fouling is unwanted deposit on a (heat transfer) surface. In food and dairy industry it is a major problem because heat transfer to the product is decreased resulting in reduced product quality and safety. Thus, plant efficiency is reduced and unsupervised cleaning has to be conducted. This limits processing time and increases plant downtime and costs. Monitoring fouling and cleaning requires high demands for the measuring and analysing system. This paper gives an overview over different fouling monitoring methods in heat exchangers. Experimental (pressure drop, temperature and heat transfer parameters, electrical parameters, acoustic methods), numerical, and computational methods are presented and compared.

Contents

1. Introduction

Fouling is unwanted deposit on (heat transfer) surfaces. When it develops thermal performance of a heat exchanger goes off-design and decreases due to an extra heat transfer resistance. Thorough product heating cannot be ensured anymore in food industry if fouling occurs. This leads to product loss and cleaning of the heat exchanger equipment using a fixed cleaning-in-place cycle. Cleaning is often time consuming, costly, and used cycles are seldom adaptable to different fouling conditions. Hence, different methods were developed to detect fouling in heat exchangers, where e.g. Prakash, Datta, and Deeth (2005) give an overview.

Fouling is a high influence in dairy industry and lead to a lot of research of fouling mechanisms, mitigation, and cleaning. Investigated methods for fouling detection are e.g. weighing of fouled and clean tubes and plates of heat exchangers (Burton, 1961; Tissier & Lalande, 1986), observing disturbances in hydrodynamics

Abbrevations: ANN, artificial neural network; DEC, deposit electric conductivity; GA, genetic algorithm; MEMS, micro-electro-mechanical system; MSS, mass surface sensor; PHE, plate heat exchanger; QCM/QCM-D, quartz micro balance/with dissipation; SMUF, simulated milk ultrafiltrate; THE, tube heat exchanger; TOF, time of flight; UHT, ultra-high temperature; WPC/WPI, whey protein concentrate/isolate; WT, wavelet transform.

* Corresponding author. Tel.: +49 8161 71 2623; fax: +49 8161 71 3883.
E-mail address: e.wallhaeusser@wzw.tum.de (E. Wallhäußer).

0956-7135/$ – see front matter
doi:10.1016/j.foodcont.2012.02.033

Nomenclature

a, b, k	constant
$A_{(0)}$	(incident) amplitude
A	area
α	attenuation coefficient
c_p	specific heat capacity at constant pressure
d	(outer) pipe diameter
D	dissipation factor
δ_f	fouling thickness
$e_{E/fl}$	electrode/fluid space
f	frequency
Δf	frequency change
Hg	Hagen number
k	calibration constant
l	heat exchanger length
$\lambda_{(f)}$	thermal conductivity (of fouling)
$\dot{m}$	mass flow rate
Δm	mass change
μ	dynamic viscosity
ν	kinematic viscosity
p	pressure
Q	heat transfer
r	reflection coefficient
$R_{el,th,dep,fluid}$	electric, thermal, deposit, fluid resistance
Re	Reynolds number
ρ	density
S	Sauerbrey constant
$\sigma_{(eq,p)}$	(equivalent, product) electric conductivity
t	time
t_f	final fouling run time
T/T_{lm}	temperature/logarithm of mean T difference
ΔT	temperature difference
τ	decay time
$\Delta\theta$	product temperature change
U	overall heat transfer coefficient
v	velocity
ξ	friction factor
z	direction
Z	acoustic impedance

(Corrieu, Lalande, & Ferret, 1986), or using heat transfer parameters as fouling indicator (Davies, Henstridge, Gillham, & Wilson, 1997; Ling & Lund, 1978). Also, electrical, optical, and acoustical methods are included (Withers, 1996). But, fouling can also occur in other places like membranes where different methods are applicable like confocal laser scanning (Ferrando, Rozek, Zator, López, & Güell, 2005), fluid dynamic gauging (Chew, Paterson, & Wilson, 2004, 2007), or ultrasonic techniques (Kujundzic, Cobry, Greenberg, & Hernandez, 2008; Kujundzic et al., 2007).

To understand fouling mechanisms and improve fouling prediction and cleaning, fouling modelling was investigated (de Jong, te Giffel, Straatsma, & Vissers, 2002; de Jong, Waalewijn, & van der Linden, 1993). Food processing in heat exchangers may be optimised by developing kinetic models for dairy fouling (Grijspeerdt, Mortier, De Block, & Van Renterghem, 2004; Petermeier, Benning, Becker, & Delgado, 2003; Petermeier et al., 2002). This may help to improve fouling detection and mitigation in and cleaning of heat exchangers. An overview about different fouling models and mitigation methods of fouling can be found in Balasubramanian and Puri (2010).

In this review article, experimental, numerical, and computational fouling detection and monitoring methods are described and compared. It would go beyond the scope of this paper to shine a light on all possible methods and on all areas where fouling occurs. Therefore, the focus lies on fouling in heat exchangers in food processing industry and dairy fouling. In the next section, a short overview over fouling is given. Then, selected experimental and computational methods are presented. At the end, these methods are compared with each other and a conclusion is drawn.

2. Fouling

Fouling is classified into macro and micro fouling. The first plays no major role in food industry. The latter is divided into precipitation, particulate fouling (colloidal particles) or sedimentation (larger particles), corrosion, chemical reaction fouling, solidification, and biofilms (Bott, 1995, 1997; Simões, Simões, & Vieira, 2010; Watkinson & Wilson, 1997) which are summarised in Table 1.

In food industry, dairy industry is one of the most affected sectors. Usually two kinds appear depending on process temperature: chemical reaction at pasteurisation (type A or protein fouling, mainly denaturated proteins, see Fig. 1 for a sketch) and scaling at ultra-high temperature (UHT) (type B or mineral fouling, mainly salts) (Bansal & Chen, 2006; Burton, 1968; Changani, Belmar-Beiny, & Fryer, 1997; Visser & Jeurnink, 1997). Cleaning is conducted due to the diminished heat transfer with fouling and the risk of unsafe food (Bohnet, 1987; Changani et al., 1997; Fryer & Asteriadou, 2009).

Dairy industry is not the only food industry affected by different fouling types. In beverage industry, particulate/sedimentation fouling during membrane filtration of beer and other fermented beverages plays an important role (Blanpain & Lalande, 1997; Czekaj, López, & Güell, 2000). In water treatment plants, mostly scaling and biofilms are present and can hinder processing (Laine, Campos, Baudin, & Janex, 2003; Müller-Steinhagen, Hartnett, Irvine, Cho, & Greene, 1999) while in crude oil processing scaling and chemical reaction occur reducing heat exchanger performance (Butterworth, 2002; Deshvannar, Rafeen, Ramasamy, & Subbaro, 2010).

Table 1
Comparison of different fouling types and their occurrence.

Fouling kind	Short description	Occurrence	Example
Precipitation	Precipitation/crystallisation of salts, oxides etc.	Heat exchangers Water treatment, desalination	Dairy fouling type B Calcium, other salts
Particulate/sedimentation	Deposition/accumulation of particles on surfaces	Combustion systems Food processing industry	Colloids Dust
Corrosion	Corrosion deposits on metal surfaces	Water treatment	Rust
Chemical reaction	Decomposition/polymerisation of proteins, hydrocarbons on heat transfer surfaces	Heat exchangers in dairy, crude oil industry Food processing industry	Dairy fouling type A Crude oil fouling
Solidification	Freezing of components on a cooled surface	Food processing industry Fine mechanical manufacture	Ice Paraffin wax
Biofilm	Growth of algae, bacteria	Water treatment	Bacterial growth on membranes

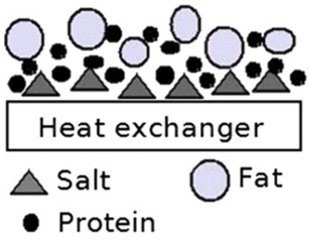

Fig. 1. Sketch of protein fouling made of proteins, salts, and fat.

3. Experimental methods for determining fouling

3.1. Pressure drop

In heat exchangers, the pressure between inlet and outlet is measured regularly. When fouling develops the mean square area in a flow channel decreases leading to a pressure drop at constant flow rate. This method is standard and can be used as input for other methods e.g. as input in an artificial neural network (ANN) for fouling detection in a plate heat exchanger (PHE) (Riverol & Napolitano, 2005). Usually, pressure drop is measured accompanying to other methods like temperature measurements.

Martin connected mass and heat transfer in heat exchangers with periodic arrangements like cross corrugated plate and tube bundles with pressure drop via the generalised Lévêque equation (Martin, 2002). So, the Hagen number Hg was derived which was used to predict heat and mass transfer over a wide range of applications and heat exchanger geometries.

$$\left(\frac{\xi}{2}\right)\mathrm{Re}^2 = \mathrm{Hg} = \left(\frac{1}{\rho}\right)\left(\frac{\Delta p}{\Delta z}\right)\frac{d^3}{\nu^2} \tag{1}$$

With ξ as friction factor, Re as Reynolds number, ρ as density, p as pressure, z as direction of flow, d as outer tube diameter, and ν as kinematic viscosity.

An advantage is that the necessary equipment for pressure measurement is present. Also, pressure drop measurement is necessary to avoid excessive pressure and thus heat exchanger damage. Disadvantageous of this method is that it is not very sensitive to thin layers and that the place of fouling remains unknown.

3.2. Temperature and heat transfer parameters

Inlet and outlet temperature of product and heating medium is routinely measured. When fouling develops heat transfer is diminished and product outlet temperature drops. If a fixed product outlet temperature is wanted the heating medium temperature is increased when former decreases. This can be used to measure fouling presence and extent: the higher the increase of the heating medium temperature the more fouling is present.

When used on its own, it is not very sensitive and gives only overall values. Still, temperature changes can be used as input for numerical fouling determination (Ingumundardottir & Lalot, 2009; Lecoeuche, Lalot, & Desmet, 2005; Riverol & Napolitano, 2005). Outlet temperature and flow parameters are also measured regularly and were used to develop a computational model to control milk sterilisation (Nema & Datta, 2005, 2006). But, fouling place is unknown and certain thicknesses are necessary to influence the temperature.

Heat transfer parameters like heat flux, overall heat transfer coefficient, and fouling resistance are based on temperature changes, mass flow rate $\dot{m}$, and thermal conductivity of the product, the heating medium, and the fouling layer. Heat transfer Q is the amount of heat transferred from heating medium to product with the overall heat transfer coefficient U given as

$$U = \frac{Q}{A\Delta T_{\mathrm{lm}}} = \frac{\dot{m}c_{\mathrm{p}}\Delta\theta}{A\Delta T_{\mathrm{lm}}} \tag{2}$$

with specific product heat capacity at constant pressure c_{p}, product temperature change $\Delta\theta$, heat transfer area A, and logarithm of mean temperature difference between heating medium and product T_{lm}. Fouling introduces an extra resistance R_{dep}. If the heat transfer is monitored via ΔT_{lm} and $\dot{m}$, fouling can be determined. Fouling thickness δ_{f} and thermal conductivity λ_{f} are related to U via

$$R_{\mathrm{dep}} = \frac{1}{U(t)} - \frac{1}{U(0)} = \frac{\delta_{\mathrm{f}}}{\lambda_{\mathrm{f}}} \tag{3}$$

where $U(0)$ is the heat transfer coefficient of a clean and $U(t)$ the one of a fouled heat exchanger. Increasing fouling thickness increases R_{dep}.

Thermal resistance R_{th} is a measurand for the heat lost during heating. It is inversely proportional to the product thermal conductivity λ and is expressed as

$$R_{\mathrm{th}} = \frac{1}{\lambda} = \frac{\Delta T \cdot A}{Q \cdot l} \tag{4}$$

temperature difference between inlet and outlet ΔT, area A, and heat exchanger length l. The parameters can be used to determine fouling or as input for other methods.

The convective heat exchanger coefficient and fouling thickness in a heat exchanger was determined via transient state estimation by comparing the global response time of a system in fouling and no fouling conditions (Perez, Ladevie, Tochon, & Batsale, 2009). For this, a transient fouling probe was developed using a sensitivity function and the probe was evaluated theoretically and experimentally. Perez et al. determined the average heat transfer coefficient and fouling thickness their tests showing good agreement with measurements. In future, the developed method shall be extended to other heat exchangers and fouling kinds.

Adaptive observers were used to monitor the performance degradation of the overall heat transfer coefficient $U(t)$ with fouling (Astorga-Zaragoza, Zavala-Río, Alvarado, Méndez, & Reyes-Reyes, 2007). An adaptive observer is a recursive algorithm estimating the system state and unknown parameters which helps to decide if preventive or corrective maintenance is necessary. Simulated and experimental temperature measurements in a counter-flow heat exchanger were used. Astorga-Zaragoza et al. monitored $U(t)$ continuously and related its variation with thermal performance of heat exchanger. Thus, the decision whether maintenance was needed or good could be made.

3.3. Electrical parameters

Electrical parameters can be used when electric heating or electrodes are present. E.g., a change in salt concentration due to precipitation induces a change in electric conductivity. Usually, electrical resistance and conductivity are chosen. Former is characterised by the electrical voltage over electrical current, latter describes the material ability to conduct an electrical current. When electric heating is applied, monitoring the heater behaviour can be used because the electrode temperature changes with fouling.

For determining fouling, a method was developed measuring the electrical and the thermal resistance (heat flux) (Chen, Li, Lin, & Özkan, 2004). Stainless steel electrodes were applied to determine the electrical resistance R_{el} and the thermal resistance R_{th} was calculated with heat flux, backside surface temperature of the fouled wall, and fluid bulk temperature. The difference of R_{el} of a reference (non-fouled) and a fouled section was determined and correlated with R_{th} with constants a and b.

$$R_{th} = aR_{el} + bR_{el}^2 \tag{5}$$

Chen et al. measured fouling build-up and cleaning with high sensitivity and showed that electrical and thermal resistance can be linked.

Electrical conductivity was used to determine growth rate of fouling (Guérin, Ronse, Bouvier, Debreyne, & Delaplace, 2007). Electrodes were implemented in a plate heat exchanger and the effect of Reynolds number, calcium concentration, and temperature on fouling made of whey protein concentrate (WPC) was investigated. Deposit thickness was determined by weighing the plate prior and after a fouling run and by a pneumatic lifting device. Kirchhoff's rule decouples fluid and deposit resistance at fixed operating conditions:

$$R_{el} = R_{fluid} + 2R_{deposit} \tag{6}$$

The deposit electrical conductivity σ with ion concentration in the layer with space of fluid e_{fl} (distance between electrodes e_E minus deposit thickness e_d), fouling run time t_f, and equivalent electrical conductivity σ_{el} is (Guérin et al., 2007)

$$\sigma_{d_{t_f}} = \left[\frac{e_E}{2e_{d_{t_f}}}\cdot\left(\frac{1}{\sigma_{eq_{t_f}}} - \frac{1}{\sigma_p}\right) + \frac{1}{\sigma_p}\right]^{-1} \tag{7}$$

with structure and volume of fouling layers dependent on Reynolds number and calcium concentration. This results can explain some cleaning difficulties because cleaning agents did not soak a layer sufficiently.

Continuous ohmic heating was investigated using a solution made of WPC and xanthan gum (Ayadi, Leuliet, Chopard, Berthou, & Lebouché, 2004). For fouling determination, dry deposit mass, pressure drop, local temperature gradient between electrodes and bulk, and consumed electrical power were monitored. It was found by Ayadi et al. that an additional electric resistance emerged with fouling lead to energy dissipation and increased temperature until boiling point was reached while electrical power consumption evolution was very sensitive to fouling. In future, Ayadi et al want to improve local electric measurements and to develop a model for deposition thickness dependent on electrical parameters evolution.

The temperature profile and temperature gradient between electrode surface and bulk of non-fouling (water, water-sucrose solution) and fouling (aqueous β-lactoglobulin solution, β-lactoglobulin–xanthan gum mixture) fluids of an ohmic cell was studied (Ayadi, Bénézech, Chopard, & Berthou, 2008). For non-fouling fluids, value and shape of temperature difference between electrode and bulk depend on flow and rheological fluid behaviour. For fouling fluids, the temperature gradient differed due to changed Reynolds number during fouling caused by different electric conductivities between bulk and deposit. Fouling adds an additional electric resistance to the existing one leading electrical energy to dissipate in the layer. Energy dissipation increases electrode temperature which can be used as measurand.

A chronoamperometric electrochemical method was used to evaluate the intensity of $CaSO_4$ scaling (Tlili, Rousseau, Ben Amor, & Gabrielli, 2008). It is based on an oxygen-reduced cathodic reaction, $O_2 + 2H_2O + 4e^- \rightarrow OH^-$, where time variations of the electrical current are measured and can be used as indicator for scaling rate and to detect nucleation time. Fouling acts as insulator reducing current intensity to zero with a compact and to very small values with a porous layer. The probe consisted of a copper rod with a nickel foil glued to one end with a gold layer on its top which acted as thermocouple. It was put into an electrolyte fluid with constant flow rate and current intensity and electrode surface temperature were measured. The chronoamperometric curve slope displayed growth rate and nucleation time. Layer porosity was determined and salt concentration was found to have a stronger influence than temperature on fouling (Tlili et al., 2008).

Electrical parameters are very sensitive to thin layers and fouling thickness can be determined. A drawback is the invasive implementation of the electrodes and that usage of electric heating of food products is not widespread.

3.4. Acoustic methods

3.4.1. Ultrasound and vibrational methods

Acoustic parameters change when fouling occurs and can be measured in transmission (one transducer as sender, one as receiver) and in pulse-echo mode (one transducer as sender and receiver). Often, time of flight (TOF) of the signal is determined:

$$\begin{aligned} \mathrm{TOF} &= \frac{d}{c} \quad \text{for transmission mode} \\ \mathrm{TOF} &= \frac{2d}{c} \quad \text{for reflection mode} \end{aligned} \tag{8}$$

with path length d and sound velocity c. Using TOF and with known c in the layer, thicknesses can be calculated. Also, characteristic acoustic impedance Z can be used which measures the resistance a medium opposes to a travelling sound wave and can be determined with density ρ and c

$$Z = \rho\cdot c \tag{9}$$

or with reflection coefficient r at an interface of two different materials

$$Z_2 = Z_1\left(\frac{1-r}{1+r}\right) \tag{10}$$

Z is typical for a material and can be used for material identification and fouling determination. The determination of TOF, Z, and echo energy E together with an explanatory signal is shown in Fig. 2.

Another parameter is signal energy which changes when fouling develops due to changing reflection/transmission and attenuation coefficients. Energy can be determined in time and frequency domain. Besides, damping and signal attenuation can be used. The attenuation coefficient α is connected to path length x and incident amplitude A_0

$$A(t) = A_0\exp(-\alpha x) \tag{11}$$

Signal damping takes place because the signal is refracted and is linked to intrinsic and thermal parameters (viscosity, thermal conductivity).

Withers used a tubular setup measuring in transmission mode to determine the thickness of different materials (adhesive tape, silicone grease, tomato paste, cheese spread, gravy, chocolate) using TOF with temperature compensation for milk and water (Withers, 1994). He determined thicknesses between 0.5 and 6.0 mm of different fouling substances with a threshold of 100 μm below which thickness could not be determined with high accuracy.

Characteristic acoustic impedance Z was used already to determine solution properties, density changes, and to characterise foodstuff (Bamberger & Greenwood, 2004; Chung, Popovics, &

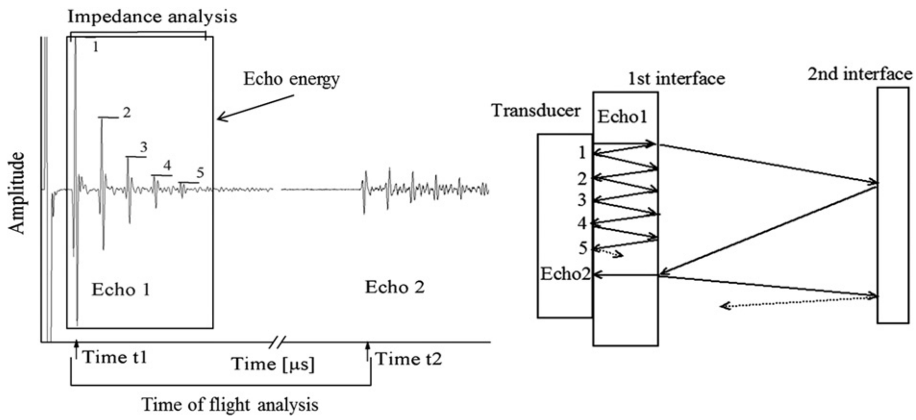

Fig. 2. Ultrasonic signal displaying some acoustic parameters (TOF, Z, E) and a sketch of the pulse-echo mode.

Struble, 2010; Greenwood, 2009; Greenwood, Adamson, & Bond Leonard, 2006). *Z* was also applied in detection of fouling by Wallhäußer, Hussein, Hussein, Hinrichs, and Becker (2011) where an ultrasonic transducer of 2 MHz in pulse-echo mode in a static setup was used together with echo energy and logarithmic decrement (signal loss) of reconstituted skim milk with different protein concentrations. Fouling developed on a stainless steel plate and the obtained parameters were combined in an ANN showing an accuracy of 98.6%. They found that acoustic impedance and energy changed significantly with protein fouling and will includes mineral fouling and flow measurements in future experiments.

A technique based on propagation of nano- and microvibrations along the deposition surface called mechatronic surface sensor (MSS) was developed by Pereira, Rosmaninho, Mendes, and Melo (2006). The MSS consisted of an actuator (piezoelectric ceramic) and an acceleration sensor. After excitation, the acceleration sensor measured the signal amplitude of a stainless steel plate vibration which changed when a layer was deposited. For mineral fouling simulated milk ultrafiltrate (SMUF) and for protein fouling whey protein isolate (WPI) was used. For both mineral and protein fouling SMUF and WPI were combined. Experiments took place at 50 °C in turbulent regime and the amplitude was found to change significantly with fouling thus build-up and cleaning could be monitored. The damping factor varied with elasticity of fouling layer making it possible to distinguish between different layer types.

A MSS was applied for monitoring different structural deposit build-ups (Pereira, Mendes, & Melo, 2008). The deposits were *Pseudomonas fluorescence* biofilms using laminar and turbulent flow and silica on PVC. A correlation between deposit amount and MSS answer was shown and confirmed by numerical simulations. Visco-elastic properties were determined and it was distinguished between organic/inorganic deposit and attached/sedimented deposit. In addition, a MSS was used to detect the end of hair shampoo removal on a stainless steel plate (Pereira, Mendes, & Melo, 2009). Different cleaning conditions were applied with changing temperature and Reynolds number. The signal amplitude was chosen and visual inspection, spectrophotometry, and contact angle measurements were applied for validation by Pereira et al. The MSS detected cleaning end correctly with different cleaning conditions resulting in different cleaning rates.

For observing fouling in a PHE, an acoustic sensor was developed which monitored low-frequency waves (Merheb, Nassar, Nongaillard, Delaplace, & Leuliet, 2007) with WPC used as fouling fluid. On one plate side, an impactor was applied and on different places on the other side acoustic sensors were attached with pressure drop and plate weighing used for validation. Power and arrival time decreased strongly with fouling but changed depending on sensor location. Low-frequency waves demonstrated a good sensitivity to fouling according to Merheb et al. In future, power and delay measurements at different locations shall be made and help to understand mechanisms and kinetics of fouling.

Ultrasonic measurements are very sensitive to material and thickness changes and can be used non-invasively. These measurements may also be used to monitor cleaning success. But, ultrasonic parameters are temperature dependent and a temperature correction has to be included and most ultrasonic transducers monitor only one point of a heat exchanger if not multiple transducers are used.

3.4.2. *Quartz crystal microbalance (QCM)*

QCM is based on the crystal oscillator principle. It consists of a piezoelectric quartz oscillating at its resonant frequency which frequency changes Δf dependent on deposited material amount. Usually, Δf decreases when material is adsorbed (compare with Fig. 3). The mass absorbed per unit surface area Δm is linked with Δf via the Sauerbrey constant S and described with the Sauerbrey equation (Sauerbrey, 1959) with $\Delta m \ll m_Q$ (quartz mass)

$$\Delta m = S\Delta f \tag{12}$$

This equation does not hold if: a) the added mass is not rigidly deposited, b) it slips, or c) it is not deposited evenly. QCM in liquids is calibrated due to liquid viscosity and density with well-known masses (Langmuir–Blodgett films). The change in Δf of a QCM from air into liquid is proportional to the square root of the liquid's density–viscosity product (Kanazawa & Gordon, 1985).

An extension to QCM is measuring energy dissipation ΔD (quartz crystal microbalance with dissipation monitoring, QCM-D). ΔD of a signal is related with rigidity of the layer. Signal damping changes when a layer attaches and viscosity and elasticity can be derived. ΔD is determined when the driving power is turned off and the exponential decay of the signal is monitored. The dissipation factor D is determined via $D = 1/\pi f\tau$ with resonant frequency $\underline{f}$ and signal decay time τ. With QCM-D, the Sauerbrey equation (Eq. (12)) can be validated, swelling and hydration of a layer can be monitored, and visco-elasticity can be modelled.

QCM was used to investigate the removal of β-lactoglobulin and commercial skim milk powder from different surfaces (Murray & Deshaires, 2000). The quartz crystals were coated with gold and chromium to determine the surface effect on attachment and removal. Calibration was done in sucrose solutions with different concentrations. Changes of Δf due to viscosity changes were

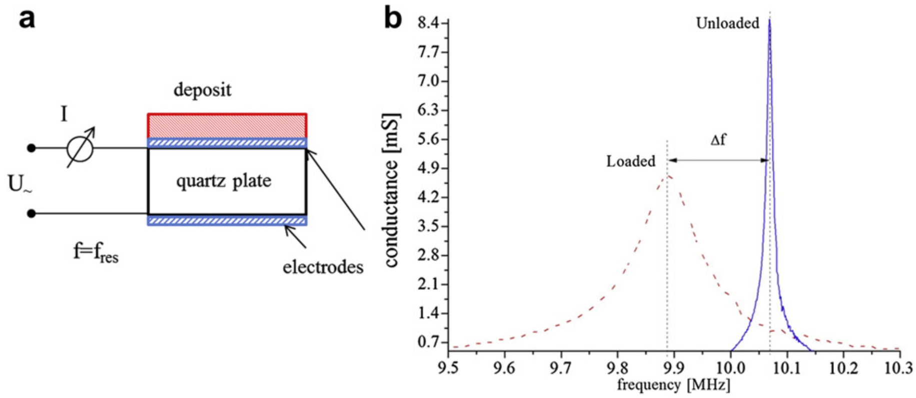

Fig. 3. QCM (a) and its frequency response (b) according to loading and no loading.

considered, Δf_V. With calibration constant k, Δm can be calculated with

$$\Delta m = k(\Delta f \sim \Delta f_V) \tag{13}$$

The setup of Murray and Deshaires was very sensitive to protein adsorption and desorption and to heating effects but it was difficult to link Δf to absorbed protein amount. Concentrated solutions led to thick, coherent films and more protein was adsorbed from skim milk compared with pure β-lactoglobulin.

QCM-D was applied to monitor the adsorption process of β-lactoglobulin on a polyethersulfone coated surface (Kim, Weber, Shin, Huang, & Liu, 2007). Energy dissipation takes place due to high visco-elastic properties of the protein layer. Atomic force microscopy imaged the protein layer showing that adsorption is randomly distributed. Fouling was found to increase with increasing protein amount, changed pH led to a decrease of protein amount. Δf and ΔD both changed rapidly when β-lactoglobulin was introduced. According to Kim et al., Δf depends on protein concentration and pH whereof ΔD and the visco-elastic behaviour depend only on protein concentration.

QCM and QCM-D is highly sensitive to material and thickness changes and the fouling kind can be investigated using QCM-D. Still, it is invasive and it has to be taken into account that the Sauerbrey equation has to be adapted to fouling material and deposition type present.

3.4.3. *Guided waves*

In contrast to conventional methods, guided waves travel alongside a structure not through it. Horizontal variation leads to signal reflection and amplitude changes. A tube is excited to oscillate in its resonance frequency and changes in frequency, velocity, and amplitude are determined. Wave excitation has to be controlled due to different oscillation modes (symmetric, non-symmetric). This can be done by mechanical impactors (hammer), piezoceramics, or piezopolymers. Symmetric reflection gives information about overall variations; mode conversion contains information about fouling extent. Fouling inside a pipe leads to a decrease in wave energy and signal arrival time. An initial lossless signal shows losses when fouling is present due to non-leakage modes in the layer.

A comb sensor with a piezopolymer (2.5 MHz) was developed to produce ultrasonic guided waves (Hay & Rose, 2003). It was applied to a stainless steel pipe and fouling was simulated using Crisco vegetable shortening at the pipe interior. The 4th longitudinal, axisymmetric mode of a Lamb wave ($L(0,4)$) was chosen displaying minimal radial and maximum axial displacement and high sensitivity to fouling. Measurements were made using longitudinal guided waves in transmission mode. Hay and Rose found that water loading did not change the amplitude strongly but an amplitude drop of 6 dB occurred with 1 mm fouling and will investigate the effect of different operating temperatures and piezopolymer ageing in future.

A piezoelectric ultrasonic transducer with 2.62 MHz was attached to a stainless steel pipe with specially designed Plexiglas angle beam shoes (Lohr & Rose, 2003). Measurements took place in transmission mode and a non-leaky S0 was used with tar as foulant showing amplitude decrease with fouling due to in-plane energy loss. The amplitude of longitudinal guided waves of the Lamb wave mode $L(0,5)$ decreased with fouling thickness. Guided waves seem to differentiate between different viscous materials (Lohr & Rose, 2003). For corrosion investigations an acoustic impact method was used with highly corroded pipes showing a strong velocity decrease (Lohr & Rose, 2003). Future work of the group shall improve sensor design, data analysis, and modelling.

Ultrasonic guided waves were used to detect fouling in duct systems (Silva, Silva, Lima, & Neto, 2008). The tubes became non-homogeneous causing non-stationary distortion with fouling. Wavelet transform (WT) was applied for analysis. It is a time-frequency method to analyse a signal in different frequency ranges by dilating and translating a mother wavelet monitoring inter alia energy distribution changes. Due to ultrasonic characteristics Daubechies 4 mother wavelets were chosen by Silva, Silva, et al. (2008). Results were analysed and 1st and 2nd scale of discrete WT was calculated. Fouling led to a decrease in energy spectrum due to signal leakage with thicknesses between 1 and 3 mm having the highest influence.

An electromagnetic displacement systems was used to control and to have reproducible excitations for hammer impact tests for fouling detection in tubes (Silva, Lima, Neff, & Neto, 2009; Silva, Lima, Neff, & Neto, 2010; Silva, Queiroz, Lima, Neff, & Neto, 2008). A commercial MEMS accelerometer was used as sensor showing an amplitude reduction and less signal duration time when fouling thickness increased (Silva, Queiroz, et al., 2008). Comparison with finite element simulations showed signal leakage in the layer. As detector for hammer impact tests, a microphone was applied (Silva et al., 2009). Resonance frequency shift and signal decay time were found to be a function of fouling thickness and resonance frequency, 1/e attenuation time, and associated amplitude decreased linearly with fouling thickness. Experiments done with oil processing plant supported the lab-scale results.

Guided waves are sensitive to material changes and different fouling layers and can be used not invasive. Cleaning of fouling can be monitored using leakage modes and monitor amplitude. Still, acoustic parameters are temperature dependent making it necessary to do temperature correlation.

4. Computational and numerical methods for fouling modelling and prediction

Heat exchanger design and fouling determination benefit from numerical methods which can be used to estimate fouling behaviour in a heat exchanger. For this, a model is usually built including parameters present in real heat exchangers. Parameter evolution with time is monitored when fouling is introduced. At the end, a modelled and a real heat exchanger are compared and the model can be adapted to real conditions and vice versa: parameters used in heat exchanger design can be changed if the fouling behaviour is improved.

The effect of fouling on heat transfer parameters was investigated numerically using ANSYS with incorporated tube geometry (Kaptan, Buyruk, & Ecder, 2008). Temperature, heat flux, and heat transfer coefficient were chosen and single and double layer fouling and Reynolds and Nusselt number were included. The equations for steady, laminar, incompressible flow with constant fluid properties were used.

$$\begin{aligned} \nabla \boldsymbol{v} &= 0 \\ \rho \boldsymbol{v} \nabla \boldsymbol{v} &= -\nabla p + \mu \nabla^2 \boldsymbol{v} \\ \rho c_\mathrm{p} \nabla T &= k \nabla^2 T \end{aligned} \tag{14}$$

with velocity v, density ρ, pressure p, dynamic viscosity μ, specific heat at constant pressure c_p, and temperature T. The parameters were compared with literature; concentric and eccentric tube geometries were modelled by Kaptan et al. (2008). Increasing fouling thickness reduced heat transfer which showed higher values in eccentric geometries. With double layer fouling (two layers with different heat conductivity) heat flux varied though heat transfer coefficients stayed nearly constant.

An offline method was derived to detect fouling in a cross-flow heat exchanger (Gudmundsson, Palsson, Palsson, & Lalot, 2009). They divided the heat exchanger in an equal number of sections on the hot and cold side and got model parameters with Kalman filtering. Temperatures represented the model state. Inlet and outlet temperature and mass flow of the hot and cold fluid were monitored using simulated data and reasonable accuracy and consistency of fouling determination was found by Gudmundsson et al. (2009). The researchers will include data from real heat exchangers and develop a more detailed model in future.

A non-linear physical state model for online detection of fouling in heat exchangers was applied (Jonsson, Lalot, Palsson, & Desmet, 2007). A cross-flow heat exchanger was split in cells and described with inlet and outlet temperatures and mass flow rates of hot and cold fluid which got using extended Kalman filtering. With parameter variation with time fouling was monitored online by Jonsson et al. (2007) using a sensitive method. Future work of the group aims on including other heat exchanger configurations, to compare the results with other models like ANN, and to include experimental data.

Another way to include intelligent methods in fouling detection is by using combinatorial decision making machines (ANN, support vector machines). Prior extracted parameters are fed into an ANN and used for fouling decision. An ANN is an emulation of a biological network connecting a setup of input vectors with a set of output vectors (Basheer & Hajmeer, 2000) with feed-forward multilayer perceptrons with an input, an output, and one or several hidden layers made of neurons with weights and transfer functions. Input can be measured parameters as well as modelling results (compare with Fig. 4). The ANN can model complex non-linear phenomena and helps in pattern recognition and controlling (Egmont-Petersen, de Ridder, & Handels, 2002; Mas & Flores, 2008) and can decide after training if a clean or a fouled heat exchanger is present.

Fouling presence in a PHE was estimated using an Adaline network (Riverol & Napolitano, 2005) with heat transfer coefficient as input parameter. Heat transfer over area was measured and fouling resistance was determined using the ANN and fouling thickness was calculated with fouling resistance. After the run it was compared with the measured thickness and found to be predicted reliable (Riverol & Napolitano, 2005). The developed method was independent on milk type because of regular ANN update with heat flux measurements.

Fouling in coal-fired utility boilers was monitored by heat flux measurements (Teruel, Cortés, Ignacio Díez, & Arauzo, 2005). A grey box ANN model was used including three kinds of network: one to predict the probability that activation of a neighbour sootblower is effective at current conditions, one to predict the increase of cleanliness of an occurrence at present conditions, and one to predict the heat flux meter evolution. Very simple feed-forward networks were applied making the computational effort efficient and the ANNs detected cleaning effectiveness correctly. After off-line training the grey box ANN model showed that real-time monitoring is possible (Teruel et al., 2005). Future work will include integration in a working plant to test longer periods of quality prediction, the development of a model for individual blowers, for fouling and cleaning, and of similar methods in other sections.

Fouling determination of a numerical and an ANN based method for a triple tube heat exchanger was compared (Lecoeuche et al., 2005). For the numerical way the heat exchanger was divided in

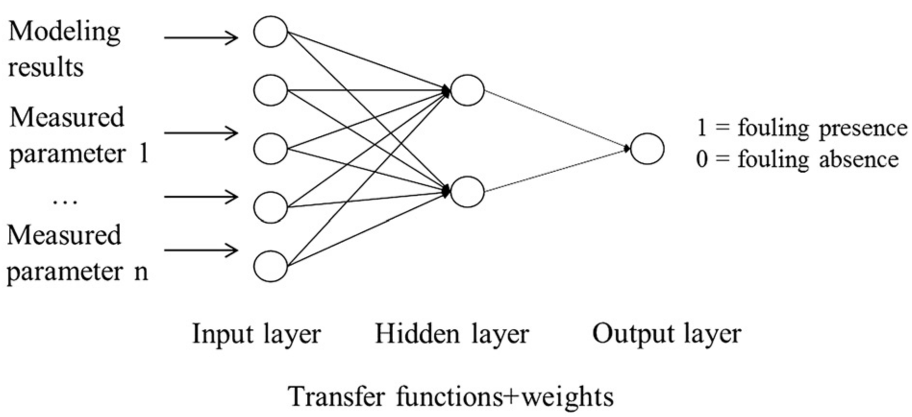

Fig. 4. Model for the task of a combinatorial method like an ANN. Different inputs can be included, computed and compared using weights and transfer functions and then give the result of fouling presence ("1") and fouling absence ("0").

N modules with inlet, outlet, outer surface temperature, and mass flow rate to calculate the outlet temperature. Changes due to fouling were detectable. Also, 50 local ANNs were coupled to include the time delay between inlet and outlet temperature. The numerical model and the coupled ANN showed comparable results with latter being significant faster (Lecoeuche et al., 2005). Next steps of Lecoeuche et al. shall consider variable mass flow for the inner fluid and other heat exchangers.

Fouling behaviour as function of time and position in a triple tube heat exchanger was predicted using hydrodynamics and heat balance concept (Sahoo, Ansari, & Datta, 2005). With local fouling rate, heated milk was simulated and fouling thickness was determined corresponding to Biot number. At the beginning of the simulation, a uniform fouling deposit was found by Sahoo et al. due to constant wall temperature. With growing time, fouling layer and Biot number increased towards the outlet and stabilised after time like expected.

ANNs with prior knowledge were included to determine independent parameters for fouling determination and to predict fouling resistance (Malayeri & Müller-Steinhagen, 2003, 2007b). An increase in error of predicting fouling resistance from 38% to 15% of was found comparing the ANN with a model from HTRI using Reynolds number, dimensionless time, and water quality as input (Malayeri & Müller-Steinhagen, 2003). The group also built an integrated model of NN with genetic algorithm (GA) to determine important variables in fouling determination of cooling water (Malayeri & Müller-Steinhagen, 2007b). Finding best combinations of input variables is a major problem in regression and non-parametric methods. GAs are used as search heuristic. The combination of GA and NN was tested with fouling data from $CaSO_4$ deposition during subcooled flow boiling with an error in training of 8.7% and in generalization phase of 13.5%.

Initial fouling deposition under pool boiling conditions of $CaSO_4$ was studied (Malayeri & Müller-Steinhagen, 2007a). As independent variables, heat flux and $CaSO_4$ concentration were chosen. Experiments took place in a test rig with an adjustable resistance band heater. An increase of heat flux increased the number of nucleation sites for fouling and big bubbles broke up into smaller ones. Increasing concentration led to lower heat transfer coefficient at constant heat flux due to increased supersaturation of solution resulting in bigger bubbles. To correlate experimental results, an ANN based on radial basis function with three neurons in the input layer and one hidden layer was used (Malayeri & Müller-Steinhagen, 2007a). The absolute error found was 8.7 % with higher accuracy for heat fluxes above 200 kW/m^2.

An advantage of numerical and computational methods is that they need no extra equipment but rely on measured or measurable parameters and can be very sensitive if appropriate models and parameters are employed. But if parameters or models are chosen wrongly or not appropriate (high) errors can occur and first results have to be validated with other methods.

5. Summary

An overview is given over different methods to detect and model fouling in heat exchangers. The conclusion is drawn that depending on the process and the requirements different methods may be more advantageous than others. Seeking a single method covering everything seems to be implausible. Rather, combination of different methods and switching between is more practical. The objectives may be besides others:

- Determination of exact place of fouling
- Determination of exact amount and/or thickness of fouling
- Determination of an overall value (fouling presence/absence)
- Monitoring and adapting of cleaning process (cleaning for how long?)
- Monitoring of fouling development (when does it start?, when is it gone?)

A combination of different methods may enhance both detection stability and the probability to reach the objectives. The first step is to determine the goals and the detection limit of the methods, and to know the fouling type(s) which may be present. It is important for industry to have a non-invasive, fast, reliable, robust and not expensive method. Several presented methods are non-invasive but cannot easily be applied to existing heat exchangers. Others are very sensitive and invasive but could be included in new heat exchangers. Thus, the different methods according to their applicability are summarised:

Table 2
Comparison of different detection methods together with their advantages and limitations.

Method	Short description	Advantages	Limitations
Pressure drop	Pressure between inlet and outlet measured	No extra equipment Usually measured Caution of excessive pressures	Not very sensitive More sensitive for PHE Fouling place unknown
Temperature	Product outlet/heating medium temperature measured	No extra equipment Usually measured	Not very sensitive Thin layers not monitored Fouling place unknown
Heat transfer parameters	Heat flux, heat transfer coefficient, thermal resistance measured	No extra equipment (despite heat flux) Flow/temperature usually measured	Certain thickness necessary Heat flux sensors not usable at high temperatures
Electrical parameters	Electrical resistance, conductivity measured Electrical behaviour of heater monitored	Very sensitive to thin layers Fouling thickness determinable	Invasive Electrical heating not popular
Acoustic/Ultrasound/QCM/QCM-D	Acoustic parameters measured Frequency change and energy dissipation monitored	Non-invasive Very sensitive to material changes, thin fouling Fouling and cleaning monitored Movable clamp-on sensor	Scattering can occur Parameters temperature dependent One transducer: only one point monitored QCM/QCM-D invasive
Numerical methods/ANN	Clean/fouled heat exchangers modelled Parameters combined in ANN	No extra equipment Very sensitive when appropriate parameters and models used	Due to parameters errors may occur First, validation with other methods necessary

- If the main task is to determine fouling presence (thick layers), pressure drop and product outlet or heating temperature is sufficient.
- If information about place and fouling amount and a sensitive method is wanted, monitoring of heat transfer parameters can be done.
- If electrical heating is applied, monitoring of heater performance helps to determine fouling presence, amount, and very thin layers.
- If the presence or absence of thin fouling layers is wanted to control e.g. cleaning better or if the fouling type is of interest, acoustic methods are suitable. All presented methods are very sensitive to these parameters. Dependent on sensor type only selected positions may be investigated but well-chosen places minimise this disadvantage. Guided waves and nanovibrations give a broader view. Acoustic parameters are temperature dependent thus temperature correction has to be included. QCM and QCM-D has to be implemented in the heat exchanger but is very sensitive to very thin layers and mechanical properties.
- If help in the decision process if a heat exchanger is fouled and how long cleaning shall take place is needed numerical methods or simulations are useful. Determined parameters of other measurements can be included and decisions of fouling presence can be made. Numerical investigations may help to improve heat exchanger design.

The process where fouling and/or cleaning is monitored as well as user demands are the main influence on which method is suitable. A short overview about advantages, limitations, and possibly fields of application of the presented methods is given in Table 2.

It is not easy to find a suitable method to monitor fouling (and cleaning) in closed systems where a variety of conditions have to be considered. The huge variance of methods makes it possible to find a suitable procedure. In future, it seems good to combine different approaches and to include numerical methods because dependent on the objectives it will be easier to adapt to changing process parameters and to enhance product quality.

References

Astorga-Zaragoza, C. M., Zavala-Río, A., Alvarado, V. M., Méndez, R. M., & Reyes-Reyes, J. (2007). Performance monitoring of heat exchangers via adaptive observers. *Measurement, 40*(4), 392–405.

Ayadi, M. A., Bénézech, T., Chopard, F., & Berthou, M. (2008). Thermal performance of a flat ohmic cell under non-fouling and whey protein fouling conditions. *LWT – Food Science and Technology, 41*(6), 1073–1081.

Ayadi, M. A., Leuliet, J. C., Chopard, F., Berthou, M., & Lebouché, M. (2004). Continuous ohmic heating unit under whey protein fouling. *Innovative Food Science & Emerging Technologies, 5*(4), 465–473.

Balasubramanian, S., & Puri, V. M. (2010, June 20–23). Fouling of food processing equipment – critical review. Paper presented at the *ASABE 10 annual international meeting*.

Bamberger, J. A., & Greenwood, M. S. (2004). Non-invasive characterization of fluid foodstuffs based on ultrasonic measurements. *Food Research International, 37*(6), 621–625.

Bansal, B., & Chen, X. D. (2006). A critical review of milk fouling in heat exchangers. *Comprehensive Reviews in Food Science and Food Safety, 5*(2), 27–33.

Basheer, I. A., & Hajmeer, M. (2000). Artificial neural networks: fundamentals, computing, design, and application. *Journal of Microbiological Methods, 43*(1), 3–31.

Blanpain, P., & Lalande, M. (1997). Investigation of fouling mechanisms governing permeate flux in the crossflow microfiltration of beer. *Filtration & Separation, 34*(10), 1065–1069.

Bohnet, M. (1987). Fouling of heat transfer surfaces. *Chemical Engineering & Technology – CET, 10*(1), 113–125.

Bott, T. R. (1995). *Fouling of heat exchangers*. Elsevier Science & Technology Books.

Bott, T. R. (1997). Aspects of crystallization fouling. *Experimental Thermal and Fluid Science, 14*(4), 356–360.

Burton, H. (1961). A laboratory method for the investigation of milk deposits on heat exchanger surfaces. *Journal of Dairy Research, 28*(3), 255–263.

Burton, H. (1968). Section G. Deposits from whole milk in heat treatment plant – a review and discussion. *Journal of Dairy Research, 35*(2), 317–330.

Butterworth, D. (2002). Design of shell-and-tube heat exchangers when the fouling depends on local temperature and velocity. *Applied Thermal Engineering, 22*(7), 789–801.

Changani, S. D., Belmar-Beiny, M. T., & Fryer, P. J. (1997). Engineering and chemical factors associated with fouling and cleaning in milk processing. *Experimental Thermal and Fluid Science, 14*(4), 392–406.

Chen, X. D., Li, D. X. Y., Lin, S. X. Q., & Özkan, N. (2004). On-line fouling/cleaning detection by measuring electric resistance-equipment development and application to milk fouling detection and chemical cleaning monitoring. *Journal of Food Engineering, 61*(2), 181–189.

Chew, J. Y. M., Paterson, W. R., & Wilson, D. I. (2004). Fluid dynamic gauging for measuring the strength of soft deposits. *Journal of Food Engineering, 65*(2), 175–187.

Chew, J. Y. M., Paterson, W. R., & Wilson, D. I. (2007). Fluid dynamic gauging: a new tool to study deposition on porous surfaces. *Journal of Membrane Science, 296*(1–2), 29–41.

Chung, C.-W., Popovics, J. S., & Struble, L. J. (2010). Using ultrasonic wave reflection to measure solution properties. *Ultrasonics Sonochemistry, 17*(1), 266–272.

Corrieu, G., Lalande, M., & Ferret, R. (1986). Mesure en ligne de l'encrassement et du nettoyage d'un sterilisateur UHT industriel. *Journal of Food Engineering, 5*(3), 231–248.

Czekaj, P., López, F., & Güell, C. (2000). Membrane fouling during microfiltration of fermented beverages. *Journal of Membrane Science, 166*(2), 199–212.

Davies, T. J., Henstridge, S. C., Gillham, C. R., & Wilson, D. I. (1997). Investigation of whey protein deposit properties using heat flux sensors. *Food and Bioproducts Processing, 75*(2), 106–110.

de Jong, P., te Giffel, M. C., Straatsma, H., & Vissers, M. M. M. (2002). Reduction of fouling and contamination by predictive kinetic models. *International Dairy Journal, 12*(2–3), 285–292.

de Jong, P., Waalewijn, R., & van der Linden, H. J. L. J. (1993). Validity of a kinetic fouling model for heat-treatment of whole milk. *Lait, 73*, 293–302.

Deshvannar, U. B., Rafeen, M. S., Ramasamy, M., & Subbaro, D. (2010). Crude oil fouling – a review. *Journal of Applied Science, 10*, 3167–3174.

Egmont-Petersen, M., de Ridder, D., & Handels, H. (2002). Image processing with neural networks-a review. *Pattern Recognition, 35*(10), 2279–2301.

Ferrando, M., Rozek, A., Zator, M., López, F., & Güell, C. (2005). An approach to membrane fouling characterization by confocal scanning laser microscopy. *Journal of Membrane Science, 250*(1–2), 283–293.

Fryer, P. J., & Asteriadou, K. (2009). A prototype cleaning map: a classification of industrial cleaning processes. *Trends in Food Science & Technology, 20*(6–7), 255–262.

Greenwood, M. S. (2009). Self-calibrating measurements of the density and velocity of sound from the reflection of ultrasound at two solid–liquid interfaces. *POMA, 6*(1), 045003–045011.

Greenwood, M. S., Adamson, J. D., & Bond Leonard, J. (2006). Measurement of the viscosity–density product using multiple reflections of ultrasonic shear horizontal waves. *Ultrasonics, 44*(Suppl. 1), e1031–e1036.

Grijspeerdt, K., Mortier, L., De Block, J., & Van Renterghem, R. (2004). Applications of modelling to optimise ultrahigh temperature milk heat exchangers with respect to fouling. *Food Control, 15*(2), 117–130.

Gudmundsson, O., Palsson, O. P., Palsson, H., & Lalot, S. (2009). Fouling detection in a cross-flow heat exchanger based on physical modeling. Paper presented at the *Proceedings of international conference on heat exchanger and fouling and cleaning VIII – 2009*.

Guérin, R., Ronse, G., Bouvier, L., Debreyne, P., & Delaplace, G. (2007). Structure and rate of growth of whey protein deposit from in situ electrical conductivity during fouling in a plate heat exchanger. *Chemical Engineering Science, 62*(7), 1948–1957.

Hay, T. R., & Rose, J. L. (2003). Fouling detection in the food industry using ultrasonic guided waves. *Food Control, 14*(7), 481–488.

Ingumundardottir, H., & Lalot, S. (2009). Detection of fouling in a cross-flow heat exchanger using wavelets. Paper presented at the *Proceedings of international conference on heat exchanger and fouling and cleaning VIII – 2009*.

Jonsson, G. R., Lalot, S., Palsson, O. P., & Desmet, B. (2007). Use of extended Kalman filtering in detecting fouling in heat exchangers. *International Journal of Heat and Mass Transfer, 50*(13–14), 2643–2655.

Kanazawa, K. K., & Gordon, J. G. (1985). Frequency of a quartz microbalance in contact with liquid. *Analytical Chemistry, 57*(8), 1770–1771.

Kaptan, Y., Buyruk, E., & Ecder, A. (2008). Numerical investigation of fouling on cross-flow heat exchanger tubes with conjugated heat transfer approach. *International Communications in Heat and Mass Transfer, 35*(9), 1153–1158.

Kim, Weber, N., Shin, G., Huang, Q., & Liu, S. (2007). The study of β-lactoglobulin adsorption on polyethersulfone thin film surface using QCM-D and AFM. *Journal of Food Science, 72*(4), E214–E221.

Kujundzic, E., Cobry, K., Greenberg, A. R., & Hernandez, M. (2008). Use of ultrasonic sensors for characterization of membrane fouling and cleaning. *Journal of Engineered Fibers and Fabrics, Special Issue*, 35–44.

Kujundzic, E., Fonseca, C. A., Evans, E. A., Peterson, M., Greenberg, A. R., & Hernandez, M. (2007). Ultrasonic monitoring of earlystage biofilm growth on polymeric surfaces. *Journal of Microbiological Methods, 68*(3), 458–467.

Laine, J. M., Campos, C., Baudin, I., & Janex, M. L. (2003). Understanding membrane fouling: a review of over a decade of research. *Water Supply, 3*(5–6).

Lecoeuche, S., Lalot, S., & Desmet, B. (2005). Modelling a non-stationary single tube heat exchanger using multiple coupled local neural networks. *International Communications in Heat and Mass Transfer, 32*(7), 913–922.

Ling, A. C., & Lund, D. B. (1978). Apparatus for studying fouling of heated surfaces by biological fluids. *Journal of Food Science, 43*, 390–393.
Lohr, K. R., & Rose, J. L. (2003). Ultrasonic guided wave and acoustic impact methods for pipe fouling detection. *Journal of Food Engineering, 56*(4), 315–324.
Malayeri, M. R., & Müller-Steinhagen, H. (2003). Analysis of fouling data based on prior knowledge. Paper presented at the *2003 ECI conference on heat exchanger fouling and cleaning: fundamentals and applications*.
Malayeri, M. R., & Müller-Steinhagen, H. (2007a). Initiation of $CaSO_4$ scale formation on heat transfer surfaces under pool boiling conditions. *Heat Transfer Engineering, 28*(3), 240–247.
Malayeri, M. R., & Müller-Steinhagen, H. (2007b). Intelligent discrimination model to identify influential parameters during crystallisation fouling. Paper presented at the *7th International conference on heat exchanger fouling and cleaning – Challenges and opportunities*.
Martin, H. (2002). The generalized Lévêque equation and its practical use for the prediction of heat and mass transfer rates from pressure drop. *Chemical Engineering Science, 57*(16), 3217–3223.
Mas, J. F., & Flores, J. J. (2008). The application of artificial neural networks to the analysis of remotely sensed data. *International Journal of Remote Sensing, 29*(3), 617–663.
Merheb, B., Nassar, G., Nongaillard, B., Delaplace, G., & Leuliet, J. C. (2007). Design and performance of a low-frequency non-intrusive acoustic technique for monitoring fouling in plate heat exchangers. *Journal of Food Science, 82*, 518–527.
Müller-Steinhagen, H., Hartnett, J. P., Irvine, T. F., Jr., Cho, Y. I., & Greene, G. A. (1999). *Cooling-water fouling in heat exchangers* (pp. 415–496)In *Advances in heat transfer, Vol. 33*. Elsevier.
Murray, B. S., & Deshaires, C. (2000). Monitoring protein fouling of metal surfaces via a quartz crystal microbalance. *Journal of Colloid and Interface Science, 227*(1), 32–41.
Nema, P. K., & Datta, A. K. (2005). A computer based solution to check the drop in milk outlet temperature due to fouling in a tubular heat exchanger. *Journal of Food Engineering, 71*(2), 133–142.
Nema, P. K., & Datta, A. K. (2006). Improved milk fouling simulation in a helical triple tube heat exchanger. *International Journal of Heat and Mass Transfer, 49*(19–20), 3360–3370.
Pereira, A., Mendes, J., & Melo, L. F. (2008). Using nanovibrations to monitor biofouling. *Biotechnology and Bioengineering, 99*(6), 1407–1415.
Pereira, A., Mendes, J., & Melo, L. F. (2009). Monitoring cleaning-in-place of shampoo films using nanovibration technology. *Sensors and Actuators B: Chemical, 136*(2), 376–382.
Pereira, A., Rosmaninho, R., Mendes, J., & Melo, L. F. (2006). Monitoring deposit build-up using a novel mechatronic surface sensor (MSS). *Food and Bioproducts Processing, 84*(4), 366–370.
Perez, L., Ladevie, B., Tochon, P., & Batsale, J. C. (2009). A new transient thermal fouling probe for cross flow tubular heat exchangers. *International Journal of Heat and Mass Transfer, 52*(1–2), 407–414.
Petermeier, H., Benning, R., Becker, T., & Delgado, A. (2003). Numero-fuzzy hybrid for modelling and simulation of the fouling of milk heat exchangers. *PAMM, 3*(1), 470–471.
Petermeier, H., Benning, R., Delgado, A., Kulozik, U., Hinrichs, J., & Becker, T. (2002). Hybrid model of the fouling process in tubular heat exchangers for the dairy industry. *Journal of Food Engineering, 55*(1), 9–17.
Prakash, S., Datta, N., & Deeth, H. C. (2005). Methods of detecting fouling caused by heating milk. *Food Reviews International Dairy Journal, 21*, 267–293.
Riverol, C., & Napolitano, V. (2005). Estimation of fouling in a plate heat exchanger through the application of neural networks. *Journal of Chemical Technology & Biotechnology, 80*(5), 594–600.
Sahoo, P. K., Ansari, I. A., & Datta, A. K. (2005). Milk fouling simulation in helical triple tube heat exchanger. *Journal of Food Engineering, 69*(2), 235–244.
Sauerbrey, G. (1959). Verwendung von Schwingquarzen zur Wägung dünner Schichten und zur Mikrowägung. *Zeitschrift für Physik A: Hadrons and Nuclei, 155*(2), 206–222.
Silva, J., Lima, A., Neff, F. H., & Neto, J. S.d. R. (2009). Non-invasive fast detection of internal fouling layers in tubes and ducts by acoustic vibration analysis. *IEEE Transactions on Instrumentation and Measurement, 58*(1), 108–114.
Silva, J., Lima, A. M., Neff, H., & Neto, J. S. R. (2010). Vibration analysis based on Hammer impact for fouling detection using microphone and accelerometers as sensors. *Sensors and Transducers Journal, 112*(1), 10–23.
Silva, J., Queiroz, I. B., Lima, A. M., Neff, F. H., & Neto, J. S. R. (2008). Vibration analysis for fouling detection using hammer impact test and finite element simulation. Paper presented at the *Instrumentation and measurement technology conference proceedings, 2008 (IMTC 2008), IEEE*.
Silva, J., Silva, K. M., Lima, A., & Neto, J. (2008). Fouling detection based on analysis of ultrasonic guided waves using wavelet transform. Paper presented at the *Industrial electronics, 2008 (ISIE 2008), IEEE international symposium*.
Simões, M., Simões, L. C., & Vieira, M. J. (2010). A review of current and emergent biofilm control strategies. *LWT – Food Science and Technology, 43*(4), 573–583.
Teruel, E., Cortés, C., Ignacio Díez, L., & Arauzo, I. (2005). Monitoring and prediction of fouling in coal-fired utility boilers using neural networks. *Chemical Engineering Science, 60*(18), 5035–5048.
Tissier, J. P., & Lalande, M. (1986). Experimental device and methods for studying milk deposit formation on heat exchange surfaces. *Biotechnology Progress, 2*(4), 218–229.
Tlili, M. M., Rousseau, P., Ben Amor, M., & Gabrielli, C. (2008). An electrochemical method to study scaling by calcium sulphate of a heat transfer surface. *Chemical Engineering Science, 63*(3), 559–566.
Visser, J., & Jeurnink, T. J. M. (1997). Fouling of heat exchangers in the dairy industry. *Experimental Thermal and Fluid Science, 14*(4), 407–424.
Wallhäußer, E., Hussein, W. B., Hussein, M. A., Hinrichs, J., & Becker, T. M. (2011). On the usage of acoustic properties combined with an artificial neural network – a new approach of determining presence of dairy fouling. *Journal of Food Engineering, 103*(4), 449–456.
Watkinson, A. P., & Wilson, D. I. (1997). Chemical reaction fouling: a review. *Experimental Thermal and Fluid Science, 14*(4), 361–374.
Withers. (1996). Ultrasonic, acoustic and optical techniques for the non-invasive detection of fouling in food processing equipment. *Trends in Food Science & Technology, 7*(9), 293–298.
Withers, P. (1994). Ultrasonic sensor for the detection of fouling in UHT processing plants. *Food Control, 5*(2), 67–72.

5.2.2. "On the usage of acoustic properties combined with an artificial neural network - A new approach of determining presence of dairy fouling", E. Wallhäußer, W.B. Hussein, M.A. Hussein, J. Hinrichs, T. Becker; Journal of Food Engineering 103 (2011), 449-456

Journal of Food Engineering 103 (2011) 449–456

Contents lists available at ScienceDirect

Journal of Food Engineering

journal homepage: www.elsevier.com/locate/jfoodeng

On the usage of acoustic properties combined with an artificial neural network – A new approach of determining presence of dairy fouling

Eva Wallhäußer[a,*], Walid B. Hussein[a], Mohamed A. Hussein[a], Jörg Hinrichs[b], Thomas M. Becker[a]

[a] (Bio-)Process Technology and Process Analysis, Life Science Engineering, Technische Universitaet Muenchen, Weihenstephaner Steig 20, 85354 Freising, Germany
[b] Animal Foodstuff Technology, Institute for Foodscience and Biotechnology, University of Hohenheim, Garbenstr. 21, 70599 Stuttgart, Germany

ARTICLE INFO

Article history:
Received 16 September 2010
Received in revised form 3 November 2010
Accepted 9 November 2010
Available online 16 November 2010

Keywords:
Ultrasound
Dairy fouling
ANN
Acoustic parameters
Pattern recognition

ABSTRACT

Fouling and cleaning in heat exchangers are severe and costly issues in food processing. In this study, a new pattern recognition method for detecting fouling on stainless steel is presented. It is based on a combination of ultrasonic parameters and a multilayer perceptron feed forward neural network. Chosen acoustic parameters change significantly with fouling compared with tap water as standard. When fouling is present echo energy of echo 2 increases up to 73.84%, characteristic acoustic impedance shows 1.802 ± 0.169 MRayl (17.54% higher than impedance for water), and logarithmic decrement seems to decrease. These acoustic parameters have been combined in an artificial neural network (ANN) with one hidden layer and back propagation algorithm to disentangle error proneness of single parameters and increase detection stability. After training with 400 and validation of 250 of 1000 samples, the ANN displayed an accuracy of 98.58% for fouling presence/absence.

1. Introduction

Milk is heated to extend shelf life and reduce microbiological hazards. Heating above 70 °C induces protein denaturation and agglomeration on heat transfer areas and results in fouling type A (protein fouling), a soft, spongy, white deposit consisting mostly of β-lactoglobulin and salt (Fig. 1) (Burton, 1968; Visser and Jeurnink, 1997). This accumulation increases heat transfer resistance, decreases thermal efficiency of heating equipment, and increases production costs (Bansal and Chen, 2006). Fouling deposition is influenced by various parameters like Reynolds number, surface characteristics, salt, and pH (Belmar-Beiny et al., 1993; Fryer and Belmar-Beiny, 1991; Law and Leaver, 2000; McKenzie and Sawyer, 1967; Pelegrine et al., 2007; Premathilaka et al., 2007; Rosmaninho et al., 2005, 2007). In particular, influence of pH and salts has been studied extensive during the last few years by various groups (Krebs et al., 2009; Renard et al., 1998; Unterhaslberger et al., 2006). It has been found that Ca^{2+} seems to screen β-lactoglobulin surface charge and that the effect of salts on deposition changes with pH (Haug et al., 2009; Simons et al., 2002; Smith and Rose, 1994; Yüksel and Erdem, 2005). Besides, it remains still unclear in which order dairy protein fouling is deposited (Changani et al., 1997). It is assumed that deposition starts with an induction layer but it is unknown if this layer is composed primarily of salts or protein even though usually salt is found as the undermost layer (Bansal and Chen, 2006). Rosmaninho and Melo (2008) proposed different kinds of deposition for SMUF (simulated milk ultrafiltrate) which depend on surface energy and temperature. The results obtained are not easily transferred to milk because it is more complex than SMUF. For measuring readily developed fouling, different methods are developed: Astorga-Zaragoza et al. (2007), Davies et al. (1997) and Truong et al. (2002) e.g. used heat flux measurements. Chen et al. (2004) measured thermal and electrical resistance to detect fouling extent. In contrast, Pereira et al. (2008, 2009) applied nano-vibrations to determine removal of shampoo films. As drawback, most of these methods are not very sensitive or hardly usable in heat exchangers.

Ultrasound has been chosen as sensitive and non-destructive measuring method. In food processes, it has been applied to monitor sucrose and ethanol concentration (Resa et al., 2005; Schoeck et al., 2010) and to detect foreign bodies (Hæggström and Luukkala, 2001; Leemans and Destain, 2009). Ultrasound has been used to detect membrane fouling (Li et al., 2006; Marselina et al., 2009) and Withers (1994) employed it to measure fouling thickness. In this paper, acoustic parameters which are sensitive to changes on heat transfer area are chosen. These are echo energies of first two echoes, signal damping, and characteristic acoustic impedance. To enhance detection stability and develop a pattern recognition method, these parameters are combined in an artificial neural network (ANN).

An ANN is an emulation of a biological network which can establish almost any relationship among data by building models between a set of input and output vectors (Basheer and Hajmeer, 2000). Usually, a feed-forward multilayer perceptron with an

* Corresponding author. Tel.: +49 (0)8161 71 2623; fax: +49 (0)8161 71 3883.
E-mail address: e.wallhaeusser@wzw.tum.de (E. Wallhäußer).

0260-8774/$ - see front matter © 2010 Elsevier Ltd. All rights reserved.
doi:10.1016/j.jfoodeng.2010.11.015

Nomenclature

α	damping coefficient
a	neuron output
A (V)	amplitude
c (m/s)	sound velocity
δ (m)	distance
d (m)	distance
E (J)	energy
E_{kin} (J)	kinetic energy
E_{pot} (J)	potential energy
I	intensity
I_i	incident intensity
I_r	reflected intensity
K	damping ratio
l (m)	length
Λ	logarithmic decrement
m	slope
n	output of transfer function
n	number of pulses
p (Pa)	pressure
ρ (kg/m^3)	density
r	reflection coefficient
R	reflectivity
SMUF	simulated milk ultrafiltrate
t (s)	time
T (s)	time
TOF (s)	time of flight
v (m/s)	particle velocity
Z (Rayl = kg/(m^2 s))	acoustic impedance

Subscripts

i, n	counter
s	sample
ss	stainless steel
w	water
0	initial value

input, one or several hidden, and an output layer consisting of various neurons is used. ANNs are preferred where traditional models fail like in modelling complex phenomena with non-linear relationships. They have been applied in image processing, pattern recognition, and pest detection (Egmont-Petersen et al., 2002; Hussein et al., 2010; Mas and Flores, 2008). ANNs have also been used in monitoring and predicting fouling in boilers (Teruel et al., 2005) and in designing cleaning in place in plate heat exchangers (Riverol and Napolitano, 2005).

The focus in this study lies on the development of a pattern recognition method which uses a combination of carefully chosen acoustic parameters and an ANN to detect presence and absence of dairy fouling on stainless steel. Initially, ultrasonic experiments have been made from which a set of five acoustic parameters has been extracted together with information about fouling presence/absence. These parameters changed significantly with fouling. Then, they have been implemented in an ANN with back propagation algorithm with five neurons in the input, two neurons in one hidden, and one neuron in the output layer displaying "0" for fouling absence and "1" for fouling presence. Hence, a stable pattern recognition method has been developed.

2. Materials and methods

2.1. Experimental setup

The experimental setup consists of a acryl glass container, two stainless steel lids, and a self-built ultrasonic transducer with a PZT-ceramic (Noliac, center frequency 2 MHz). A fast Fourier transform (FFT) with rectangular windowing and sampling interval of 0.04 of one reflection has been applied in Origin displaying a center frequency of 2.13 ± 0.34 MHz (Fig. 2b). An in-house electronic with a sampling frequency of 40 ns and 20 V excitation voltage is used. Tap water has been chosen as reference and measured because it is used in cleaning and has well known properties (e.g. Marczak, 1997).

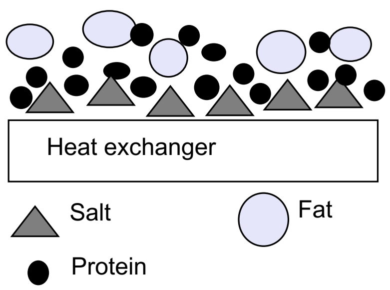

Fig. 1. Schematic of protein fouling.

As acoustic parameters, energies of echo 1 and 2, signal damping and characteristic acoustic impedance at the interface stainless steel–probe chamber have been chosen (Fig. 3a–c).

2.2. Fouling procedure

The setup has been filled with ca. 50 g of reconstituted milk made from skim milk powder (34% protein, 7.2–8.2% ash). The reconstituted milk showed a pH of between 6.5 and 6.9. The milk protein content varied (2–9%) and milk has been heated to 90 ± 1 °C for 90 ± 5 min to produce fouling (see Table 1). Then, waste milk has been poured out and the fouled setup has been cooled to 25 ± 1 °C. After filling with water, the ultrasonic transducer has been attached to the stainless steel lid with fouling (see Fig. 2a) using an oil-based coupling gel (Sonatest) and measurements were made in pulse-echo mode under static conditions. Experiments on five different days took place with 30 measurements per protein content and day.

2.3. Energy calculation

Acoustic energy E can be calculated by summing kinetic E_{kin} and potential energy E_{pot}. Sound energy in a fluid is then given by $E = E_{pot} + E_{kin} = \frac{p^2}{2\rho_0 c^2} + \frac{\rho_0 v^2}{2}$ with p as sound pressure, ρ_0 as initial density, c as sound velocity, and v as particle velocity. Because echo energy is wanted, the integral over intensity I in an echo is calculated. As boundaries, starting time t_1 (start of echo) and ending time t_2 (intensity indistinguishable from noise) are chosen (see Fig. 4):

$$E = \int_{t_1}^{t_2} I dt \qquad (1)$$

The energy depends on the material the signal travels through and on reflection and transmission coefficients at interfaces. Energy $E1$ is the energy from echo 1 prior entering the chamber,

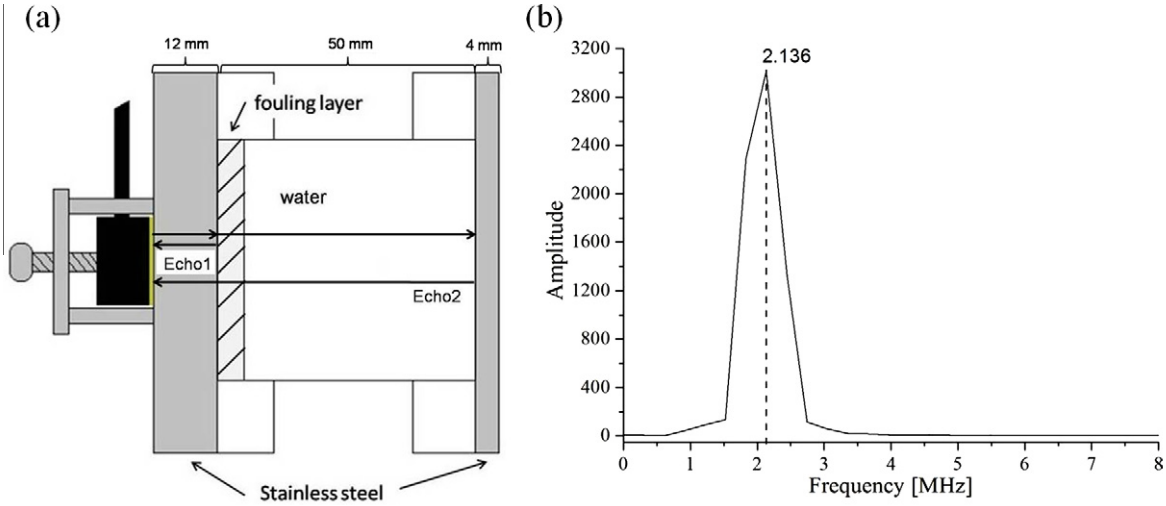

Fig. 2. (a) An ultrasonic wave is partly reflected at the interface wall–probe chamber (echo 1), partly transmitted. After travelling through the chamber it is reflected at the interface chamber–back wall (echo 2). (b) FFT of one ultrasonic reflection displaying a center frequency of 2.13 ± 0.34 MHz.

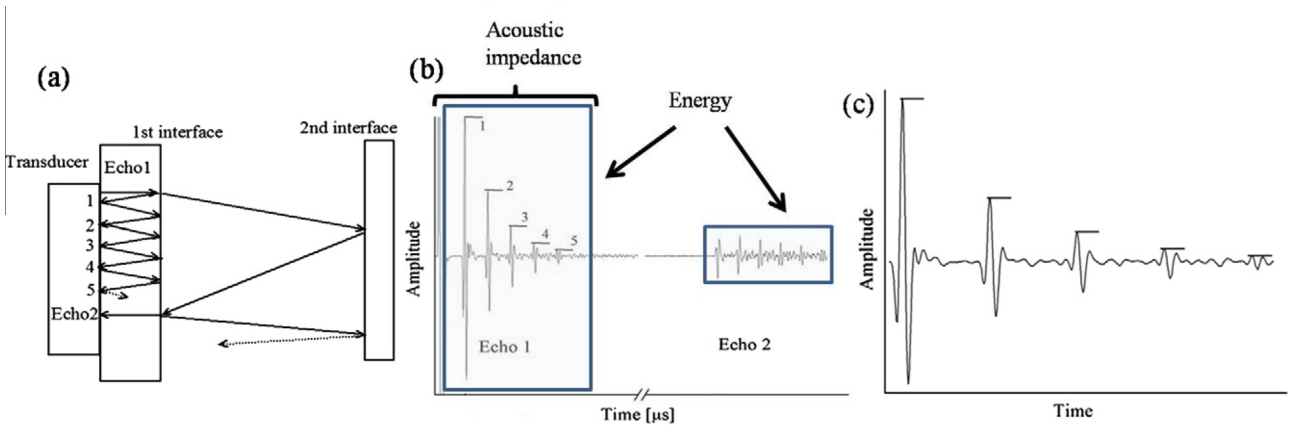

Fig. 3. (a) An echo is the reflected signal at an interface. It consists of several reflections in the wall. (b) For acoustic impedance, succeeding reflections of echo 1 are used, for energy, echo 1 and 2 is integrated. (c) Damping is calculated by logarithmising and fitting succeeding reflections in echo 1.

Table 1
Protein content in reconstituted milk, heating temperature and time for fouling production.

Protein content (%)	Temperature (°C)	Heating time (min)
0 (water)	–	–
2	90	90
3	90	90
6	90	90
9	90	90

E2 is the energy from echo 2 after travelling through the chamber. For both *E1* and *E2* attenuation in the stainless steel wall and for *E2* in water is negligible for frequencies and temperatures used here. Energy *E1* depends mostly on reflection and transmission coefficients at the first interface. These are governed by material properties at this interface with similar materials resulting in low reflection and high transmission and differing materials showing higher reflection and low transmission. For *E2*, material properties in the chamber play an important role, in particular attenuation in a fouling layer and scattering by air bubbles and uneven fouling layers.

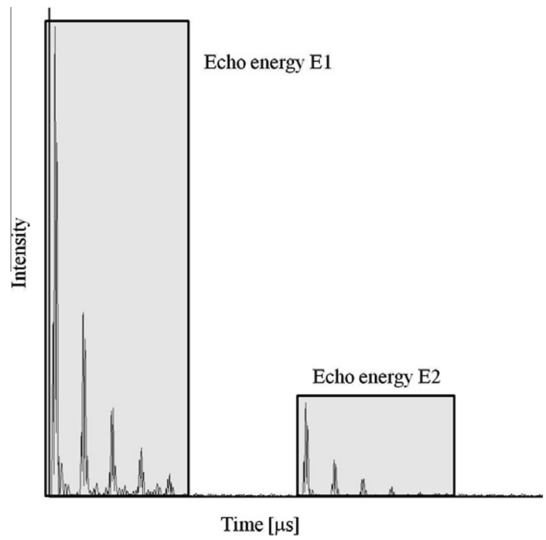

Fig. 4. Echo energy *E1* and *E2*.

2.4. Determination of logarithmic decrement

Signal damping at the interface prior entering the probe chamber has been chosen because it depends on material properties at this interface. It can be determined via comparing incident I_i and reflected intensity I_r. The signal is damped by a damping factor α after travelling a distance d, $I_r = I_i \exp(-\alpha d)$. Incident intensity is unknown thus logarithmic decrement Λ is used. It displays the ratio between successive peaks of the amplitudes A_n and A_{n+1} differing by one oscillation period $(t + T)$ with constant damping ratio K:

$$K = \frac{A_n}{A_{n+1}} = \frac{A(t)}{A(t+T)} = \exp(\delta T) \Rightarrow \Lambda = \ln \exp(\delta T) = \delta T \tag{2}$$

Logarithmised amplitudes are plotted against number of amplitude and fit linear where slope m resembles Λ (see Fig. 5). Here, the signal has been squared and intensities of consecutive reflections have been logarithmised. Least square regression took place to determine the slope which is twice Λ because intensity is used. Due to signal variations, Λ is calculated twice: one with all intensities and another one excluding intensities with a residuum higher than standard error.

2.5. Determination of characteristic acoustic impedance

Characteristic acoustic impedance Z is a measure for the resistance a medium opposes to a travelling sound wave. With density ρ and sound velocity c at one temperature in the far field of a sound source it can be calculated with $Z = \rho \cdot c$. When ρ and c are unknown Z_2 at an interface can be obtained via reflection coefficient r and reference impedance Z_1.

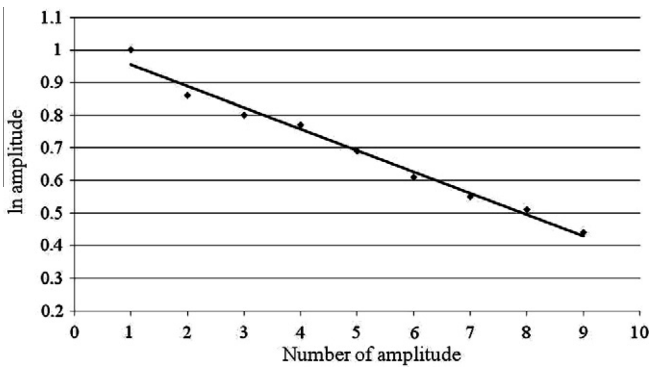

Fig. 5. Amplitude is logarithmised and fit over number with slope m as logarithmic decrement Λ.

$$Z_2 = Z_1 \cdot \left(\frac{1-r}{1+r}\right) \tag{3}$$

An ultrasonic signal can be described as n consecutive amplitudes $A_{1,\ldots,n}$ with incident amplitude A_0, reflection coefficient at interface transducer-wall r_1, reflection coefficient at interface wall-chamber r_2, attenuation coefficient α, and wall thickness l.

$$\begin{aligned} A_1 &= A_0 \cdot r_2 \cdot \exp(-2\alpha_1 \cdot l_1) \\ A_2 &= A_0 \cdot r_2^2 \cdot r_1 \cdot \exp(-4\alpha_1 \cdot l_1)\ldots \\ A_n &= A_0 \cdot r_2^n \cdot r_1^{n-1} \cdot \exp(-2n\alpha_1 \cdot l_1) \end{aligned} \tag{4}$$

With $I \propto A^2$ and $R = r^2$, Eq. (6) can be written as $I_n = I_0 \cdot const. \cdot R_2^n \cdot R_1^{n-1} \cdot \exp(-4n\alpha_1 \cdot l_1)$ and energy E of i succeeding reflections is

$$E = \int I \cdot F dt \cong \sum_n I_n \cdot F\Delta t \tag{5}$$

with intensity I, area of ultrasonic transducer F, and integration timestep Δt. With incident energy $E_0 = const \cdot \sum_n A_0^{2n} \cdot \frac{1}{R_1} \cdot F\Delta t$ energy E is defined as $E = E_0 \cdot (R_2 \cdot R_1)^n \exp(-4nl_1 \cdot \alpha_1)$. Due to exponential decay E can be logarithmised resulting in

$$\underset{y}{\ln E} = \underset{b}{\ln E_0} + \underset{x}{n} \cdot \underbrace{[\ln(R_2 R_1) - 4\alpha_1 l_1]}_{m} \tag{6}$$

This resembles the linear equation where slope m depends on material properties (see Fig. 6).

Material changes at the interface can be detected when slope m is compared with a reference.

$$\frac{m_s}{m_w} = \frac{\ln(R_s \cdot R_{ss}) - 4\alpha_1 l_1}{\ln(R_w \cdot R_{ss}) - 4\alpha_1 l_1} \tag{7}$$

with s for sample, w for water, and ss for stainless steel. This relation is simplified when both denominator and numerator are exponentiated and compared.

$$\exp(m_s - m_w) = R_s / R_w \tag{8}$$

With Eq. (10), reflectivity $R_2 = R_s$ and reflection coefficient r_2 can be calculated

$$R_s = R_w \cdot \exp(m_s - m_w) \Rightarrow r_s = \sqrt{R_s} \tag{9}$$

After that, the acoustic impedance Z at an interface can be determined using Eq. (3).

2.6. Statistical analysis

Fitting for determination of logarithmic decrement and characteristic acoustic impedance has been done via a self-written least square regression algorithm. Statistical data analysis has been

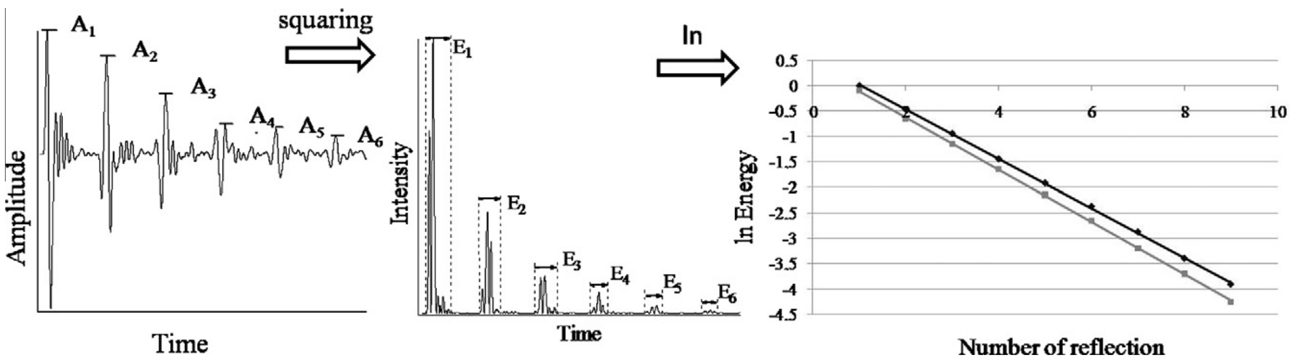

Fig. 6. Signal is squared and energies are calculated and logarithmised. Slope m of a reference (water) and a sample (fouling) are got. Via slope comparison characteristic acoustic impedance can be calculated.

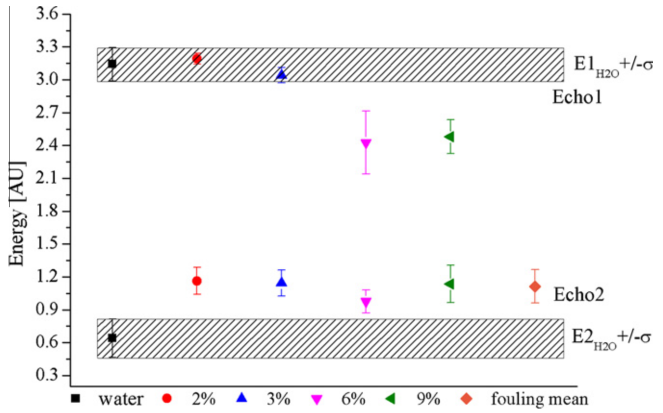

Fig. 7. Energy of echo 1 (*E1*) and echo 2 (*E2*) for different protein contents in milk. In contrast to *E1*, *E2* shows higher values when fouling is present due to higher transmission at the interface wall–probe chamber.

performed in Origin 8.0 using the build-in ANOVA test. Mean value, standard deviation, and standard error of mean have been calculated. Percentage difference with respect to mean has been calculated using $\%\text{error} = \frac{|\text{measured}-\text{mean}|}{\text{mean}} \times 100$ [%].

3. Results and discussion

3.1. Energy

Energies of echo 1 and 2 of surfaces with and without fouling have been compared. The results are displayed in Fig. 7.

Energy of echo 1, *E1*, prior entering the probe chamber does not show a clear tendency. Only fouling made of 6% and 9% protein milk are significantly lower than water even though this is expected for all fouling layers. Energy of echo 2, *E2*, shows a clearly higher value compared with water. A mean of 1.112 ± 0.153 AU has been calculated which is 73.84% higher compared with *E2* of water (0.640 ± 0.176 AU). This increase depends on the change of reflection and transmission at the interface when fouling is present. Differences between stainless steel and fouling are less than between steel and water leading to lower reflection and higher transmission of the signal at the interface. Even though only thin layers (<800 μm) are present changes are high enough to affect the signal. Energy *E2* seems to be better applicable for fouling detection. Attenuation in fouling layer is outweighed by higher transmission but may introduce an error in measurements. In Table 2, *E1* and *E2* for water and fouling are displayed with standard deviation and percentage error.

The high error in *E2* of water is explained by a high variance of measured values. This can be due to changing experimental surrounding conditions over 10 different days affecting water. Altogether, error in *E2* is higher because more error sources are present. These could be e.g. uneven fouling surface, different compositions in fouling layer or air bubbles in water.

3.2. Logarithmic decrement

Damping of the ultrasonic wave at the interface prior entering the probe chamber is got. Clean and surfaces with fouling have been compared. In Fig. 8, the results are presented.

For logarithmic decrement, two values have been calculated. Logarithmic decrement *Λ1* resembles the slope got by least square regression when all intensities of the reflections in echo 1 are taken. After fitting, intensity values with a residuum higher than standard error have been excluded and a second least square regression took place giving slope *Λ2*. Logarithmic decrement *Λ1* does not show a clear trend whereas *Λ2* seems to decrease when fouling is present. This decrease can be explained by less reflection and higher transmission at the interface wall–probe chamber leading to a faster decay of the reflected part which is connected to stronger signal damping. Logarithmic decrement seems to be independent on milk protein amount. For detecting fouling, *Λ2* seems to be more appropriate but due to high errors this trend is not easy to see and has to be verified or falsified by further measurements. The high error may be explained by imperfections in data analysis and differing fouling layers. The values of *Λ1* and *Λ2* are summarised in Table 3 together with standard deviation and error.

3.3. Characteristic acoustic impedance

The characteristic acoustic impedance at an interface of surfaces with and without fouling has been determined; the obtained results are shown in Fig. 9.

Characteristic acoustic impedance seems to be independent on protein content in milk. Thus, a mean of 1.802 ± 0.169 MRayl has been calculated. This value for solid-like fouling is significantly higher than for liquid water (1.486 MRayl, calculated using Bilaniuk (Bilaniuk and Wong, 1993)) and liquid milk (1.558 MRayl, calculated using Kessler (Kessler, 1996)). A fouling layer has to be

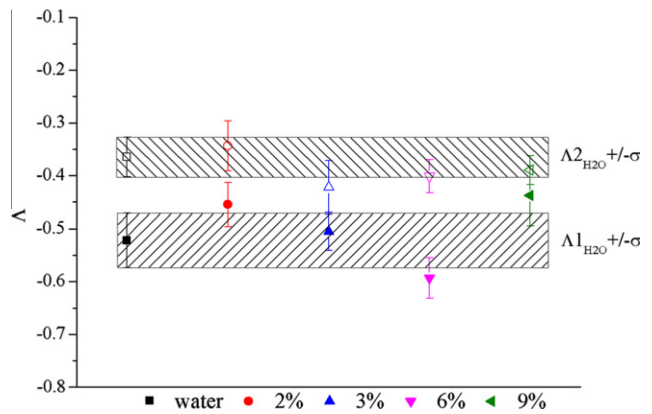

Fig. 8. Logarithmic decrement of water and fouling made of milk with different protein content. Due to high error of logarithmic decrement of water a trend is hard to see. Logarithmic decrement *Λ2* seems to decrease when fouling is present due to less reflection and thus faster intensity decay at the interface. Logarithmic decrement *Λ1* is displayed in closed, *Λ2* in open symbols.

Table 2
Energies for echo 1 and 2 for water and fouling made of milk with different protein content along with standard deviation (SD) and error.

Material	Energy *E1* (AU)	SD (AU)	Error (%)	Energy *E2* (AU)	SD (AU)	Error (%)	% Difference with respect to mean
Water	3.142	0.153	4.88	0.640	0.176	27.47	–
2% protein	3.197	0.049	1.54	1.163	0.123	10.53	4.57
3% protein	3.041	0.070	2.29	1.144	0.120	10.47	2.82
6% protein	2.426	0.287	11.84	0.976	0.105	10.74	12.24
9% protein	2.480	0.154	6.21	1.135	0.171	15.03	2.07
Mean				1.112	0.153	13.73	0.00

Table 3
Logarithmic decrement of water and fouling made of milk with different protein contents with standard deviation (SD) and error.

Material	Λ1	SD	Error (%)	Λ2	SD	Error (%)
Water	−0.522	0.052	9.90	−0.365	0.038	10.34
2% protein	−0.455	0.042	9.23	−0.344	0.047	13.79
3% protein	−0.505	0.036	7.12	−0.422	0.051	12.06
6% protein	−0.593	0.038	6.44	−0.401	0.032	7.928
9% protein	−0.438	0.057	12.95	−0.389	0.027	7.028

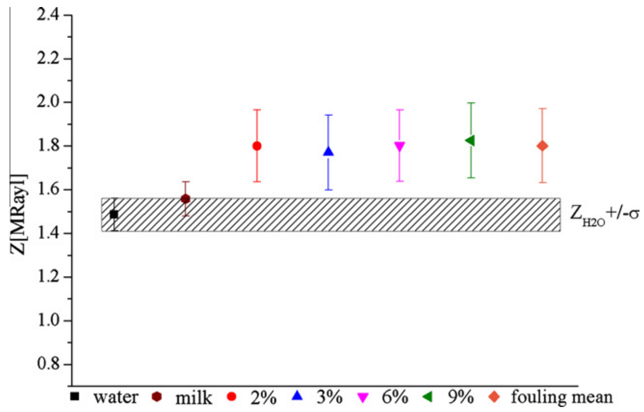

Fig. 9. Characteristic acoustic impedance of water, milk, and fouling made of milk with different protein content. Values for water (calculated using Bilaniuk Bilaniuk and Wong, 1993) and milk (calculated using Kessler, 1996) are similar. When solid-like fouling is present the acoustic impedance is significant higher. The error of water and milk represents a standard deviation of 5%.

considered as visco-elastic material being neither a liquid nor a solid but solid-like. Its material properties vary strongly enough compared with water and milk to change reflection and transmission coefficients at an interface. Reflection decreases when fouling is present which leads to a faster signal decay and increases characteristic acoustic impedance. Thus, a solid-like layer can be clearly distinguished from liquids present at an interface. Table 4 displays the values for acoustic impedances of water, milk, and fouling with standard deviation, standard error of mean, and percentage error.

The error for water and milk matches a standard deviation of 5%. Errors in characteristic acoustic impedance for fouling are mostly caused by irregularities of the fouling layer like uneven spreading on the surface. Fouling layers differed every day in spreading on the surface and composition even though reconstituted milk has been used.

3.4. Artificial neural network (ANN)

A feed-forward multilayer perceptron ANN (see Fig. 10) has been designed based on the back propagation algorithm to develop a pattern recognition method. The input layer is made of five neurons for the acoustic parameters energies of echo 1 and 2, signal damping (two values), and characteristic acoustic impedance. One hidden layer with two neurons has been chosen while the output layer contains one neuron for the fouling decision.

Each neuron weights the input and sums it up with a bias. Then, it presents it to the next layer using a transfer function. The behaviour of an ANN depends on both the weights and the transfer function. The implemented back propagation algorithm tries to minimise the network error by modifying the weights. The transfer functions for the neurons should ensure the smallest available total mean square error (MSE). Iterations on type and order of the transfer functions have been applied and the best results were obtained when LOGSIG (Eq. (2)), LOGSIG, TANSIG (Eq. (1) transfer functions were chosen.

$$a = \frac{2}{(1 + \exp(-2n))} - 1 \qquad (10)$$

$$a = \frac{1}{(1 + \exp(-n))} \qquad (11)$$

where n and a are the input to the transfer function and the neuron output, respectively. Prior training, the network inputs were scaled to be in their mean-centered form so that the network sets the same priority to each input. Altogether, 1000 experiments of water and milk (clean surface) and surfaces with fouling have been investigated whereof 40% (400 samples) has been used for training, 25% (250 samples) for validation, and 35% (350 samples) for testing.

Since the result of the output TANSIG neuron is a finite value (i.e., not {0,1}), a step function with a suitable threshold has to be applied producing "1" for fouling presence and "0" for fouling absence. Sensitivity analysis for several thresholds has been investigated with respect to the number of wrongly detected samples (see Fig. 11). The best results were obtained with thresholds of 0.5, 0.6, and 0.7. However, a threshold of 0.5 had been selected to avoid over-fitting that may occur when testing the designed model with samples of different experimental environment.

After repeating the training 29 times, a mean square error (MSE) of 6.75E−13 has been obtained (see Fig. 12). Then, the ability of the ANN to accurately detect fouling presence has been tested. For this, 207 samples without fouling have been chosen whereof

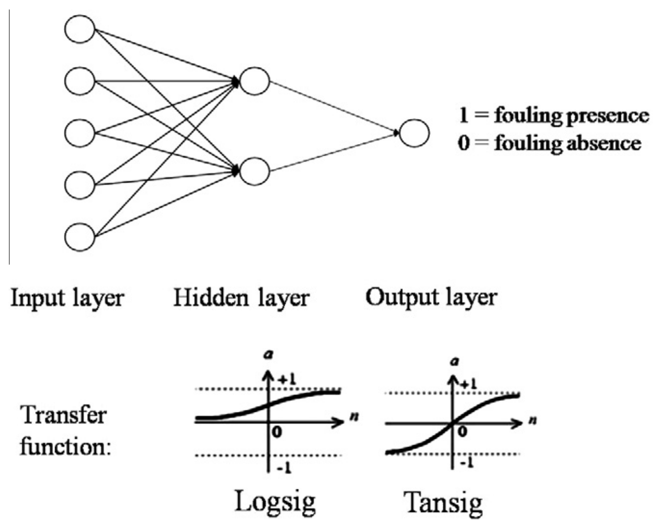

Fig. 10. Architecture of the designed ANN. The input layer has five neurons for the selected acoustic parameters (LOGSIG transfer function), the hidden layer two neurons (LOGSIG transfer function), and the output layer one neuron (TANSIG transfer function) giving "1" for fouling presence, "0" for absence.

Table 4
Characteristic acoustic impedances of water, milk, and fouling together with standard deviation (SD), standard error of mean (SE of mean), and error.

Material	Z (MRayl)	SD (MRayl)	SE of mean (MRayl)	Error (%)	% Difference with respect to mean
Water	1.486	0.074	0.0041	4.99	–
Milk	1.558	0.078	0.0043	5.00	–
2% protein	1.800	0.165	0.0014	9.15	0.07
3% protein	1.771	0.172	0.0015	9.70	1.74
6% protein	1.802	0.163	0.0014	9.05	0.01
9% protein	1.826	0.171	0.0013	9.36	1.31
Mean	1.802	0.169	0.0072	9.36	0.00

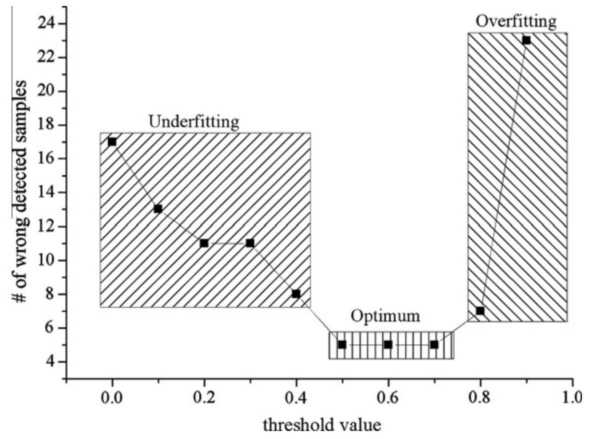

Fig. 11. Number of wrong detected samples out of 350 test samples with different thresholds applied to the ANN output (0 matches no threshold). Values between 0.5 and 0.7 show an optimum.

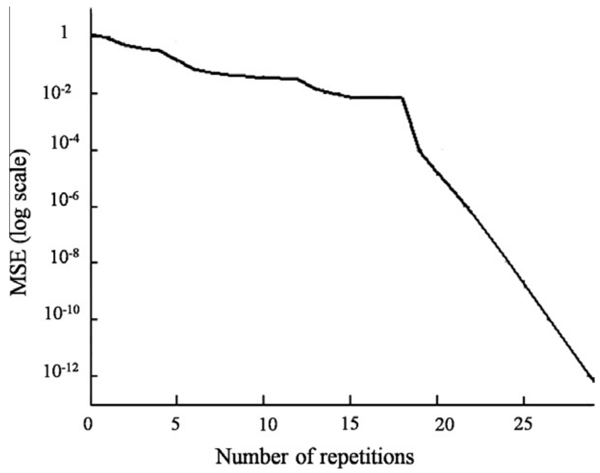

Fig. 12. Performance of the ANN during training: variation of MSE with number of repetitions of training samples. The training process stopped after 29 repetitions when MSE reached a minimum of 6.75×10^{-13}.

203 samples have been identified correctly resembling a detection stability of 98.07%. The residual 143 of all 350 testing samples have been with fouling present. Of them, 142 have been recognised correctly corresponding to 99.29% (compare with Fig. 13).

In Table 5, the number of samples used is displayed in more detail and number of correctly and incorrectly detected samples as well as percentage error are given.

Table 5
Number of testing samples in total and for fouling presence and absence together with error and number of samples detected correctly and incorrectly.

	# Of samples	Detection correct	Detection incorrect	% Error
Fouling	143	142	1	0.70
No fouling	207	203	4	1.93
Total	350	345	5	1.42

Out of 350 test samples 345 have been detected correctly (98.58%) indicating the efficiency of the designed network with the selected acoustic parameters as input. To improve detection efficiency, more samples with and without fouling have to be included in designing and testing of the ANN as well as an outlier algorithm could be included.

4. Conclusions

In this study a new pattern recognition method for determining fouling presence and absence is presented. It is based on a combination of acoustic parameters from ultrasonic measurements and an artificial neural network (ANN). Dairy fouling type A has been made using reconstituted milk with varying protein content and measured using ultrasound. The acoustic parameters chosen as input for the ANN are energies of echo 1 and 2, logarithmic decrement (two values), and characteristic acoustic impedance. Energy of echo 1 did not show a clear tendency whereas energy of echo 2 increased up to 73.84% when fouling was present compared to tap water. This increase is due to less difference between solid-like fouling and stainless steel leading to higher signal transmission. Logarithmic decrement resembles damping at the interface prior entering the probe chamber and seemed to decrease up to 14% with fouling. This may be disputable due to high variance which may be caused by uneven fouling spreading and errors in analysis. Characteristic acoustic impedance increased from 1.486 ± 0.074 MRayl for water by 17.54% to 1.802 ± 0.169 MRayl for fouling. This is caused by changed material state from liquid to solid-like at the interface wall–probe chamber. Errors in the measurements are mainly due to uneven spreading of fouling on the measured surface. All parameters seem to be independent of protein content and show significant changes with fouling presence even though usage of logarithmic decrement may be disputable. The parameters have been used as input in an ANN to disentangle fouling detection from error proneness of single acoustic parameters. Single parameters may vary strongly and give false results easily whereas a combination of them will decrease error proneness and increase detection stability and efficiency. The ANN is based on a back propagation algorithm with one hidden layer and displays "1" for

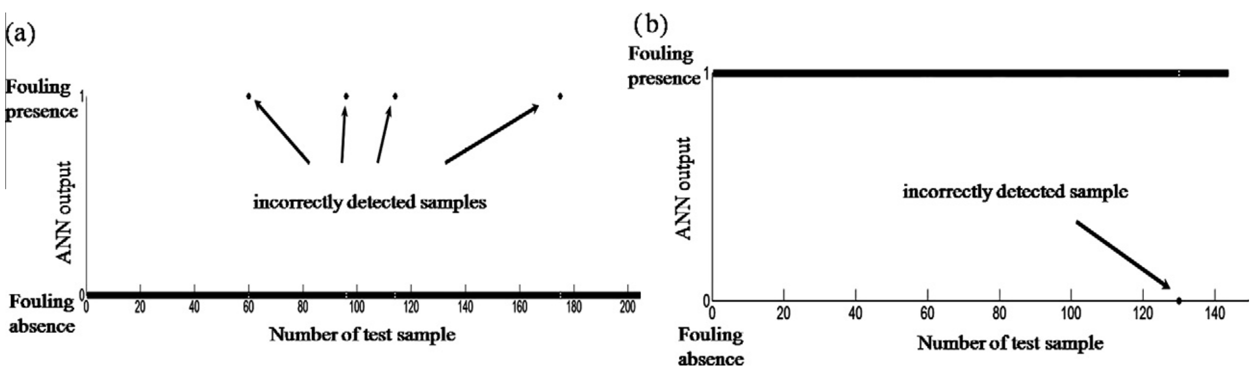

Fig. 13. Performance of the ANN during testing. (a) 207 samples without fouling, 203 samples have been identified correctly. (b) 143 samples with fouling, 142 samples have been recognised correctly.

presence and "0" for absence of fouling. Sensitivity analysis showed a threshold of 0.5 for the output neuron as best applicable. After training with 400 samples (40% of data), 350 samples have been tested (35% of data). In 98.58% of the tested samples correct identification of fouling presence and absence has been found. Increasing number of samples and decreased errors in single parameters may increase correct detection further. Wrong detection may be caused by the decision in the last layer where values are rounded up to 1 and down to 0 when not displaying definite value, respectively. This may be improved by including outlier analysis and making the threshold more flexible. Also, other or more acoustic parameters may increase detection stability.

Fouling is a complex process and fouling detection is prone to many errors. Using a combination of ultrasonic parameters and an ANN a stable and efficient pattern recognition method for fouling detection has been developed. In future, dairy fouling type B shall be included to extend the analysis method to other fouling kinds. Also, differing flow and temperatures and their influence on acoustic parameters shall be added. Following, fouling and cleaning processes shall be monitored to adapt the developed method to real processes.

Acknowledgements

This work has been supported by the FEI (Forschungskreis der Ernährungsindustrie), the AiF, and Ministry of Economics and Technology. AIF project number: 16302N.

References

Astorga-Zaragoza, C.M., Zavala-Río, A., Alvarado, V.M., Méndez, R.M., Reyes-Reyes, J., 2007. Performance monitoring of heat exchangers via adaptive observers. Measurement 40 (4), 392–405.
Bansal, B., Chen, X.D., 2006. A critical review of milk fouling in heat exchangers. Comprehensive Reviews in Food Science and Food Safety 5 (2), 27–33.
Basheer, I.A., Hajmeer, M., 2000. Artificial neural networks: fundamentals, computing, design, and application. Journal of Microbiological Methods 43 (1), 3–31.
Belmar-Beiny, M.T., Gotham, S.M., Paterson, W.R., Fryer, P.J., Pritchard, A.M., 1993. The effect of Reynolds number and fluid temperature in whey protein fouling. Journal of Food Engineering 19 (2), 119–139.
Bilaniuk, N., Wong, G.S.K., 1993. Speed of sound in pure water as a function of temperature. The Journal of the Acoustical Society of America 93 (3), 1609–1612.
Burton, H., 1968. Section G. Deposits from whole milk in heat treatment plant – a review and discussion. Journal of Dairy Research 35 (02), 317–330.
Changani, S.D., Belmar-Beiny, M.T., Fryer, P.J., 1997. Engineering and chemical factors associated with fouling and cleaning in milk processing. Experimental Thermal and Fluid Science 14 (4), 392–406.
Chen, X.D., Li, D.X.Y., Lin, S.X.Q., Ozkan, N., 2004. On-line fouling/cleaning detection by measuring electric resistance-equipment development and application to milk fouling detection and chemical cleaning monitoring. Journal of Food Engineering 61 (2), 181–189.
Davies, T.J., Henstridge, S.C., Gillham, C.R., Wilson, D.I., 1997. Investigation of whey protein deposit properties using heat flux sensors. Food and Bioproducts Processing 75 (2), 106–110.
Egmont-Petersen, M., de Ridder, D., Handels, H., 2002. Image processing with neural networks – a review. Pattern Recognition 35 (10), 2279–2301.
Fryer, P.J., Belmar-Beiny, M.T., 1991. Fouling of heat exchangers in the food industry: a chemical engineering prespective. Trends in Food Science & Technology 2, 33–37.
Hæggström, E., Luukkala, M., 2001. Ultrasound detection and identification of foreign bodies in food products. Food Control 12 (1), 37–45.
Haug, I.J., Skar, H.M., Vegarud, G.E., Langsrud, T., Draget, K.I., 2009. Electrostatic effects on β-lactoglobulin transitions during heat denaturation as studied by differential scanning calorimetry. Food Hydrocolloids 23 (8), 2287–2293.
Hussein, W.B., Hussein, M.A., Becker, T., 2010. Detection of the red palm weevil using its bioacoustics features. Journal of Bioacoustics 19 (2), 177–194.
Kessler, H.G., 1996. Lebensmittel- und Bioverfahrenstechnik – Molkereitechnologie, fourth ed. A. Kessler.
Krebs, M.R.H., Devlin, G.L., Donald, A.M., 2009. Amyloid fibril-like structure underlies the aggregate structure across the pH range for β-lactoglobulin. Biophysical Journal 96 (12), 5013–5019.
Law, A.J.R., Leaver, J., 2000. Effect of pH on the thermal denaturation of whey proteins in milk. Journal of Agricultural and Food Chemistry 48 (3), 672–679.
McKenzie, H.A., Sawyer, W.H., 1967. Effect of pH on β-lactoglobulins. Nature 214 (5093), 1101–1104.
Leemans, V., Destain, M.-F., 2009. Ultrasonic internal defect detection in cheese. Journal of Food Engineering 90 (3), 333–340.
Li, J.-X., Sanderson, R.D., Chai, G.Y., 2006. A focused ultrasonic sensor for in situ detection of protein fouling on tubular ultrafiltration membranes. Sensors and Actuators B: Chemical 114 (1), 182–191.
Marczak, W., 1997. Water as a standard in the measurements of speed of sound in liquids. Journal of the Acoustical Society of America 102 (5), 2776–2779.
Marselina, Y., Lifia, Le-Clech, P., Stuetz, R.M., Chen, V., 2009. Characterisation of membrane fouling deposition and removal by direct observation technique. Journal of Membrane Science 341 (1–2), 163–171.
Mas, J.F., Flores, J.J., 2008. The application of artificial neural networks to the analysis of remotely sensed data. International Journal of Remote Sensing 29 (3), 617–663.
Pelegrine, D.H., Oliviera, K.F., Gomes, M.T.M.S., 2007. Milk protein fouling in a tubular heat exchanger: effect of milk temperature and Reynolds number. In: Müller-Steinhagen, H., Malayari, M.R., Watkinson, A.P. (Eds.), 7th International Conference on Heat Exchanger Fouling and Cleaning - Challenges and Opportunities, Tomar, Portugal, pp. 147–149.
Pereira, A., Mendes, J., Melo, L.F., 2008. Using nanovibrations to monitor biofouling. Biotechnology and Bioengineering 99 (6), 1407–1415.
Pereira, A., Mendes, J., Melo, L.F., 2009. Monitoring cleaning-in-place of shampoo films using nanovibration technology. Sensors and Actuators B: Chemical 136 (2), 376–382.
Premathilaka, S.S., Hyland, M.M., Chen, X.D., Watkins, L.R., Bansal, B., 2007. Interaction of whey protein with modified stainless steel surfaces. In: Müller-Steinhagen, H., Malayari, M.R., Watkinson, A.P. (Eds.), 7th International Conference on Heat Exchanger Fouling and Cleaning - Challenges and Opportunities, Tomar, Portugal, pp. 150–161.
Renard, D., Lefebvre, J., Griffin, M.C.A., Griffin, W.G., 1998. Effects of pH and salt environment on the association of β-lactoglobulin revealed by intrinsic fluorescence studies. International Journal of Biological Macromolecules 22 (1), 41–49.
Resa, P., Luis, E., Montero de Espinosa, F.R., Gómez-Ulltate, Y., 2005. Ultrasonic velocity in water–ethanol–sucrose mixtures during alcoholic fermentation. Ultrasonics 43 (4), 247–252.
Riverol, C., Napolitano, V., 2005. Estimation of fouling in a plate heat exchanger through the application of neural networks. Journal of Chemical Technology and Biotechnology 80, 594–600.
Rosmaninho, R., Melo, L.F., 2008. Protein–calcium phosphate interactions in fouling of modified stainless-steel surfaces by simulated milk. International Dairy Journal 18 (1), 72–80.
Rosmaninho, R., Gizzo, G., Müller-Steinhagen, H., Melo, L.F., 2005. Anti-Fouling stainless steel based surfaces for milk heating processes. In: Müller-Steinhagen, H., Malayari, M.R., Watkinson, A.P. (Eds.), 6th International Conference on Heat Exchanger Fouling and Cleaning - Challenges and Opportunities, Kloster Irsee, Germany, pp. 97–102.
Rosmaninho, R., Santos, O., Nylander, T., Paulsson, M., Beuf, M., Benezech, T., 2007. Modified stainless steel surfaces targeted to reduce fouling - Evaluation of fouling by milk components. Journal of Food Engineering 80 (4), 1176–1187.
Schoeck, T., Hussein, M.A., Becker, T., 2010. Konzentrationsbestimmung in Wasser-Zucker-Ethanol-Gemischen mittels adiabatischer Kompressibilität und Dichte. Tm-Technisches Messen 77 (1), 30–37.
Simons, J.-W.F.A., Kosters, H.A., Visschers, R.W., de Jongh, H.H.J., 2002. Role of calcium as trigger in thermal β-lactoglobulin aggregation. Archives of Biochemistry and Biophysics 406 (2), 143–152.
Smith, D.M., Rose, A.J., 1994. Gel properties of whey protein concentrates as influenced by ionized calcium. Journal of Food Science 59 (5), 1115–1118.
Teruel, E., Cortés, C., Ignacio Díez, L., Arauzo, I., 2005. Monitoring and prediction of fouling in coal-fired utility boilers using neural networks. Chemical Engineering Science 60 (18), 5035–5048.
Truong, T., Anema, S., Kirkpatrick, K., Chen, H., 2002. The use of a heat flux sensor for in-line monitoring of fouling of non-heated surfaces. Food and Bioproducts Processing 80 (4), 260–269.
Unterhaslberger, G., Schmitt, C., Sanchez, C., Appolonia-Nouzille, C., Raemy, A., 2006. Heat denaturation and aggregation of β-lactoglobulin enriched WPI in the presence of arginine HCl, NaCl and guanidinium HCl at pH 4.0 and 7.0. Food Hydrocolloids 20 (7), 1006–1019.
Visser, J., Jeurnink, T.J.M., 1997. Fouling of heat exchangers in the dairy industry. Experimental Thermal and Fluid Science 14 (4), 407–424.
Withers, P., 1994. Ultrasonic sensor for the detection of fouling in UHT processing plants. Food Control 5 (2), 67–72.
Yüksel, Z., Erdem, Y.K., 2005. The influence of main milk components on the hydrophobic interactions of milk protein system in the course of heat treatment. Journal of Food Engineering 67 (3), 301–308.

5.2.3. "Detection of dairy fouling: Combining ultrasonic measurements and classification methods", E. Wallhäußer, W.B. Hussein, M.A. Hussein, J. Hinrichs, T. Becker; Engineering in Life Science 13 (2013), 292-301

Engineering in Life Sciences

www.els-journal.com

E. Wallhäußer[1]
W.B. Hussein[1]
M.A. Hussein[1]
J. Hinrichs[2]
T. Becker[1]

[1] (Bio-)Process Technology and Process Analysis, Life Science Engineering, Technische Universitaet Muenchen, Freising, Germany

[2] Animal Foodstuff Technology, Institute for Foodscience and Biotechnology, University of Hohenheim, Stuttgart, Germany

Research Article

Detection of dairy fouling: Combining ultrasonic measurements and classification methods

Fouling and cleaning in heat exchangers are severe and costly (up to 0.3% of gross national product) issues in dairy and food processing. Therefore, reducing cleaning time and cost is urgently needed. In this study, two classification methods [artificial neural network (ANN) and support vector machine (SVM)] for detecting protein and mineral fouling presence and absence based on ultrasonic measurements were presented and compared. ANN is based on a multilayer perceptron feed forward neural network, whereas SVM is based on clustering between fouling and no fouling using a hyperplane. When both fouling types (1239 datasets) were combined, ANN showed an accuracy of 71.9% while SVM displayed an accuracy of 97.6%. Separate fouling detection of mineral/protein fouling by ANN/SVM was comparable: dependent on fouling type detection accuracies of 100% (protein fouling, ANN and SVM), and 98.2% (SVM), and 93.5% (ANN) for mineral fouling was reached. It was shown that it was possible to detect fouling presence and absence offline in a static setup using ultrasonic measurements in combination with a classification method. This study proved the applicability of combining classification methods and fouling measurements to take a step toward reducing cleaning costs and time.

Keywords: Artificial neural network (ANN) / Classification method / Dairy fouling / Support vector machine (SVM) / Ultrasound

Additional supporting information may be found in the online version of this article at the publisher's web-site

Received: June 28, 2012; *revised:* October 29, 2012; *accepted:* December 14, 2012

DOI: 10.1002/elsc.201200081

1 Introduction

To extend shelf life and reduce microbiological hazards, milk is heated in heat exchangers where temperatures from 72°C to 75°C (pasteurization) and from 135°C to 150°C (ultra-high-temperature processing) are used. At these temperatures, proteins denaturate and agglomerate and minerals precipitate on heat transfer surfaces producing fouling. Fouling is classified in protein fouling (type A) a soft, spongy, white deposit consisting mostly of β-lactoglobulin and developing at pasteurization processes and mineral fouling (type B) that is grayish, brittle, and gritty and made mostly of calcium phosphates ($Ca_3(PO_4)_2$) developing mostly at ultra-high temperature processing [1]. Fouling deposition is influenced by various parameters like Reynolds number [2], salt content, age of milk [3], protein concentration [4], and pH [5]. Fouling starts with an induction layer but it remains unknown if this layer is composed primarily of salts or proteins [6–8]. When fouling occurs heat transfer resistance and production costs are increased wile thermal efficiency is decreased and unsupervised cleaning will take place [9]. Thus, it is of great importance for dairy industry to determine fouling presence and monitor its progress and cleaning success. To achieve these goals different approaches were made like monitoring heat transfer measurands [10, 11], electric parameters [12–14], or acoustical quantities for fouling detection [15–17]. Another approach is to feed measured values to a computational or numerical method that then states fouling presence [18–20]. All these methods proved to be usable for fouling detection and have different advantages and disadvantages. Heat and electric parameters are, e.g. very sensitive to fouling thickness but may

Correspondence: Dipl.-Eng. E. Wallhäußer (e.wallhaeusser@wzw.tum.de), (Bio-)Process Technology and Process Analysis, Life Science Engineering, Technische Universitaet Muenchen, Weihenstephaner Steig 20, 85354 Freising, Germany.

Abbreviations: ANN, artificial neural network; **MSE**, mean square error; **SCF**, spectral crest factor; **SSMOOTH**, spectral smoothness; **STE**, short-time energy; **SVM**, support vector machine; **TCF**, temporal crest factor; **Z**, characteristic acoustic impedance

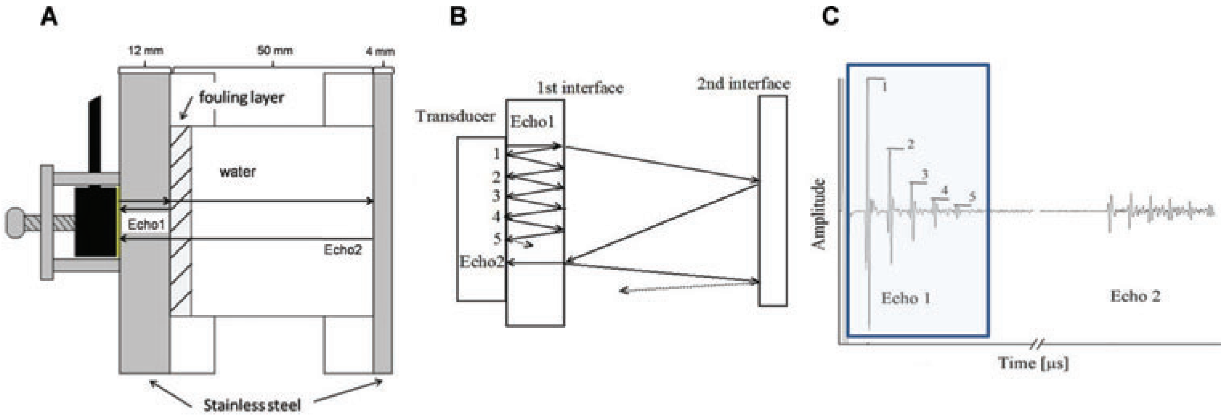

Figure 1. (A) Experimental setup: an ultrasonic wave runs through the setup and is reflected and transmitted at interfaces. (B) An echo is the reflected signal at an interface consisting of several reflections in the wall. (C) For the chosen signal parameters echo 1 is analyzed (framed).

be only local, invasive, or not stand very high temperatures. For example acoustic methods are noninvasive and are highly sensitive to fouling but are temperature dependent. Numerical approaches can be used to get an impression about fouling behavior and occurrence but have to be compared with experimental results and are usually simplifications of complex processes. Dependent on the application a suitable method has to be chosen.

This work deals with a combination of an ultrasonic measuring method and classification techniques that are used to determine fouling presence and absence where parameters were extracted from an ultrasonic signal and fed into a decision machine. Ultrasound (20 kHz–2 GHz) is a well-known method for noninvasive inspection and used in many applications like nondestructive testing in aerospace industry [21], to determine polymer properties [22], and to characterize dairy products and fermentation in food industry [23, 24]. As classification machines, artificial neural networks (ANN) and support vector machines (SVM) were chosen. An ANN is an emulation of a biological network that can establish a relationship among data by building models between input and output vectors [25]. ANNs were already applied, e.g. in image processing, pattern recognition, and pest detection [26, 27] and in supervising cleaning in place in plate heat exchangers [28]. A SVM is a decision machine and was first introduced by Vapnik et al. [29, 30] where objects are classified such that a clear gap between them is found by using a hyperplane that is defined by support vectors from the distinguished classes. SVMs were already applied in pattern recognition [31,32], regression [33], and computational biology [34,35].

The focus in this study lied on the development of a decision method independent on fouling type. The method uses a combination of carefully chosen acoustic and signal parameters and a pattern recognition or classification method to detect fouling presence and absence on stainless steel in a static setup.

2 Materials and methods

2.1 Experimental setup

The setup consists of an acrylic glass container (length 50 mm, diameter 50 mm) closed with two stainless steel lids where the self-built ultrasonic transducer with a lead zirconate titanate-ceramic (Noliac, center frequency 2.13 ± 0.34 MHz, theoretically detectable fouling thickness below 50 μm) was pressed to one side using a screw (Fig. 1A) with the path of the ultrasonic wave schematically shown in Fig. 1B. An adjustable in-house electronic was used (sampling frequency of 12.5 kHz, 20 V excitation voltage) and tap water was chosen as reference. For protein fouling, reconstituted milk and for mineral fouling reconstituted permeate was heated. Different acoustic and signal parameters were chosen to determine fouling presence and absence and calculated using the first echo of the signal (Fig. 1C). The parameters showed a difference between a fouled and a clean surface.

2.2 Procedure for protein and mineral fouling

For protein fouling, the setup was filled with 50 g of reconstituted milk made from skim milk powder (Instant C, Schwarzwaldmilch, 34 w/w% protein) with a pH of 6.7 ± 0.2. Protein content varied (2–9 w/w%) and milk was heated to 90 ± 1°C for 90 ± 5 min to produce fouling. Supernatant milk was poured out, the fouled setup was cooled to 25 ± 1°C, the setup was filled with water, the ultrasonic transducer was attached to the fouled stainless steel lid using an oil-based coupling gel (Sonatest) and measurements were made in pulse-echo mode under static conditions. All 238 measurements were combined because it was found that protein content did not have a significant impact on the signal and its parameters [36].

For mineral fouling, the setup was filled with 50 g of reconstituted permeate made of permeate powder (Bayolan PT, Bayerische Milchindustrie eG). After preliminary tests, a mineral content of 4 w/w% and pH 9 were chosen. Permeate was filtered to reduce the amount of fats and sugars, heated for 180 ± 5 min at 95 ± 1°C, then supernatant permeate was poured out, and the setup was cooled to 25 ± 1°C. After that, the same procedure as for protein fouling was followed (317 measurements). No fouling resembles the setup filled only with water (648 measurements).

2.3 Acoustic and signal processing parameters

Different acoustic and signal processing parameters that showed high sensitivity toward fouling presence and absence were combined in pattern recognition methods. The features and classification methods are shortly presented together with their mathematical description.

2.3.1 Acoustic impedance

The characteristic acoustic impedance (Z) stands for the resistance a medium opposes to the traveling sound wave. It is calculated by determining the reflection coefficient r at the interface between wall and medium that changes dependent on material present [Eq. (1)].

$$Z_{\text{sample}} = Z_{\text{steel}} \left(\frac{1-r}{1+r} \right) \tag{1}$$

2.3.2 Short time energy

Short-time energy (STE) resembles the energy content of the pattern (here first echo). It is calculated by summing up the area under the curve of echo 1 (framed in Fig. 1C).

$$\text{STE} = \sum_{n=1}^{N} [x(n)]^2 \tag{2}$$

It changes due to different reflection and transmission coefficients at the considered interface that are changing due to different media.

2.3.3 Temporal/spectral crest factor

Temporal crest factor (TCF) and spectral crest factor (SCF) are the ratio between the maximum amplitude/magnitude in time/frequency domain to the average amplitude/magnitude and are unique for a signal. For this investigation, maximum and average of echo 1 were chosen.

$$\text{TCF} = \frac{\max(|x(n)|)}{1/N \sum_{n=1}^{N} |x(n)|} \tag{3}$$

$$\text{SCF} = \frac{\max(|X(m)|)}{1/1024 \sum_{m=1}^{1024} |X(m)|} \tag{4}$$

The bigger it is the higher is the amount of harmonics in the signal that is not wanted because many harmonics may decrease detection stability and accuracy.

2.3.4 Spectral smoothness

The spectral smoothness (SSMOOTH) stands for the smoothness variation of the amplitude of the chosen pattern with respect to its two neighbors. This was done for echo 1.

$$\text{SSMOOTH} = 20 \cdot \sum_{m=2}^{1023} \left| \log|X(m)| - \frac{\log|X(m-1)| + \log|X(m)| + \log|X(m+1)|}{3} \right| \tag{5}$$

The smoother a signal is, the less deviated is its waveform, which is indicated by low SSMOOTH whereas high values indicate stronger decrease.

2.4 Pattern recognition methods

2.4.1 Artificial neural network

A feed-forward multilayer perceptron ANN (Fig. 2) was designed based on the back propagation algorithm to develop a pattern recognition method. One input (five neurons), one hidden (two neurons), and one output layer (one neuron) were chosen. The output neuron displayed “1” for a fouled and “0” for a clean plate.

Each neuron weights the input, sums it up with a bias, and presents it to the next layer via a transfer function where ANN behavior depends on both weights and transfer function. The implemented back propagation algorithm minimizes network error by weight modifying the transfer functions to obtain the smallest total mean square error (MSE). Iterations on type and order of the transfer function were applied and tangent sigmoid transfer function [Eq. (6)] transfer function was chosen for both fouling types.

$$a = \frac{2}{[1 + \exp(-2n)]} - 1 \tag{6}$$

Where n and a are the input to the transfer function and neuron output, respectively. Prior training, the inputs were scaled to be mean centered.

2.4.2 Support vector machine

A SVM creates and defines the maximal margin hyperplane to separate two clouds of points. The classification training algorithm builds a decision model capable of predicting whether a new point falls into one category or the other [Eq. (7)].

$$F(x) = \sum_{i=1}^{N} w_i \cdot x + b = \sum_{i=1}^{N} \alpha_i y_i (x_i \cdot x) + b \tag{7}$$

where b is the distance between the separating hyperplane and the origin in the perpendicular direction, N the number of support vectors, α the nonnegative Lagrange multiplier, y the decision value $\in\{-1,1\}$, and F the decision function that allocates a test sample to one cloud if its sign is positive and to the other cloud if its sign is negative.

If the clouds are clearly separated (Fig. 3A) a linear SVM can be used. The applied hyperplane is the one with largest distance to nearest points (i.e. support vectors) of each cloud that define the hyperplane and guide the decision process.

Since the samples are not linear separable in input space the separation is sought in an appropriate chosen kernel-induced feature space (Fig. 3B).

Nonlinear separable data can be made linear separable such that a dot product can be used by applying the kernel trick. With it the data is transferred from input to feature space making it linear separable and Eq. (7) is modified [Eq. (8)]. The solution

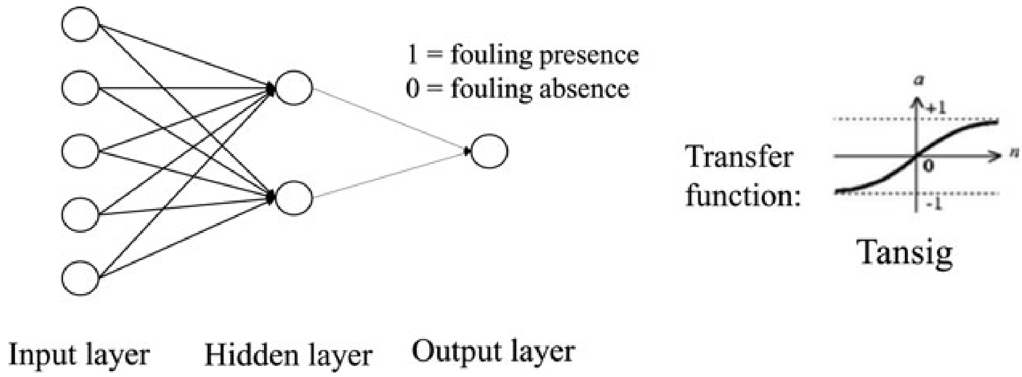

Figure 2. Architecture of the designed ANN. The input layer has five neurons (five inputs), the hidden layer two neurons, and the output layer one neuron giving "1" for fouling presence, "0" for absence. tangent sigmoid transfer function was used.

of the problem lies in finding b, α's, and an appropriate kernel.

$$F(x) = \sum_{i=1}^{N} \alpha_i y_i \left[\Phi(x_i) \cdot \Phi(x)\right] + b = \sum_{i=1}^{N} \alpha_i y_i K(x_i, x) + b \tag{8}$$

Where $\Phi(x)$ is the transform of sample x from input to feature space, and K is the kernel to represent feature space.

Choosing a kernel is a challenging task and is usually done following other studies in the same area or by trial and error. For a polynomial kernel it can be shown that it can be linked with regression analysis [Eq. (9)]. This is proven by mathematical induction.

$$\begin{array}{lll} & \text{Polynomial fit} & \text{Polynomial kernel} \\ & y = A + \sum_n B_i \cdot x_i^n & K = \left(A + x_i^* \cdot x_i\right)^n \\ n = 1: & y = A + B_1 x_1^1 \quad B_1 = x_1^* & K = A + x_1^* x_1 \\ n = n: & y = A + B_n x_n^n + \cdots + B_1 x_1 & K = A^n + x_n^{n*} x_n^n + \cdots \\ & & \quad + (n-1)\, A^{n-1} x_1^* x_1 \\ & B_n = x_n^{n*}, \ldots, B_1 = (n-1) A^{n-1} x_1^* & \end{array} \tag{9}$$

If mean values can be fitted with polynomial regression this may help to choose a kernel as starting point for further investigation. Still, radial basis function or perceptron kernels may give better results and may be tested.

3 Results and discussion

3.1 Fouling layer

Protein layer was spongy and thick with thicknesses of 400 ± 100 μm (measured with caliper). Thickness is in the same range as described, e.g. by Withers [37] with fouling made under static conditions in this study. Different protein concentrations led to similar layer thicknesses when same heating time and temperature was applied. Increasing heating time, temperature, and protein concentration is known to increase fouling deposition rate and thickness [14,38,39]. Mineral fouling on the other side was very thin, brittle, hard to obtain, and its thickness could not be measured easily but is estimated to be below 50 μm. Fouling resembled layers described in literature [6,40] and only one thickness for every fouling type was investigated because fouling detection in principle was of interest.

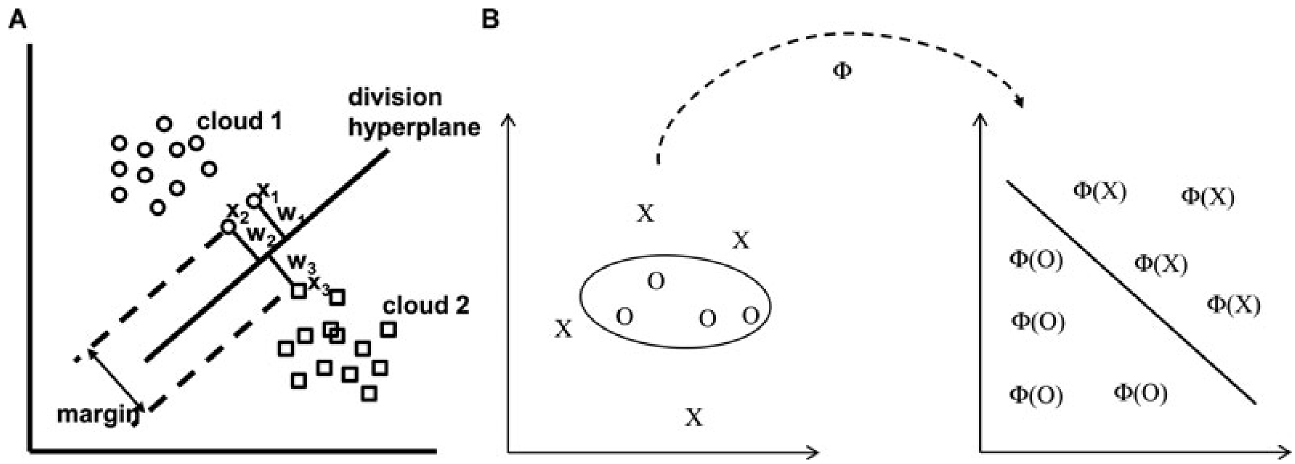

Figure 3. (A) Classification problem of two classes (cloud 1, cloud 2) modeled by a linear SVM with three support vectors (x_1, x_2, x_3) of three weights (w_1, w_2, w_3). (B) Schematic display of the transformation Φ of nonlinear separable samples from input to feature space at which a linear separating hyperplane can be constructed.

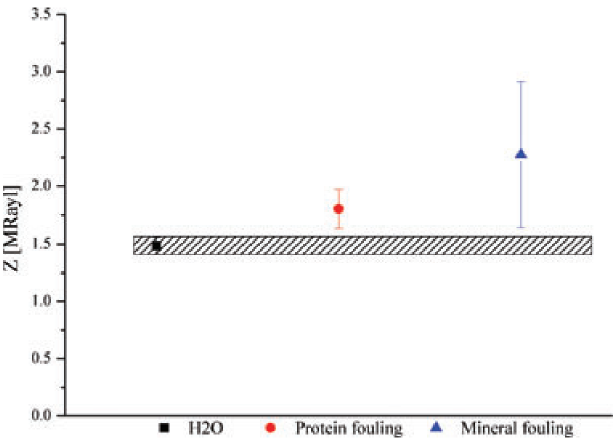

Figure 4. Characteristic acoustic impedance (Z) of water, protein, and mineral fouling. Value for water was calculated using $Z = \rho \cdot c$ with sound velocity c after Bilaniuk [37], SD of 5%. With solid-like fouling acoustic impedance is significant higher. Error bars stand for SD.

3.2 Acoustic and signal processing parameters

3.2.1 Characteristic acoustic impedance

The Z at an interface of surfaces with and without fouling was determined; the results are shown in Fig. 4.

Z for both fouling types is higher than for water and one-way analysis of variance calculated with Minitab® and Origin®, respectively, showed significant difference between both fouling types and water (for both fouling types $p < 0.0005$, H0 hypothesis stated no difference, H1 hypothesis stated difference between fouling and water, H0 hypothesis was rejected due to low p-value). Characteristic acoustic impedance for water is 1.49 MRayl (calculated using Bilaniuk [41]), for protein fouling 1.80 ± 0.17 MRayl, and for mineral fouling 2.28 ± 0.64 MRayl. Fouling is considered as visco-elastic, solid-like material thus its material properties vary strongly compared with a liquid and change the reflection coefficient at an interface even if only thin layers are present. This change leads to a change in Z that in turn can be used to distinguish fouling at an interface from a liquid.

3.2.2 STE and TCF

STE of fouled and not fouled surfaces were compared (Fig. 5A). It is seen that STE of protein fouling displayed a difference from water where mineral fouling is very similar ($p < 0.0005$ for protein fouling, $p = 0.14263$ for mineral fouling). STE may be influenced by layer thickness because a higher amount of signal energy is lost into the layer decreasing the reflected energy. This may explain why STE of protein fouling shows a statistical significant difference while mineral fouling shows no significant difference.

TCF of protein fouling shows a smaller value than and differs from water more strongly whereas mineral fouling shows a higher mean but lays inside the error bars (Fig. 5B) and statistical differences between both fouling types and water is found ($p < 0.0005$). Lower TCF can be explained by a thick protein-fouling layer that may increase noise in a signal and lead to lower TCF due to less harmonics.

3.2.3 SCF and SSMOOTH

SCF showed visible differences only for protein fouling (Fig. 5C) that displays smaller SCF because it introduces a layer behind the interface, decreases the reflected amplitude, and may increase noise and thus mean amplitude where the reflected wave seems to include fewer harmonics compared to water. From this it follows that fouling seems to deform the ultrasonic signal less.

SSMOOTH showed a difference for protein fouling (Fig. 5D) and seems to increase when fouling is present. This indicates that the signal is more pronounced and decays faster when fouling present. SCF and SSMOOTH showed statistical differences for protein fouling ($p < 0.0005$) while for mineral fouling no statistical difference was found ($p = 0.75136$ and $p = 0.57278$, respectively). Still, both spectral features were used for ANN and SVM for both fouling types because detection was stabilized. Table 1 gives an overview over all determined features.

Error sources for both fouling are uneven spreading on the surface and slightly different fouling composition from day to day. In the case of mineral fouling, complex experimental conditions made it difficult to obtain reproducible fouling and only very thin layers were produced [below 50 μm (estimated value)]. For protein fouling all temporal and spectral features showed statistical significance while for mineral fouling no statistical significance was found for STE and the spectral features. Some features like STE may depend on layer thickness because they showed significant difference for (thick) protein fouling but none for (thin) mineral fouling. This has to be investigated in more detail in future. Still, all features were included into ANN and SVM, respectively, to increase the accuracy and to compare detection accuracy.

3.3 Pattern recognition methods

3.3.1 Artificial neural network

Altogether, 1239 datasets with and without fouling were used. Of these, 238 datasets with protein fouling, 317 datasets of mineral fouling, and 684 datasets of no fouling were present. Of the data, 60% were used for training and 40% for testing. Three ANNs were built, one for protein fouling, one for mineral fouling, and one for both fouling types together.

The ANN for protein fouling showed a MSE of 3.0×10^{-12} and a detection accuracy of nearly 100% (error 2.3×10^{-5}%). When mineral fouling was investigated a MSE of 2.3×10^{-12} was found and the detection accuracy was 93.5%. The ANN that should detect both fouling types had a MSE of 3.8×10^{-12} but displayed a detection accuracy of only 71.9%. Both fouling types were combined because in dairy industry usually both types do occur regularly. Results for the three developed ANN together with amount of training and testing data, MSE, and accuracy is presented in Supporting information, Table 1. For protein fouling, ANN showed very good results where for mineral fouling and mixture of both fouling types ANN performance was less

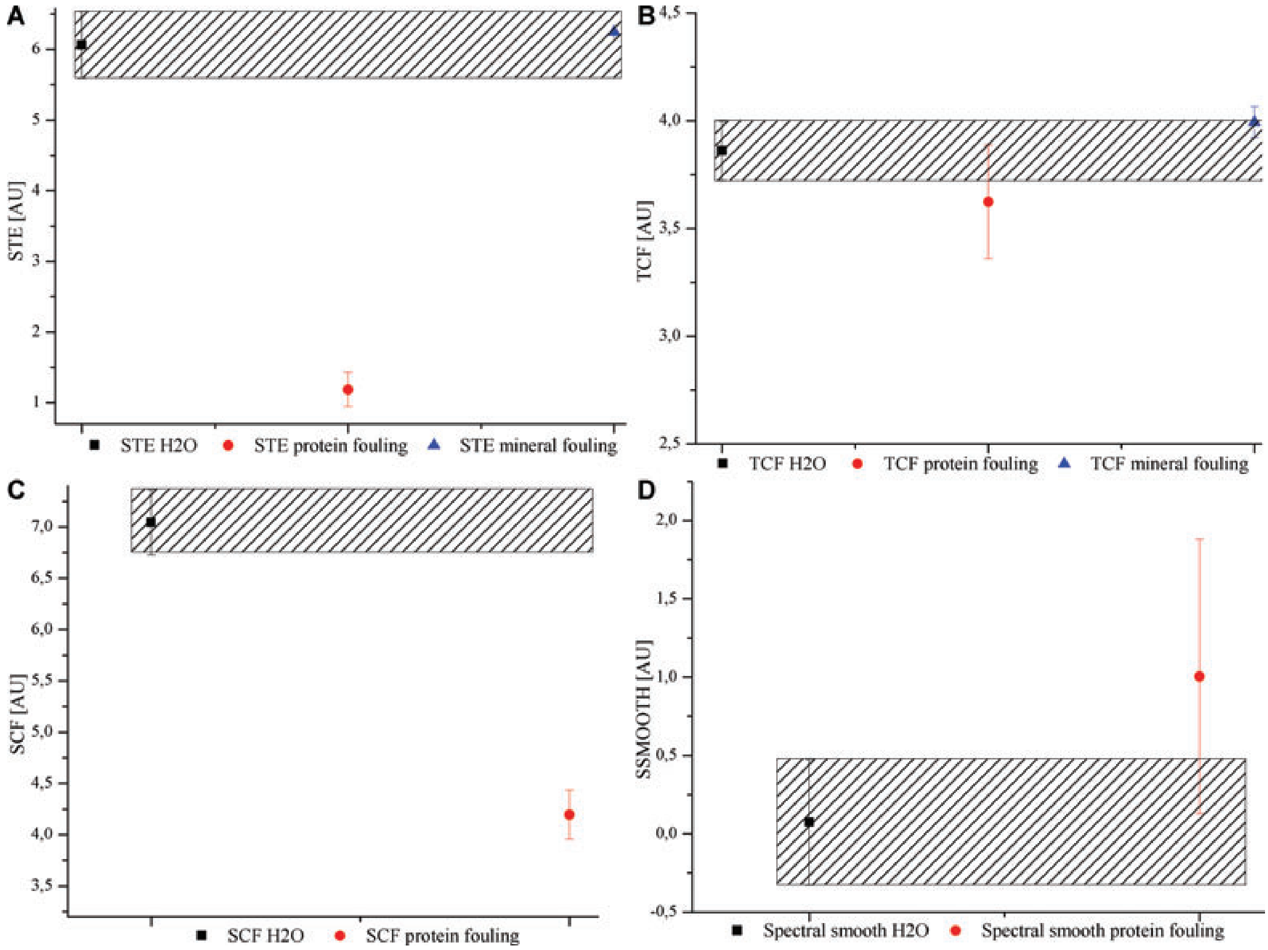

Figure 5. (A) STE of water, protein, and mineral fouling. STE of protein fouling differs significantly from water. (B) TCF of water, protein, and mineral fouling. Protein fouling is easily distinguished from water. (C) SCF and (D) SSMOOTH of water and protein fouling can be distinguished. For mineral fouling, the value is not shown but included in ANN and SVM. Error bars stand for SD.

good. This may be due to higher variations of determined values and less stability of used network.

ANNs are applied for fouling detection in different applications like microfiltration membranes [42] and utility boilers [43]. For heat exchangers, ANN was used successfully for simulation and estimation of fouling usually using inlet/outlet temperatures, mass flow rate, and more as ANN input parameters [44,45]. Even though input parameters based on ultrasonic measurements were used in this study comparison shows good applicability for detection of dairy protein fouling in heat exchangers by ANN. For mineral fouling fewer studies are present and comparison, e.g. with Malayeri and Müller-Steinhagen [46,47] show applicability of ANN for crystallization and $CaSO_4$ fouling formation with similar error range. ANN seems to be better applicable for detection of protein fouling than for mineral fouling with higher accuracy.

3.3.2 *Support vector machine*

As kernel functions homogeneous polynomial of first, second, third, and fourth orders [Eq. (10)] and Gaussian radial basis function [Eq. (11)] were investigated.

$$K(x_i, x) = (x_i \cdot x)^d,\ d = 1, 2, 3... \tag{10}$$

$$K(x_i, x) = \exp(-\gamma \|x_i - x\|^2) \tag{11}$$

Half of the samples were used to design the hyperplane, the other half to validate and test the designed model where model efficiency was found to be dependent on the selected kernel. A polynomial kernel of third order showed highest accuracy for all fouling types as expected from fitting mean data (Supporting information, Fig. 1).

Figure 6 shows exemplary for protein fouling why a polynomial kernel of third order is a good choice. STE and TCF were held fix because they displayed lowest SD and can be considered as constant whereas Z, SCF, and SSMOOTH are plotted. These three features are displayed prior and after multiplication with the kernel function. Prior multiplication using the found third order polynomial kernel no clear separation between fouling and no fouling data is visible due to overlapping of data (Fig. 6A). However, a clear separation between fouling and no

Table 1. Determined features of water, permeate, protein, and mineral fouling together with SD and SEM determined by built-in analysis of variance in origin and experimental error. SCF and SSMOOTH for water is distinguished between protein and mineral fouling

	Water	Protein fouling	Mineral fouling
Z [MRayl]	1.486	1.802	2.277
SD	0.074	0.169	0.636
SE of mean	0.004	0.007	0.042
Exp. error [%]	5	9	28
STE [AU]	6.064	1.184	6.247
SD	0.474	0.242	0.001
SE of mean	0.018	0.016	6.493E-5
Exp. error [%]	8	20	0
TCF [AU]	3.86	3.632	3.993
SD	0.138	0.264	0.072
SE of mean	0.005	0.017	0.004
Exp. error [%]	4	5	2
SCF [AU]	7.043/17.508	4.196	17.291
SD	0.139/1.467	0.239	1.901
SEM	0.017/0.078	0.016	0.107
Exp. error [%]	2/8	6	11
SSMOOTH [AU]	0.073/38.053	1.004	38.076
SD	0.4/1.859	0.875	1.827
SEM	0.022/0.099	0.057	0.103
Exp. error [%]	548/5	87	5

Table 2. Comparison of the accuracy and performance of the SVM and ANN

	SVM accuracy	ANN accuracy	Difference
Protein fouling	100	100	0
Mineral fouling	98.2	93.5	4.7
Both fouling kinds	97.6	71.9	25.7

fouling data is visible after multiplication of the data with the third order polynomial kernel due to data separation. This is shown in Fig. 6B) with no fouling data being framed for easier identification.

Input parameters for the SVM were Z, STE, TCF, SCF, and SSMOOTH and for protein fouling, an accuracy of 100% was determined with 30 support vectors and a bias of 0.49. The SVM for mineral fouling showed an accuracy of 98.2% with 80 support vectors and a bias of 1.98. When both fouling types were combined, SVM accuracy was 97.6% using 116 support vectors and a bias of 1.69 (see Supporting information, Table 2 for comparison of different SVM structures).

SVM is a newly developed technique and often used for classification in computational biology (e.g. [34, 48, 49]) or online monitoring and updating of fault systems [50]. For fouling prediction in heat exchangers SVM was just recently applied for protein fouling [51–53] showing very good results with low errors. As for ANN, input parameters based on different features were used compared with this study. Still, SVM showed low errors and high accuracy making SVM a good tool for detection of mineral and protein fouling.

In Table 2, the accuracy of SVM and ANN are compared. Both methods show comparable results for protein and mineral fouling, respectively, but for the detection of both fouling types SVM is more accurate. SVM displays an accuracy of 97.6% compared with 71.9% of the ANN (difference 25.7%). Protein and mineral fouling are very different in layer structure (thick, spongy for protein; thin, brittle for mineral fouling). This may lead to high variations of calculated features and may introduce errors in detection. SVM seems to deal better with

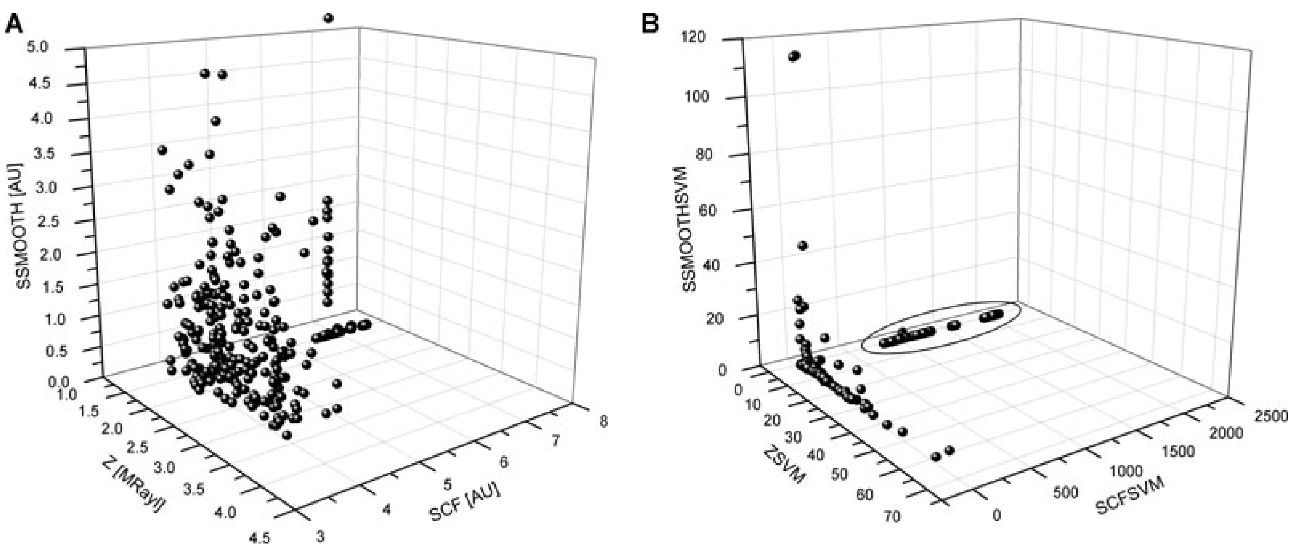

Figure 6. (A) Protein fouling prior multiplication with SVM kernel function where TCF and STE are kept constant because they displayed lowest SD. (B) Protein fouling after multiplication with SVM kernel function (third order polynomial). Fouling and no fouling (framed) data can be clearly separated.

the variation of calculated features because contrary to ANN it finds an absolute maximum of the error function and not a local one. SVM also shows higher stability and seems to be independent of fouling type and thickness compared to ANN. Thus, even though both methods can be used to determine fouling presence SVM seems to be advantageous concerning thin layers.

Both ANN and SVM were shown to be usable for fouling detection with SVM as younger and until now not so often applied method. However, SVM seems to be less prone to data variation and can be used additional to or even as replacement for ANN if necessary.

4 Concluding remarks

In this study, two decision methods were compared for determining fouling presence and absence. Protein fouling from reconstituted milk and mineral fouling from reconstituted permeate was made. ANN and SVM were applied as decision method. Measurements of fouling and no fouling (only water) were made using an ultrasonic transducer. From the ultrasonic signal, five parameters (acoustic impedance, STE, TCF, SCF, SSMOOTH) were extracted and used as input in the ANN and SVM that decided offline if fouling was present or absent. For protein fouling, all chosen features showed statistical significance ($p < 0.0005$) while STE and the spectral features for mineral fouling showed $p > 0.05$. This may be due to very thin fouling layers for mineral fouling (<50 μm) and may change with thicker layers. The ANN was built with one input layer (five neurons), one hidden layer (two neurons), and one neuron in the output layer displaying "1" for fouling presence and "0" for absence, between all layers tangent sigmoid transfer function was applied. The ANN for protein fouling showed an accuracy of nearly 100% (error $2.3 \times 10^{-5\%}$), for mineral fouling the accuracy was 93.5%, and when both fouling types were combined an accuracy of 71.9% was found. Due to the high error of the ANN for combined fouling and longish calculation SVM was used. It classifies data into different groups (fouling/no fouling) with an area around the border without any objects using a kernel function. SVM for protein fouling had an accuracy of 100%, for mineral fouling, it showed an accuracy of 98.2% and when both fouling types were combined, the accuracy was 97.6%.

It was shown that ANN and SVM can be applied for detection of fouling presence and absence. For protein and mineral fouling, both methods show high accuracy and detection stability. When both fouling types are combined as may happen in industry SVM showed a higher accuracy than ANN because of very differing layer occurrence: mineral fouling had only thin, brittle layers whereas for protein fouling thick, spongy layers were present. This led to high variation in parameters and higher complexity of the data. SVM manages this better than ANN and seems to be less dependent on fouling type. All measurements were done static and analysis was done offline that shall be changed to flow measurements and online analysis in future.

Practical application

We present a method to determine dairy protein fouling presence and absence in heat exchangers using a combination of ultrasonic measurements and classification methods such as artificial neural networks and support vector machines. This will help to monitor the cleaning process in a heat exchanger and adapt it if necessary. The change from a fouled to a cleaned heat exchanger can be determined. Adjusting cleaning cycles to fouling amount and type will help to reduce cleaning costs (effluent, cleaning agent, water, temperature), shorten plant down time, and increase production time.

This work was supported by the FEI (Forschungskreis der Ernährungsindustrie), the AiF, and Ministry of Economics and Technology. AIF project number: 16302 N. The authors acknowledge Schwarzwaldmilch GmbH for the provision of skim milk powder and Bayerische Milchindustrie e.G., Landshut, for the permeate powder.

The authors have declared no conflict of interest.

5 References

[1] Burton, H., Section, G., Deposits from whole milk in heat treatment plant-a review and discussion. *J. Dairy Res.* 1968 *35*, 317–330.

[2] Belmar-Beiny, M. T., Gotham, S. M., Paterson, W. R., Fryer, P. J. et al., The effect of Reynolds number and fluid temperature in whey protein fouling. *J. Food Eng.* 1993, *19*, 119–139.

[3] Fryer, P. J., Belmar-Beiny, M. T., Fouling of heat exchangers in the food industry: a chemical engineering prespective. *Trends Food Sci. Technol.* 1991, *2*, 33–37.

[4] Fickak, A., Al-Raisi, A., Chen, X. D., Effect of whey protein concentration on the fouling and cleaning of a heat transfer surface. *J. Food Eng.* 2011, *104*, 323–331.

[5] Law, A. J. R., Leaver, J., Effect of pH on the thermal denaturation of whey proteins in milk. *J. Agric. Food Chem.* 2000, *48*, 672–679.

[6] Bansal, B., Chen, X. D., A critical review of milk fouling in heat exchangers. *Compr. Rev. Food Sci. Food Safety* 2006, *5*, 27–33.

[7] Changani, S. D., Belmar-Beiny, M. T., Fryer, P. J., Engineering and chemical factors associated with fouling and cleaning in milk processing. *Exp. Thermal Fluid Sci.* 1997, *14*, 392–406.

[8] Yang, M., Young, A., Niyetkaliyev, A., Crittenden, B., Modelling the fouling induction period, in: Mueller-Steinhagen, H., Malayeri, M. R., Watkinson, A. P. (Eds.), *Proceedings of International Conference on Heat Exchanger Fouling and Cleaning VIII—2009*, Schladming, Austria 2009, pp. 69–75.

[9] Fryer, P. J., Asteriadou, K., A prototype cleaning map: a classification of industrial cleaning processes. *Trends Food Sci. Technol.* 2009, *20*, 255–262.
[10] Truong, T., Anema, S., Kirkpatrick, K., Chen, H., The use of a heat flux sensor for in-line monitoring of fouling of non-heated surfaces. *Food Bioprod. Process.* 2002, *80*, 260–269.
[11] Perez, L., Ladevie, B., Tochon, P., Batsale, J. C., A new transient thermal fouling probe for cross flow tubular heat exchangers. *Int. J. Heat Mass Tran.* 2009, *52*, 407–414.
[12] Chen, X. D., Li, D. X. Y., Lin, S. X. Q., Özkan, N., On-line fouling/cleaning detection by measuring electric resistance-equipment development and application to milk fouling detection and chemical cleaning monitoring. *J. Food Eng.* 2004, *61*, 181–189.
[13] Ayadi, M. A., Benezech, T., Chopard, F., Berthou, M., Thermal performance of a flat ohmic cell under non-fouling and whey protein fouling conditions. *LWT: Food Sci. Technol.* 2008, *41*, 1073–1081.
[14] Guérin, R., Ronse, G., Bouvier, L., Debreyne, P. et al., Structure and rate of growth of whey protein deposit from in situ electrical conductivity during fouling in a plate heat exchanger. *Chem. Eng. Sci.* 2007, *62*, 1948–1957.
[15] Pereira, A., Mendes, J., Melo, L. F., Using nanovibrations to monitor biofouling. *Biotechnol. Bioeng.* 2008, *99*, 1407–1415.
[16] Silva, J. J. da, Lima, A., Neff, F. H., da Rocha Neto, J. S., Non-invasive fast detection of internal fouling layers in tubes and ducts by acoustic vibration analysis. *IEEE Trans. Instrum. Meas.* 2009, *58*, 108–114.
[17] Merheb, B., Nassar, G., Nongaillard, B., Delaplace, G. et al., Design and performance of a low-frequency non-intrusive acoustic technique for monitoring fouling in plate heat exchangers. *J. Food Sci.* 2007, *82*, 518–527.
[18] Kaptan, Y., Buyruk, E., Ecder, A., Numerical investigation of fouling on cross-flow heat exchanger tubes with conjugated heat transfer approach. *Int. Comm. Heat Mass Tran.* 2008, *35*, 1153–1158.
[19] Sahoo, P. K., Ansari, I. A., Datta, A. K., Milk fouling simulation in helical triple tube heat exchanger. *J. Food Eng.* 2005, *69*, 235–244.
[20] Malayeri, M. R., Müller-Steinhagen, H., Analysis of fouling data based on prior knowledge, *2003 ECI Conference on Heat Exchanger Fouling and Cleaning: Fundamentals and Applications,* Santa Fe, USA 2003.
[21] Schnars, S., Henrich, R., Application of NDT methods on composite structures in aerospace industry. *CDCM* 2006, 1–8.
[22] McHugh, J., Döring, J., Stark, W., Guey, J. L., Relationship between the mechanical and ultrasound properties of polymer materials. *ECNDT* 2006, *11*, 1–9.
[23] Lamberti, N., Ardia, L., Albanese, D., Di Matteo, M., An ultrasound technique for monitoring the alcoholic wine fermentation. *Ultrasonics* 2009, *49*, 94–97.
[24] Dukhin, A. S., Goetz, P. J., Travers, B., Use of ultrasound for characterizing dairy products. *J. Dairy Sci.* 2005, *88*, 1320–1324.
[25] Basheer, I. A., Hajmeer, M., Artificial neural networks: fundamentals, computing, design, and application. *J. Microbiol. Methods* 2000, *43*, 3–31.
[26] Egmont-Petersen, M., de Ridder, D., Handels, H., Image processing with neural networks—a review. *Pattern Recogn.* 2002, *35*, 2279–2301.
[27] Hussein, W. B., Hussein, M. A., Becker, T., Detection of the red palm weevil using its bioacoustics features. *J. Bioacoustics* 2010, *19*, 177–194.
[28] Riverol, C., Napolitano, V., Estimation of fouling in a plate heat exchanger through the application of neural networks. *J. Chem. Technol. Biotechnol.* 2005, *80*, 594–600.
[29] Cortes, C., Vapnik, V., Support-vector networks. *Mach. Learn.* 1995, *20*, 273–297.
[30] Boser, B. E., Guyon, I. M., Vapnik, V. N., A training algorithm for optimal margin classifier, *COLT 92—Proceedings of the Fifth Annual Workshop on Computational Learning Theory*, Pittsburgh, PA, USA 1992, pp. 144–152.
[31] Burges, C. J. C., A tutorial on support vector machines for pattern recognition. *Data Min. Knowl. Disc.* 1998, *2*, 121–167.
[32] Kazuhiro, H., Robust face recognition under partial occlusion based on support vector machine with local Gaussian summation kernel. *Image Vision Comput.* 2008, *26*, 1490–1498.
[33] Grimm, M., Kroschel, K., Narayanan, S., Support vector regression for automatic recognition of spontaneous emotions in speech, *IEEE International Conference on Acoustics, Speech and Signal Processing, 2007.* ICASSP 2007, pp. IV-1085–IV-1088.
[34] Komura, D., Nakamura, H., Tsutsumi, S., Aburatani, H. et al., Multidimensional support vector machines for visualization of gene expression data. *Bioinformatics* 2005, *21*, 439–444.
[35] Qiu, J., Sheffler, W., Baker, D., Noble, W. S., Ranking predicted protein structures with support vector regression. *Proteins* 2008, *71*, 1175–1182.
[36] Wallhäußer, E., Hussein, W. B., Hussein, M. A., Hinrichs, J. et al., On the usage of acoustic properties combined with an artificial neural network—a new approach of determining presence of dairy fouling. *J. Food Eng.* 2011, *103*, 449–456.
[37] Withers, P., Ultrasonic sensor for the detection of fouling in UHT processing plants. *Food Control* 1994, *5*, 67–72.
[38] Nema, P. K., Datta, A. K., Improved milk fouling simulation in a helical triple tube heat exchanger. *Int. J. Heat Mass Tran.* 2006, *49*, 3360–3370.
[39] Ayadi, M. A., Leuliet, J. C., Chopard, F., Berthou, M. et al., Continuous ohmic heating unit under whey protein fouling. *Innov. Food Sci. Emerg. Technol.* 2004, *5*, 465–473.
[40] Visser, J., Jeurnink, T. J. M., Fouling of heat exchangers in the dairy industry. *Exp. Thermal Fluid Sci.* 1997, *14*, 407–424.
[41] Bilaniuk, N., Wong, G. S. K., Speed of sound in pure water as a function of temperature. *JASA* 1993, *93*, 1609–1612.
[42] Liu, Q.-F., Kim, S.-H., Lee, S., Prediction of microfiltration membrane fouling using artificial neural network models. *Sep. Purif. Technol.* 2009, *70*, 96–102.
[43] Teruel, E., Cortes, C., Ignacio Diez, L., Arauzo, I., Monitoring and prediction of fouling in coal-fired utility boilers using neural networks. *Chem. Eng. Sci.* 2005, *60*, 5035–5048.

[44] Riverol, C., Napolitano, V., Estimation of fouling in a plate heat exchanger through the application of neural networks. *J. Chem. Technol. Biotechnol.* 2005, *80*, 594–600.

[45] Lalot, S., Palsson, H., Detection of fouling in a cross-flow heat exchanger using a neural network based technique. *Int. J. Thermal Sci.* 2010, *49*, 675–679.

[46] Malayeri, M. R., Müller-Steinhagen, H., Initiation of $CaSO_4$ scale formation on heat transfer surfaces under pool boiling conditions. *Heat Tran. Eng.* 2007, *28*, 240–247.

[47] Malayeri, M. R., Müller-Steinhagen, H., Intelligent discrimination model to identify influential parameters during crystallisation fouling, *Seventh International conference on Heat Exchanger Fouling and Cleaning—Challenges and Opportunities*, Tomar, Portugal 2007.

[48] Nouretdinov, I., Costafreda, S. G., Gammerman, A., Chervonenkis, A. et al., Machine learning classification with confidence: application of transductive conformal predictors to MRI-based diagnostic and prognostic markers in depression. *Neuroimage 56*, 809–813.

[49] Martin, T. C., Moecks, J., Belooussov, A., Cawthraw, S. et al., Classification of signatures of Bovine Spongiform Encephalopathy in serum using infrared spectroscopy. *Analyst* 2004, *129*, 897–901.

[50] Dehestani, D., Eftekhari, F., Guo, Y., Ling, S. et al., Online support vector machine application for model based fault detection and isolation of HVAC systems. *Int. J. Mach. Learn. Comput.* 2011, *1*, 1–7.

[51] Lingfang, S., Yingying, Z., Rina, S., Fouling prediction of heat exchanger based on genetic optimal SVM algorithm, *International Conference on Genetic and Evolutionary Computing*, Montréal, Canada 2009, pp. 112–116.

[52] Lingfang, S., Yingying, Z., Xinpeng, Z., Shanrang, Y. et al., Research on the fouling prediction of heat exchanger based on support vector machine, *International Conference on Intelligent Computation Technology and Automation*, Changsha, China 2008, pp. 240–244.

[53] Kaneko, H., Inasawa, S., Inokuchi, H., Funatsu, K., Construction of high predictive fouling models using statistical methods, in: Mueller-Steinhagen, H., Malayeri, M. R., Watkinson, A. P. (Eds.), *Proceedings of International Conference on Heat Exchanger Fouling and Cleaning VIII*, Schladming, Austria 2009, pp. 260–262.

5.2.4. "Investigating and understanding fouling in a planar setup using ultrasonic methods", E. Wallhäußer, M.A. Hussein, T. Becker; Review of Scientific Instruments 83 (2012), 094904-01-094914-10

AIP | Review of Scientific Instruments

Investigating and understanding fouling in a planar setup using ultrasonic methods

E. Wallhäußer, M. A. Hussein, and T. Becker

Citation: Rev. Sci. Instrum. **83**, 094904 (2012); doi: 10.1063/1.4753992
View online: http://dx.doi.org/10.1063/1.4753992
View Table of Contents: http://rsi.aip.org/resource/1/RSINAK/v83/i9
Published by the American Institute of Physics.

Investigating and understanding fouling in a planar setup using ultrasonic methods

E. Wallhäußer,[a)] M. A. Hussein, and T. Becker
(Bio-)Process Technology and Process Analysis, Life Science Engineering, Technische Universitaet Muenchen, Weihenstephaner Steig 20, 85354 Freising, Germany

(Received 28 June 2012; accepted 5 September 2012; published online 26 September 2012)

Fouling is an unwanted deposit on heat transfer surfaces and occurs regularly in foodstuff heat exchangers. Fouling causes high costs because cleaning of heat exchangers has to be carried out and cleaning success cannot easily be monitored. Thus, used cleaning cycles in foodstuff industry are usually too long leading to high costs. In this paper, a setup is described with which it is possible, first, to produce dairy protein fouling similar to the one found in industrial heat exchangers and, second, to detect the presence and absence of such fouling using an ultrasonic based measuring method. The developed setup resembles a planar heat exchanger in which fouling can be made and cleaned reproducible. Fouling presence, absence, and cleaning progress can be monitored by using an ultrasonic detection unit. The setup is described theoretically based on electrical and mechanical lumped circuits to derive the wave equation and the transfer function to perform a sensitivity analysis. Sensitivity analysis was done to determine influencing quantities and showed that fouling is measurable. Also, first experimental results are compared with results from sensitivity analysis. [http://dx.doi.org/10.1063/1.4753992]

NOMENCLATURE

b	=	damping constant
B	=	blockage factor
C	=	capacity
c_0	=	sound velocity
d	=	thickness
e_{33}	=	piezoelectric constant in direction 33
E	=	Young's modulus
f	=	function
F	=	force
G	=	Laplace transformed
I	=	current
k	=	spring constant
k	=	wave vector
KLM	=	Krimholtz, Leedom, Mattaei
KV	=	Kelvin-Voigt
L	=	inductance
m	=	mass
M	=	matrix/matrix element
Δp	=	pressure drop
R	=	resistance
Re	=	Reynold's number
s	=	parameter
t	=	time
TF	=	transfer function
U	=	voltage
v	=	velocity
V	=	voltage
x	=	value
Δx	=	variance of x
X	=	Laplace transformed x
Z	=	impedance

Greek

δ	=	damping factor
$\varepsilon^s{}_{33}$	=	permittivity at constant strain in direction 33
η	=	strain
λ	=	friction factor
ν	=	frequency
θ	=	length times wave vector
π	=	pi factor
σ	=	stress
ω	=	angular frequency
ω	=	frequency

Subscripts

0	=	incident
1–4	=	number of part
ac	=	acoustic
B	=	backing
delay	=	delay line
el	=	electric
fouling	=	fouling layer
ges	=	overall (gesamt)
i	=	counter
liquid	=	liquid
medium	=	medium
n	=	counter
US	=	ultrasound
wall	=	wall

I. INTRODUCTION

In dairy industry, milk is heated to extend shelf life and to reduce microbiological hazards. Temperatures around 75 °C

a)Author to whom correspondence should be addressed. Electronic mail: e.wallhaeusser@wzw.tum.de. Tel.: 0049-(0)8161-71-2623. Fax: 0049-(0)8161-71-3883.

(pasteurization) and above 130 °C (ultra-high-temperature processing) are used. The protein β-lactoglobulin starts to denaturate and aggregate when heated above 70 °C (protein fouling) and salts start to precipitate above 110 °C (mineral fouling).[1–3] As a result, a solid layer composed of proteins and salts develops on the heat transfer wall. This decreases heat transfer and increases costs,[4] leads to possible heat exchanger damage, and results in unavoidable cleaning.[2,5,6] Different methods were developed to detect fouling and to supervise cleaning to reduce both costs and risks for heat exchangers. These methods are based on different methods like heat flux,[7–9] electrical and thermal resistance,[10] nano-vibrations,[11,12] and ultrasound.[13,14]

Ultrasound is sound with frequencies between 20 kHz and 2 GHz and can be used non-destructively in food processes,[15–21] medical application,[22–26] and non-destructive testing.[27–30] Ultrasound is a well-known technique and often used when opaque materials are present where visible light cannot be applied. Ultrasound generation is based on the piezoelectric effect and can be described in both mechanical and electrical ways using lumped circuits[31–34] or port notation.[35–40] These descriptions can be used to determine the wave equation of a system as well as to model ultrasonic systems based on integrated circuits[41–44] or finite elements.[45–47] Different models of an ultrasonic transducer using lumped circuits and port notation are shortly presented. Van Dyke model[32] is a straightforward model and often used to describe the behaviour of an ultrasonic transducer, but it holds only near resonance frequency due to its simplicity. Mason[33] presented an electromechanical representation of a piezoactive material using three port theory (one electrical, two acoustical ports) where the representation includes a transformer for the connection between the mechanical and the electrical part. It is more complex and includes a negative resistance but allows to model the behaviour of a piezoplate in more detail at many different frequencies. Redwood[48] showed that this negative resistance can be transferred to the mechanical part of the three port while the remaining model stayed the same. Krimholtz, Leedom, and Mattaei[34] developed another three port with a different description of the electrical transducer port and excluded the negative resistance (KLM model). It can be easily used to model piezoelectric behaviour across a wide range of frequencies. Mason and KLM model show comparable results when compared also when losses are introduced in the model.[49] Here, due to the demand of matching the ultrasonic transducer to the load, KLM model was chosen to describe the electromechanical part of the ultrasonic transducer. A purely mechanical or electrical description of an ultrasonic setup can also be done using mechanical and electrical components. Starting from electrical and mechanical lumped circuits, a sensitivity analysis can be performed to determine the parameters with highest influence on the ultrasonic signal. Sensitivity analysis can be used to determine the influence of different parameters and the variance of output due to input variation.[50,51]

II. LUMPED CIRCUITS

An ultrasonic transducer (electromechanical part) as well as every other mechanical part of the setup can be described with electrical and mechanical circuits, respectively. The circuits together with their wave equations are shortly presented. Using the wave equation, the system can be modeled and described in detail, and the system answer to different stimuli can be found. The following system was considered: ultrasonic transducer (1), delay line (2), stainless steel wall (3), fouling (4). Coupling was not included in the calculation even though it plays a role in experiments for introducing a sound wave into the medium. The lumped circuits can be used for sensitivity analysis to determine the influence of the parameters.

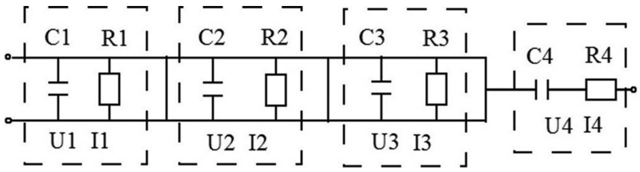

FIG. 1. Electrical circuit to describe the system transducer (1)—delay line, (2)—wall, (3)—fouling, (4) with resistors R_i, capacitors C_i, voltage U_i, and current I_i of every subcircuit i.

A. Electrical circuit description

An ultrasonic transducer as well as every part of the setup can be described by its equivalent electrical circuit. The setup can be circumscribed with the electrical circuit shown in Fig. 1 (inductors are not displayed but included in calculation). For solids, the Kelvin-Voigt model was used (1)–(3), whereas for fouling the Maxwell model was applied[52] (4).

The wave equation for voltage U_{ges} of the circuit with overall resistivity R_{ges}, overall capacity C_{ges}, and overall inductance L_{ges} was found to be

$$U_{ges}(t) + R_{ges} \cdot C_{ges} \cdot \dot{U}_{ges}(t) + L_{ges} \cdot C_{ges} \cdot \ddot{U}_{ges}(t) = 0 \tag{1}$$

with

$$U_{ges} = U_{KV} + U_4, R_{ges} = R_{KV} + R_4, \frac{1}{C_{ges}} = \frac{1}{C_{KV}} + \frac{1}{C_4},$$

$$L_{ges} = L_{KV} + L_4, \tag{2}$$

where for the solid parts (1)-(3) (Kelvin-Voigt, KV) $U_{KV} = U_1 = U_2 = U_3$, $C_{KV} = C_1 + C_2 + C_3$, $1/R_{KV} = 1/R_1 + 1/R_2 + 1/R_3$, and $1/L_{KV} = 1/L_1 + 1/L_2 + 1/L_3$.

Using Kirchhoff's circuit laws, Eq. (1) can be solved and gives for $R_{ges}^2/4L_{ges}^2 < 1/(L_{ges} \cdot C_{ges})$

$$U(t) = U_0 \cdot \exp(-\delta t) \cdot (\cos \omega t + \delta/\omega \cdot \sin \omega t). \tag{3}$$

Where damping factor δ and frequency ω are defined as

$$\delta = \frac{R_{ges}}{C_{ges}} \text{ and } \omega = \sqrt{\frac{1}{L_{ges} \cdot C_{ges}} - \frac{R_{ges}^2}{4L_{ges}^2}}. \tag{4}$$

B. Mechanical circuit description

The setup can also be described with a mechanical circuit (see Fig. 2). Masses are not displayed but included in calculation.

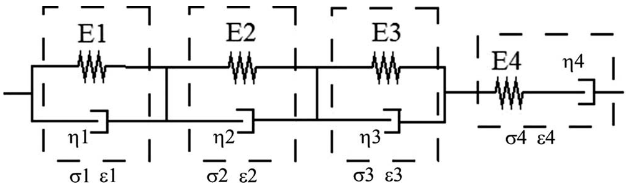

FIG. 2. Mechanical circuit of the system transducer (1)—delay line, (2)—steel wall, (3)—fouling, (4) using springs E_i, dashpots η_i, stress σ_i, and strain ε_i for every subcircuit i.

The mechanical wave equation is determined using a combination of Kelvin-Voigt chain for solids and Burger model for fouling. The result is

$$\sigma_{ges}(t) + \eta_{ges} \cdot E_{ges} \cdot \dot{\sigma}_{ges}(t) + m_{ges} \cdot E_{ges} \cdot \ddot{\sigma}_{ges}(t) = 0. \tag{5}$$

With overall stress $\sigma_{ges} = \sigma_1 = \ldots = \sigma_4$, overall strain $\eta_{ges} = \sum_{i=1}^{4} \eta_i$, overall Young's modulus $1/E_{ges} = \sum_{i=1}^{4} 1/E_i$, and overall mass $m_{ges} = \sum_{i=1}^{4} m_i$, the solution is

$$\sigma(t) = \sigma_0 \cdot \exp(-\delta \cdot t) \cdot (\cos \omega \cdot t + \delta/\omega \cdot \sin \omega \cdot t). \tag{6}$$

Where the damping factor δ and frequency ω are

$$\delta = \frac{\eta_{ges}}{2m_{ges}} \text{ and } \omega = \sqrt{\frac{E_{ges}}{m_{ges}}}. \tag{7}$$

So, a transfer function between the input and output of the system can be found.

III. SENSITIVITY ANALYSIS

Sensitivity analysis helps to understand the influence of input parameters on output parameters and can be used to improve a setup by identifying possible error sources. It varies the quantities of interest to determine the weight and thus the impact of a quantity on the system investigated and helps to find out if the quantity of interest is measurable. There are different ways to calculate the weights, here, central difference equation was chosen.

A. Port notation

Port notation can be used to describe the setup. An equivalent circuit model for the ultrasonic transducer is applied (KLM model). The ultrasonic transducer is described with an electromechanical three port. With fixed backing impedance, Z_b, the three port is reduced to a series of two ports, one electromechanical, one purely mechanical. The description of the electromechanical two port matrix follows Higuti *et al.*[40] All passive parts are considered as transmission lines where the two port matrix is defined by port thickness.[47] Figure 3 shows the used three port for the ultrasonic transducer.

The considered structure is composed of an ultrasonic transducer, a voltage source, a delay line, a stainless steel wall, fouling, water, a second stainless steel wall, and air (compare with Fig. 4). The transducer is divided into backing (sheer resistance) and piezoplate, which is described by one electromechanical and one mechanical two port. All other two ports are purely mechanical.

B. Sensitivity analysis of the electrical circuit following port notation

The parts are connected in series giving a transfer matrix M describing the transformation from the electrical (voltage V, current I) to the mechanical part (force F, velocity v),

$$\begin{bmatrix} V \\ I \end{bmatrix} = \underline{\underline{M}} \begin{bmatrix} F \\ v \end{bmatrix}. \tag{8}$$

The matrix M for fouling presence is found by multiplication of the matrices of all two ports,

$$\underline{\underline{M}} = \prod_i \underline{\underline{M}}_i = \underline{\underline{M}}_{US} \cdot \underline{\underline{M}}_{delay} \cdot \underline{\underline{M}}_{wall1} \cdot \underline{\underline{M}}_{fouling} \cdot \underline{\underline{M}}_{medium} \cdot \underline{\underline{M}}_{wall2}. \tag{9}$$

The electromechanical two port matrix of the ultrasonic transducer follows Higuti *et al.*[40] Abbreviations are explained in

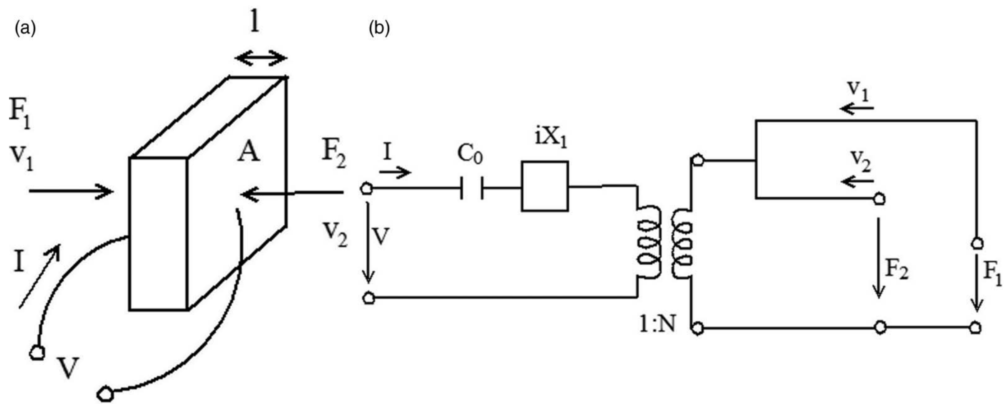

FIG. 3. Three port notation of an ultrasonic transducer. (a) The forces $F_{1,2}$ and velocities $v_{1,2}$ at the surfaces of the transducer with area A and thickness l are connected with the electrical port (voltage V, current I). (b) KLM model with capacitance C_0, reactance X_1, and transformer (ratio 1:N) from the electrical to the mechanical part.

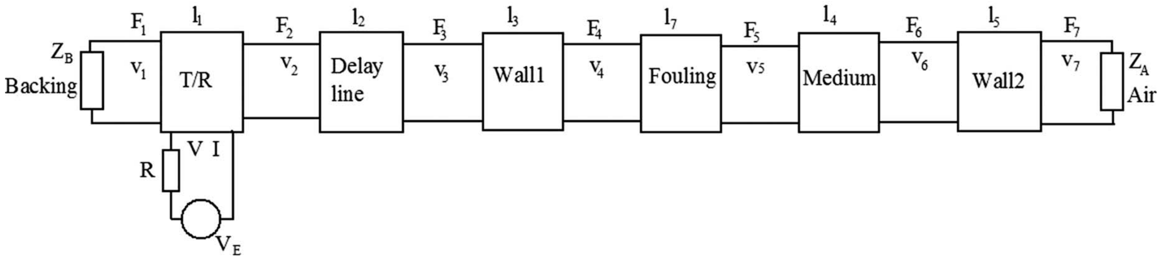

FIG. 4. Used ports for description of the equivalent circuits: Setup with fouling.

the Appendix.

$$\underline{\underline{M}}_{US} = \begin{bmatrix} M_{11} & M_{12} \\ M_{21} & M_{22} \end{bmatrix} \text{with}$$

$$\begin{aligned}
M_{11} &= \frac{\varepsilon_{33}^S}{e_{33}c_0} \cdot \frac{\cos\theta + i\varsigma\sin\theta}{\cos\theta - 1 + i\varsigma\sin\theta} - \frac{e_{33}}{i\omega\varepsilon_{33}^S} \\
&\quad \cdot \frac{\sin\theta}{\cos\theta - 1 + i\varsigma\sin\theta}, \\
M_{12} &= \frac{-e_{33}}{i\omega\varepsilon_{33}^S} \cdot \frac{2(\cos\theta - 1) + i\varsigma\sin\theta}{\cos\theta - 1 + i\varsigma\sin\theta} + \frac{\varepsilon_{33}^S}{e_{33}c_0} \\
&\quad \cdot \frac{Z_B(\varsigma\cos\theta + i\sin\theta)}{\cos\theta - 1 + i\varsigma\sin\theta}, \\
M_{21} &= \frac{i\omega\varepsilon_{33}^S}{e_{33}} \cdot \frac{\cos\theta + i\varsigma\sin\theta}{\cos\theta - 1 + i\varsigma\sin\theta}, \; M_{22} = \frac{i\omega\varepsilon_{33}^S}{e_{33}} \\
&\quad \cdot \frac{Z_0(\varsigma\cos\theta + i\sin\theta)}{\cos\theta - 1 + i\varsigma\sin\theta}.
\end{aligned} \tag{10}$$

The matrix for every passive layer i (only mechanical ports, according to Lerch *et al.*[53]) is

$$\begin{bmatrix} F_i \\ v_i \end{bmatrix} = \begin{bmatrix} \cosh kl & Z\sinh kl \\ (\sinh kl)/Z & \cosh kl \end{bmatrix} \begin{bmatrix} F_j \\ v_j \end{bmatrix}. \tag{11}$$

If fouling is present, the matrix elements M_{ij} of the overall transfer matrix M are

$$\begin{aligned}
M_{11} &= \left(\frac{b\cdot c}{a} - \frac{d}{a}\sin\theta_{US}\right)\cdot\Gamma - \left(\frac{d\cdot g}{a} + \frac{b\cdot e}{a}Z_{US}\right)\cdot\Omega, \\
M_{12} &= \left(\frac{b\cdot c}{a} - \frac{d}{a}\sin\theta_{US}\right)\cdot\Xi - \left(\frac{d\cdot g}{a} - \frac{b\cdot e}{a}Z_{US}\right)\cdot\Upsilon, \\
M_{21} &= \frac{f\cdot c}{a}\cdot\Gamma + \frac{f\cdot e}{a}Z_{US}\cdot\Omega, \\
M_{22} &= \frac{f\cdot c}{a}\cdot\Xi + \frac{f\cdot e}{a}Z_{US}\cdot\Upsilon,
\end{aligned} \tag{12}$$

TABLE I. Parameters used for the sensitivity analysis of the electrical circuit.

Parameter	Mean	Unit	Parameter	Mean	Unit
Z_{ac}	72.192×10^5	Pa	θ_{US}	2.92	...
Z_{el}	9	Ω	θ_{delay}	148.93	...
Z_B	14×10^6	Rayl	θ_{wall}	2.2	...
Z_{US}	22.5×10^6	Rayl	$\theta_{fouling}$	3.14	...
Z_{delay}	32×10^6	Rayl	θ_{liquid}	99.69	...
Z_{wall}	40.1×10^6	Rayl	$\varepsilon^S{}_{33}$	1400	F/m
$Z_{fouling}$	2.1×10^6	Rayl	e_{33}	15×10^{-12}	m^2/N
Z_{liquid}	1.5×10^6	Rayl	c_0	4300	m/s

where $\theta_{US} = k \cdot d_{US}$ with k as wave number and d_{US} as ultrasonic (*US*) transducer thickness. The long writing for the abbreviations can be found in the Appendix.

The transfer function (TF_{el}) of pulse echo mode can be described with the multiplication of the one for the emitting (TF_{FV}) and the receiving transducer (TF_{VF}).

$$\begin{aligned}
TF_{el} &= TF_{FV} \cdot TF_{VF} \\
&= \frac{Z_{ac}\cdot Z_{el}}{(M_{11}Z_{el} + M_{12} + M_{21}Z_{ac}Z_{el} + M_{22}Z_{ac})^2}.
\end{aligned} \tag{13}$$

From TF_{el}, derivatives with respect to the chosen parameters are made. These parameters are presented in Table I with a chosen variation for every parameter of ±5%.

Concerning the parameters, a sensitivity analysis was done and central difference equation was used to calculate the parameter weights.

$$\frac{\partial f(x_n)}{\partial x_n} = \frac{f(x_{n+1}) - f(x_{n-1})}{2\cdot\Delta x}. \tag{14}$$

Here, $f(x_n)$ resembles *TF* at one parameter. The variance δx is ±5% of this value. With Eq. (14), the weight Δx of every parameter is calculated and its influence is determined.

C. Sensitivity analysis of the mechanical circuit

Sensitivity analysis was done for the mechanical description by writing x instead of σ and the transfer function (*TF*) was found by substituting $E_{ges} = 1/k$, $\eta_{ges} = b$, $x_1 = x$, and $x_2 = \dot{x}$.

$$m\cdot\ddot{x} + b\cdot\dot{x} + k\cdot x = F \rightarrow m\cdot\dot{x}_2 + b\cdot x_2 + k\cdot x_1 = F. \tag{15}$$

TABLE II. Parameters used for the sensitivity analysis of the mechanical circuit.

Parameter	Mean value	Unit	Parameter	Mean value	Unit
m_1	100.0×10^{-3}	kg	E_4	4.86×10^9	Pa
m_2	38.6×10^{-3}	kg	η_0	4.95×10^3	Pa
m_3	32.2×10^{-3}	kg	η_1	1.47×10^{10}	Pa
m_4	4.0×10^{-3}	kg	η_2	8.60×10^8	Pa
E_1	1.47×10^{11}	Pa	η_3	2.65×10^{10}	Pa
E_2	8.60×10^9	Pa	η_4	4.86×10^8	Pa
E_3	2.65×10^{11}	Pa			

Thus,

$$\begin{pmatrix} \dot{x}_1 \\ \dot{x}_2 \end{pmatrix} = \begin{pmatrix} 0 & 1 \\ -k/m & -b/m \end{pmatrix} \cdot \begin{pmatrix} x_1 \\ x_2 \end{pmatrix} + \begin{pmatrix} 0 \\ 1/m \end{pmatrix} \cdot F. \tag{16}$$

With this, TF_{mech} is found

$$TF_{\mathrm{mech}} = \frac{Z_m^2}{\left(mZ_m^2 - Z_m b - k\right)^2} \tag{17}$$

with

$$Z_m = \frac{\omega \cdot \eta_{ges} - i(E_1 + E_2 + E_3 + E_4)}{\eta_4 \omega E_4 (i\omega^3 \alpha_m + \omega^2(\beta_m E_3 + \delta_m E_1) + \omega(\gamma_m E_2 - i\eta_3\lambda - i\eta_1\mu_m - i\eta_2\nu_m) - \pi_m)}, \tag{18}$$

where $\omega = 2\pi\nu$, $\alpha_m = \eta_1\eta_2\eta_3$, $\beta_m = \eta_1\eta_2$, $\delta_m = \eta_2\eta_3$, $\gamma_m = \eta_1\eta_3$, $\lambda_m = E_1E_2$, $\mu_m = E_2E_3$, $\nu_m = E_1E_3$, and $\pi_m = E_1E_2E_3$.

Besides, Laplace transformation can be used to determine the *TF*. With $\dot{x}(t) = s \cdot X(s)$,

$$\begin{aligned} & m \cdot s^2 \cdot X(s) + b \cdot s \cdot X(s) + k \cdot X(s) = F(s) \\ & \rightarrow G(s) = \frac{input}{output} = \frac{s}{m \cdot s^2 + b \cdot s + k}. \end{aligned} \tag{19}$$

Back transformation and the fact that the transducer serves as emitter and receiver gives the same TF_{mech} as in Eq. (17). Sensitivity analysis was done concerning the parameters shown in Table II with a variation of ±5%.

E stands for the real part of Young's modulus describing the elastic part and η is the imaginary part including the viscous part of a material. η_0 describes the transducer backing (only damping considered). For sensitivity analysis, Eq. (14) was applied.

IV. EXPERIMENT

An experimental setup was constructed to test the predictions from sensitivity analysis and to produce and measure fouling presence and absence. The setup was also compared with industrial heat exchangers.

A. Experimental setup

The experimental setup consists of an ultrasonic transducer with a resonance frequency of 2.2 ± 0.1 MHz and an epoxy-tungsten backing in a polyoxymethylene housing. It is used in pulse echo mode and attached to a delay line made of polymethyl methacrylate (PMMA), which is affixed to a rectangular stainless steel channel (498 × 94 × 32 mm, wall thickness 2 mm, Fig. 5). The excitation is carried out via in-house electronics and measurements are done using the program Virtual Expert on a personal computer. The ultrasonic transducer was coupled to the PMMA delay line (length 30 mm) using a water-based coupling gel from AB Angelika Busch (UCA-2M). This is the ultrasonic measuring section and it is pressed on the rectangular channel using a spring (Federnshop Bayern, V2A). Solid coupling is used (thickness 2 mm, Aqualene™, Olympus) between delay line and wall. A rectangular channel was chosen because no refraction due to curved surfaces has to be taken into account.

The rectangular channel is connected with two connections to hot water hoses (DN 20). With an adjustable pump (Nirostar 2000-A/PT, ZUWA-Pumpe GmbH), a liquid (water, milk) can be pumped through the piping, the planar channel and a feed tank (20l). The rectangular channel is heatable using an electrical heating band (ELWA-VA, 6.0, 294 W) and the liquid can be heated in the feed tank via a heating rod (1000 W @ 220 V) to produce dairy fouling and measure water at different temperatures.

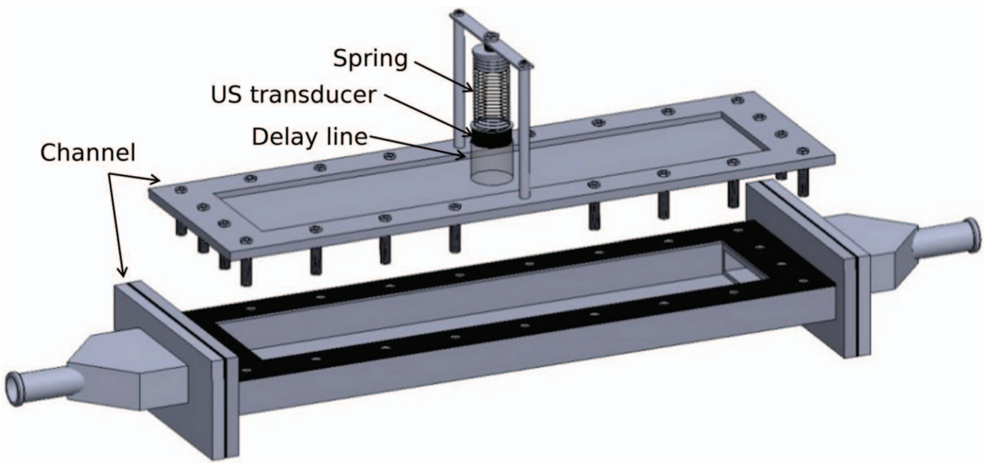

FIG. 5. Sketch of the flow channel where fouling is produced with the ultrasonic detection unit.

TABLE III. Comparison of different fluid dynamic parameters.

Factor	Industry scale	Lab scale	Industry/lab ratio
Blockage factor B	1.085	1.006	1.078
Friction coefficient λ	1.899×10^{-2}	2.293×10^{-2}	0.827
Pi parameter π_1	0.154	1.538×10^{-2}	10
Pi parameter π_2	0.247	1.716×10^{-2}	13.849
Pressure drop Δp	2.256×10^4	2.531×10^3	8.915
Reynolds number *Re*	7.703×10^4	3.628×10^4	2.436

Sensitivity analysis (SA) can be used to improve the setup, e.g., the ultrasonic measuring unit. It helps to determine influencing parameters on the ultrasonic signal such that they can be overcome by hardware or software adaption during measuring and signal preparation for analysis. SA was used to estimate the influence of the different setup parts on the ultrasonic signal and to see if it is possible to measure fouling presence and absence.

B. Comparing the experimental setup and an industrial heat exchanger

The developed measuring section and an industrial monotube heat exchanger with same length as the measuring section are compared to determine the adequacy of the developed setup concerning fouling build-up using different factors (blockage factor, Reynolds number, non-dimensional π parameters, friction coefficient (after Ref. 54), pressure drop). Blockage factor includes information about how strongly a channel is blocked, friction coefficient is the friction loss during pipe flow, Reynolds number can be used to compare flow behaviour, and pressure drop can be applied to compare pressure loss during flow. π_1 is similar to Biot number and π_2 describes the heat transfer together with mass flow rate. The used equations and values can be found in the Appendix. The results are displayed in Table III.

Blockage factor and friction coefficient are nearly the same for both setups, thus, the setups behave similarly concerning channel blockage and friction loss. Both Reynolds number and pressure drop of the industrial heat exchanger are higher showing a higher pressure drop for an industrial heat exchanger, and Reynolds number is in the same order of magnitude compared, thus, the fouling is made under similar flow conditions. Both non-dimensional π-parameters are ca. 10 times bigger for industry leading to a higher heat transfer. This does not alter fouling composition but may lead to different fouling times and thicknesses. From this, it can be concluded that the developed setup and an industrial monotube heat exchanger are comparable which should result in similar fouling layers. It has to be kept in mind that different scale ups have to be considered regarding the lab scale heat exchanger.

C. Experimental procedure

The setup can be used to produce dairy protein fouling similar to the one found in industrial heat exchangers and to determine the phase transition of a material from liquid to solid (fouling) and reverse (cleaning). Measurements are done using an ultrasonic measuring section. Reconstituted skim milk (15 kg) was produced by dissolving skim milk powder (Schwarzwaldmilch GmbH) in water (40 ± 2 °C) for 10 min using a stirrer. Milk (protein content 7.2%) was pumped in circulation ($\dot{V} = 4.07 l/\min$) and heated up to 76 ± 2 °C (140 ± 0.5 °C on top plate) and held for 5 h. Then, the heating band was removed. After cooling down the planar channel for 15 min (fluid temperature 62 ± 1 °C), the ultrasonic measuring section was attached and measurements were done every 20 s for 30 min (fluid temperature 56 ± 1 °C at the end, ultrasonic measuring section 28 ± 1 °C). The transducer was excited with 40 V and 17.5 kHz were used as sampling frequency. Water at 60 ± 1 °C was measured with the same pump settings as reference. Generated fouling was similar to the one in dairy industry making the measurements comparable.

V. RESULTS AND DISCUSSION

The results for SA of the electrical and the mechanical lumped circuits will be presented and compared. Then, experimental results will be shown and compared with SA results.

A. Sensitivity analysis for the electrical circuit

The weight Δx of every parameter was calculated using Eq. (14) providing information about the influence of an input parameter on the ultrasonic signal. The ranking for the weights of the electrical circuit is displayed in Table IV.

Highest weight is seen for delay line thickness Θ_{delay} and characteristic acoustic impedance of the wall Z_{wall} where former influences the amount of signal transmitted to the

TABLE IV. Ranking of the weights from the sensitivity analysis for the electrical circuit.

Rank	Parameter	Weight	Weight/mean	Rank	Parameter	Weight	Weight/mean
1	θ_{delay}	1.96×10^7	1.32×10^5	9	Z_{ac}	1.44×10^4	1.99×10^{-3}
2	Z_{wall}	1.60×10^7	3.99×10^{-1}	10	e_{33}	278.58	1.86×10^{13}
3	θ_{liquid}	7.62×10^6	7.64×10^4	11	θ_{US}	0.75	2.57×10^{-1}
4	Z_{US}	4.50×10^6	2×10^{-1}	12	$\theta_{fouling}$	0.64	2.04×10^{-1}
5	Z_B	2.80×10^6	2×10^{-1}	13	θ_{wall}	0.46	1.09×10^{-1}
6	Z_{delay}	6.40×10^5	2×10^{-2}	14	Z_{el}	3.90×10^{-3}	4.33×10^{-4}
7	$Z_{fouling}$	4.43×10^5	1.46×10^{-1}	15	$\varepsilon^S{}_{33}$	2.99×10^{-12}	2.14×10^{-15}
8	Z_{liquid}	3.06×10^5	2.04×10^{-1}	16	c_0	8.63×10^{-15}	2.01×10^{-18}

TABLE V. Ranking of the weights from the sensitivity analysis of the mechanical circuit.

Rank	Parameter	Weight	Weight/mean	Rank	Parameter	Weight	Weight/mean
1	η_1	1.05×10^9	7.14×10^{-2}	8	η_4	9.44×10^7	1.94×10^{-1}
2	E_3	6.33×10^8	2.39×10^{-3}	9	m_1	2.0×10^{-2}	2×10^{-1}
3	η_3	5.73×10^8	2.16×10^{-2}	10	m_3	6.4×10^{-3}	1.99×10^{-1}
4	E_1	4.00×10^8	2.72×10^{-3}	11	m_2	7.6×10^{-3}	1.97×10^{-1}
5	E_4	3.53×10^8	7.26×10^{-2}	12	m_4	8.0×10^{-4}	2×10^{-1}
6	E_2	2.54×10^8	2.95×10^{-2}	13	η_0	6.53×10^{-8}	1.32×10^{-11}
7	η_2	1.63×10^8	1.89×10^{-1}				

measuring section and latter ultrasonic behaviour at the interface. Also, characteristic acoustic impedances of the ultrasonic transducer Z_{US}, backing Z_B, delay line Z_{delay}, and liquid Z_{liquid} show high weights. However, all of these parameters should stay nearly constant varying less than during SA and thus can be considered as negligible on ultrasonic signal (as long as variations are not too high). The acoustic impedance of the setup Z_{ac} is also considered as constant during measurements and thus negligible. Thickness of the liquid behind the fouling layer Θ_{liquid} shows a high influence if thick fouling layers (above 500 μm) are present which change Θ_{liquid} strongly and is usually not the case. Surprisingly, the material parameters of the piezoplate, which govern the production of the ultrasonic wave show only low weight, which was not expected.

The parameters for fouling show different results: whereas layer thickness Θ_{fouling} shows only low weight, characteristic acoustic impedance of fouling $Z_{fouling}$ displays a high weight on the ultrasonic signal. Fouling is not present at the beginning of a production cycle, develops during production, and disappears again during cleaning (as does its characteristic impedance) from which it follows that it is possible to determine fouling presence and absence during cleaning.

The thicknesses regulate how much wave energy is lost during the travel. Thus, delay line thickness is important for the complete ultrasonic signal but the influence during measuring is negligible because thickness change during measurements at constant temperature is nil. The same is true for thickness of liquid behind the fouling layer because it is only affected if fouling thickness is high. Acoustic impedance of different materials determines reflection and transmission at interfaces and signal shape. The former is used to determine fouling presence and absence at the interface stainless steel wall-measuring section because when fouling presence changes so does the acoustic impedance and reflection coefficient at this interface, while all other acoustic impedances stay constant if temperature stays constant. If this is not the case, influences particularly from the delay line are present. From the characteristic acoustic impedance $Z_{fouling,}$ it is visible that fouling presence and absence should be detectable.

B. Sensitivity analysis for the mechanical circuit

The weights for the parameters of the mechanical circuit (Fig. 2) are calculated and the ranking is shown in Table V.

The highest weight is displayed by η_1 of the piezoplate, which determines the damping of the ultrasonic wave inside the plate. Also, its elastic counterpart E_1 and the elastic and viscous part of the stainless steel wall (E_3, η_3) and of the delay line (E_2, η_2) have high weights. These parameters should stay roughly constant during measurement and thus can be neglected and subtracted out of the signal influences. As can be seen, also the elastic and viscous part of the fouling layer (E_4, η_4) shows high weights. This can be used to determine the presence and absence of fouling because both parameters are not present on a clean but only at a fouled surface. The masses $m_{1\text{-}4}$ do not seem to have any influence on the ultrasonic signal. E describes the material answer and can be compared with the spring constant, the higher it is the higher is the material resistance to the deformation. This will change significantly if fouling develops. η on the other side governs the signal loss due to damping.

Comparing both SA, it is seen that the mechanical and acoustic parameters E, η, and Z influence the signal strongly. Characteristic acoustic impedance Z and real part of Young's modulus E are comparable because both describe the answer of a material to the travelling sound wave. For both, high weights for the piezoplate, stainless steel plate, and delay line were expected and found. Z also gives information about interfaces between two materials and changes at these interfaces. Imaginary part η and "thickness" Θ both contain information about signal loss where Θ includes not only thickness but also the wave vector. Losses should never be underestimated because they determine the amount of signal received and thus the detection accuracy and stability. Most parameters with high weight like delay line and stainless steel wall can be considered as nearly constant and thus negligible. This can be used for improving the setup. Fouling also shows a high weight and is thus measurable.

C. Experimental results

First, the experiments showed that it is possible to produce dairy protein fouling in this setup, which was similar to the one found in dairy industry (Fig. 6). A procedure is developed to get every time a similar fouling layer.

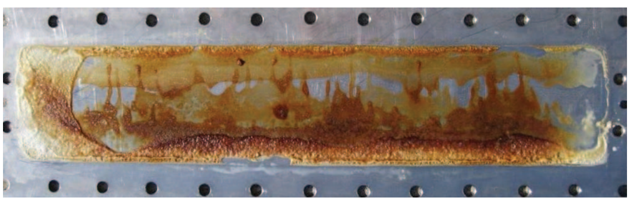

FIG. 6. Fouling made in developed setup.

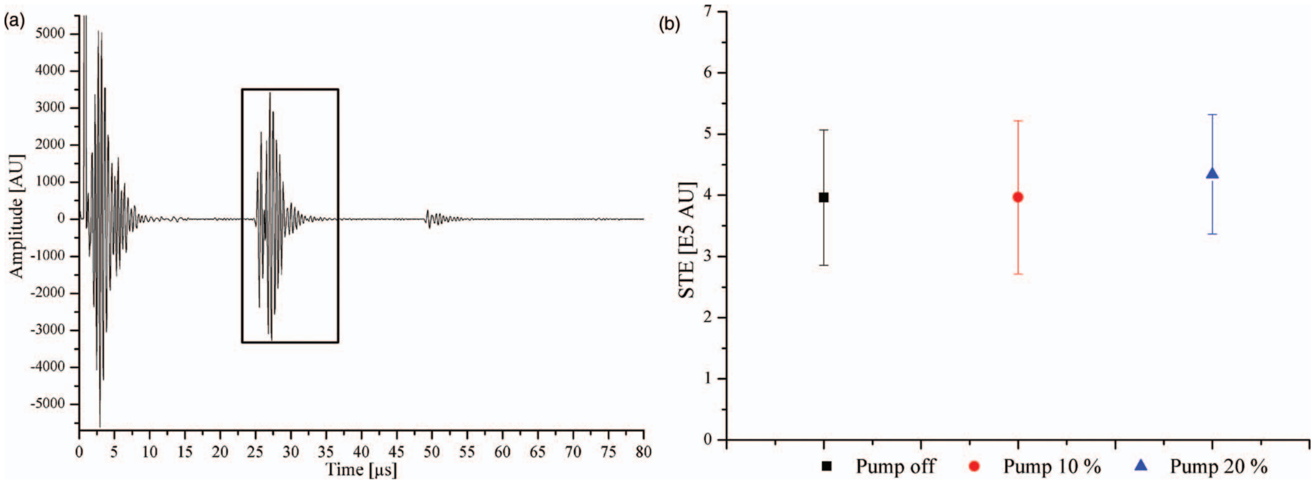

FIG. 7. (a) Typical signal of the ultrasonic transducer on the planar measuring section. The echo used for analysis is framed. (b) Short time energy (*STE*) with standard deviation for different pumping rates measured at different days. *STE* does not differ strongly.

Experiments were made to compare the results with the results from SA. Different measurements were made at different days, daytimes, and pumping rates to exclude environmental factors like temperature and vibration. Figure 7(a) displays a typical signal measured with the described setup. The analysed signal part (1st echo) is framed. It was found that neither outside temperature nor vibrations showed a high influence on the signal and the chosen signal and acoustic parameters characteristic acoustic impedance *Z*, short time energy *STE*, temporal crest factor *TCF*, and spectral crest factor *SCF*. *STE* was chosen to be displayed as model parameter. Vibrations of the setup caused by the pump did not influence *STE* strongly (pump turned off 306 measurements, 10% 309 measurements, 20% 204 measurements, Fig. 7(b)). Errors are around 33%.

Different solid couplings were used between delay line and measuring section. Aqualene (Olympus) was used in thicknesses of 2 mm and 0.5 mm and silicone rubber was applied with different hardnesses (40°SH, 60°SH) and thicknesses (0.3 mm, 0.5 mm, 0.6 mm, 1.0 mm). The results are shown in Fig. 8(a)). All errors were between 0.3% and 1% besides the silicone foil with 40°SH and a thickness of 0.5 mm (6%). Even though the hard silicon foil (60°SH) with 0.3 mm and 0.5 mm showed the highest *STE*, Aqualene demonstrated better heat and mechanical stability for long term use. The influence of the (solid) coupling on the ultrasonic signal (particular its energy content) should not be underestimated.

A delay line was used between ultrasonic transducer and planar channel. It was necessary to separate the echoes from the different interfaces of the setup. Different materials were investigated namely polyether ether ketone (PEEK) and PMMA. Latter was used as solid and as cylinder filled with demineralised water. The water-filled PMMA showed the highest transmitted *STE* but also the highest variation of 70% due to difficulties in excluding air bubbles between delay line and ultrasonic transducer. PMMA showed the best result with lowest error of 36% and thus was chosen (Fig. 8(b)); the error for PEEK was 56%.

In SA, it was shown that delay line has a high influence on the ultrasonic signal when non-stable conditions apply. This influence is confirmed by experimental results when different materials (same length all) were investigated.

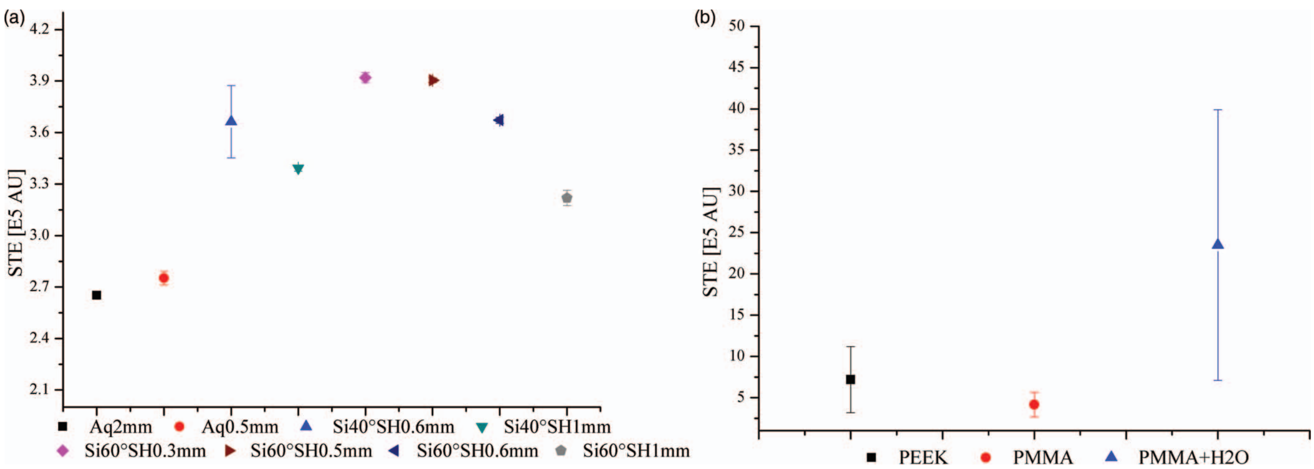

FIG. 8. (a) *STE* of different solid couplings used between delay line and planar channel. The silicone foil (Si) with 60 °SH and thicknesses of 0.3 mm and 0.5 mm showed highest *STE* but Aqualene (Aq) displayed better heat and mechanical stability (all results with standard deviation). (b) PEEK, PMMA, and a PMMA cylinder filled with water were used as delay line. PMMA showed highest *STE* (with standard deviation).

Coupling was found in experiments to be important even though it was primarily excluded in SA. The influence of the stainless steel wall was not investigated in experiments because wall thickness is considered constant such that the influence can be neglected. More experiments with fouling have to be made to see the effect of fouled surfaces but a difference is seen as predicted by SA.

It is known that the mechanical pressure applied to the ultrasonic transducer influences the transmitted and received signal. For repeatable measurements, the same force was applied using a spring (Federnshop Bayern, V2A, k = 7.77 N/mm) which was compressed a defined way (11 mm) with a screw. The force applied was F = 93.24 N for all measurements.

VI. CONCLUSION

A setup is presented in which dairy protein fouling can be produced and measured using ultrasound. The theoretical and experimental descriptions are given and the influence of different parameters on the ultrasonic signal is determined using sensitivity analysis. The wave equation for the electrical and mechanical lumped circuit is derived and the transfer function between input and output is obtained. SA was performed and high weights were found for characteristic acoustic impedance Z, thickness θ, real and imaginary parts of the elastic modulus E, and η of the delay line, the stainless steel wall, and the piezoplate as expected. All parameters are considered constant during measurement and thus their influence can be thought as nil. Z, E, and η of fouling also showed high weights, thus, it is concluded that fouling is measurable because fouling presence and absence change during fouling production and cleaning. Experiments confirmed the results of SA concerning the influence of the delay line (if conditions are not controlled) and also showed high influence of (solid) coupling. In first tests, it was possible to make reproducible dairy protein fouling which was also measurable again confirming SA results.

Small variations in signal stability and transducer excitation are investigated further and will be excluded using appropriate filtering, digital lock-in amplifiers, and impedance matching. In future, it shall be possible to detect cleaning of dairy protein fouling using ultrasound. During cleaning processes fouling presence changed to its absence. Monitoring the time where fouling absence is determined can help to adapt cleaning cycles in industry.

ACKNOWLEDGMENTS

This work was funded by the Forschungskreis der Ernährungsindustrie FEI/AiF, Grant No. AIF 16302 N. We want to thank Schwarzwaldmilch GmbH for the free provision of the used skim milk powder.

[1]H. Burton, J. Dairy Res. **35**(02), 317–330 (1968).
[2]J. Visser and T. J. M. Jeurnink, Exp. Therm. Fluid Sci. **14**(4), 407–424 (1997).
[3]B. Bansal and X. D. Chen, Compr. Rev. Food Sci. Food Saf. **5**(2), 27–33 (2006).
[4]S. Balasubramanian and V. M. Puri, presented at the *ASABE 10 Annual International Meeting*, Pittsburgh, PA, 20–23 June 2010.
[5]P. J. Fryer and M. T. Belmar-Beiny, Trends Food Sci. Technol. **2**, 33–37 (1991).
[6]S. D. Changani, M. T. Belmar-Beiny, and P. J. Fryer, Exp. Therm. Fluid Sci. **14**(4), 392–406 (1997).
[7]C. M. Astorga-Zaragoza, A. Zavala-Río, V. M. Alvarado, R. M. Méndez, and J. Reyes-Reyes, Measurement **40**(4), 392–405 (2007).
[8]T. J. Davies, S. C. Henstridge, C. R. Gillham, and D. I. Wilson, Food Bioprod. Process. **75**(2), 106–110 (1997).
[9]T. Truong, S. Anema, K. Kirkpatrick, and H. Chen, Food Bioprod. Process. **80**(4), 260–269 (2002).
[10]X. D. Chen, D. X. Y. Li, S. X. Q. Lin, and N. Özkan, J. Food Eng. **61**(2), 181–189 (2004).
[11]A. Pereira, J. Mendes, and L. F. Melo, "Cleaning monitoring using controlled nano-vibrations," presented at the *7th International Conference on Heat Exchanger Fouling and Cleaning—Challenges and Opportunities*, 1–7 June 2007, Tomar, Portugal, pp. 483–488.
[12]A. Pereira, J. Mendes, and L. F. Melo, Sens. Actuators B **136**(2), 376–382 (2009).
[13]Peters M. Withers, Trends Food Sci. Technol. **7**(9), 293–298 (1996).
[14]E. Wallhäußer, W. B. Hussein, M. A. Hussein, J. Hinrichs, and T. M. Becker, J. Food Eng. **103**(4), 449–456 (2011).
[15]P. Resa, L. Elvira, C. Sierra, and F. M. d. Espinosa, Anal. Biochem. **384**(1), 68–73 (2009).
[16]P. Resa, E. Luis, and F. R. Montero de Espinosa, Food Res. Int. **37**(6), 587–594 (2004).
[17]T. Schöck and T. Becker, Food Control **21**(4), 362–369 (2010).
[18]V. Leemans and M.-F. Destain, J. Food Eng. **90**(3), 333–340 (2009).
[19]J. Li, D. K. Hallbauer, and R. D. Sanderson, J. Membr. Sci. **215**(1–2), 33–52 (2003).
[20]J.-X. Li, R. D. Sanderson, and G. Y. Chai, Sens. Actuators B **114**(1), 182–191 (2006).
[21]Y. Marselina, Lifia, P. Le-Clech, R. M. Stuetz, and V. Chen, J. Membr. Sci. **341**(1–2), 163–171 (2009).
[22]E. G. Moros, X. Fan, and W. L. Straube, Ultrasound Med. Biol. **25**(8), 1275–1287 (1999).
[23]S. B. Barnett, Semin Ultrasound CT MR **23**(5), 387–391 (2002).
[24]S. B. Barnett, G. R. Ter Haar, M. C. Ziskin, H.-D. Rott, F. A. Duck, and K. Maeda, Ultrasound Med. Biol. **26**(3), 355–366 (2000).
[25]M. C. Ziskin and S. B. Barnett, Ultrasound Med. Biol. **27**(7), 875–876 (2001).
[26]C. M. Rumack, S. I. Wilson, W. J. Charboneau, and D. Levine, *Diagnostic Ultrasound*, 4th ed. (Mosby, 2011).
[27]J. McHugh, J. Döring, W. Stark, and J. L. Guey, "Relationship between the mechanical and ultrasound properties of polymer materials," presented at *ECNDT*, Berlin, Germany, 25–29 September 2006.
[28]L. B. Zuev, B. S. Semukhin, A. G. Lumev, and S. Y. Zavodchikov, "Use of acoustic parameter measurements for evaluating the reliability criteria of machine parts and metal work," presented at *ECNDT*, Berlin, Germany, 25–29 September 2006.
[29]H. Tohmyoh and M. Saka, presented at the *12th Asia Pacific Conference of NDT*, Auckland, New Zealand, 5–10 November 2006.
[30]S. Schnars and R. Henrich, see http://www.ndt.net/ for open access NDT database with information about conference proceedings, articles, exhibitions, and more (2006).
[31]S. Butterworth, Proc. Phys. Soc. (London) **27**(1), 410 (1914).
[32]K. S. Van Dyke, Proc. IRE **16**(6), 742–764 (1928).
[33]W. P. Mason, Proc. IRE **23**(10), 1252–1263 (1935).
[34]R. Krimholtz, D. A. Leedom, and G. L. Mattaei, Electron. Lett. **6**(13), 398–399 (1970).
[35]K. K. Shung and M. Zippuro, IEEE Eng. Med. Biol. Mag. **15**(6), 20–30 (1996).
[36]N. Aouzale, A. Chitnalah, H. Jakjoud, and D. Kourtiche, in *14th IEEE International Conference on Electronics, Circuits and Systems, ICECS 2007* (Marrakech, 2007), pp. 54–57.
[37]C. G. Hutchens and S. A. Morris, "A three port model for thickness mode transducers using SPICE II," presented at *IEEE Ultrasonics Symposium 1984*, 14–16 November 1984, Dallas, Texas, USA, pp. 897–902.
[38]S. A. Morris and C. G. Hutchens, IEEE Trans. Ultrason. Ferroelectr., Freq. Control **UFFCC-33**, 295–198 (1986).
[39]D. Parenthoine, L. P. Tran-Huu-Hue, L. Haumesser, F. Vander Meulen, M. Lematre, and M. Lethiecq, Ultrasonics **51**(2), 109–114 (2011).
[40]R. T. Higuti, F. Buiochi, J. C. Adamowski, and F. M. de Espinosa, Ultrasonics **44**(3), 302–309 (2006).

[41]N. Aouzale, A. Chitnalah, and H. Jakjoud, IEEE Trans. Circuits Syst., II: Express Briefs **56**(12), 911–915 (2009).
[42]J. van Deventer, T. Lofqvist, and J. Delsing, IEEE Trans. Ultrason. Ferroelectr. Freq. Control **47**(4), 1014–1024 (2000).
[43]J. W. M. Leach, IEEE Trans. Ultrason. Ferroelectr. Freq. Control **41**(1), 60–66 (1994).
[44]L. Jian, T. Watanabe, N. Kijima, M. Haruta, Y. Murayama, and S. Omata, in *Proceedings of the Second International Conference on Sensor Technologies and Applications, SENSORCOMM '08, Cap Esterel, France, 2008*, pp. 592–597.
[45]S. R. Ghorayeb, E. Maione, and V. La Magna, IEEE Trans. Ultrason. Ferroelectr. Freq. Control **48**(4), 1124–1131 (2001).
[46]N. N. Abboud, G. L. Wojcik, D. K. Vaughan, J. Mould, D. J. Powell, and L. Nikodyn, "Finite element modelling for ultrasonic transducers," in *Proceedings of the SPIE International Symposium on Medical Imaging*, 21–27 February 1998, San Diego, CA, USA, pp. 19–42.
[47]R. Lerch, "Finite element analysis of piezoelectric transducers," in *Ultrasonics Symposium*, Chicago, IL, USA, 1–5 October 1988 (IEEE Proceedings, 1988), Vol. 2, pp. 643–654.
[48]M. Redwood, J. Acoust. Soc. Am. **33**(4), 527–536 (1961).
[49]S. Sherrit, S. P. Leary, B. P. Dolgin, and Y. Bar-Cohen, in *IEEE Ultrasonics Symposium* (1999), pp. 1–6.
[50]J. Johansson and P. E. Martinsson, "Incorporation of diffraction effects in simulations of ultrasonics systems using PSPICE models," presented at the *Ultrasonics Symposium*, Atlanta, GA, USA, 7–10 October 2001, Vol. 1, pp. 405–410.
[51]A. Saltelli, S. Tarantola, and K. P.-S. Chan, Technometrics **41**(1), 39–56 (1999).
[52]W. Fluegge, *Viscoelasticity* (Springer, Berlin / Heidelberg, 1975).
[53]R. Lerch, G. Sessler, and D. Wolf, *Technische Akustik - Grundlagen und Anwendungen* (Springer, 2009).
[54]P. R. H. Blasius, Mitteilungen ueber Forschungsarbeiten auf dem Gebiete des Ingenieurswesen **131**, 1–41 (1913).

5.2.5. "Determination of cleaning end of protein fouling using an online system combining ultrasonic and classification methods", E. Wallhäußer, A. Sayed, S. Nöbel, M.A. Hussein, J. Hinrichs, T. Becker; Food and Bioprocess Technology 6 (1) (2013), 1-10

Determination of cleaning end of dairy protein fouling using an online system combining ultrasonic and classification methods

Eva Wallhäußer, Ahmed Sayed, Stefan Nöbel, Mohamed A. Hussein, Jörg Hinrichs & Thomas Becker

Food and Bioprocess Technology
An International Journal

ISSN 1935-5130

Food Bioprocess Technol
DOI 10.1007/s11947-012-1041-0

Food Bioprocess Technol
DOI 10.1007/s11947-012-1041-0

ORIGINAL PAPER

Determination of cleaning end of dairy protein fouling using an online system combining ultrasonic and classification methods

Eva Wallhäußer · Ahmed Sayed · Stefan Nöbel · Mohamed A. Hussein · Jörg Hinrichs · Thomas Becker

Received: 25 September 2012 / Accepted: 20 December 2012

Abstract Fouling and cleaning of heat exchangers in food industry are severe and costly issues and of high importance. In this study, a planar heat exchanger was constructed to produce and clean milk protein fouling similar to industry. Using a combination of an ultrasonic measuring method and classification machines cleaning should be monitored online to adapt cleaning time. After reproducible fouling deposit was built, cleaning started which was monitored using an ultrasonic measuring unit. The measured ultrasonic signal was analyzed for seven acoustic features and fed together with temperature and mass flow rate (both measured) into a classification method for decision of fouling presence or absence. For classification, artificial neural network (ANN) and support vector machine (SVM) was applied displaying detection accuracies of more than 80 % (ANN) and 94 % (SVM), respectively. Besides, the slope change of the seven acoustic features was monitored with time resulting in a cleaning time of at least 21±4 min. The cleaning time determined by the new sensor system is comparable with previously determined cleaning times for this setup. This study demonstrated that ultrasound based sensor systems offer a new tool to determine presence or absence of fouling and to monitor cleaning processes in the food industry with high accuracy.

Keywords Ultrasound · Artificial neural network · Support vector machine · Dairy fouling · Acoustic features · Classification method

Introduction

Milk is heated in heat exchangers using temperatures between 72 to 75 °C (pasteurization) and 135 to 150 °C (ultra-high temperature processing) to extend shelf life and reduce microbiological hazards. At these temperatures, proteins denaturate and agglomerate, and minerals precipitate on heat transfer surfaces. The resulting fouling is classified in protein fouling (type A, develops above 72 °C), a soft, spongy, white deposit consisting mostly of β-lactoglobulin and in mineral fouling (type B, develops above 110 °C) which is grayish, brittle and gritty and made mostly of calcium phosphates ($Ca_3(PO_4)_2$) (Burton 1968; Visser and Jeurnink 1997). Fouling formation is influenced by various parameters like Reynolds number (Belmar-Beiny et al. 1993; Pelegrine et al. 2007), surface characteristics (Premathilaka et al. 2007; Rosmaninho and Melo 2008), age of milk (Fryer and Belmar-Beiny 1991), protein concentration (Fickak et al. 2011), and pH (Law and Leaver 2000). The accumulation of salts and proteins increase heat transfer resistance, decreases thermal efficiency, lets the thermal equipment to go off-design, and increases production costs. Unfortunately, only unsupervised and unadapted cleaning of the equipment takes place (Fryer and Asteriadou 2009; Gillham et al. 1999). Thus, it is important for dairy industry to determine fouling presence and to monitor its cleaning success to adapt cleaning. To achieve these goals different approaches were followed. Often, heat transfer parameters like heat flux is monitored (Astorga-Zaragoza et al. 2007; Perez et al. 2009; Truong et al. 2002), electric parameters are used (Chen et al. 2004; Guérin et al. 2007), or acoustic parameters are measured

E. Wallhäußer (✉) · A. Sayed · M. A. Hussein · T. Becker
(Bio-)Process Technology and Process Analysis, Life Science Engineering, Technische Universitaet Muenchen, Weihenstephaner Steig 20, 85354 Freising, Germany
e-mail: e.wallhaeusser@wzw.tum.de

S. Nöbel · J. Hinrichs
Animal Foodstuff Technology, Institute of Food Science and Technology, Universitaet Hohenheim, Garbenstr. 21, 70593 Stuttgart, Germany

S. Nöbel · J. Hinrichs
Dairy Science and Technology, Institute of Food Science and Biotechnology, Universitaet Hohenheim, Garbenstr. 21, 70593 Stuttgart, Germany

Published online: 15 January 2013

(Merheb et al. 2007; Pereira et al. 2009; Silva et al. 2009; Withers 1994). Weaknesses in these besides other studies are, e.g., that some sensors cannot withstand high temperatures, that some methods are difficult to apply in food industry heat exchangers at the moment, or that results currently depend strongly on sensor position. A new method, compared with already used acoustic methods, is the combination of acoustic measurements with classification methods.

Ultrasound is high frequency sound and is used non-destructively, e.g., in medical applications (Wang and Olbricht 2011) or non-destructive testing (McHugh et al. 2006; Schnars and Henrich 2006). Ultrasound is well-known and was already applied in different applications in food industry, e.g., in dairy industry (Dukhin et al. 2005), bread crumb (Elmehdi et al. 2003), or alcoholic fermentation (Lamberti et al. 2009). Here, acoustic and signal features from an ultrasonic signal were chosen to determine fouling presence and absence. They were extracted from an ultrasonic signal and then fed into different decision machines like artificial neural networks (ANN) and support vector machines (SVM). An ANN is an emulation of a biological network (Basheer and Hajmeer 2000) and most often used as feed-forward multilayer perceptron. ANNs classify into the trained classes and were already applied in image processing (Egmont-Petersen et al. 2002), pest detection (Hussein et al. 2010), to monitor and predict fouling in boilers (Teruel et al. 2005) and static setups (Wallhäußer et al. 2011), and to design cleaning cycles in plate heat exchangers (Riverol and Napolitano 2005). SVM is a decision machine and was first introduced by Vapnik et al. (Boser et al. 1992; Cortes and Vapnik 1995). Objects are classified such that a clear gap between them can be found which is defined by a hyperplane and its support vectors. For this, the dual problem is solved which always gives an absolute extremum contrary to ANN. SVMs were already applied in pattern recognition (Burges 1998), regression (Grimm et al. 2007), and in computational biology (Komura et al. 2005; Qiu et al. 2008).

The study was aligned to the development of an online detection system to monitor cleaning success in a pilot plant dairy heat exchanger. Ultrasonic online measurements were combined with classification methods developed via offline analysis and implemented to perform online. Following a fixed fouling and cleaning procedure, cleaning success was monitored using the developed method. As decision machines an ANN and a SVM, respectively, was tested. Besides, a new method based on the slope change of the calculated features was investigated. The goal of this study was to develop an ultrasonic based method with which cleaning and cleaning success of dairy protein fouling can be monitored.

Material and Methods

Experimental Setup

The experimental setup consists of two process tanks (40 l), two pumps (Durietta 0/2K32/25/0.75/2, Hilge GmbH und Co KG, CRN 1–2 A-FGJ-G-E HQQE, Grundfos GmbH), two plate heat exchangers for preheating and cooling (Tetra Plex MS3-SR, TetraPak Processing GmbH), one planar measuring section (self-built), and tubing. The substrate is pumped in circuit from the process tanks to the planar measuring section where it is heated up to 120 °C via a heating plate (G. Maier Elektrotechnik GmbH) and afterwards cooled down to 50 °C. The setup and a sketch of the planar measuring section are shown in Fig. 1.

The channel of the planar measuring section is rectangular (497×94×32 mm) and connected to the tubing via a diminution. An ultrasonic transducer is attached to the planar channel via a delay line made of polymethyl methacrylate (PMMA) for fouling detection. The ultrasonic transducer (piezoceramic PZT, center frequency of 2.2±2 MHz, epoxy-tungsten backing) is coupled using a water-based coupling gel (UCA-2M, AB Angelika Busch) to the PMMA delay line. The delay line is coupled using a solid coupling (2 mm thickness, Aqualene, Olympus) to the stainless steel and everything is pressed to the channel using a spring (V2A, Federnshop Bayern, F=93.24 N). The transducer is excited with an in-house electronic (40 V, sampling rate 12.5 kHz) and measured using Virtual Expert (gimbio mbH) reading a signal every 10 s.

Procedure for protein fouling formation and cleaning cycle

As standard substrate for milk protein fouling, skim milk concentrate were used (Dairy for Research and Training, Universitaet Hohenheim, Stuttgart, Germany). Protein content was increased up to 30 % (*w*/*w*) by dispersing skim milk powder (Instant C, Schwarzwaldmilch) in pasteurized skim milk because higher protein content increases amount of fouling (Schraml 1993). For fouling production, 20 l of 20 % DM skim milk concentrate was heated up to 65 °C and circulated in the pilot plant at a mass flow rate of 410 kg/h for 128 min (laminar flow range increasing fouling formation (Graßhoff 1988; Guérin et al. 2007)). Thereby, standard substrate was heated up to 120 °C for each passage in the planar measuring section with a wall temperature difference of $\Delta\vartheta_w = 5-15K$ where high wall temperature differences decrease induction phase (Chen et al. 2004; Yang et al. 2009). For cleaning, milk was exchanged with water, then NaOH (0.1 % *w*/*w*, Anti-Germ, AGFX) was circulated at 70 °C, and at the end water was used for rinsing.

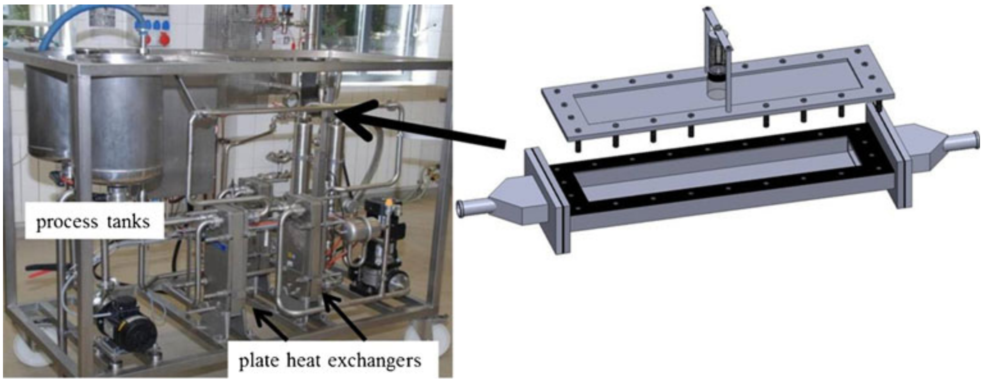

Fig. 1 Experimental setup with the process tanks, pumps, and plate heat exchangers for preheating and cooling; the planar measuring section together with an ultrasonic measuring section can be included instead of a tube (*indicated by arrow*)

Signal and acoustic parameters

Characteristic acoustic impedance (Z)

The characteristic acoustic impedance Z is the resistance of a medium to a sound wave and is calculated with the reflection coefficient r at the interface between wall and medium.

$$Z_{\text{sample}} = Z_{steel}\left(\frac{1-r}{1+r}\right) \tag{1}$$

It depends on the material behind the considered interface because the reflection coefficient r used for calculation changes due to the material properties at this interface. Liquids lead to higher r and lower Z, solids like fouling lead to lower r and higher Z.

Short time energy

Short time energy (STE) resembles the energy content of one echo and is determined by summing up the area under the signal curve.

$$\text{STE} = \sum_{n=1}^{N} (x(n))^2 \tag{2}$$

As Z, STE depends on the material and changes due to different reflection and transmission coefficients at the considered interface, and was highly influenced by temperature.

Temporal/spectral crest factor

Temporal/spectral crest factor (TCF/SCF) is the ratio between the maximum signal amplitude/magnitude in time/frequency domain to the average amplitude/magnitude.

$$\text{TCF} = \frac{\max(|x(n)|)}{1/N\sum_{n=1}^{N}|x(n)|} \tag{3}$$

$$\text{SCF} = \frac{\max(|X(m)|)}{1/1024\sum_{m=1}^{1024}|X(m)|} \tag{4}$$

High values indicate high amounts of harmonics in a signal which are usually not wanted in a clear signal.

Spectral smoothness

Spectral smoothness (SSMOOTH) stands for the smoothness variation of the amplitude of the chosen pattern with respect to its two neighbors.

$$\text{SSMOOTH} = 20\cdot\sum_{m=2}^{1023}\left|\log|X(m)| - \frac{\log|X(m-1)| + \log|X(m)| + \log|X(m+1)|}{3}\right| \tag{5}$$

High values lead to an unsmooth amplitude whereas low values show a smooth course.

Temporal slope

Temporal slope (TSLOPE) describes the signal decrease between 0.8×maximum and 0.08×maximum and provides an impression about damping and losses at interfaces.

Descent time

Descent time (TDESCENT) is the time which is scanned by the temporal slope and thus is dependent on how strongly the signal decreases.

Temperature (*T*)

Temperature is included in SVM and ANN to make the decision independent on temperature influence of the different features and was measured in the planar section.

Mass flow rate $\left(\dot{m}\right)$

The mass flow rate is included to exclude its possible influence on the features due to irregular flow or vibrations and was measured after the pump.

Detection Methods

Artificial Neural Network

A feed-forward multilayer perceptron ANN (Fig. 2) was designed based on the back propagation algorithm. The ANN is composed of an input layer with nine neurons (seven signal features, temperature, mass flow rate), one hidden layer with 14 neurons, and an output layer with nine neurons to compare the output with the input. The ANN stated "1" for fouling presence and "0" for its absence.

Each neuron weighted its input, summed it up with a bias, and presented it to the next layer via LOGSIG (Eq. (6)) and TANSIG transfer function (Eq. (7)) with n and a as the input to the transfer function and the neuron output, respectively,

$$a = \frac{1}{1 + \exp(-n)} \tag{6}$$

$$a = \frac{2}{(1 + \exp(-2n))} - 1 \tag{7}$$

while PURELIN transfer function solely transfers the input to the output without any changes.

Inputs were scaled to be mean-centered to exclude influences due to feature magnitude. The used back propagation algorithm minimized network error by weight modifying where the transfer functions ensures the smallest available total mean square error.

Support Vector Machine

A SVM finds a hyperplane defined by support vectors (SV) to separate two categories of points (in direction to the normal vector w, +1, and opposite to it, −1) (Belousov et al. 2002; Burges 1998; Smola and Schoelkopf 2004). Usually, a canonical hyperplane normalized to N training data is applied with maximized margin. The maximized margin is found by minimizing the Lagrangian L (Eq. (8)) with regard to the normal vector w and the bias b while the Lagrange multiplicators α_i are maximized. The SV x_i define the location of the hyperplane and have $\alpha_i \neq 0$. Every decision can thus be expressed by a scalar product between the SV x_i and the data x.

$$L(w, b, \alpha) = \frac{1}{2}\|w\|^2 - \sum\nolimits_{i=1}^{N} \alpha_i(y_i(\langle x_i, w\rangle + b) - 1) \tag{8}$$

where y is the decision value.

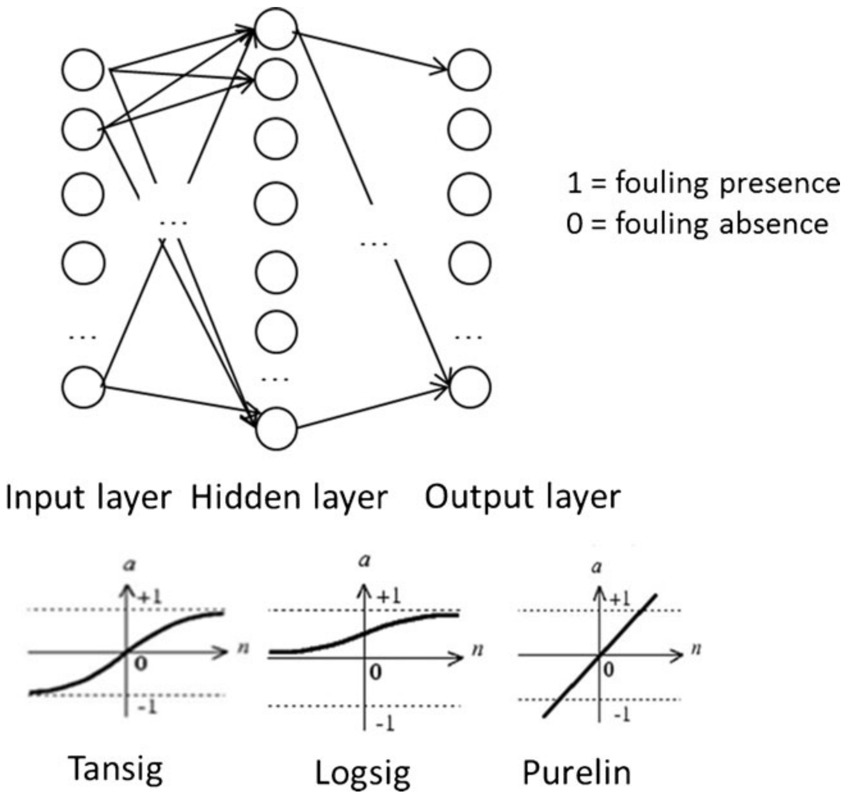

Fig. 2 ANN architecture. The input layer has nine neurons (seven ultrasonic parameters, mass flow rate, temperature), the hidden layer 14 neurons, and the output layer nine neurons (TANSIG, LOGSIG, PURELIN transfer function). A clean surface is identified if output layer equals input layer

Non-linear separable data can be made linear separable by transferring data to feature space using a transfer function $\mathfrak{F}$ (Fig. 3). There a dot product can be found with an appropriate kernel K and a linear separating hyperplane can be applied (kernel trick) (Eq. (9)). The solution of the problem lies in determining the values of b and α's and in finding the appropriate K.

$$F(x) = \sum_{i=1}^{N} \alpha_i y_i \left(\mathfrak{F}(x_i) \cdot \mathfrak{F}(x) \right) + b = \sum_{i=1}^{N} \alpha_i y_i K(x_i, x) + b \tag{9}$$

K describes a scalar product in the feature space, is symmetrical and positive definite (Mercer 1909). A kernel function may be a polynomials of nth degree $K(x, x_i) = (\langle x, x_i \rangle)^n$, a radial basis functions (rbf) with width $\sigma K(x, x_i) = \exp\left(-\|x - x_i\|^2 / 2\sigma^2\right)$, or a neural network $K(x, x_i) = \tanh(\kappa\langle x, x_i\rangle + \theta)$. Usually, a soft margin hyperplane is applied which allows errors while looking for the hyperplane while introducing a cost term.

Different kernels were tested and a rbf kernel with σ=0.7 proofed best. Of the 7,722 values, 50 % were used for training and 50 % were used for testing and the same input as for the ANN was used.

Online Detection Method

To detect the cleaning process, a code was developed in Matlab including the ANN and the SVM, respectively, and later implemented in C++ for online analysis. The code able for online detection reads in the ultrasonic signal and then calculates the seven acoustic features mentioned above. They are fed into an offline trained ANN/SVM together with the measured temperature and the mass flow rate and a decision is made. Fouling presence is stated with a red long bar representing “1”, fouling absence is a green short bar representing “0”. Figure 4 displays the process flow chart. To improve detection stability data mining tasks like outlier detection and exceptional handling were introduced.

Results and Discussion

Fouling Layer and Cleaning Results

To evaluate suitable cleaning cycles, different cleaning times of NaOH with fixed concentration (0.1 % *w/w*, pH11.05±0.06) were investigated. NaOH determines the cleaning of protein fouling where soaking time, temperature and other parameters play an important role (Fryer and Asteriadou 2009; Mercade-Prieto et al. 2007). Cleaning times ranged from 10 to 180 min whereby swelling, layer thickness, and layer composition was analyzed by different methods. Layer thickness was determined using eddy current (Leptoskop, Karl Deutsch Prüf- und Messgerätebau GmbH) following DIN EN ISO 2360 and layer composition was characterized concerning protein, mineral, and ash content by applying Dumas method, ashing, and atomic emission spectroscopy with the results displayed in Table 1. To determine reproducibility of fouling, five experiments were made, the plate was weighed prior and after drying, and the layer was photographed.

The protein content was found to be 78.8 % with an ash content of 10.5 % and layer thicknesses around 316 µm. Error for thickness measurement was below 6 %, for protein and ash content below 2 %, and fouling was similar to the one found in industry.

Fouling removal was investigated dependent on cleaning time. During the investigation it was found that first a strong removal was seen where 42 % of the fouling layer was removed after 10–20 min; followed by only small removal

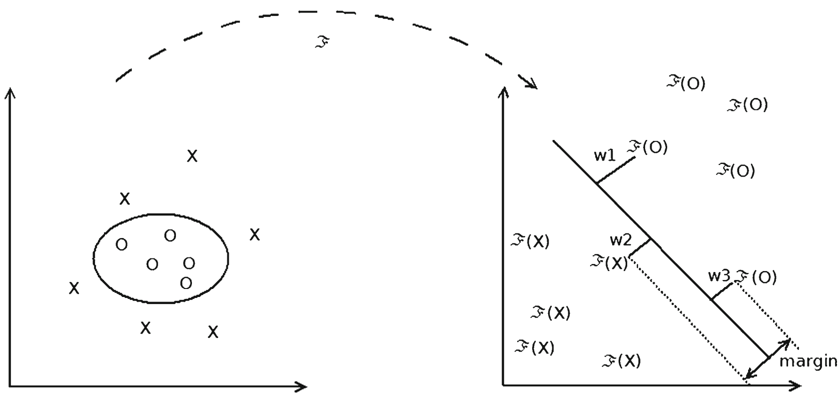

Fig. 3 Classification of two classes (X, O) by a SVM which transfers data from input to feature space using the transform $\mathfrak{F}$ where data is linear separable. The hyperplane is defined by the normal vector *w* and is surrounded by a margin

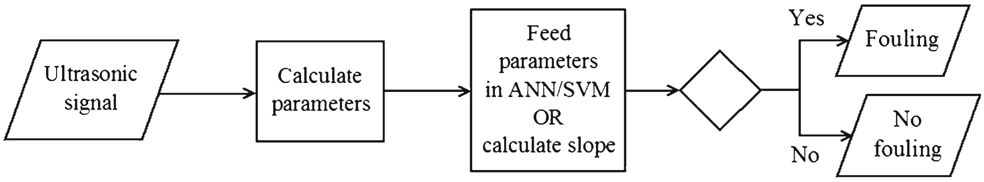

Fig. 4 Flowchart of the developed code which can be used online and offline

between 40 and 120 min. Figure 5 gives an overview over fouling distribution and thickness for different cleaning times.

After contact with the cleaning agent NaOH the deposit started to swell and build a gel which collapsed after drying for analysis having a brownish color. When cleaning lasted 60 min or longer, only the edges of the plate remained unclean, the place where the transducer is located was cleaned down to 30–40 µm. Protein content of the remaining layer decreased to 60 % whereas mineral content increased up to 15–16.5 and 6–12 % sodium because the cleaning agent was integrated into the fouling layer. Structure and surface of fouling changed during cleaning, the amount of pores in direction to the plate decreased until at the end nearly no pores were present. During cleaning, crystals developed on the surface with a length of 4–5 µm due to the usage of drinking water which precipitates calcite when heated (cleaning was done at 70 °C).

Table 1 Reproducibility of the fouling layer and its composition: skim milk concentrate (20 % DM); heating temperature: 120 °C, five independent experiments

	MV±SE[a]	Repetitions	Variation (%)
Thickness (µm)	316±23	5	5.87
Deposit mass (g/m^2)			
Wet	253±29	5	9.07
Drying 20 °C, 18 h	149±17	5	9.11
Drying 20 °C, 18 h and 105 °C, 4 h	138±17	5	9.89
Mass portion in dry matter (%)			
Protein	78.8±1.3	5	1.33
Lactose[b]	10.6±1.4	5	10.5
Ash	10.5±0.3	5	1.93
Mass portion of minerals in ash (%)[c]			
Calcium	37.4±1.3	5	2.77
Phosphate	52.4±1.1	5	3.56
Magnesium	2.16±0.18	3	3.52
Potassium[d]	1.49±0.86	5	46.0
Sodium[d]	0.78±0.37	5	35.9
Iron[d]	0.04±0.05	3	26.1

[a] Mean value and standard error

[b] Overall mass—(protein+ash)

[c] ICP-OES

[d] Minor components outside confidence range ICP-OES

Statistical Significance

All chosen features from the ultrasonic signal (*Z*, STE, TCF, SCF, SSMOOTH, TSLOPE, TDESCEND) showed statistical significance difference between a clean and a surface with deposit ($p<0.0005$, significance level 0.05). Statistical analysis was done with built-in one-way ANOVA in Origin®.

Ultrasonic Detection of Fouling

Ultrasound and sound were already applied in different application of fouling detection (see, e.g., Lemos et al. 2011; Silva et al. 2010), or for cleaning supervision (Kujundzic et al. 2008; Pereira et al. 2009) in heat exchangers and membranes. In membranes, other methods like confocal microscope or gravimetric methods can be used (Chai et al. 2007; Ferrando et al. 2005; Peiris et al. 2010) whereas in heat exchangers often numerical/computational methods are applied (Jonsson et al. 2007; Lalot and Palsson 2010).

Artificial Neural Network

ANN already was applied in fouling detection showing good applicability (Lyons et al. 2001; Wallhäußer et al. 2011). ANN was first trained offline using data of a clean heat exchanger (water at 70 °C) and was tested with both a clean and a fouled heat exchanger and with data from cleaning cycles. ANN showed an accuracy of more than 80 % after introduction of a LOGSIG neuron which weighted the different features.

Support Vector Machine

The SVM was trained offline using data of both a clean and a fouled heat exchanger (3861 values) and it was tested with signals of cleaning cycles and of a clean as well as a fouled heat exchanger (3861). The SVM used a rbf-kernel with a width of 0.7 and 1179 support vectors and showed an accuracy of 94 %.

Slope Change

It was found that the determined values of the features may be variable and that this may diminish the detection accuracy. Thus, a method was investigated which follows the change of a feature and not its actual value. To make the method as easy as possible, not the whole cleaning cycle

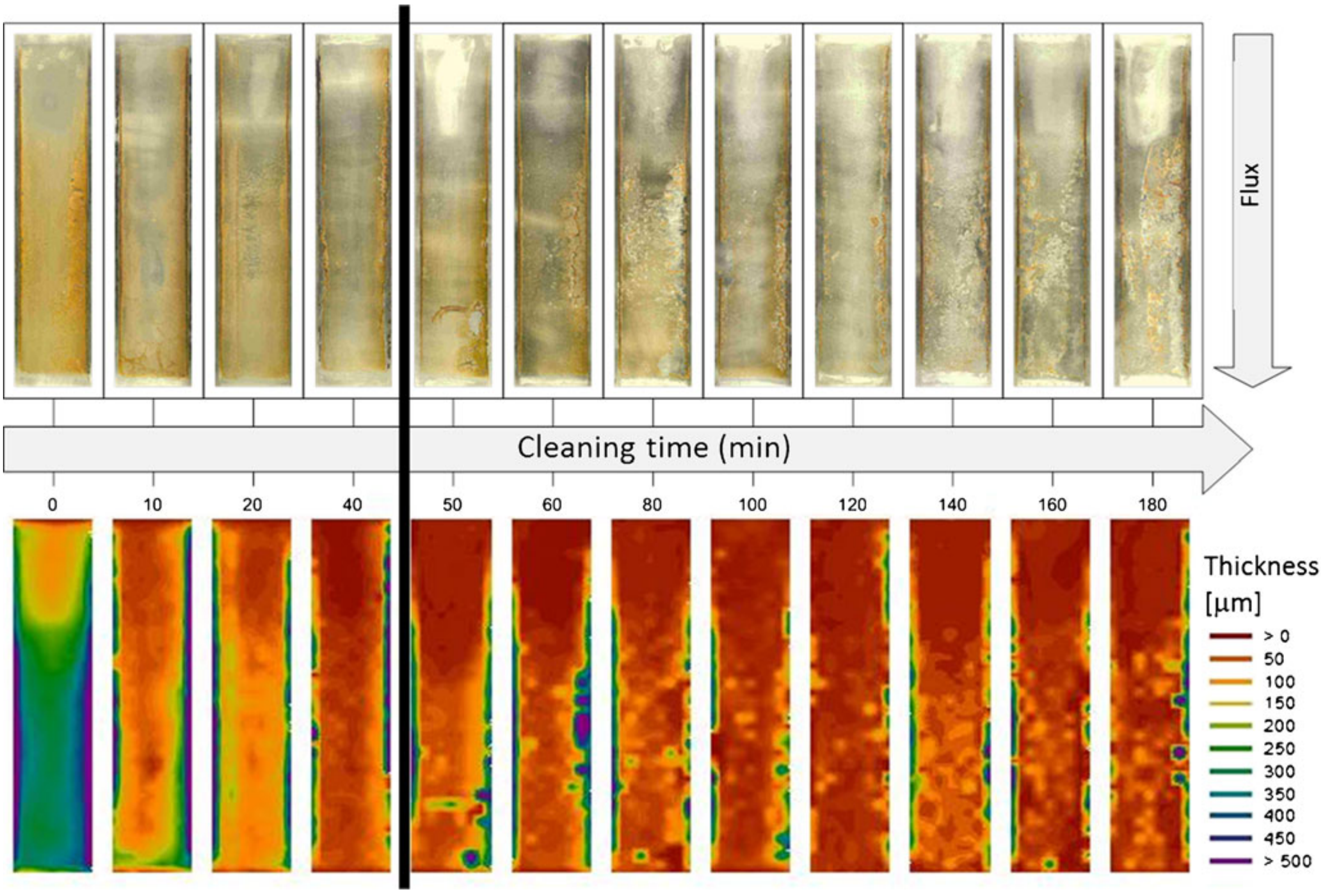

Fig. 5 Cleaning progress and deposit height with time. Fouling deposit was removed strongly in the first 40 min from approx. 300 μm to ca. 50 μm, afterwards the removal was slower. This is indicated by a *black line*

was investigated at once but frame-wise. That way, a linear fit can be applied if the frame is small enough but not too small (a frame of ten signals was chosen). The algorithm can be described as follows:

- Wait until ten ultrasonic signals are measured and the features are determined
- Fit for every feature a line to the values and determine the slope

Fig. 6 Change of slope of short time energy (STE) for three different cleaning runs. Change of slope to around zero takes place after around 20–22 min

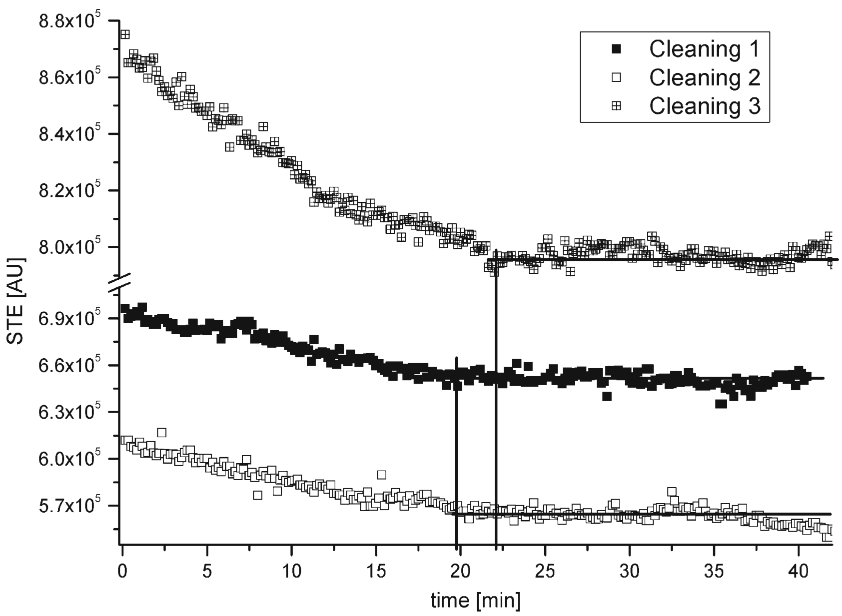

- If the slope≠0 then take the next determined value, skip the first value and fit again
- Do so until the slope≈0 for at least 3 min (20 values)

If the slope change is unequal zero for at least four out of seven features, fouling is decided if it equals zero no fouling is concluded. The slope change is exemplary shown in Fig. 6 for short time energy for three different cleaning runs at different days. If the slope is monitored, a change to about zero at 21±4 min for different features is found resembling a fouling thickness of below 50 μm. A factor of safety of 3 min can be added because the time until setup changes are effective is in the same range.

Outlier Detection

Outlier detection is applied to exclude data which do not fit into the general data distribution. Angle-based outlier detection (ABOD) was chosen because it is more stable in high dimensional space considering locations in both x and y axis. ABOD is based on the angles between distance vectors: The smaller the angle and its variation the more likely point p is an outlier. A point of the data group has a high angle variation because it is surrounded by many other points whereas an outlier is not surrounded by many points.

Following Kriegel et al. (2008), the definition for ABOD is given as:

$$ABOF\left(\vec{A}\right) = VAR_{\vec{B},\vec{C}\in D}\left(\frac{\langle \overline{AB},\overline{AC}\rangle}{\|\overline{AB}\|^2\cdot\|\overline{AC}\|^2}\right)$$
$$= \frac{\sum\limits_{\vec{B}\in D}\sum\limits_{\vec{C}\in D}\left(\frac{1}{\|\overline{AB}\|\cdot\|\overline{AC}\|}\cdot\frac{\langle \overline{AB},\overline{AC}\rangle}{\|\overline{AB}\|^2\cdot\|\overline{AC}\|^2}\right)^2}{\sum\limits_{\vec{B}\in D}\sum\limits_{\vec{C}\in D}\frac{1}{\|\overline{AB}\|\cdot\|\overline{AC}\|}} - \left(\frac{\sum\limits_{\vec{B}\in D}\sum\limits_{\vec{C}\in D}\frac{1}{\|\overline{AB}\|\cdot\|\overline{AC}\|}\cdot\frac{\langle \overline{AB},\overline{AC}\rangle}{\|\overline{AB}\|^2\cdot\|\overline{AC}\|^2}}{\sum\limits_{\vec{B}\in D}\sum\limits_{\vec{C}\in D}\frac{1}{\|\overline{AB}\|\cdot\|\overline{AC}\|}}\right) \tag{10}$$

Any value which did neither display "0" nor "1" but a value in between was transformed to "0" or "1". This smoothed the displayed results and helped not to connect the seen bar with cleaning progress (e.g., high green bar means partially cleaned). Besides, any classification method has a detection accuracy of 100 % leading to false decisions. To overcome this, a combination of ABOD and exceptional handling was applied using a window with adaptable frame size which was moved over the data with no overlap between two windows. If at least half of the window size values display fouling/no fouling all other values are considered the same. The decision when both ABOD and exceptional handling were applied is shown in Fig. 7.

When both methods were applied a time delay occurred due to the windows tendency check. This means if the end of cleaning is reached inside a window, it may not be shown until the next window because in this window maybe more values display fouling. Time delay due to ABOD and exceptional handling is only of importance if window size is chosen to large.

Conclusion

In this study, a method is presented to monitor online cleaning of milk fouling and to provide a decision concerning fouling presence and absence. This method is based on a combination of different classification methods and ultrasonic measurements. A specially designed experimental setup with a planar measuring section was developed and built to enable reproducible fouling and cleaning. Heat-induced fouling was comparable to fouling emerging in continuous heating processes in dairy industry. In analogy, after rinsing, an alkaline-based cleaning cycle was developed. Clean and fouled heat exchangers as well as different cleaning procedures were monitored using an ultrasonic transducer (resonance frequency 2 MHz) and signals were analyzed concerning seven different acoustic features. ANN and SVM were applied using acoustic features, mass flow rate, and temperature. Fouling presence or absence was determined with accuracies of 80 % (ANN) and 94 % (SVM). An additional method concerning the change of the slope of the seven acoustic features was also investigated. Thus, a clean surface was detected after 21±4 min independent on differing starting values at various days. This proposed cleaning time implies a fouling deposit thickness below 50 μm determined in cleaning time experiments. Higher frequencies may lead to thinner detectable deposits. ANN showed also usable for online detection showing similar cleaning times but due to less detection accuracy sophisticated outlier detection was necessary. SVM was not tested online so far but seems to be promising concerning offline detection accuracy. Thus, it was shown that

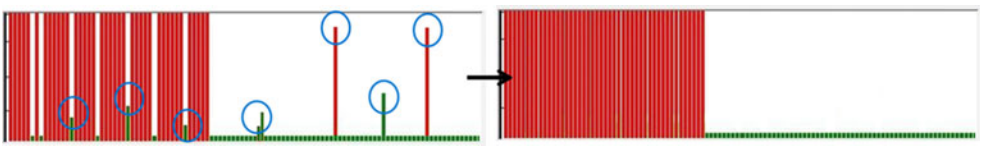

Fig. 7 Outlier detection and exceptional handling (window: 10 signals). All outliers displaying not an exact value are transformed to an exact value. If five or more signals display e.g. fouling, all other signals are considered being the same. *Red, long bars* stand for fouling, *green, short bars* for no fouling

monitoring cleaning success of dairy protein fouling is possible using a combination of ultrasonic measurements and classification methods.

In the future, the planar setup will be exchanged by a tubular double pipe setup (monotube approach, outer pipe transmitting water, inner pipe carrying substrate) and cleaning success will be monitored using the same system combining ultrasonic measurements and a classification method.

Another application site of the developed ultrasonic sensor together with its method is to apply waffled plate heat exchangers (PHE). PHE are advantageous concerning transducer mounting (no adaption for round surfaces has to be found) but multiple refractions of the ultrasonic signal have to be taken into account in the analysis. Also, adding up of multiple signals coming of different plates have to be investigated concerning detection accuracy and new challenges.

Acknowledgments This work was supported by the FEI (Forschungskreis der Ernährungsindustrie), the AiF, and Ministry of Economics and Technology. AIF project number: 16302N. The authors thank Schwarzwaldmilch GmbH Offenburg for the provision of skim milk powder, Tetra Pak AG for providing the plate heat exchangers, M. Sprunk for performing most experiments in Hohenheim, and W. Hussein for help designing the ANN.

References

Astorga-Zaragoza, C. M., Zavala-Río, A., Alvarado, V. M., Méndez, R. M., & Reyes-Reyes, J. (2007). Performance monitoring of heat exchangers via adaptive observers. *Measurement, 40*(4), 392–405.

Basheer, I. A., & Hajmeer, M. (2000). Artificial neural networks: fundamentals, computing, design, and application. *Journal of Microbiological Methods, 43*(1), 3–31.

Belmar-Beiny, M. T., Gotham, S. M., Paterson, W. R., Fryer, P. J., & Pritchard, A. M. (1993). The effect of Reynolds number and fluid temperature in whey protein fouling. *Journal of Food Engineering, 19*(2), 119–139.

Belousov, A. I., Verzakov, S. A., & von Frese, J. (2002). Applicational aspects of support vector machines. *Journal of Chemometrics, 16* (8–10), 482–489.

Boser, B. E., Guyon, I. M., & Vapnik, V. N. (1992). A training algorithm for optimal margin classifier. In: COLT 92—Proceedings of the fifth annual workshop on computational learning theory, 1992, 144–152.

Burges, C. J. C. (1998). A tutorial on support vector machines for pattern recognition. *Data Mining and Knowledge Discovery, 2*(2), 121–167.

Burton, H. (1968). Section G. Deposits from whole milk in heat treatment plant-a review and discussion. *The Journal of Dairy Research, 35*(02), 317–330.

Chai, G. Y., Greenberg, A. R., & Krantz, W. B. (2007). Ultrasound, gravimetric, and SEM studies of inorganic fouling in spiral-wound membrane modules. *Desalination, 208*(1–3), 277–293.

Chen, X. D., Li, D. X. Y., Lin, S. X. Q., & Özkan, N. (2004). On-line fouling/cleaning detection by measuring electric resistance-equipment development and application to milk fouling detection and chemical cleaning monitoring. *Journal of Food Engineering, 61*(2), 181–189.

Cortes, C., & Vapnik, V. (1995). Support-vector networks. *Machine Learning, 20*(3), 273–297.

Dukhin, A. S., Goetz, P. J., & Travers, B. (2005). Use of ultrasound for characterizing dairy products. *Journal of Dairy Sciences, 88*(4), 1320–1324.

Egmont-Petersen, M., de Ridder, D., & Handels, H. (2002). Image processing with neural networks—a review. *Pattern Recognition, 35*(10), 2279–2301.

Elmehdi, H. M., Page, J. H., & Scanlon, M. G. (2003). Using ultrasound to investigate the cellular structure of bread crumb. *Journal of Cereal Science, 38*(1), 33–42.

Ferrando, M., Rozek, A., Zator, M., López, F., & Güell, C. (2005). An approach to membrane fouling characterization by confocal scanning laser microscopy. *Journal of Membrane Science, 250*(1–2), 283–293.

Fickak, A., Al-Raisi, A., & Chen, X. D. (2011). Effect of whey protein concentration on the fouling and cleaning of a heat transfer surface. *Journal of Food Engineering, 104*(3), 323–331.

Fryer, P. J., & Asteriadou, K. (2009). A prototype cleaning map: a classification of industrial cleaning processes. *Trends in Food Science & Technology, 20*(6–7), 255–262.

Fryer, P. J., & Belmar-Beiny, M. T. (1991). Fouling of heat exchangers in the food industry: a chemical engineering prespective. *Trends in Food Science & Technology, 2*, 33–37.

Gillham, C. R., Fryer, P. J., Hasting, A. P. M., & Wilson, D. I. (1999). Cleaning-in-place of whey protein fouling deposits: mechanisms controlling cleaning. *IChemE, 77*, 127–136.

Graßhoff, A. (1988). Studien über die Belagbildung auf Wärmeaustauschflächen beim Erhitzen von Milch mit einer Labor-Wärmeaustauscher-Apparatur. *Milchwissenschaft, 43*(12), 780–783.

Grimm, M., Kroschel, K., & Narayanan, S. (2007). Support vector regression for automatic recognition of spontaneous emotions in speech. In IEEE International Conference on Acoustics, Speech and Signal Processing, 2007. ICASSP 2007, 15–20 April 2007, 4, IV-1085-IV-1088.

Guérin, R., Ronse, G., Bouvier, L., Debreyne, P., & Delaplace, G. (2007). Structure and rate of growth of whey protein deposit from in situ electrical conductivity during fouling in a plate heat exchanger. *Chemical Engineering Science, 62*(7), 1948–1957.

Hussein, W. B., Hussein, M. A., & Becker, T. (2010). Detection of the red palm weevil using its bioacoustics features. *Journal of Bioacoustics, 19*(2), 177–194.

Jonsson, G. R., Lalot, S., Palsson, O. P., & Desmet, B. (2007). Use of extended Kalman filtering in detecting fouling in heat exchangers. *International Journal of Heat and Mass Transfer, 50*(13–14), 2643–2655.

Komura, D., Nakamura, H., Tsutsumi, S., Aburatani, H., & Ihara, S. (2005). Multidimensional support vector machines for visualization of gene expression data. *Bioinformatics, 21*(4), 439–444.

Kriegel, H.-P., Schuber, M., & Zimek, A. (2008). Angle-based outlier detection in high-dimensional data. In Proc. of the 14th ACM SIGKDD International conference on knowledge discovery and data mining (KDD'08), 2008.

Kujundzic, E., Cobry, K., Greenberg, A. R., & Hernandez, M. (2008). Use of ultrasonic sensors for characterization of membrane fouling and cleaning. *Journal of Engineered Fibers and Fabrics*, Special Issue, 35–44.

Lalot, S., & Palsson, H. (2010). Detection of fouling in a cross-flow heat exchanger using a neural network based technique. *International Journal of Thermal Sciences, 49*(4), 675–679.

Lamberti, N., Ardia, L., Albanese, D., & Di Matteo, M. (2009). An ultrasound technique for monitoring the alcoholic wine fermentation. *Ultrasonics, 49*(1), 94–97.

Law, A. J. R., & Leaver, J. (2000). Effect of pH on the thermal denaturation of whey proteins in milk. *Journal of Agricultural and Food Chemistry, 48*(3), 672–679.

Lemos, L. C., Neto, J. M. R. S., Silva, J. J., & Neto, J. S. R. (2011). Fouling detection using hammer impact test and wireless comunication. In Instrumentation and Measurement Technology Conference (I2MTC), 2011 IEEE, 10–12 May 2011, 1–5.

Lyons, W. B., Ewald, H., Flanagan, C., Lochmann, S., & Lewis, E. (2001). A neural networks based approach for determining fouling of multi-point optical fibre sensors in water systems. *Measurement Science and Technology, 12*(7), 958–965.

McHugh, J., Döring, J., Stark, W., & Guey, J. L. (2006). Relationship between the mechanical and ultrasound properties of polymer materials. ECNDT, 1–9.

Mercade-Prieto, R., Paterson, W. R., & Wilson, D. I. (2007). The science of cleaning of dairy fouling layers. In Proceedings of the 7th International Conference on Heat Exchanger Fouling and Cleaning—Challenges and Opportunities, 2007/07, RP5, 119–127.

Mercer, J. (1909). Functions of positive and negative type, and their connection with the theory of integral equations. *Philosophical Transactions of the Royal Society of London. Series A, 209*(441–458), 415–446. Containing Papers of a Mathematical or Physical Character.

Merheb, B., Nassar, G., Nongaillard, B., Delaplace, G., & Leuliet, J. C. (2007). Design and performance of a low-frequency non-intrusive acoustic technique for monitoring fouling in plate heat exchangers. *Journal of Food Science, 82*, 518–527.

Peiris, R. H., Hall, C., Budman, H., Moresoli, C., Peldszus, S., Huck, P. M., & Legge, R. L. (2010). Identifying fouling events in a membrane-based drinking water treatment process using principal component analysis of fluorescence excitation-emission matrices. *Water Research, 44*(1), 185–194.

Pelegrine, D. H., Oliviera, K. F., & Gomes, M. T. M. S. (2007). Milk protein fouling in a tubular heat exchanger: effect of milk temperature and Reynolds number. In 7th International Conference on Heat Exchanger Fouling and Cleaning—Challenges and Opportunities, July, Tomar, Portugal, RP5, 147–149.

Pereira, A., Mendes, J., & Melo, L. F. (2009). Monitoring cleaning-in-place of shampoo films using nanovibration technology. *Sensors and Actuators B: Chemical, 136*(2), 376–382.

Perez, L., Ladevie, B., Tochon, P., & Batsale, J. C. (2009). A new transient thermal fouling probe for cross flow tubular heat exchangers. *International Journal of Heat and Mass Transfer, 52*(1–2), 407–414.

Premathilaka, S. S., Hyland, M. M., Chen, X. D., Watkins, L. R., & Bansal, B. (2007) Interaction of whey protein with modified stainless steel surfaces. In 7th International Conference on Heat Exchanger Fouling and Cleaning—Challenges and Opportunities, July, Tomar, Portugal, 150–161.

Qiu, J., Sheffler, W., Baker, D., & Noble, W. S. (2008). Ranking predicted protein structures with support vector regression. *Proteins: Structure, Function, and Bioinformatics, 71*(3), 1175–1182.

Riverol, C., & Napolitano, V. (2005). Estimation of fouling in a plate heat exchanger through the application of neural networks. *Journal of Chemical Technology and Biotechnology, 80*, 594–600.

Rosmaninho, R., & Melo, L. F. (2008). Protein-calcium phosphate interactions in fouling of modified stainless-steel surfaces by simulated milk. *International Dairy Journal, 18*(1), 72–80.

Schnars, S., & Henrich, R. (2006). Application of NDT methods on composite structures in aerospace industry. ndt.net.

Schraml, J. (1993). Zum Verhalten konzentrierter Produkte bei der Belagbildung an heißen Oberflächen. PhD Thesis. Technische Universität München.

Silva, J., Lima, A., Neff, F. H., & da Rocha Neto, J. S. (2009). Non-invasive fast detection of internal fouling layers in tubes and ducts by acoustic vibration analysis. *IEEE Transactions on Instrumentation and Measurement, 58*(1), 108–114.

Silva, J., Lima, A. M., Neff, H., & Neto, J. S. R. (2010). Vibration analysis based on Hammer impact for fouling detection using microphone and accelerometers as sensors. *Sensors and Transducers Journal, 112*(1), 10–23.

Smola, A. J., & Schoelkopf, B. (2004). A tutorial on support vector regression. *Statistics and Computing, 14*(3), 199–222.

Teruel, E., Cortés, C., Ignacio Díez, L., & Arauzo, I. (2005). Monitoring and prediction of fouling in coal-fired utility boilers using neural networks. *Chemical Engineering Science, 60*(18), 5035–5048.

Truong, T., Anema, S., Kirkpatrick, K., & Chen, H. (2002). The use of a heat flux sensor for in-line monitoring of fouling of non-heated surfaces. *Food and Bioproducts Processing, 80*(4), 260–269.

Visser, J., & Jeurnink, T. J. M. (1997). Fouling of heat exchangers in the dairy industry. *Experimental Thermal and Fluid Science, 14* (4), 407–424.

Wallhäußer, E., Hussein, W. B., Hussein, M. A., Hinrichs, J., & Becker, T. M. (2011). On the usage of acoustic properties combined with an artificial neural network—A new approach of determining presence of dairy fouling. *Journal of Food Engineering, 103*(4), 449–456.

Wang, P., & Olbricht, W. L. (2011). Fluid and solid mechanics in a poroelastic network induced by ultrasound. *Journal of Biomechanics, 44*(1), 28–33.

Withers, P. (1994). Ultrasonic sensor for the detection of fouling in UHT processing plants. *Food Control, 5*(2), 67–72.

Yang, M., Young, A., Niyetkaliyev, A., & Crittenden, B. (2009). Modelling the fouling induction period. In: Proceedings of International Conference on Heat Exchanger Fouling and Cleaning VIII - 2009, 2009, 69–75.

6. Conclusion and Outlook

Summary and Discussion

This thesis addresses the development of a system which can monitor online cleaning of dairy fouling in industrial-like heat exchangers. Fouling is one of the most costly factors particularly in foodstuff industry because it cannot be avoided. In dairy industry, milk is heated for safety and shelf life reasons. Heating leads to denaturation of proteins and aggregation of salts and consequential fouling in industrial heat exchangers. To overcome this problem, cleaning is conducted on a daily basis using fixed cleaning in place (CIP) cycles. At the moment, CIP cycles cannot be adapted to amount and kind of fouling present and is conducted without knowledge of actual fouling. Thus, cleaning is often conducted too long for small batches and small- and medium-sized companies. Online monitoring of cleaning will help to adapt CIP cycles. This will help to save costs for example for energy and cleaning agents and will increase production time because plant downtime can be minimised and production time can be maximised.

For monitor fouling progress and cleaning success in dairy heat exchangers it is necessary to understand fouling process and the properties of the fouling layer. Focus in most fouling studies is protein fouling because it is one major factor in dairy industry. As known, protein fouling mainly consists of β-lactoglobulin (β-lg). β-lg is a globular protein and naturally present in cow milk. β-lg denaturates at used pasteurisation temperatures. Its denaturation behaviour is summarised in table C.1. Denaturated and/or aggregated β-lg is attached to heat exchanger surface via molecular interactions (van der Waals and electrostatic double layer forces). Thus, deposition of β-lg is the crucial step which leads to fouling in heat exchangers.

Detection of fouling is necessary to monitor cleaning success and adapt CIP cycles. To do so, several research approaches were done focusing on monitoring fouling presence. All known approaches show different advantages and drawbacks where general overviews can be found in [127], [165], or [167]. Most of the investigated methods are sensitive but cannot be easily applied to existing heat exchangers. In contrast, heat exchangers have to be adapted to the developed detection system. Ultrasound promises remedy because it is a sensitive method which can be applied and used in various areas and environnments. Ultrasound can also be easily applied to existing heat exchangers because it can be attached from the outside. Drawbacks are that ultrasound is dependent on the system and influenced by parameters like temperature and excitation variations. These points have to be kept in mind but can be dealt with: the detection system (ultrasonic transducer, excitation and reception electronics, cables, connections, coupling system) has to be adjusted to each part. Also, analysis software can be adapted such that most influences can be included in it and thus compensated. Detailed analysis was done for the system developed in this thesis where detailed results can be found in Appendix D.

Ultrasound is promising for monitoring fouling and cleaning success also due to another reason: it is very sensitive to changes of medium state at interfaces. Here, the change of fluid milk to solid fouling and back is explicitly addressed. Fouling deposition on the heat exchanger surfaces leads to changes in reflection and transmission of signals and medium properties like characteristic acoustic impedance. Therefore, ultrasound can detect changes caused by thin and thick fouling layers. Thin layers can be detected mainly by changes at the interface heat exchanger wall-medium because reflection and transmission coefficients are influenced. Thick layers on the other hand change time of flight of signal, damp and refract the signal differently (e.g. via air/water bubbles inside the layer), or additional echoes may appear. Thus, there is no limitation of using ultrasound to fouling layers thickness. A detailed investigation of interactions between fouling layer and ultrasound can be found in Appendix C.

Ultrasonic methods are investigated in different foodstuff areas since several decades. E.g., ultrasound was applied for viscosity/density measurements [60] [61], non-invasive characterisation of foodstuff [9] [38] [106], and process monitoring [69] [70] [107]. Ultrasound was also used to determine sugar content in fruit juices [31], to characterise dairy products [39], and to detect internal cheese defects [90].

As mentioned above reliable excitation of the ultrasonic signal as well as analysis of measured signal is crucial. During this work signal analyses was a major topic which was realised in software. Variable methods of signal analysis are present and can be used in time and/or frequency domain. In both domains different features can be determined like amplitude (both domains), time of flight (time domain), or phase angle (frequency domain). Often, signal analysis is focused on time domain because signal is measured in time domain e.g. [92] [93] [101] [107]. For analysis in frequency domain, mainly fast Fourier transform (FFT) is undertaken. FFT has to be applied with care because it can easily introduce unwanted errors. Still, with FFT it is possible to determine influences which are not visible or not strongly distinctive in time domain [112] [122] [123] [126].

Determined features can be used directly or can be introduced into smart systems like classification methods as done in this work. Classification methods are applied in many different areas showing good results. One kind of classification is undertaken by artificial neural networks (ANN) which behave similar to neurons in brains. Overviews over ANN and how it can be applied are given in e.g. [13] (general), [94] (one-class classification), or [104] (remote sensing). Applications of ANN are image processing [42] [67] and detection of fluid structures at interfaces [71]. ANNs were also used for modeling fouling in heat exchangers e.g. [89] or crossflow ultrafiltration of dairy products e.g. [134] [133]. ANNs are often used for processing of signals like in image analysis or for modelling like in dairy industry. In this thesis ANNs have been used to detect fouling presence and to monitor cleaning success with ultrasonic measurements for the first time.

Another smart system for classification and pattern recognition is support vector machine (SVM). Compared with ANN, SVM is a newer technique where overviews are given by [152] and [163] concerning the theoretical background. Recently, SVM was applied in computational biology [15] because it is predestined for sorting and classifying complex data. This holds for e.g. gene expression where huge amount of complex data has to be sorted in multiple dimensions [81] and for protein structure prediction where the three dimensional structure of proteins is to be modeled by amino acid sequence [130]. Also, SVM was applied in speech recognition and analysis where SVM is e.g. used for automatic recognition of emotions in speech [63]. In that work, SVM showed best results compared with other methods like fuzzy logic and fuzzy k-nearest neighbour. SVM was applied in foodstuff area for the first time in this thesis.

Different ultrasonic methods were applied for monitoring fouling. Ultrasonic frequency domain reflectometry was chosen for monitoring early stage growth of biofilms on polymeric surfaces which are used for membranes in foodstuff industry [85]. Biofilm growth could be monitored successfully but measuring approach is too complicated to be easily applied in industrial heat exchangers. Also, ultrasonic time domain reflectometry (UTDR) can be applied for monitoring fouling in paper waste water as well as protein fouling [92] [93] [95]. Ultrasound was used during ultrafiltration to monitor fouling as well as cleaning success of both flat and round membranes by UTDR technique. This method shows good approaches with good accuracy yet it is based on time-of-flight measurements of reflection of different layers of the filtration membrane. Each echo of each membrane layer can be analysed and compared because all are effected by fouling. Drawback of this method is that it cannot be used for monitoring cleaning success in industrial heat exchangers.

Another method to monitor fouling and cleaning in heat exchangers is using a mechatronic surface sensor (MSS) [121] [122] [123]. Here, the evolution of an ultrasonic surface wave is investigated between actuator and sensor. Amplitude decreases with fouling presence and different fouling kinds as well as cleaning can be monitored. A drawback for industrial heat exchangers with this sensor is at the moment that temperature range for the developed sensor is much lower than pasteurisation temperature (maximum temperature in the conducted studies was around 50°C) and mainly one feature is used (signal amplitude). Amplitude variations due to excitation variation or changes in the system independent of fouling may introduce errors in detection.

Until now, there are not many studies in literature which used ultrasound for monitoring cleaning success of dairy fouling. Also, most ultrasonic methods focus on one single feature. This approach may reduce detection efficiency and accuracy if variations in excitation signal or changes in measured system during measurements occur. Closest to the work done here are the studies undertaken by Pereira et al. [121] [122] [123]. Still, they did not apply classical ultrasonic sensors but developed a mechatronic surface sensor. Pereira et al. also investigated dependencies of the signal on e.g. mass flow rate and temperature. Indeed, this was not included into analysis for increasing detection stability. For reliable online monitoring of cleaning and adaption of CIP cycles based on monitoring, a method is necessary which combines a reliable measuring method like ultrasound with reliable signal analysis which can adapt to changing conditions.

Here, a gap opens which was bridged by the work underdone in this thesis. In this thesis an ultrasonic measuring unit was developed together with an intelligent analysis to detect fouling and monitor cleaning online. To achieve this goal several steps were undertaken and several milestones were reached. First milestone was to determine what kind of detection and measurement systems are present and what is needed. Ultrasound was selected due to above mentioned advantages: it is easy to apply, a known method, sensitive to surface changes, as well as sensitive to thin layers. Next goal was the development of a well defined prototype at lab scale. A planar and linear heat exchanger was chosen such that different ultrasonic sensors could be applied easily. Furthermore modelling can be underdone easily and external influences can be controlled and minimised. The heat exchanger section can be opened to obtain information about fouling layer and cleaning success.

Based on this planar setup, the group of Prof. J. Hinrichs developed a reliable and reproducible method to produce and clean dairy protein fouling. To achieve this important milestone protein enriched milk was used and pumped in a circle through the planar measuring section were fouling was produced by electric heating. A cleaning procedure was developed using sodium hydroxide. To find best cleaning time, the measuring section was opened and cleaning success was determined visible during several cleaning runs.

At the same time an ultrasonic measuring section was developed which fits to the designed heat exchanger and could be easily applied to industrial systems. Also, error analysis of the excited and measured ultrasonic signal was done. The used materials were investigated and characterised in detail concerning electrical and thermal properties to reduce

thermal effects of the ultrasonic measuring section on the signal. During this development different coupling agents and their interactions with the ultrasonic signal were investigated. Here, both solid and liquid coupling was compared. At the end, a solid couplant (Aqualene™) was used together with a water-based coupling gel.
Ultrasonic excitation was investigated to determine influence of sheer capacities and ultrasonic transducer on the signal. This is important for analysis because electric impedance mismatch between excitation/reception and ultrasonic sensor may influence measured signals. For better analysis error analysis of the signal was done concerning extra echoes which were not introduced by the electronics. This extra echo can be neglected because it did not carry information about the investigated system and was easily distinguished by the signal of interest. Also, influence of temperature of excitation box was investigated. Signal amplitude drift was found with temperature of excitation electronics. For time of flight measurements the determination of exact arrival time of the echo is most important. Found signal drift is of no interest for time of flight measurements for which the electronics was first developed. For signal analysis underdone in this work signal amplitude was the superior parameter. Thus, signal drift with temperature was investigated and excluded. The found signal drift could be easily overcome by turning the excitation on at least 30 min prior start of measuring or not turning it off at all. Also, signal amplitude was influenced by temperature variation of system where measurements took place. This influence was taken care by introducing temperature measurements into signal analysis. More details concerning found errors can be found in Appendix D.

Besides having reproducible fouling and cleaning procedures using a reliable setup and excluding influences via hardware (coupling agent, used frequency, excitation electronics) signal analysis was investigated in detail. The milestone was to have a reliable signal analysis for monitoring fouling and cleaning online. To achieve this, first different signal parameters and features were determined both in time and frequency domain. A variety of features was chosen at the end because it was found that detection stability increased. Still, only features where chosen which showed an influence on signal with fouling presence and absence. Namely the following features of the ultrasonic signal were chosen together with temperature and mass flow rate: characteristic acoustic impedance, short time energy, temporal slope, temporal/spectral crest factor, spectral smoothness, and descent time. All chosen features displayed sensitivity to dairy protein fouling and changed with fouling. In this work, a variety of features were used to improve detection stability. This advantage helps to reduce the influence of varying signals and to get wrong results. A disadvantage is that signal analysis gets more complex and may be prone to errors if signal analysis is not undertaken with care. Chosen features were not used directly for detection of fouling presence and absence but were used as input to a sophisticated analysis system. As mentioned above, ANN, SVM, and a third method called slope change were chosen. Both ANN and SVM can be applied for complex applications and showed comparable results in speech recognition [91]. Thus both methods were chosen for detection of fouling and monitoring of cleaning success. This is one the first times that SVM was applied for detection of fouling and monitoring of cleaning. As mentioned above both methods are sophisticated and need a lot of computation time. So, a third method was developed which was less sophisticated and more efficient in calculation. All methods were compared to each other to determine which method showed best results under which conditions. Chosen benchmark was offline detection of fouled and clean surfaces and online monitoring of cleaning of fouled surfaces using the ultrasonic measuring unit. Offline training was undertaken with Matlab while signal analysis code was written with C++. Determined results were compared with each other and with literature:

- ANN was used as one-class classification and showed high accuracy (80 %) for detection of fouling presence and absence. ANN can be easily implemented into the signal analysis code and was trained offline in this thesis. Still, ANN showed highest susceptibility and thus did show drawbacks during online monitoring of cleaning. Comparing ANNs trained for protein and salt fouling showed that they cannot be easily swept. Hence, ANN can be used for detection of fouling after training but for every kind of fouling single ANNs have to be found and trained.

- SVM was used with a radial basis function kernel and showed very high accuracies (94 %) for detection of fouled and clean surfaces. Stability against signal variation was high for SVM because contrary to ANN SVM is looking for an absolute extremum during training. Training of SVM is easy but finding the best suitable kernel is a delicate work. Also, implementation into the signal analysis code was sophisticated because the code used for training has to be known in detail such that weighting is the same for the trained and the implemented SVM. As shown in this thesis SVM showed highest reliability in monitoring cleaning success and is the best candidate for industrial application. So far, SVM was not implemented for detection or modelling of fouling in foodstuff area.

- Slope change is the less sophisticated method because it only monitors the change of the determined features. Implementation into the signal analysis code is very easy and computational time is low. Slope change monitors cleaning success with high accuracy if stable and reliable experimental conditions are present. Further investigation has to be undertaken to determine the applicability of this method to other fouling types. This method is new and was not used in literature so far.

- All investigated methods can be combined with each other to improve stability and accuracy. Slope change is the most ressource serving method and it is advantageous to couple this method with ANN or SVM. The results of the methods can then be compared with each other. Consequently weaknesses and errors of the methods can be found and the real time of cleaning end can be determined with higher precision.

To improve detection stability of investigated methods outlier detection was necessarily introduced into signal analysis code. Angle-based outlier detection (ABOD) was used because it is more stable in higher dimensions. Result of ANN/SVM were given binary: 1 for fouling presence, 0 for fouling absence (clean conditions). ABOD transformed any value between 0 and 1 to one of both dependent on a threshold and compared each result in a choosable window of width n. If at least $n/2$ are greater than 0 all values were considered as 0 otherwise they were displayed as 1. ABOD helped to detect the turning point between fouled and clean conditions better. But it has to be taken into mind that turning point may be shown at a later time than it actually happened due to chosen window.
On the whole all three methods are comparable and can be used for determination of fouling presence and online monitoring of cleaning in a planar heat exchanger. ANN and SVM have to be trained offline with both fouled and clean surfaces to find best suitable ANN and SVM. Afterwards suitable ANN and SVM, respectively, were applied online. Slope change on the other hand can be used without any training. Thus is can be applied to unknown systems. ANN and slope change can be more easily implemented into the developed signal analysis code than SVM. But, ANN and slope change are prone to vary when signal varies. SVM showed higher stability against all kinds of variation of the ultrasonic signal but is the most sophisticated method. Still, SVM can be used for different fouling kinds without loss of accuracy. For each demand all investigated method show different advantages and drawbacks. Thus the suitable analysis method has to be found dependent on demand. Combination of two or all three methods helps to switch easily without loosing information or time during cleaning.
Comparing the obtained results of this thesis with literature is challenging because there is a high variation of determination of fouling and cleaning. Acoustic methods often use a different approach as applied in this PhD thesis e.g. low frequency waves travelling on plates [112] or mechatronic surfaces sensors (MSS) [121] [122] [123]. Here, [112] uses a different acoustic technique compared with the method used in this thesis. Also, different

features were chosen, namely power spectral density and propagation time of acoustic wave. Latter decreased with fouling and increased with cleaning. Advantage of the method of [112] is that it can easily be applied with plate heat exchangers. However, it cannot be used with tubular heat exchangers in contrast to the method developed in this thesis.

The MSS which was developed by Pereira et al. [121] [122] [123] and is promising for monitoring fouling and cleaning success. Still, method and chosen wave type is different from the investigated detection system here. Simulated milk ultrafiltrate was used as foulant which is very different from protein enriched milk as was used in this thesis. Protein enriched milk resembles indutrial milk more. Another difference is chosen feature (normalised amplitude in frequency domain). Cleaning was only investigated until now using shampoo films. However, this cannot be compared with cleaning of dairy protein fouling as undertaken in this thesis because both materials are very different from each other. Another drawback of the MSS at the moment is the material the flow cell is made of which only stands temperatures below 70°C while the ultrasonic detection unit developed here withstands temperatures up to 120°C.

In a nutshell the combination of ultrasonic measurements together with sophisticated pattern recognition methods is unique in foodstuff industry at the moment. Comparison with results from literature shows that this method is one of the few who detect not only fouling presence but also monitors cleaning success online. It was shown that both is feasible with the developed method and the obtained results are promising. Still several adaption have to be made such that this method can be easily implemented into industrial heat exchangers environment.

In this thesis, a combined approach of ultrasonic measurements and pattern recognition methods was applied to determine dairy protein fouling in closed heat exchangers. This approach in the used combination was new and not investigated earlier. Ultrasound was chosen because it is a well-known technique and can be used non-destructively. Classification methods were applied for signal analysis of ultrasonic signals because they are known to provide reliable results (see above). The combination of non-invasive ultrasonic measurements and classification methods can be used to monitor cleaning and adapt cleaning cycles. To accomplish the overall goal of monitoring cleaning of dairy fouling different steps were reached which are briefly summarised:

- The importance of detecting dairy fouling in closed heat exchangers was investigated. Literature was reviewed in detail to determine research missing and to evaluate different possible methods including their advantages and drawbacks. Besides, demands of industry concerning cleaning of heat exchangers was summarised. Many different methods for fouling detection were developed over the years. These methods are based on experimental methods like pressure drop, temperature and heat transfer paramters or electric and acoustic features. Others apply numerical or computational methods like neural networks or wavelet analysis using measured or simulated data as input.

The drawback of most methods is that they cannot be easily applied for online monitoring of cleaning success. Here, numerical/computational methods are advantageous compared to experimental ones because they can be more easily adapted to changing conditions. Still, numerical/computational methods first have to be validated experimentally. Dependent on industrial demands it is advantageous not to focus on one single method but to combine different ones. This increases stability and accuracy of results and analysis can be adapted more easily to changing conditions. Combination of experimental and numerical/computational methods are suggested to achieve these goals. This will help to improve cleaning of closed heat exchangers, to adapt cleaning cycles to fouling, and to be less dependent on the process investigated.

The results of this investigation are presented in paper 1 ("Detection methods of fouling in heat exchangers in the food industry").

- For determination of fouling ultrasound was chosen because it is sensitive to material changes which are happening during fouling formation and cleaning. Thus, investigations were undertaken to find a suitable detection and analysis method. This was done by using a small static setup in which both protein and mineral fouling was made reproducible. A fouling procedure for both fouling kinds was developed where the setup was filled with reconstituted milk/permeate and heated.

  After fouling formation, ultrasonic measurements were made and cleaning by hand was undertaken. Cleaning as well as fouling build-up could not be monitored but clean (before and after fouling build-up) as well as fouled surfaces were measured using an ultrasonic transducer (resonance frequency 2 MHz). Ultrasonic signals were used to determine most promising classification method for fouling detection. As classification methods, artificial neural networks (ANN) and support vector machines (SVM) were chosen. These methods were developed and evaluated to determine fouling presence and absence.

  Protein and mineral fouling were investigated to find similarities and differences between both fouling types and their influence on detection. Three different cases

were investigated: detection of only protein fouling, detection of only mineral fouling, and detection of both fouling types together. Three ANNs and three SVMs were developed and compared. Binary classification was used for ANN and SVM.
ANN showed accuracies between 70 % for both fouling mixed together and up to 100 % for only protein fouling. ANN showed high accuracy when only protein fouling was investigated but drawbacks when mineral fouling or both fouling types were present. This may be due to higher variation of data and higher susceptibility of ANN concerning data variation. Still, it was applicable for fouling determination. Accuracies for SVM varied between 97 % for both fouling types and 98 % for mineral and 100 % for protein fouling. SVM was less dependent on fouling type and data variation and also proofed a good method for fouling detection.
It follows that both classification methods can be used for determination of fouled and cleaned surfaces. Next steps are including flow and monitor cleaning to improve developed detection methods. This will test their applicability in more realistic cases.
Work done together with detailed results is presented in papers 2 ("On the usage of acoustic properties combined with an artifical neural network – A new approach of determining presence of dairy fouling") and 3 ("Detection of dairy fouling: Combining ultrasonic measurements and classification methods").

- Determination of suitable methods for fouling detection and cleaning monitoring is a very important point. An experimental setup was developed to monitor cleaning and measure fouling with flow. Most important part of the developed setup was a planar measuring section which can be inserted into a setup with pumps, tanks, and preheaters or can be used by its own with electric heating. The planar measuring section can be disassembled to investigate the fouling layer in more detail. Also, pilot plant scale experiments can be undertaken and different fouling procedures and cleaning cycles can be investigated.
An ultrasonic detection unit was attached to the planar measuring section and used for monitoring fouling presence and cleaning. Fouling build-up could not be monitored. The ultrasonic measuring section consisted of a delay line made of polymethylmethacrylate (PMMA) and an ultrasonic transducer (resonance frequency 2 MHz). Coupling was done with water-based gel and solid coupling (Aqualene).
The planar measuring section was investigated both experimentally and theoretically. Experimental characterisation was done concerning reproducible signals and influence of different parameters (temperature, vibration) on ultrasonic signals. It

was shown that most influences on ultrasonic signal are negligible. Detailed theoretical description was given using lumped circuits and by performing sensitivity analysis. Latter can help to determine error sources and influences which then can be investigated in more detail. Sensitivity analysis showed influence of different features on the ultrasonic signal but most features can be considered constant during cleaning and fouling build-up, e.g. stainless steel wall and delay line. Fouling particularly its characteristic acoustic impedance had a high weight. Because fouling develops and is diminished during cleaning a changing characteristic acoustic impedance at the interface stainless steel wall-medium ist presen. Thus, it can be concluded that fouling is measurable and cleaning can be monitored.
Work done is summarised in paper 4 ("Investigating and understanding fouling in a new setup using ultrasonic detection methods").

- After investigating different classification methods and developing an experimental setup cleaning monitoring has to be done to determine accuracies and improve developed methods. To do so, the developed classification methods ANN and SVM were implemented in an online monitoring code which was used to determine fouling presence and monitor cleaning success in the planar measuring section.
First, a fouling procedure for reproducible fouling build-up and a cleaning cycle for defined cleaning was developed. Then, ultrasonic measurements of the clean and fouled heat exchanger as well as cleaning cycles were performed. Ultrasonic measurements were analysed and ANN and SVM showed accuracies between 80 % (ANN) and 94 % (SVM). One-class classification was used for ANN and binary classification was used for SVM. SVM showed higher accuracy and was less influenced by data variation than ANN making it a better applicable method for online detection. Data variation may be introduced by slightly varying fouling layers. Angle based outlier detection and exceptional handling were applied to reduce outliers and improve detection accuracy of the measurements.
Both classification methods were usable for online detection but a third method was developed which proofed to be easier applicable for direct monitoring of cleaning time. This method monitors the slope of measured ultrasonic features which were also used for ANN and SVMN. Values of the ultrasonic features stayed nearly constant after fouling developed and process parameters were fixed. When cleaning started, values changed until cleaning was finished after which they showed nearly constant values again. Thereby not the value itself was of importance but the change during cleaning was investigated. Cleaning time could be monitored offline and was

determined to be 22 ± 3 min. This was in good agreement with experimental results where cleaning was stopped and cleaning success was determined. Still, thickness of fouling layer was not 0 but determined to be below 50 μm. Further improvement has to be done to determine even thinner layers. It was shown that it is possible to monitor fouling and cleaning success in a planar heat exchanger using a combination of ultrasonic measurements and classification methods.

The achieved results are summarised in Paper 5 ("Monitoring fouling presence and absence by an online measuring method of combined ultrasonic measurements and classification methods").

Further Work

Further work concerning detection of dairy fouling and monitoring of cleaning cycles in heat exchangers can be done in a variety of directions. Some of these ways will be discussed in short. This may help to improve detection and gives an opportunity to industry to adapt cleaning cycles and to safe money.

One way to improve detection of dairy fouling and monitoring of cleaning cycles is using phase locked loop (PLL): an output signal generated by a control system is related to phase of an input signal. Thus, phase of the signal can be detected and matched. So, frequency of the input signal can be tracked which may help to detect low fouling thicknesses. PLL is used in various electronic applications and measurement and control technology. E.g., for atomic force microscopy PLL is applied where frequencies can be detected with 0.1 Hz accuracy using a measuring frequency of 32 kHz and a resolution of atomic scale.

Another way to improve measurements for fouling detection and cleaning monitoring is to perform computational simulations. Simulation using different models are possible. SPICE for example can be used to improve electronics and get rough impressions of the behaviour of the ultrasonic wave during fouling and cleaning. Finite element (FE) modelling on the other side can provide more details concerning the interaction of ultrasonic waves and media. If fouling deposition and cleaning models are included cleaning supervision can be modelled and compared with ultrasonic experiments. This will help to adapt cleaning better to fouling present and to reduce costs and amounts of experiments. Also, developed signal analysis can be tested without or with less experiments made and adapted if drawbacks are shown. Fundamental understanding of fouling and cleaning processes and their measurements using ultrasound will also be provided.

To make signal analysis better adaptable to changed process parameters (e.g. changed product, changed temperatures) analysis training and testing of classification methods can be done online. This can be achieved by using one-class classification where the classification system is trained to the status "clean" which is always the case at the beginning of a batch. If any changes occur between this batch and batches prior the analysis system can adapt easily and provide the used with reliable results. Changes during operation can be included more easily and decisions about cleaning success can be made more secure. This can also be combined with simutational results improving detection accuracy even more.

One way to adapt fouling detection and cleaning monitoring to different fouling types and cleaning cycles may be using frequency sweep techniques. Here, the frequency of a signal is scanned (sweeped) during a fixed band. Power spectrum versus frequency is measured. Different fouling kinds and layer thickness may react differently to various frequencies. Advantage of this can be taken to improve detection accuracy. E.g. higher frequencies are more sensitive to thin layers than lower frequencies. Also, performance of electronic and measuring system can be determined to reduce false negative or false positive results.

Measurement accuracy can be improved if more than one ultrasonic transducer is used because different places in one heat exchanger can be monitored at the same time. This overcomes the drawback of ultrasonic transducers which are monitoring only one point. If several transducers are placed at points prone to fouling cleaning could be improved. Still, different measurement signals have to be combined in enhanced signal analysis to determine reasonable results.

One important step is to attach the ultrasonic detection unit to round tubes to fit the developed ultrasonic measuring system better to industry. This can be done by adapting transducer design such that no flat-round but round-round design is used. Here, flexible piezo foils or using an adaptor which fits the planar piezo ceramic to the round tube can be used. Transducer design has also to be adapted which means resonance frequency used, backing, and coupling of the transducer. This will improve measured signal and increase signal-to-noise ratio which in turns increases detection accuracy and stability. Refraction will play a more important role with round tubes than in the system investigated here. Thus, refraction corrections have to be included into signal analysis. On the other hand, an adaptor and signal refraction of the round tubes may be used to build a kind of acoustic lens which focus on the area of interest (compare with a microscope). Here, thinner layers may be detected and cleaning may be even better adapted in time. Time of flight measurements may be done to determine also fouling layer thickness if this is of interest. Pulse-echo technique on the other side does not have to cope with changed medium properties behind the fouling layer. In this thesis, pulse-echo technique was applied using one transducer. For round tubes, also through-transmission technique may be applied using two transducer because signal may be less influenced during through transmission. A fixed position of the ultrasonic measuring section should be chosen on a heat exchanger. Ultrasonic transducer should not be deattached as long as it is not necessary because attaching and deattaching may include unwanted signal variations. Besides cleaning cycles fouling build-up can be monitored with such a system. This may help to define starting point of cleaning and adapt cleaning not only in cleaning length. Here, production cycles may be elongated and costs concerning downtime can be reduced. Combination of different detection systems increases detection stability and fault-tolerances due to increased redundancy. Results of the different methods can be compared and weaknesses of one single method can be found and compensated by other methods. Combining methods with higher and less computational time can be chosen and compared.

Conclusion

In summary, it was shown in this thesis that it is possible to determine fouling presence and absence and monitor cleaning success in a planar heat exchanger using a combination of ultrasonic measurements and classification methods. Different classification methods (ANN, SVM) were investigated and compared. Accuracies of classification methods were between 80 % (ANN) and 94 % (SVM). Cleaning time was determined using another method (slope change) and was comparable with cleaning time found by experiments. Cleaning time found by slope change was 22 ± 3 min. This resembled a fouling thickness below 50 μm. Comparing all three methods showed that they are comparable showing different advantages and drawbacks. In a nutshell, a reliable online detection system was developed using a combined approach of ultrasonic measurements and classification methods.

The focus for further investigations lies in adapting signal analysis and ultrasonic measuring unit (ultrasonic transducer, delay line if necessary, coupling) to round tubes. Next steps will include measurements in industrial heat exchangers to enhance signal analysis and make the system adaptable for industry. Simulations done with FE or other tools will help to improve measurements, signal analysis, and transducer design and can reduce costs. So, a reliable method for fouling detection and online monitoring of cleaning success can be provided for industrial processes.

List of Publications

List of Reviewed Publications

1. Wallhäußer, E., Sayed, A., Nöbel, S., Hussein, M.A., Hinrichs, J., Becker, T., Determination of cleaning end of protein fouling using an online system combining ultrasonic and classification methods, Food and Bioprocess Technology 6 (1) (2013), 1–10

2. Wallhäußer, E., Nöbel, S., Sayed, A., Hussein, M.A., Hinrichs, J., Becker, T., Kontinuierliche Detektion von Milchfouling mittels einer Kombination von Ultraschall und Klassifizierungsmethoden, Chemie-Ingenieur-Technik 85 (2013), 1589–1596

3. Wallhäußer, E., Hussein, M.A., Becker, T., Investigating and understanding fouling in a planar setup using ultrasonic methods, Review of Scientific Instruments 83 (9) (2012), 094904–094914

4. Wallhäußer, E., Hussein, W.B., Hussein, M.A., Hinrichs, J., Becker, T., Detection of dairy fouling: Combining ultrasonic measurements and classification methods, Engineering in Life Science 13 (2013), 292–301

5. Wallhäußer, E., Hussein, M.A., Becker, T., Detection methods of fouling in heat exchangers in the food industry, Food Control 27 (2012), 1–10

6. Wallhäußer, E., Hussein, W.B., Hussein, M.A., Hinrichs, J., Becker, T., On the usage of acoustic properties combined with an artificial neural network – A new approach of determining presence of dairy fouling, Journal of Food Engineering 103 (2011), 449–456

List of Conferences

1. Wallhäußer, E., Hussein, M.A., Hinrichs, J., Becker, T., Detecting fouling using different methods, (talk) AMA conference 2013, Nürnberg, Deutschland, 14.05. – 16.05.2013

2. Wallhäußer, E., Hussein, M.A., Becker, T., How to detect protein fouling and cleaning in heat exchangers using ultrasound, (talk) 76. DPG-Frühjahrstagung, Berlin, Deutschland, 25.03. – 30.03.2012

3. Nöbel, S., Sprunk, M., Wallhäußer, E., Becker, T., Hinrichs, J., Option zur Online-Quantifizierung des Reinigungserfolgs in Milcherhitzern, DECHEMA-Jahrestreffen des Fachausschusses Lebensmittelverfahrenstechnik, Rheologie und Trocknungstechnik, Stuttgart, Deutschland, 19.03. – 21.03.2012

4. Wallhäußer, E., Hussein, W.B., Hussein, M.A., Becker, T., Usage of ultrasound in detecting dairy fouling on stainless steel, (poster)International Workshop "Online sensors for fouling monitoring", Frankfurt a.M., Deutschland, 29.11. – 30.11.2010

5. Wallhäußer, E., Hussein, M.A., Becker, T., Usage of ultrasound in detecting fouling presence on stainless steel, (talk) 14. Deutsche Physikerinnentagung, Münnchen, Deutschland, 04.11. – 07.11.2010

6. Wallhäußer, E., Úbeda Trillo, M.A., Hussein, M.A., Becker, T., Acoustic impedance analysis for determining presence and cleaning success of dairy fouling, (talk) Fouling and Cleaning in Food Processes 2010, Cambridge, UK, 22.03.2010 – 24.03.2010

7. Wallhäußer, E., Hussein, M.A., Becker, T., The acoustic impedance – an indicator for concentrations in alcoholic fermentation and cleaning progress of fouled tube heat exchangers, (talk) CIGR 2009, Potsdam, Deutschland, 31.08.2009 – 02.09.2009

8. Wallhäußer, E., Becker, T., Potenziale zur Validierung des Reinigungserfolgs von Erhitzungsanlagen mittels Ultraschallmessung, (talk) 3. Lebensmittelwissenschaftliches Kolloquium, Stuttgart, Deutschland, 25.06.2008

9. Wallhäußer, E., Neugart, F., Zappe, A., Buk, D. Graeve, L., Tietz, C., Wrachtrup, J., Investigation of the first steps of the CNTF mediated signal reception by means of fluorescence correlation spectroscopy in living cells, (poster) DPG-Frühjahrstagung, Regensburg, Deutschland, 26.0.3 – 30.03.2007

List of Abbrevations

ABOD angle based outlier detection
ANN artificial neural network
CIP cleaning in place
DLVO Derjaguin-Landau-Verwey-Overbeek
FE finite elements
HNO_3 nitric acid
IEP isoelectric point
KLM Krimholtz-Leedom-Mattaei
NaOH sodium hydroxide
NDT non-destrucrtive testing
PZT lead zirconate titanate
SA sensitivity analysis
SCF spectral crest factor
S/N ratio signal to noise ratio
SPICE simulation program with integrated circuit emphasis
SSMOOTH spectral smoothness
STE short time energy
SVM support vector machine
TCF temporal crest factor
TDESCEND temporal descend
TSLOPE temporal decrease
vdW van der Waals
Z characteristic acoustic impedance
β-lg beta-lactoglobulin

List of Symbols

A amplitude

A Hamaker constant

a output

ABO_3 Perowskite structure

B amplitude

B monomer

B* activated monomer

b bias

C amplitude

C capacity

$c_{p,v}$ specific heat capacity at constant pressure/volume

$c_{(0)}$ sound velocity

D amplitude

D dielectric displacement

d piezoelectric constant

d diameter

E Young's modulus

E electric field

E_A activation energy

e piezoelectric constant

F force

F outer body force

f function

G shear modulus

G conductance

G acoustic field due to changing volume

g gravity

I current

K compression modulus

K reaction rate constant

K kernel function

m slope

N number of datapoints

n input

n number of signal

p pressure

R gas constant

R resistance

R reflectivity

r reflection coefficient

r radius

S strain

s^E elasticity constant

T stress

$T_{i,j}$ protein aggregate

t time

u displacement vector

V voltage

v (particle) velocity

X compliance

X magnitude

x data point

x amplitude

x direction

x_i support vector

L inductance

1:N transformer ratio

Greek Symbols

α real part of propagation constant

α_i Lagrange multiplier

β imaginary part of propagation constant

Φ flux

γ adiabatic coefficient

γ propagation constant

δ Kronecker symbol

$\underline{\epsilon}$ deformation tensor

ε^T permittivity at constant stress

ε electric permittivity of a medium

η imaginary part of the elastic modulus

η viscosity

η_B bulk viscosity

Θ thickness

κ reciprocal Debyle length

ρ_0 density

$\underline{\sigma}$ stress tensor

τ shear stress

φ velocity potential

Ψ wave function

Ψ electric surface potential

Ψ_0 amplitude

ω angular frequeny

ω vorticity

Subtitle

0 incident

1,2 number of solution

11,22,33 direction of tensor

A activity

a,b,c number of component

ads adsorbed

agg aggregated

B bulk

c characteristic

calc calculated

D deposition

denat denaturated

el electrostratic

i,j,k (tensor) direction

i counter

m counter

n counter

R removal

sample investigated sample

steel stainless steel

tube siphon tube

wall wall

water water

Bibliography

[1] N. N. Abboud, G. L. Wojcik, D. K. Vaughan, J. Mould, D. J. Powell, and L. Nikodym. Finite element modelling for ultrasonic transducers. In *Proc. SPIE Int. Symp. Medical Imaging*, 1998.

[2] A. Al-Janabi, M.R. Malayeri, and H. Müller-Steinhagen. Minimisation of $CaSO_4$ deposition through surface mitigation. In H. Müller-Steinhagen, M.R. Malayeri, and A.P. Watkinson, editors, *Proceedings of International Conference on Heat Exchanger and Fouling and Cleaning VIII - 2009*, 2009.

[3] N. Alvarez, G. Daufin, and G. Gesan-Guiziou. Recommendations for rationalizing cleaning-in-place in the dairy industry: Case study of an ultra-high temperature heat exchanger. *Journal of Dairy Science*, 93(2):808–821, February 2010.

[4] N. Aouzale, A. Chitnalah, and H. Jakjoud. Experimental validation of spice modeling diffraction effects in a puls-echo ultrasonic system. *IEEE Transactions on Circuits and Systems II: Express Briefs*, 56(12):911–915, 2009.

[5] N. Aouzale, A. Chitnalah, H. Jakjoud, and D. Kourtiche. PSPICE modelling diffraction effects in pulse echo ultrasonic system. In *14th IEEE International Conference on Electronics, Circuits and Systems, ICECS 2007*, pages 54–57, Marrakech, 2007.

[6] N. W. Ashcroft and N. D. Mermin. *Festkörperphysik*. Oldenburg Verlang München Wien, 2 edition, 1995.

[7] W. Augustin, T. Geddert, and S. Scholl. Surface treatment for the mitigation of whey protein fouling. In H. Müller-Steinhagen, M.R. Malayeri, and P. Watkinson, editors, *Proceedings of the 7th International Conference on Heat Exchanger Fouling and Clenaing - Challenges and Opportunities*, volume RP5, pages 206 – 214, July 2007.

[8] S. Balasubramanian and V. M. Puri. Fouling of food processing equipment – critical review. In *ASABE 10 Annual Internatial Meeting*, pages –, 2010.

[9] Judith Ann Bamberger and Margaret S. Greenwood. Non-invasive characterization of fluid foodstuffs based on ultrasonic measurements. *Food Research International*, 37(6):621–625, July 2004.

[10] B. Bansal and X. D. Chen. A critical review of milk fouling in heat exchangers. *Comprehensive Reviews in Food Science and Food Safety*, 5(2):27–33, 2006.

[11] B. Bansal, X.D. Chen, and S. X. Q. Lin. Skim milk fouling during ohmic heating. In M.R. Müller-Steinhagen, H.and Malayeri and A.P. Watkinson, editors, *Proceedings of the 6th International Conference on Heat Exchanger Fouling and Clenaing - Challenges and Opportunities*, volume RP2, pages 133 – 140, June 2005.

[12] S. B. Barnett, G. R. Ter Haar, M. C. Ziskin, H.-D. Rott, F. A. Duck, and K. Maeda. International recommendations and guidelines for the safe use of diagnostic ultrasound in medicine. *Ultrasound in Medicine & Biology*, 26(3):355–366, March 2000.

[13] I. A. Basheer and M. Hajmeer. Artificial neural networks: fundamentals, computing, design, and application. *Journal of Microbiological Methods*, 43(1):3–31, December 2000.

[14] M. T. Belmar-Beiny and P. J. Fryer. Preliminary stages of fouling from whey protein solutions. *Journal of Dairy Research*, 60(04):467–483 M3 – 10.1017/S0022029900027837, 1993.

[15] A. Ben-Hur, C. S. Ong, S. Sonnenburg, B. Schölkopf, and G. Rärtsch. Support vector machines and kernels for computational biology. *PLoS Comput Biol*, 4(10):e1000173–, October 2008.

[16] P. Blanpain-Avet, A. Hédoux, Y. Guinet, L. Paccou, J. Petit, T. Six, and G. Delaplace. Analysis by Raman spectroscopy of the conformational structure of whey proteins constituting fouling deposits during the processing in a heat exchanger. *Journal of Food Engineering*, 110(1):86–94, May 2012.

[17] P.R.H. Blasius. Das Ähnlichkeitsgesetz bei Reibungsvorgängen in Flüssigkeiten. *Mitteilungen über Forschungsarbeiten auf dem Gebiete des Ingenieurswesen*, 131:1–41, 1913.

[18] K. Bode, R.J. Hooper, W. Augustin, W. R. Paterson, D. I. Wilson, and S. Scholl. Pulsed flow cleaning of whey protein fouling layers. In H. Müller-Steinhagen, M.R. Malayari, and A.P. Watkinson, editors, *Proceedings of the 6th International Conference on Heat Exchanger Fouling and Clenaing - Challenges and Opportunities*, volume RP2, pages 165 – 173, June 2005.

[19] K. Bode, R.J. Hooper, W.R. Paterson, D.I. Wilson, W. Augustin, and S. Scholl. Reinigung von Molkeproteinablagerungen mit pulsierender Strömung. *Chemie Ingenieur Technik*, 78(5):613–620, 2006.

[20] T.R. Bott. *Fouling of Heat Exchangers*. Elsevier Science & Technology Books, April 1995.

[21] S. Bourne. Novel solid contact ultrasonic couplants based on hydophilic polymers. *NDTnet*, unkown:1–13, 2000. Roma 2000 15th WCNDT.

[22] H. Burton. A laboratory method for the investigation of milk deposits on heat exchanger surfaces. *Journal of Dairy Research*, 28(03):255–263, 1961.

[23] H. Burton. Section G. Deposits from whole milk in heat treatment plant–a review and discussion. *Journal of Dairy Research*, 35(02):317–330, 1968.

[24] S. Butterworth. On electrically-maintained vibrations. *Proceedings of the Physical Society of London*, 27(1):410–, 1914.

[25] R. Carrotta, R. Bauer, R. Waninge, and C. Rischel. Conformational characterization of oligomeric intermediates and aggregates in beta-lactoglobulin heat aggregation. *Protein Science*, 10(7):1312–1318, 2001.

[26] M.S. Celnik, M.J. Patel, M. Pore, D.M. Scott, and D. I. Wilson. Modelling laminar pulsed flow for the enhancement of cleaning. *Chemical Engineering Science*, 61:2079 – 2084, 2006.

[27] S. D. Changani, M. T. Belmar-Beiny, and P. J. Fryer. Engineering and chemical factors associated with fouling and cleaning in milk processing. *Experimental Thermal and Fluid Science*, 14(4):392–406, May 1997.

[28] X. D. Chen, D. X. Y. Li, S. X. Q. Lin, and N. Özkan. On-line fouling/cleaning detection by measuring electric resistance–equipment development and application to milk fouling detection and chemical cleaning monitoring. *Journal of Food Engineering*, 61(2):181–189, 2004.

[29] J. Y. M. Chew, W. R. Paterson, and D. I. Wilson. Fluid dynamic gauging for measuring the strength of soft deposits. *Journal of Food Engineering*, 65(2):175–187, November 2004.

[30] G. Chikenji and M. Kikuchi. What is the role of non-native intermediates of beta-lactoglobulin in protein folding? *Proceedings of the National Academy of Sciences of the United States of America*, 97(26):14273–14277, 2000.

[31] Norma I. Contreras, Peter Fairley, David J. McClements, and Malcolm J. W. Povey. Analysis of the sugar content of fruit juices and drinks using ultrasonic velocity measurements. *International Journal of Food Science and Technology*, 27(5):515–529, 1992.

[32] J. Curie and P. Curie. Développment par compression de l'électricité polaire dans les cristaux hérmièdres à faces inclinées. *Bulletin de la Societe Mineralogie de France*, 3:90, 1881.

[33] P. Curie and J. Curie. Contractions et dilatations produites par des tension electrique dans les cristaux hérmièdres à faces inclinées. *Comptes rendus de l'Academie des Sciences*, XCIII:1137, 1881.

[34] P. de Jong. Impact and control of fouling in milk processing. *Trends in Food Science & Technology*, 8(12):401–405, December 1997.

[35] P. de Jong, R. Waalewijn, and H.J.L.J. van der Linden. Validity of a kinetic fouling model for heat-treatment of whole milk. *Lait*, 73:293 – 302, 1993.

[36] F. Delplace, J. C. Leuliet, and D. Leviex. A reaction engineering approach to the analysis of fouling by whey proteins of a six-channels-per-pass plate heat exchanger. *Journal of Food Engineering*, 34(1):91–108, October 1997.

[37] A. M. Donald. Aggregation in β-lactoglobulin. *Soft Matter*, 4(6):1147–1150, 2008.

[38] A.S. Dukhin and P.J. Goetz. Ultrasound for characterizing liqiud based food products. 1. acoustic spectroscopy. *Dispersion Technology Inc.*, 1:1–26, 2002.

[39] A.S. Dukhin, P.J. Goetz, and B. Travers. Use of ultrasound for characterizing dairy products. *Journal of Dairy Sciences*, 88(4):1320–1324, Apr 2005.

[40] H. Dürr. Milk heat exchanger cleaning: Modelling of deposit removal II. *Food and Bioproducts Processing*, 80(4):253–259, December 2002.

[41] H. Dürr and A. Grasshoff. Milk heat exchanger cleaning: Modelling of deposit removal. *Food and Bioproducts Processing*, 77(2):114–118, June 1999.

[42] M. Egmont-Petersen, D. de Ridder, and H. Handels. Image processing with neural networks–a review. *Pattern Recognition*, 35(10):2279–2301, October 2002.

[43] M. H. Eide, J. P. Homleid, and B. Mattsson. Life cycle assessment (LCA) of cleaning-in-place processes in dairies. *Lebensmittel-Wissenschaft und-Technologie*, 36(3):303–314, May 2003.

[44] W. N. Eigel, J. E. Butler, C. A. Ernstrom, Jr. Farrell, H. M., V. R. Harwalkar, R. Jenness, and R. McL. Whitney. Nomenclature of proteins of cow's milk: Fifth revision. *J. Dairy Sci.*, 67(8):1599–1631, 1984.

[45] N. Epstein. Thinking about heat transfer fouling: A 5x5 matrix. *Heat Transfer Engineering*, 4(1):43–56, 1981.

[46] A. Fickak, A. Al-Raisi, and X. D. Chen. Effect of whey protein concentration on the fouling and cleaning of a heat transfer surface. *Journal of Food Engineering*, 104(3):323–331, June 2011.

[47] M. Foerster and M. Bohnet. Modification of molecular interactions at the interface crystal/heat transfer surface to minimize heat exchanger fouling. *International Journal of Thermal Sciences*, 39(7):697–708, July 2000.

[48] A. Friis and B.B.B. Jensen. Prediction of hygiene in food processing equipment using flow modeling. *Food and Bioproducts Processing*, 80(4):281–285, December 2002.

[49] P. J. Fryer and M. T. Belmar-Beiny. Fouling of heat exchangers in the food industry: a chemical engineering prespective. *Trends in Food Science & Technology*, 2:33–37, 1991.

[50] P. J. Fryer, G. K. Christian, and W. Liu. How hygiene happens: physics and chemistry of cleaning. *International Journal of Dairy Technology*, 59(2):76–84, 2006.

[51] P. J. Fryer, P. T. Robbins, and K. Asteriadou. Current knowledge in hygienic design: can we minimize fouling and speed cleaning? *Procedia Food Science*, 1:1753–1760, 2011.

[52] P. J. Fryer, P. T. Robbins, P. M. Cole, K. R. Goode, Z. Zhang, and K. Asteriadou. Populating the cleaning map: can data for cleaning be relevant across different lengthscales? *Procedia Food Science*, 1(0):1761–1767, 2011.

[53] P.J. Fryer and K. Asteriadou. A prototype cleaning map: A classification of industrial cleaning processes. *Trends in Food Science & Technology*, 20(6-7):255–262, July 2009.

[54] M. C. Georgiadis, G. E. Rotstein, and S. Macchietto. Optimal design and operation of heat exchangers under milk fouling. *AIChE Journal*, 44(9):2099–2111, 1998.

[55] S.R. Ghorayeb, E. Maione, and V. La Magna. Modelling of ultrasonic wave propagation in teeth using pspice: a comparison with finite element models. *IEEE Transactions on Ultrasonics, Ferroelectrics and Frequency Control*, 48(4):1124–1131, 2001.

[56] C. R. Gillham, P. J. Fryer, A. P. M. Hasting, and D. I. Wilson. Cleaning-in-place of whey protein fouling deposits: Mechanisms controlling cleaning. *IChemE*, 77:127 – 136, June 1999.

[57] C. R. Gillham, P. J. Fryer, A. P. M. Hasting, and D. I. Wilson. Enhanced cleaning of whey protein soils using pulsed flows. *Journal of Food Engineering*, 46(3):199–209, November 2000.

[58] P. W. Gordon, A. D. M. Brooker, J. Y. M. Chew, I. A. Wilson, and D. W. York. A scanning fluid dynamic gauging technique for probing surface layers. *Measurement Science and Technology*, 21(8):085103, 2010.

[59] S. M. Gotham, P. J. Fryer, and A. M. Pritchard. β-lactoglobulin denaturation and aggregation reactions and fouling deposit formation: a DSC study. *International Journal of Food Science & Technology*, 27(3):313–327, 1992.

[60] Justus D. & Bond Leonard J. Greenwood, Margaret S.; Adamson. Measurement of the viscosity-density product using multiple reflections of ultrasonic shear horizontal waves. *Ultrasonics*, 44(Supplement 1):e1031–e1036, 2006.

[61] M. S. Greenwood, J.R. Skorpik, J. A. Bamberger, and R. V. Harris. On-line ultrasonic density sensor for process control of liqiuds and slurries. *Ultrasonics*, 37:159 – 171, 1999.

[62] K. Grijspeerdt, L. Mortier, J. De Block, and R. Van Renterghem. Applications of modelling to optimise ultra high temperature milk heat exchangers with respect to fouling. *Food Control*, 15(2):117–130, March 2004.

[63] M. Grimm, K. Kroschel, and S. Narayanan. Support vector regression for automatic recognition of spontaneous emotions in speech. In *IEEE International Conference on Acoustics, Speech and Signal Processing, 2007. ICASSP 2007*, volume 4, pages IV–1085–IV–1088–, 2007.

[64] O. Gudmundsson, O.P. Palsson, H. Palsson, and S. Lalot. Fouling detection in a cross-flow heat exchanger based on physical modelling. In H. Müller-Steinhagen, M.R. Malayari, and A.P. Watkinson, editors, *Proceedings of International Conference on Heat Exchanger and Fouling and Cleaning VIII - 2009*, 2009.

[65] D. Hamada and C. M. Dobson. A kinetic study of β-lactoglobulin amyloid fibril formation promoted by urea. *Protein Science*, 11(10):2417–2426, 2002.

[66] D. Hamada, T. Tanaka, G. G. Tartaglia, A. Pawar, M. Vendruscolo, M. Kawamura, A. Tamura, N. Tanaka, and C. M. Dobson. Competition between folding, native-state dimerisation and amyloid aggregation in β-lactoglobulin. *Journal of Molecular Biology*, 386(3):878–890, February 2009.

[67] M.A. Hannan, A. Hussain, S.A. Samad, K.A. Ishak, and A. Mohamed. A unified robust algorithm for detection of human and non-human object in intellegent safety application. *International Journal of Signal Processing*, 4(3):207 – 214, 2008.

[68] I.J. Haug, H.M. Skar, G.E. Vegarud, T. Langsrud, and K.I. Draget. Electrostatic effects on β-lactoglobulin transitions during heat denaturation as studied by differential scanning calorimetry. *Food Hydrocolloids*, 23(8):2287–2293, December 2009.

[69] P. Hauptmann, N. Hoppe, and A. Puettmer. Application of ultrasonic sensors in the process industry. *Measurement Science and Technology*, 13:R73 – R83, 2002.

[70] B. Henning, R. Lucklum, and P. Kupfernagel, B and; Hauptmann. Ultrasonic sensor system for characterization of liquid systems. *Sensors and actuators. A, Physical*, 42(1-3):476–480, 1994.

[71] M.I.P. Hidayat and B. Ariwahjoedi. Radial basis function neural networks for velocity-field reconstruction in fluid-structure interaction problem. In *Computer Applications and Industrial Electronics (ICCAIE), 2010 International Conference on*, pages 506–510, 2010.

[72] R.J. Hooper, W.R. Paterson, and D.I. Wilson. Comparison of whey protein model foulants for studying cleaning of milk fouling deposits. *Food and Bioproducts Processing*, 84(4):329–337, December 2006.

[73] Y. Hu, X. Zhang, J. Yang, and Q. Jiang. Transmitting electric energy through a metal wall by acoustic waves using piezoelectric transducers. *IEEE Transactions on Ultrasonics, Ferroelectrics and Frequency Control*, 50(7):773–781, 2003.

[74] C.G. Hutchens and S.A. Morris. A three port model for thickness mode transducers using spice ii. In *Ultrasonics Symposia Proceedings*, 1984.

[75] J. Johansson and P.-E. Martinsson. Incorporation of diffraction effects in simulations of ultrasonic systems using PSPICE models. In *Ultrasonics Symposium, 2001 IEEE*, volume 1, pages 405–410, 2001.

[76] S. Jun and M.V. Puri. Fouling models for heat exchangers in dairy processing: a review. *Journal of Food Process Engineering*, 28:1 – 34, 2005.

[77] C. A. C. Karlsson, M. C. Wahlgren, and C. A. Trägårdh. Some surface-related aspects of the cleaning of new and reused stainless-steel surfaces fouled by protein. *International Dairy Journal*, 8(10-11):925–933, October 1998.

[78] H.-G. Kessler and H.-J. Beyer. Thermal denaturation of whey proteins and its effect in dairy technology. *International Journal of Biological Macromolecules*, 13(3):165–173, June 1991.

[79] L.E. Kinsler, A. R. Frey, A. B. Coppens, and J. V. Sanders. *Fundamentals of Acoustics*. John Wiley & Sons, Ltd., 2000.

[80] A. E. Kobryn and F. Hirata. Statistical-mechanical theory of ultrasonic absorption in molecular liquids. *J. Chem. Phys.*, 126(4):044504–13, January 2007.

[81] D. Komura, H. Nakamura, S. Tsutsumi, H. Aburatani, and S. Ihara. Multidimensional support vector machines for visualization of gene expression data. *Bioinformatics*, 21(4):439–444–, 2005.

[82] G. Kontopidis, C. Holt, and L. Sawyer. Invited review: β-lactoglobulin: Binding properties, structure, and function. *J. Dairy Sci.*, 87(4):785–796, 2004.

[83] M. R.H. Krebs, G. L. Devlin, and A. M. Donald. Amyloid fibril-like structure underlies the aggregate structure across the pH range for β-lactoglobulin. *Biophysical Journal*, 96(12):5013–5019, June 2009.

[84] R. Krimholtz, D.A. Leedom, and G.L. Mattaei. New equivalent circuits for elementary piezoelectric transducers. *Electronic Letters*, 6(13):398–399, June 1970.

[85] Elmira Kujundzic, A. Cristina Fonseca, Emily A. Evans, Michael Peterson, Alan R. Greenberg, and Mark Hernandez. Ultrasonic monitoring of early-stage biofilm growth on polymeric surfaces. *Journal of Microbiological Methods*, 68(3):458–467, March 2007.

[86] K. Kuwata, M. Hoshino, V. Forge, S. Era, C. A. Batt, and Y. Goto. Solution structure and dynamics of bovine β-lactoglobulin A. *PRS*, 8(11):2541–2545, 1999.

[87] W.M. Leach, Jr. Controlled-source analogous circuits and spice models for piezoelectric transducers. *IEEE Transactions on Ultrasonics, Ferroelectrics, and Frequency Control*, 41(1):60–66, January 1994.

[88] M.-N. Leclercq-Perlat and M. Lalande. Cleanability in relation to surface chemical composition and surface finishing of some materials commonly used in food industries. *Journal of Food Engineering*, 23(4):501–517, 1994.

[89] S. Lecoeuche, S. Lalot, and B. Desmet. Modelling a non-stationary single tube heat exchanger using multiple coupled local neural networks. *International Communications in Heat and Mass Transfer*, 32(7):913–922, July 2005.

[90] Vincent Leemans and Marie-France Destain. Ultrasonic internal defect detection in cheese. *Journal of Food Engineering*, 90(3):333–340, February 2009.

[91] J. Li. An empirical comparison between svms and anns for speech recognition. In *First instructional Conference on Machine Learning (iCML-2003)*, Decmber 2-3 2003.

[92] J. Li, D. K. Hallbauer, and R. D. Sanderson. Direct monitoring of membrane fouling and cleaning during ultrafiltration using a non-invasive ultrasonic technique. *Journal of Membrane Science*, 215(1-2):33–52, April 2003.

[93] Jian-Xin Li, R.D. Sanderson, and G.Y. Chai. A focused ultrasonic sensor for in situ detection of protein fouling on tubular ultrafiltration membranes. *Sensors and Actuators B: Chemical*, 114(1):182–191, March 2006.

[94] Jianwu Li, Zhanyong Mao, and Yao Lu. Adapting radial basis function neural networks for one-class classification. In *Neural Networks, 2008. IJCNN 2008. (IEEE World Congress on Computational Intelligence). IEEE International Joint Conference on*, pages 3766–3770, 2008.

[95] Jianxin Li, R. D. Sanderson, D. K. Hallbauer, and V. Y. Hallbauer-Zadorozhnaya. Measurement and modelling of organic fouling deposition in ultrafiltration by ultrasonic transfer signals and reflections. *Desalination*, 146(1-3):177–185, September 2002.

[96] G. Lippmann. Principe de la conservation de l'électricité. *Annales de chimie et de physique*, 24:145, 1881.

[97] W. Liu, G.K. Christian, Z. Zhang, and P.J. Fryer. Direct measurement of the force required to disrupt and remove fouling deposits of whey protein concentrate. *International Dairy Journal*, 16(2):164–172, February 2006.

[98] A. L. Lopez-Sanchez and L. W. Schmerr. Simplified method for complete characterization of an ultrasonic NDE measurement system. *Research in Nondestructive Evaluation*, 18(1):23–43, 2007.

[99] A.L. Lopez-Sanchez and L.W. Schmerr. Determination of an ultrasonic transducer's sensitivity and impedance in a pulse-echo setup. *IEEE Transactions on Ultrasonics, Ferroelectrics and Frequency Control*, 53(11):2101–2112, 2006.

[100] G. C. Low and R. V. Jones. Design and construction of short pulse ultrasonic probes for non-destructive testing. *Ultrasonics*, 22(2):85–95, March 1984.

[101] A. P. Mairal, A. R. Greenberg, and W. B. Krantz. Investigation of membrane fouling and cleaning using ultrasonic time-domain reflectometry. *Desalination*, 130(1):45–60, September 2000.

[102] G. A. Manderson, M. J. Hardman, and L. K. Creamer. Effect of heat treatment on bovine β-lactoglobulin A, B, and C explored using thiol availability and fluorescence. *Journal of Agricultural and Food Chemistry*, 47(9):3617–3627, September 1999.

[103] R. M. Martin. Piezoelectricity. *Phys. Rev. B*, 5(4):1607–1613, February 1972.

[104] J. F. Mas and J. J. Flores. The application of artificial neural networks to the analysis of remotely sensed data. *International Journal of Remote Sensing*, 29(3):617–663, 2008.

[105] W.P. Mason. An electromechanical representation of a piezoelectric crystal used as a transducer. *Proceedings of the Institute of Radio Engineers*, 23(10):1252–1263, 1935.

[106] D. J. McClements, M. J. W. Povey, M. Jury, and E. Betsanis. Ultrasonic characterization of a food emulsion. *Ultrasonics*, 28(4):266–272, July 1990.

[107] D. Julian McClements. Advances in the application of ultrasound in food analysis and processing. *Trends in Food Science & Technology*, 6(9):293–299, September 1995.

[108] H. A. McKenzie and W. H. Sawyer. Effect of pH on β-lactoglobulins. *Nature*, 214(5093):1101 – 1104, 1967.

[109] T.R. Meeker. Thickness mode piezoelectric transducers. *Ultrasonics*, 10(1):26–36, January 1972.

[110] R. Mercade-Prieto, R.J. Falconer, W.R. Paterson, and D.I. Wilson. Effect of gel structure on the dissolution of heat-induced β-lactoglobulin gels in alkali. *Journal of Agricultural and Food Chemistry*, 54(15):5437–5444, 2006.

[111] R. Mercade-Prieto, W. R. Paterson, and D. I. Wilson. The science of cleaning of dairy fouling layers. In H. Müller-Steinhagen, M.R. Malayeri, and A.P. Watkinson, editors, *Proceedings of the 7th International Conference on Heat Exchanger Fouling and Cleaning - Challenges and Opportunities*, volume RP5, pages 119 – 127, July 2007.

[112] B. Merheb, G. Nassar, B. Nongaillard, G. Delaplace, and J. C. Leuliet. Design and performance of a low-frequency non-intrusive acoustic technique for monitoring fouling in plate heat exchangers. *Journal of Food Science*, 82:518 – 527, 2007.

[113] D. Meschede. *Gerthsen Physik*. Springer Berlin/Heidelberg, 21 edition, 2002.

[114] E. G. Moros, X. Fan, and W. L. Straube. Ultrasound power deposition model for the chest wall. *Ultrasound in Medicine & Biology*, 25(8):1275–1287, October 1999.

[115] K. Nakanishi, T. Sakiyama, and K. Imamura. On the adsorption of proteins on solid surfaces, a common but very complicated phenomenon. *Journal of Bioscience and Bioengineering*, 91(3):233–244, 2001.

[116] B. T. Nielsen, H. Singh, and J. M. Latham. Aggregation of bovine β-lactoglobulins a and b on heating at 75 Â°C. *International Dairy Journal*, 6(5):519–527, May 1996.

[117] R. Oliveira. Understanding adhesion: A means for preventing fouling. *Experimental Thermal and Fluid Science*, 14(4):316–322, May 1997.

[118] Y.-H. Pao and V. Varatharajulu. Huygens' principle, radiation conditions, and integral formulas for the scattering of elastic waves. *J. Acoust. Soc. Am.*, 59(6):1361–1371, June 1976.

[119] M. Z. Papiz, L. Sawyer, E. E. Eliopoulos, A. C. T. North, J. B. C. Findlay, R. Sivaprasadarao, T. A. Jones, M. E. Newcomer, and P. J. Kraulis. The structure of β-lactoglobulin and its similarity to plasma retinol-binding protein. *Nature*, 324(6095):383–385, November 1986.

[120] D. Parenthoine, L.-P. Tran-Huu-Hue, L. Haumesser, F. Vander Meulen, M. Lematre, and M. Lethiecq. Modelling nonlinearity in piezoceramic transducers: From equations to nonlinear equivalent circuits. *Ultrasonics*, 51(2):109–114, February 2011.

[121] A. Pereira, J. Mendes, and L.F. Melo. Cleaning monitoring using controlled nanovibrations. In H. Müller-Steinhagen, M.R. Malayeri, and A.P. Watkinson, editors, *Proceedings of the 7th International Conference on Heat Exchanger Fouling and Cleaning - Challenges and Opportunities*, volume RP5, pages 483 – 488, July 2007.

[122] A. Pereira, J. Mendes, and L.F. Melo. Monitoring cleaning-in-place of shampoo films using nanovibration technology. *Sensors and Actuators B: Chemical*, 136(2):376–382, March 2009.

[123] Ana Pereira, Joaquim Mendes, and Luis F. Melo. Using nanovibrations to monitor biofouling. *Biotechnology and Bioengineering*, 99(6):1407–1415, 2008.

[124] H. Petermeier, R. Benning, A. Delgado, U. Kulozik, J. Hinrichs, and T. Becker. Hybrid model of the fouling process in tubular heat exchangers for the dairy industry. *Journal of Food Engineering*, 55(1):9–17, November 2002.

[125] J. Petit, A.-L. Herbig, A. Moreau, and G. Delaplace. Influence of calcium on β-lactoglobulin denaturation kinetics: Implications in unfolding and aggregation mechanisms. *Journal of Dairy Science*, 94(12):5794–5810, December 2011.

[126] Malcolm J. W. Povey. Particulate characterization by ultrasound. *Pharmaceutical Science & Technology Today*, 3(11):373–380, November 2000.

[127] S. Prakash, N. Datta, and H.C. Deeth. Methods of detecting fouling caused by heating milk. *Food Reviews International Dairy Journal*, 21:267 – 293, 2005.

[128] S.S. Premathilaka, M.M. Hyland, X.D. Chen, L.R. Watkins, and B. Bansal. Interaction of whey protein with modified stainless steel surfaces. In H. Müller-Steinhagen, M.R. Malayeri, and A.P. Watkinson, editors, *Proceedings of the 7th International Conference on Heat Exchanger Fouling and Clenaing - Challenges and Opportunities*, volume RP5, pages 150 – 161, July 2007.

[129] A. Püttmer, P. Hauptmann, R. Lucklum, O. Krause, and B. Henning. SPICE model for lossy piezoceramic transducers. *Ultrasonics, Ferroelectrics and Frequency Control, IEEE Transactions on DOI - 10.1109/58.585191*, 44(1):60–66, 1997.

[130] Jian Qiu, Will Sheffler, David Baker, and William Stafford Noble. Ranking predicted protein structures with support vector regression. *Proteins: Structure, Function, and Bioinformatics*, 71(3):1175–1182–, 2008.

[131] S.S. Ramachandra, S. Wiehe, M.M. Hyland, X.D. Chen, and B. Bansal. A preliminary study of the effect of surface coating on the initial deposition mechanisms of dairy fouling. In H. Müller-Steinhagen, M.R. Malayeri, and A.P. Watkinson, editors, *Proceedings of the 6th International Conference on Heat Exchanger Fouling and Clenaing - Challenges and Opportunities*, volume RP2, pages 88 – 96, June 2005.

[132] S.N. Ramadas, G. Hayward, R.L. O'Leary, T. McCunnie, A.J. Mulhollandt, A. Troge, R.A. Pethrick, D. Robertson, and V. Murray. A three-port acoustic lattice model for piezoelectric transducers containing opposing zones of polarization. In *Ultrasonics Symposium, 2006. IEEE*, pages 1899–1902, 2006.

[133] Mohamed A. Razavi, Ali Mortazavi, and Mahmoud Mousavi. Application of neural networks for crossflow milk ultrafiltration simulation. *International Dairy Journal*, 14(1):69–80, January 2004.

[134] Mohammad A. Razavi, Ali Mortazavi, and Mahmoud Mousavi. Dynamic modelling of milk ultrafiltration by artificial neural network. *Journal of Membrane Science*, 220(1-2):47–58, August 2003.

[135] K. S. Reddy, C. V. Krishnamurthy, K. Balasubramaniam, and T. Balasubramanian. Hugen-fresnel diffraction model (H-FDM) for the simulation of ultrasonic time-of-flight diffraction technique in 2d geometries. *AIP Conf. Proc.*, 1211(1):2031–2037, February 2010.

[136] M. Redwood. Transient performance of a piezoelectric transducer. *J. Acoust. Soc. Am.*, 33(4):527–536, April 1961.

[137] D. Renard, J. Lefebvre, M. C. A. Griffin, and W. G. Griffin. Effects of pH and salt environment on the association of β-lactoglobulin revealed by intrinsic fluorescence studies. *International Journal of Biological Macromolecules*, 22(1):41–49, February 1998.

[138] C. Riverol and V. Napolitano. Estimation of fouling in a plate heat exchanger through the application of neural networks. *Journal of Chemical Technology & Biotechnology*, 80(5):594–600, 2005.

[139] R. Rosmaninho, G. Gizzo, H. Müller-Steinhagen, and L.F. Melo. Anti-fouling stainless steel based surfaces for milk heating processes. In H. Müller-Steinhagen, M.R. Malayeri, and A.P. Watkinson, editors, *Proceedings of the 6th International Conference on Heat Exchanger Fouling and Clenaing - Challenges and Opportunities*, volume RP2, pages 97 – 102, June 2005.

[140] R. Rosmaninho, G. Gizzo, H. Müller-Steinhagen, and L.F. Melo. Flow cell studies on fouling caused by protein-calcium phosphate deposition in turbulent flow. In H. Müller-Steinhagen, M.R. Malayari, and A.P. Watkinson, editors, *Proceedings of the 7th International Conference on Heat Exchanger Fouling and Clenaing - Challenges and Opportunities*, volume RP5, pages 128 – 137, July 2007.

[141] R. Rosmaninho and L. F. Melo. Protein-calcium phosphate interactions in fouling of modified stainless-steel surfaces by simulated milk. *International Dairy Journal*, 18(1):72–80, January 2008.

[142] R. Rosmaninho, O. Santos, T. Nylander, M. Paulsson, M. Beuf, T. Benezech, S. Yiantsios, N. Andritsos, A. Karabelas, G. Rizzo, H. Müller-Steinhagen, and F. Melo. Modified stainless steel surfaces targeted to reduce fouling – evaluation of fouling by milk components. *Journal of Food Engineering*, 80(4):1176–1187, June 2007.

[143] K. Sakurai, T. Konuma, M. Yagi, and Y. Goto. Structural dynamics and folding of beta-lactoglobulin probed by heteronuclear NMR. *Biochimica et Biophysica Acta (BBA) - General Subjects*, 1790(6):527–537, June 2009.

[144] K. Sakurai, M. Oobatake, and Y. Goto. Salt-dependent monomer-dimer equilibrium of bovine β-lactoglobulin at pH 3. *Protein Science*, 10(11):2325–2335, 2001.

[145] N. Sava, I. Van der Plancken, W. Claeys, and M. Hendrickx. The kinetics of heat-induced structural changes of β-lactoglobulin. *Journal of Dairy Science*, 88(5):1646–1653, May 2005.

[146] S. Schnars and R. Henrich. Application of NDT methods on composite structures in aerospace industry. website, ndt.net, 2006.

[147] P. J. R. Schreier and P. J. Fryer. Heat exchanger fouling: A model study of the scaleup of laboratory data. *Chemical Engineering Science*, 50(8):1311–1321, April 1995.

[148] S. Sherrit. An accurate equivalent circuit for the unloaded piezoelectric vibrator in the thickness mode. *Journal of Physics D: Applied Physics*, 30(16):2354–, 1997.

[149] S. Sherrit, S. P. Leary, B. P. Dolgin, and Y. Bar-Cohen. Comparison of the Mason and the KLM equivalent circuits for piezoelectric resonators in the thickness mode. In *IEEE Ultrasonics Symposium*, pages 1–6, 1999.

[150] S. Sherrit and B.K. Mukherjee. The use of complex material constants to model the dynamic response of piezoelectric materials. In *Ultrasonics Symposium, 1998. Proceedings., 1998 IEEE*, volume 1, pages 633–640 vol.1, 1998.

[151] J.-W. F. A. Simons, H. A. Kosters, R. W. Visschers, and H. H. J. de Jongh. Role of calcium as trigger in thermal β-lactoglobulin aggregation. *Archives of Biochemistry and Biophysics*, 406(2):143–152, October 2002.

[152] Alex J. Smola and Bernhard Schoelkopf. A tutorial on support vector regression. *Statistics and Computing*, 14(3):199–222, 2004.

[153] R. Steinhagen, H. Müller-Steinhagen, and K. Maani. Problems and costs due to heat exchanger fouling in New Zealand industries. *Heat Transfer Engineering*, 14(1):19–30–, 1993.

[154] A. Stirpe, B. Rizzuti, M. Pantusa, R. Bartucci, L. Sportelli, and R. Guzzi. Thermally induced denaturation and aggregation of β-lg-a: effect of the Cu^{2+} and Zn^{2+} metal ions. *European Biophysics Journal*, 37(8):1351–1360, October 2008.

[155] V. A. Sutilov. *Physik des Ultraschalls*. Akademie Verlag, 1984.

[156] E. Teruel, C. Cortes, L. Ignacio Diez, and I. Arauzo. Monitoring and prediction of fouling in coal-fired utility boilers using neural networks. *Chemical Engineering Science*, 60(18):5035–5048, September 2005.

[157] H. Tohmyoh and M. Saka. Rubber-coupled acoustic microscopy for industrial applications. In *12th A-PCNDT 2006 - Asia Pacific Conference of NDT*, 5th - 10th November 2006.

[158] A. Tolkach and U. Kulozik. Reaction kinetic pathway of reversible and irreversible thermal denaturation of β-lactoglobulin. *Lait*, 87(4-5):301–315, July 2007.

[159] T. Truong, S. Anema, K. Kirkpatrick, and H. Chen. The use of a heat flux sensor for in-line monitoring of fouling of non-heated surfaces. *Food and Bioproducts Processing*, 80(4):260–269, December 2002.

[160] G. Unterhaslberger, C. Schmitt, C. Sanchez, C. Appolonia-Nouzille, and A. Raemy. Heat denaturation and aggregation of β-lactoglobulin enriched WPI in the presence of arginine HCl, NaCl and guanidinium HCl at pH 4.0 and 7.0. *Food Hydrocolloids*, 20(7):1006–1019, October 2006.

[161] J. van Deventer, T. Lofqvist, and J. Delsing. PSPICE simulation of ultrasonic systems. *IEEE Transactions on Ultrasonics, Ferroelectrics and Frequency Control*, 47(4):1014–1024, 2000.

[162] K.S. Van Dyke. The piezo-electric resonator and its equivalent betwork. *Proceedings of the Institute of Radio Engineers*, 16(6):742–764, 1928.

[163] V.N. Vapnik. An overview of statistical learning theory. *Neural Networks, IEEE Transactions on*, 10(5):988–999, 1999.

[164] J. Visser and Th. J. M. Jeurnink. Fouling of heat exchangers in the dairy industry. *Experimental Thermal and Fluid Science*, 14(4):407–424, May 1997.

[165] E. Wallhäusser, M.A. Hussein, and T. Becker. Detection methods of fouling in heat exchangers in the food industry. *Food Control*, 27(1):1–10, September 2012.

[166] P. Wang and W. L. Olbricht. Fluid and solid mechanics in a poroelastic network induced by ultrasound. *Journal of Biomechanics*, 44(1):28–33, January 2011.

[167] Peter M. Withers. Ultrasonic, acoustic and optical techniques for the non-invasive detection of fouling in food processing equipment. *Trends in Food Science & Technology*, 7(9):293–298, September 1996.

[168] G.L. Wojcik, D.K. Vaughan, N. Abboud, and Jr. Mould, J. Electromechanical modeling using explicit time-domain finite elements. In *Ultrasonics Symposium, 1993. Proceedings., IEEE 1993*, pages 1107–1112 vol.2, 1993.

[169] H. Xin, X. D. Chen, and N. Özkan. Removal of a model protein foulant from metal surfaces. *AIChE Journal*, 50(8):1961–1973, 2004.

[170] H. Xin, X.D. Chen, and N. Özkan. A mathematical model of the removal of milk protein deposit. In P. Watkinson, H. Müller-Steinhagen, and M.R. Malayeri, editors, *ECI Conference on Heat Exchanger Fouling and Cleaning: Fundamentals and Applications*, 2003.

[171] X. Xu, J. Li, H. Li, Y. Cai, Y. Cao, B. He, and Y. Zhang. Non-invasive monitoring of fouling in hollow fiber membrane via UTDR. *Journal of Membrane Science*, 326(1):103–110, January 2009.

[172] T. Xue, W. Lord, and S. Udpa. Numerical analysis of the radiated fields of ultrasonic transducers. *Journal of Nondestructive Evaluation*, 14(3):137–146, September 1995.

[173] S.G. Yantsios and A.J. Karabelas. Deposition of micron-sized particles on flat surfaces: effects of hydrodynamic and physicochemical conditions on particle attachment efficiency. *Chemical Engineering Science*, 58:3105 – 3113, 2003.

[174] Z. Yüksel and Y. K. Erdem. The influence of main milk components on the hydrophobic interactions of milk protein system in the course of heat treatment. *Journal of Food Engineering*, 67(3):301–308, April 2005.

[175] L.B. Zuev, B.S. Semukhin, A.G. Lunev, and S.Y. Zavodchikov. Use of acoustic parameter measurements for evaluating the reliability criteria of machine parts and metalwork. In *ECNDT*, 2006.

A. Derivation of the Linear Wave Equation

In ultrasonics the ideal linear wave equation is used even though nonlinear effects like absorption and damping are present. Still, most nonlinear effects are small and the linear wave equation can be derived from the nonlinear one.

$$\Delta p = \frac{1}{c^2} \cdot \frac{\partial^2}{\partial t^2} \tag{A.1}$$

with **p** as pressure, t as time, and c as medium sound velocity.
The nonlinear wave formula considering viscosity, gravitational effects, acoustic fields from volume changes, moving acoustic fields, and (nonlinear) effects from vortices is (after [79])

$$\left(1 + \tau \cdot \frac{\partial}{\partial t}\right)\Delta p - \frac{1}{c^2} \cdot \frac{\partial^2 p}{\partial t^2} - \nabla(\rho_0 \cdot g) - \frac{\partial G}{\partial t} - \nabla F - \frac{\partial^2(\rho u_i uj)}{\partial x_i \partial x_j} = 0 \text{with } \tau = \frac{4/3 \cdot \eta + \eta_B}{\rho - 0 \cdot c^2}. \tag{A.2}$$

τ is absorption due to viscosity, ρ_0 medium density of rest, g gravity, G an acoustic field due to changing volume, F outer body force, $u_{i,j}$ particle velocity in i and j direction, η shear viscosity, and η_B bulk viscosity. To derive the linear wave equation starting from the nonlinear wave equation above every term of the nonlinear one will be investigated in detail.

Absorption Effects

Absorption due to viscosity plays an important role for fluids with high viscosity, low fluidity, and high inner friction which is true for non-Newtonian and some Newtonian fluids. For water and milk this kind of absoption is negligible but damping of an ultrasonic wave.

$$\tau \frac{\partial}{\partial t} = \frac{4/3 \cdot \eta + \eta_B}{\rho - 0 \cdot c^2} \ll 1 \tag{A.3}$$

because $\eta_{water} \leq 1mPa$ and $\eta_{B,water} \leq 1mPa$.

Gravitational Effects

Effects of gravity can often be neglected because in most cases $\nabla g \equiv 0$. Gravitational effects do play a role if medium and/or flow is inhomogeneous.

$$\nabla \rho_0 \cdot g \approx 0. \tag{A.4}$$

Acoustic Field due to Volume Changes

G describes injected mass into space at a rate per unit volume and is generated by a closed surface with changing volume, e.g. the surface of an explosion or an imploding bubble. Because no mass is injected and no explosion/implosions are present acoustic fields due to volume changes can be neglected

$$\frac{\partial G}{\partial t} \approx 0. \tag{A.5}$$

Body Forces

Body forces are introduced by sources which do not change its volume while moving through a fluid like vibrating spheres or bubbles of constant volume. This may play a role if air bubbles are present but in food processing the focus lies on air-free processing.

$$\nabla F \approx 0. \tag{A.6}$$

Vortices

This term takes into account effects of spatial changes of momentum flux inside a fluid produced by regions of turbulences e.g. in the exhaust of a jet engine. These turbulences are partially caused by viscosity inhomogenities and of interest at high flow fields and high energies. Here, flow fields and (ultrasonic) energies are low and they can be excluded in most cases in food industry

$$\frac{\partial(\rho \cdot u_i \cdot u_j)}{\partial x_i \partial x_j} \approx 0. \tag{A.7}$$

Result

Thus, the linear lossless wave equation can be derived from a lossy nonlinear wave equation

$$\left(1 + \tau \cdot \frac{\partial}{\partial t}\right)\Delta p - \frac{1}{c^2} \cdot \frac{\partial^2}{\partial t^2} - \nabla(\rho_0 \cdot g) - \frac{\partial G}{\partial t} - \nabla F - \frac{\partial^2(\rho u_i u j)}{\partial x_i \partial x_j} \Rightarrow \Delta p = \frac{1}{c^2} \cdot \frac{\partial^2}{\partial t^2}. \tag{A.8}$$

B. Description of the Developed Code

The subroutines of the developed online monitoring code are briefly presented where all features have the following steps together:

- Read in signal.
- Determine wanted echo.
- Calculated wanted feature.
- Feed calculated feature into a classification method.
- Decide for fouling presence and absence.

Calculation of Acoustic Impedance *Z*

Characteristic acoustic impedance is calculated as follows:

- Determine reflections inside wanted echo.
- Determine energy of every reflection.
- Logarithmise these energies.
- Fit a linear regression to logarithmised reflection.
- Determine slope of linear regression.
- Use slope to calculate reflectivity at interface: $R_{sample} = R_{water} \cdot exp(m_{sample} - m_{water})$.
- Calculate reflection coefficient: $r = \sqrt{R}$.
- Determine characteristic acoustic impedance Z_{sample}: $Z_{sample} = r_{calc} \cdot [(1 - Z_{steel})/(1 + Z_{steel})]$.
- Feed Z into a classification machine.

Calculation of Other Features

Other features used are briefly presented with their equation and description.

- Short time energy (STE): $STE = \sum_{n=1}^{N} \big(x(n)\big)^2$. Describes energy content of echo.
- Temporal crest factor (TCF): $TCF = \Big(max\big(|x(n)|\big)\Big) / \Big((1/N) \sum_{n=1}^{N} |x(n)|\Big)$. Ratio between maximal and average amplitude (time domain).
- Spectral crest factor (SCF): $SCF = \Big(max\big(|X(m)|\big)\Big) / \Big((1/1024) \sum_{m=1}^{1024} |X(m)|\Big)$. Ratio between maximal and average magnitude (frequency domain).
- Spectral smoothness (SSMOOTH): $SSMOOTH = 20 \cdot \sum_{2}^{1023} \Big| log|X(m)| - \Big(log|X(m-1)| + log|X(m)| + log|X(m+1)|\Big)/(3)\Big|$. Variation of a point with respect to its two nearest neighbours.
- Temporal slope (TSLOPE): Slope between 0.8*maximum and 0.08*maximum.
- Descent time (TDESCENT): Time which is scanned by TSLOPE.

All features are calculated and then fed into classification methods like ANN or SVM to determine fouling and to monitor cleaning success. These features were chosen because they showed high sensitivity to fouling and can be determined from the echo at the interface between stainless steel wall and fouling. For higher detection stability, temperature T and mass flow rate $\dot{m}$ were included.

Artificial Neural Network (ANN)

An 1-class classification ANN was trained offline to determine weights and bias and determined values were implemented into the online code. As transfer functions between the layers TANSIG, LOGSIG, and PURELIN were applied.

$$TANSIG : a = \Big(\frac{2}{1 + exp(-2 \cdot n)}\Big) - 1 \tag{B.1}$$

$$LOGSIG : a = \frac{1}{1 + exp(n)} \tag{B.2}$$

$$PURELIN : a = n \tag{B.3}$$

where a is output and n is input of one neuron.

If input and output layers were the same net output equaled zero and a clean heat exchanger was determined. If the layers were different net output equaled one and a fouled heat exchanger was present.

Support Vector Machine (SVM)

The SVM was trained offline and values for bias b, support vectors x_i, direction in or opposite to the direction of the normal vector of the hyperplane y_i, Lagrange multipliers $\alpha_i \neq 0$, and kernel function K were load into the online monitoring code.

$$F(x) = \sum_{i=1}^{N} \alpha_i y_i K(x, x_i) + b \tag{B.4}$$

with radial basis function as kernel. SVM classified the features stating fouling or no fouling dependent on the direction of the vector from feature to hyperplane.

Monitoring the Slope

The slope of the calculated features was monitored using a gliding fit with n as number of investigated features:

- Wait until ten values of one feature is determined.
- Fit linear using linear regression.
- Determine slope of linear fit.
- IF $m \neq 0$ THEN include the next determined value, drop the first value, and fit again. State "fouled heat exchanger" if at least $n/2$ features state the same.
- ELSEIF $m = 0$ THEN include the next value, drop the first value and fit again. State "clean heat exchanger" if at least $n/2$ features state the same.

It is recommended to wait for ten consecutive fits if a clean heat exchanger is stated before cleaning is stopped. This corresponds to ca. 2.5 min and lies inside setup reaction time.

Outlier Detection

Outlier detection was done using a combination of angle based outlier detection (ABOD) and windows tendency check where outliers were values neither displaying "0" nor "1".

- IF ANN/SVM decision is 0 or 1 do not change it.

- ELSEIF compare if decision is closer to 0 or 1.
- IF decision is closer to 0 change decision and displayed bar to 0.
- IF decision is closer to 1 do so accordingly.

In doing so a user is not mislead to connect length of bar with cleaning success.
Windows tendency check is used to compare the ANN/SVM decisions in a frame of n signals without overlapping.

- Check every decision inside frame.
- IF $n/2$ or more signals display fouling change all decisions to fouling.
- IF $n/2$ or more signals display no fouling do so accordingly.

This smoothens the displayed decision but introduces a time delay in the range of $n \cdot 10s$.

C. β-lactoglobulin and Ultrasound

β-lactoglobulin: Properties and Fouling

Bovine β-lactoglobulin (β-lg) is a globular protein (diameter ca. 3nm) belonging to lipocalin family, made of 162 amino acids, and has an IEP of ca. 5.13 [44]. Average weight is 18kDa and its concentration in raw cow milk is 0.2 g/100 ml where β-lg exists in three genetic variants (A, B, C). β-lg consists of eight-stranded β-sheets and α-helices (Fig. C.1) [37] [82] and ternary structure is stabilised via two disulfide bonds. A free thiol and one tryptophane residue is buried in the conical hydrophobic β-barrel, a second tryptophane is exposed to the solvent forming covalently bound dimers [86] [143].

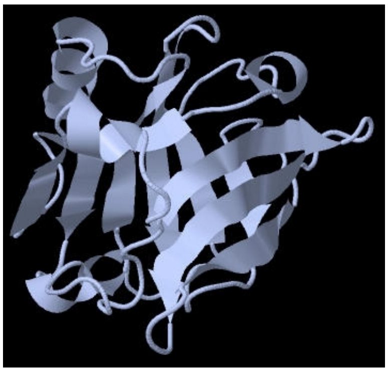

Figure C.1.: Molecular modelled β-lactoglobulin where β-sheet configuration can be seen.

Folding of β-lg follows an $\alpha-\beta$-transition and proceeds via intermediate states [143]. During heating, β-lg denaturates (reversible), agglomerates with β-lg, α-lactalbumin and/or caseins (irreversible), and adsorbs on heat transfer surfaces. Dependent on pH β-lg forms particulates (pH near IEP) or amyloid fibrils (pH away from IEP) [83] while fibrils can assemble into suprafibrillar structures [65] [66].

Denaturation and aggregation of β-lg is influenced by different factors like pH [108] [137] [160], salts [144] [151] [154], temperature, β-lg concentration, and other whey proteins [174]. Denaturation is rate limited at low temperature, pH at IEP, and high ionic strength while aggregation is slowed at high temperatures, pH far away from IEP, and low ionic strength. The influence of some factors are summarised in Table C.1.

Table C.1.: Effect of different factors on β-lg denaturation and behaviour.

Factor	**Influence**
Concentration	Increasing concentration increases average size of aggregates Protein association is influenced
Genetic variant	Thermostability at pH 6.7: C>A>B Variant A shows enhanced oligomerisation and gelation, lower solubility, changed polarity
pH	Conversion rate of native β-lg into aggregates increases with pH, molecular mass decreases; high pH facilitates unfolding and dissociation 7<pH<8.5: conformational change, refolding of protein chain (Tanford transition) $\rightarrow$ higher acitivity of thiol group pH8: thiol group more ready for reactions <pH7: molecule unfolds and exposes thiol group 6.4<pH<8: intermolecular disulphide bonds play an important role 2-3pH: β-lg has positive charge (21) $\rightarrow$ electrostatic interactions repulsive $\rightarrow$ screening via salts $\rightarrow$ increasing aggregation rate and ionic strength pH=2.5: only non-covalent binding
Whey proteins	α-lactalbumin binds via disulphide bonds and hydrophobic interactions Bovine Serum Albumin also binds to disulphide bonds
Salt	Overall mechanisms unchanged but rate and intensity reinforced (charge screening), stabilising/destabilising effects follow Hofmeister series pH 3: Charge repulsion suppressed (counterion binding) $\rightarrow$ more dimers pH 4: Positive charged protein, aggregation when negatively charged ions present (e.g. Cl^-), hydrophobic interactions due to high protein stability in acidic condition pH 7: Negatively charged protein $\rightarrow$ positively charged ions important (e.g. Na^+) Transition metals influence dissociation/aggregation: Cu^{2+} interacts specific, makes kinetics 4.6-fold faster, Zn^{2+} interacts less specific, favours aggregation by forming intermolecular bonds between denaturated polypeptide chains

Absorption of fouling depends on protein and surface characteristics, solution, flow conditions, transport phenomena, and heat exchanger design [47] [115] [117]. As soon as the first fouling layer is present its properties take over surface characteristics. For adhesion on surfaces different forces play an important role like mechanical forces, molecular interactions (DLVO, Derjaguin, Landau, Verwey, Overbeek), and others (Fig. C.2).

Forces like Lewis acid-base interactions and ion bridging are not important in fouling while DLVO forces are dominant which combine van der Waals ($F \propto 1/r^3$) and electrostatic double layer forces ($F \propto exp(-r)$) (see Table C.2). The resultive potential can be repulsive

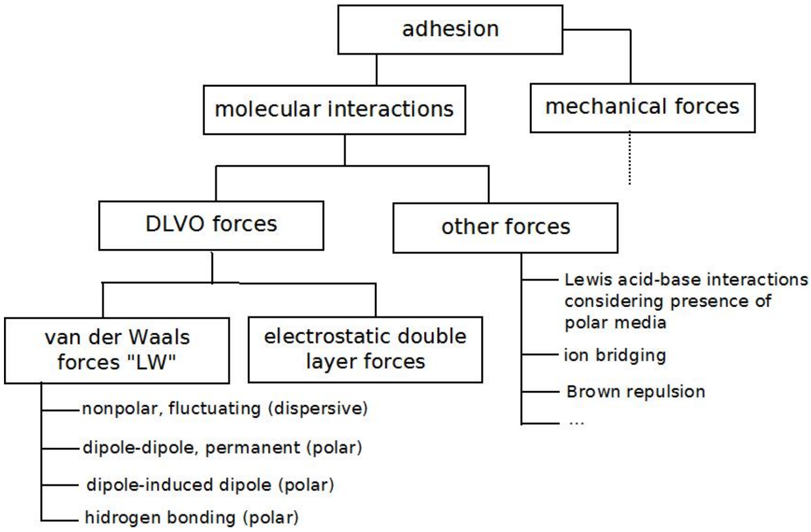

Figure C.2.: For fouling adsorption DLVO forces play an important role (after [47]).

or attractive dependent on force distribution and it influences fouling behaviour.

Table C.2.: van der Waals and electro-static double layer forces together with equations and brief explanation.

Force	**Equation (round particle, flat surface)**	**Description**
van der Waals (vdW), attractive	$F_{vdW} = (A \cdot r)/(6d^2) + A/(6\pi d^3) \cdot \pi z^2$	Non-covalent binding dependent on geometry, physical/chemical properties
Electro-static double layer, repulsive	$F_{el} = (\varepsilon r)/2 \cdot (\Psi_{01}^2 + \Psi_{02}^2) \cdot (\kappa exp(-\kappa d))/(1 - exp(-2\kappa d)) \cdot \left[(2\Psi_{01}\Psi_{02})/(\Psi_{01}^2 + \Psi_{02}^2) - exp(-\kappa d)\right]$	Particle: tendency to acquire electric surface charge (mostly negative at neutral pH), close to surface double layer is developed

Interactions between Ultrasound and Fouling Layer

Composition of fouling layers changes with time due to ageing where e.g. deposit hardness, thickness, and thermal conductivity are influenced. Fouling composition changes because fouling reduces overall heat transfer and influences temperature difference between surface (stainless steel or fouling layer) and medium (milk). This feeds back on deposition rate because deposition rate is controlled by temperature difference: lower temperature difference influences deposition → influences thermal conductivity → influences layer composition (different strata) and so on. Fouling is not evenly distributed on the wall leading to uneven spreading, varying thicknesses, and rough surfaces. This influences ultrasonic signals and its reflection at the interface where fouling is located (C.3).

Table C.3.: Fouling layers can influence an ultrasonic signal in varies ways.

Fouling layer	**Influence on ultrasonic signal**
Layer thickness	Pathway is changed → time of flight (TOF) is influenced Minimum thickness necessary to influence TOF Signal attenuated/damped due to visco-elastic layer → signal may be lost Minimal thickness and clear signal: Additional echoes may appear Affects ultrasonic reflection due to changed mass (interface, reflection changes) and changed height (can influence e.g. frequency of reflected wave)
Fouling surface	Ultrasonic signal may be scattered due to rough surface → signal may be lost, noise will increase
Different strata	Different composition may alter ultrasonic features Inhomogeneties (air/water bubbles) increase scattering → signal-to-noise ratio decreases Inhomogenities may lead to broadened signal
Fouling presence	Reflection and transmission at interface changed → amplitude and damping of signal influenced Ultrasonic features influenced due to changed oscillating behaviour at the interface

Ultrasonic features seem to be best suitable for fouling detection and cleaning monitoring when they can be determined from the ultrasonic reflection at the interface stainless steel wall-fouling. Features are promising which are sensitive to changes at this interface via e.g. reflection/transmission coefficients and amplitude. Fouling thickness may influence ultrasonic features indirectly which are not sensitive to thickness because changed height of an oscillating system changes oscillation behaviour. This in turn influences e.g. frequency and amplitude and can be determined (compare with different rope lengths and changed oscillation behaviour of a pendulum).

D. Material Properties and Error Analysis

Ultrasonic Measuring Unit and Coupling

Different materials were tested for the ultrasonic measuring unit (PZT ceramic, polyvinylchloride (PVC) housing, epoxy-tungsten backing, delay line, coupling). A delay line was necessary because echoes at the interface were not clearly separable with 2 MHz ultrasonic transducers. Polymethylmethacrylate (PMMA) was chosen as delay line because it showed best S/N ratio and was easy to use. A second reason to use a delay line was to buffer temperature between hot stainless steel wall and ultrasonic transducer to heat the transducer less as if it would be attached directly to the wall. This helps to elongate transducer life time and to reduce damage due to temperature. Electrical and thermal properties vary between different materials but effects were negligible for most cases (Table D.1 with water as reference).

Table D.1.: Electrical and thermal properties of materials used for ultrasonic measuring unit (PZT ceramic, PVC housing, epoxy-tungsten backing, PMMA delay line).

	PZT ceramic	**PVC**	**Tungsten**	**Epoxy**	**Epoxy-tungsten mixture**	**PMMA**	**Water**
Thermal conductivity $[10^{-6} W/m \cdot K]$	1.1	1.01	164	0.19	Unknown	0.19	0.6
Thermal expansion coefficient $[10^{-6} 1/K]$	-4 - -6 in direction, 4 - 8 perpendicular to polarization	50.4	4.2	45 - 65	Unknown	70 (at 80°C: 700)	200
Electrical conductivity $[A/Vm]$	Insulator (dieletric)	Insulator	$18 \cdot 10^6$ (for solids)	Insulator	Insulator?	Insulator	0.03
Density $[kg/m^3]$	7.8	1.4	19.3	Ca. 1	Unknown	1.19	0.99
Specific heat capacity $[kJ/kgK]$	0.35	0.9	0.14	Ca. 1.5	Unknown	1.47	4.18
Glass temperature $[^{\circ}C]$	-	Ca. 100	-	Ca. 70	Unknown	Ca. 105	-

Coupling of the measuring unit to the stainless steel wall was investigated where different coupling agents (solid and liquid) were examined in detail (Table D.2). Liquid coupling (water-based gel) was chosen to couple ultrasonic transducer and delay line and solid coupling (Aqualene) for coupling delay line to stainless steel wall. This helped to improve signal and accuracy of ultrasonic measurements.

Table D.2.: Attenuation of solid and liquid couplings. Aqualene is a professional solid coupling distributed by Olympus, the other coupling agents were bought at different place, Si stands for silicone.

Coupling agent	**Attenuation [Np]**	**Attenuation (dB)**
Honey	0.0	0.0
Gel (oil-based)	0.98	0.11
Gel (water-based)	-0.52	-0.06
Aluminium sheet	60.58	6.97
Plastic sheet	57.17	6.58
Si foil, 40°SH, 0.6mm	39.38	4.53
Si foil, 40°SH, 1.0mm	40.98	4.71
Si foil, 60°SH, 0.3mm	48.61	5.60
Si foil, 60°SH, 0.5mm	33.67	3.88
Si foil, 60°SH, 0.6mm	38.01	4.38
Si foil, 60°SH, 1.0mm	32.26	3.71
Aqualene, 0.5mm	17.26	1.99
Aqualene, 2.0mm	18.37	2.11
Aqualene, 6.4mm	23.57	2.71

Ultrasonic Transducer and Excitation Electronics

Electric impedance mismatch between ultrasonic transducer and excitation electronics has a high influence on ultrasonic signals. Capacity of ultrasonic transducer used was unknown thus to determine its influence on the rectangular excitation pulse different capacities were used and compared. Capacities ranged from 10 pF to 13 nF because estimated value was calculated to be around 10 nF (Fig. D.1). For excitation, 10 V were applied and influence of capacity was monitored with an oscilloscope (Picoscope).

Capacities below 2 nF did not influence excitation while higher capacities showed an influence (output of electronics was set to 50 Ω). The ultrasonic transducer showed lower influence than sheer capacity and the oscillation of the transducer (2 MHz) can be seen. Care has to be taken with measurements made due to influences of the transducer on excitation and also on reception process.

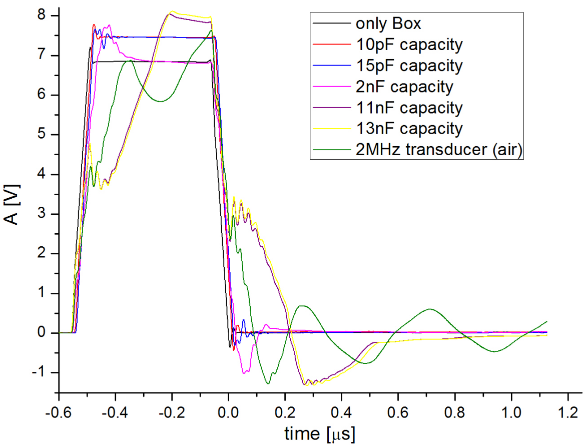

Figure D.1.: Various capacities influence the excitation differently: below 2 nF no influence is seen, above 2nF the signal is distorted, while the ultrasonic transducer imprints its oscillation.

Error Analysis

Error analysis was investigated in detail of the echo used for fouling detection because it sometimes consisted of two parts, a main echo between 22 μs and 38 μs and a second one between 44 μs and 50 μs (Fig. D.2). Most features were not strongly affected by this extra oscillation but characteristic acoustic impedance was.

This oscillation may be introduced by electronics, setup, or other sources but can be excluded using filters: bandpass filters showed signal improvement while features were not influenced. Also, time was adapted for signal analysis because echoes were clearly separable and the extra echo did not carry necessary information for analysis.

Another effect was an oscillation of the signal where amplitude varied with time independent on used excitation board (SatLin and SatScan), firmware, and setup. The boards used different ways for amplifying the ultrasonic signal: one amplified linearly, one exponential. The oscillation had a very low frequency and a period in the range of minutes after which the amplitude stabilised (Table D.3).

This oscillation may be introduced by heating of electrical components of the excitation. This is important particularly for components which are used for voltage and current amplification because high power ($\propto I^2$) leads to high temperatures influencing current and may influence measured signals if measurements with high accuracy are to be made. To investigate temperature inside the box, temperature was measured in the air inside the

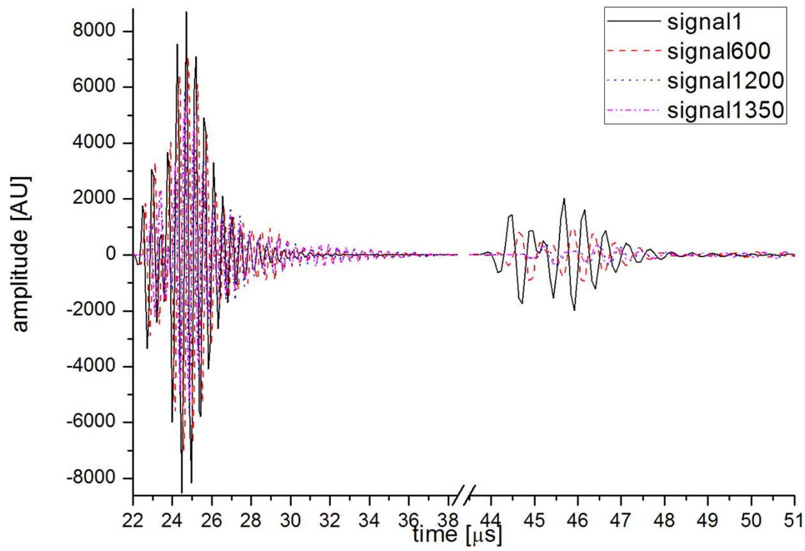

Figure D.2.: First echo of some signals. Besides investigated echo between 22μs and 38μs an extra echo between 44μs and 50μs was found but neglected in analysis.

Table D.3.: The ultrasonic signal showed an oscillation in the range of minutes independent on excitation board and setup used.

	Hohenheim	**Freising**		
Period	ca. 264 s	ca. 320 s	ca. 308 s	ca. 216 s
Type of board	SatLin	SatLin	SatScan	SatScan
Setup	Planar channel	Different	Planar channel	Planar channel

box (three measurements) and at an output amplifier (seven measurements). Temperature reached a stable value after 20 min and an increase of ca. 2 °C (Fig. D.3). Thus, temperature changes inside the box may lead to variations in the signal at the beginning of the measurements. This is no problem if at least 20 min are waited until measurements are made.

Other influencing quantities were investigated some having a higher, a lower, or no influence. The quantitites affected the features differently and in the following are summarised together with their exclusion.

- Influence on electronics
  - Pumps (frequency inverter) → excluded via filtering
  - Heating cartridge (voltage peak, thermal drift) → excluded (minor influence)
  - Switch control box in setup (voltage peaks) → excluded (minor influence)

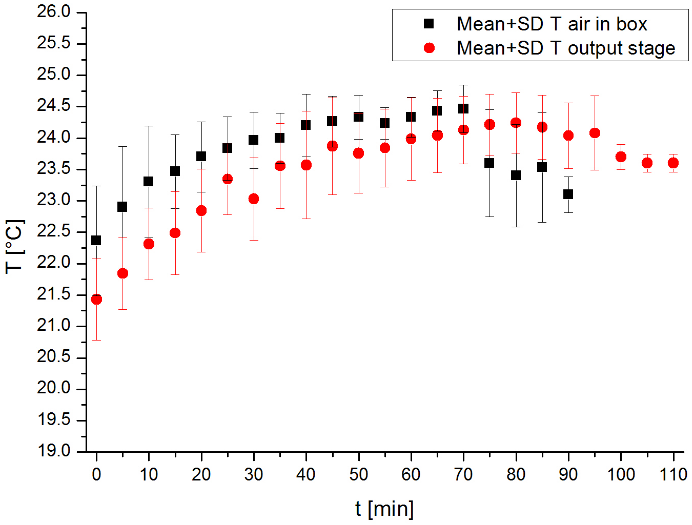

Figure D.3.: Temperature inside the box (measured in air) and at an output stage was monitored. Temperatures increased with operating time and stabilised after ca. 20min.

- Mass flow and conductivity measuring device (voltage peaks) → excluded (minor influence)
- Power supplies (voltage peaks) → excluded (minor influence)
- Air conditioning (voltage peaks, thermal influence)→ excluded (minor influence)

• Influence on transducer/measurement apparatus
  - Pumps (setup vibration) → excluded (vibrations negligible)
  - Heating cartridge (thermal infuence) → excluded (minor influence)
  - Power supplies (voltage peak) → excluded (minor influence)
  - Fluid behaviour → excluded by including mass flow rate into decision
  - Pressure used for attaching ultrasonic transducer → excluded by defined pressure

• Influence on computer
  - Power supplies (voltage peaks) → excluded (minor influence)
  - Communication between VE, Moxa, DAQFactory → excluded (minor influence)

Medium and setup temperature was investigated because it showed an influence on some features. This was visible when medium temperature was not constant e.g. at the beginning of an measurement when parts had different temperatures and heated up. Signal amplitude showed a high influence where fouling seemed to weaken the effect.

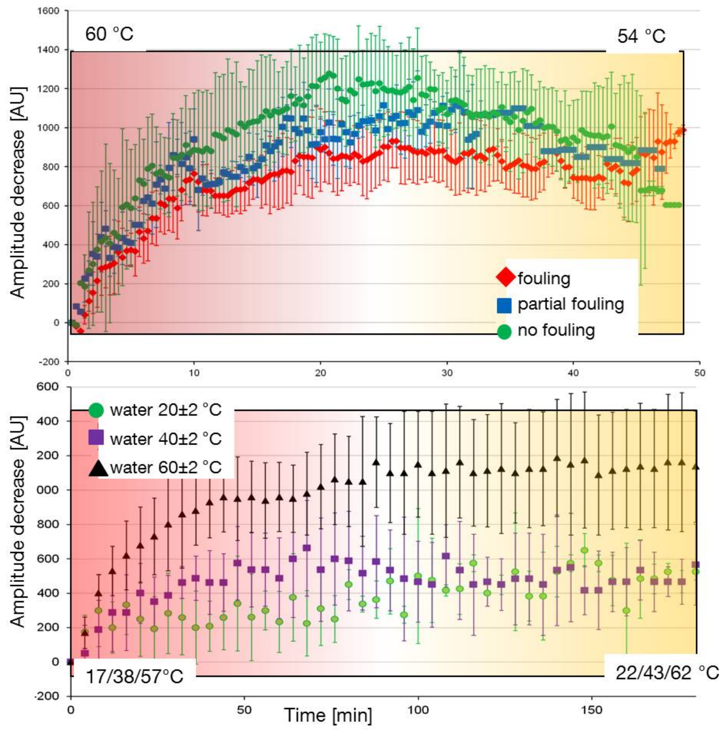

Figure D.4.: Temperature of medium and setup (channel+ultrasonic measuring unit) influenced signal amplitude ($A(0) - A(t)$, 0 is start and t later time). a) Amplitude change where fouling seems to have a weakening effect. b) Influence of medium temperature (water): lower medium temperature leads to less decrease in amplitude.

In Fig. D.4 amplitude difference between amplitude at time $t = 0$ (beginning of measurement) and at later times t are compared. Temperature influence was dependent on medium temperature: higher temperatures showed higher influences. This may be partially caused by heating of the ultrasonic measuring system. Different features were investigated concerning amplitude change to get an impression of the extend this influence was and if it may cause problems. Most features were only slightly influenced like temporal crest factor (TCF) while short time energy (STE) was strongly influenced (Fig. D.5). STE depends directly on signal amplitude while TCF measures a ratio between maximum and average amplitude which seems not to be influenced strongly.

To overcome temperature influence different strategies were followed: temperature measurements inside the measuring section were included into classification methods and prior

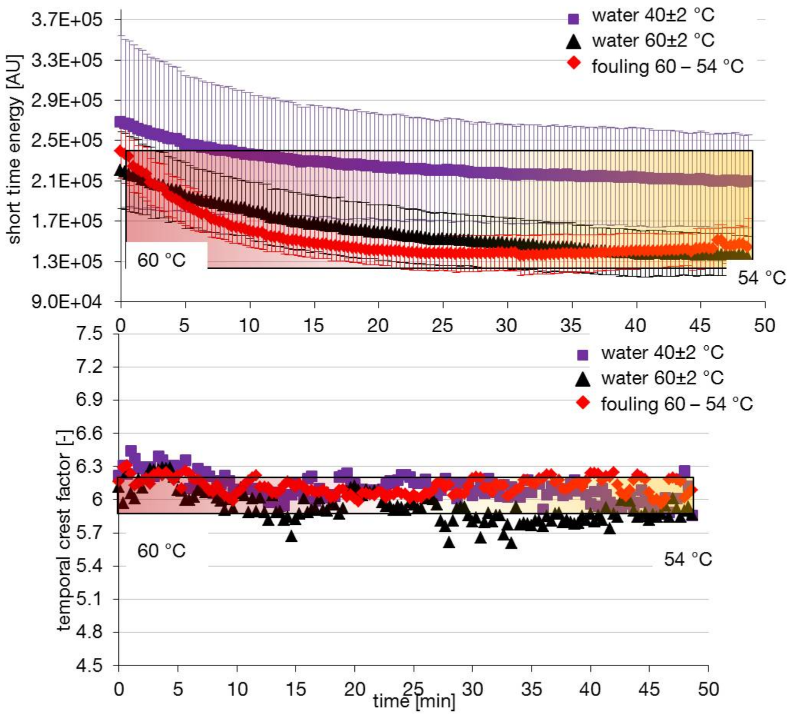

Figure D.5.: STE was strongly influenced by temperature, TCF only slightly. STE directly depends on amplitude while TCF compares maximum and average amplitude and the ratio seemed not to be influenced strongly.

every measurements 15 min were waited until ultrasonic measuring section showed a stable temperature. The effect of temperature could be minimised, errors could be reduced, and measurement accuracy was improved.

Lebenslauf

Personalien

Name und Adresse	Eva Wallhäußer Auf der Heide 10 70565 Stuttgart
Telefon	+49(0)171/50 44 31 93
Mobil	+49(0)170/53 70 45 2
E-mail	Eva.Wallhaeusser@gmx.net
Geburtsdatum	29.10.1981
Geburtsort	Pforzheim

Ausbildung

1988 – 1992	Pestalozzischule, Stuttgart
1992 – 2001	Fanny-Leicht-Gymnasium, Stuttgart
2001	Schulabschluss: **Abitur,** Note 2,1 Leistungsfächer: **Physik**, Latein
2001 – 2007	**Studium der Physik** (Diplom) an der Universität Stuttgart
2003	Abschluss: **Vordiplom Physik**, Note 3
März 2007	Abschluss: **Diplom Physik**, „Untersuchung von frühen zytokinvermittelten Signalprozessen mittels Fluoreszenzkorrelationsspektroskopie (FCS) in lebenden Zellen“, Note 2
Seit 2008	Doktorarbeit bei Herrn Prof. Becker (Ende voraussichtlich 2013)
2008 – 2009	Doktorarbeit an der Universität Hohenheim
Seit Juli 2009	Doktorarbeit an der TU München, Weihenstephan
Seit 11/2012	Zuverlässigkeitsingenieurin bei der Robert Bosch GmbH

Praktika

Juli 2001	Praktikum am **Max-Planck-Institut für Metallforschung**, Stuttgart
April – August 2004	Praktikum am **Ian-Wark-Institute der University of South Australia**, Adelaide, South Australia, Australien

Tätigkeiten neben dem Studium

2001 – 2009	Mitglied beim **Arbeitskreis Astronomie** der Universität Stuttgart
2003 – 2004	**Leitung des Arbeitskreises Astronomie** der Universität Stuttgart
2005 – 2009	Mitglied beim „Philharmonischen Orchesterchen“ der Universität Stuttgart
WS 2001/02, 2002/03, 2006/07	Helferin bei „Probiert die Uni aus – Naturwissenschaften und Technik für Schülerinnen der Oberstufe“
Seit 2010	Mentorin bei CyberMentor

Besondere Kenntnisse

Sprachen	Deutsch	Muttersprache
	Englisch	fließend
	Französisch	gut
	Portugiesisch	Grundkenntnisse
	Spanisch	Grundkenntnisse
EDV-Kenntnisse	MS-Office, MatLab, P-SPICE/LT-SPICE, Origin, LabView, LaTeX, Statgraphics, Virtual Expert	

Veröffentlichungen

E. Wallhäußer, F. Neugart, A. Zappe, D. Buk, L. Graeve, C. Tietz, J. Wrachtrup
“Investigation of the first steps at the CNTF mediated signal transduction by means of fluorescence correlation spectroscopy (FCS) in living cells“ (Poster), Frühjahrstagung der Deutschen Physikalischen Gesellschaft (DPG), Regensburg, 2007

E. Wallhäußer, T. Becker
"Potenziale zur Validierung des Reinigungserfolgs von Erhitzungsanlagen mittels Ultraschallmessung" (Vortrag), 3. Lebensmittelwissenschaftliches und Biotechnologisches Kolloquium, Stuttgart, 2008

E. Wallhäußer, M.A. Hussein, T. Becker
"The acoustic impedance – an indicator for concentrations in alcoholic fermentation and cleaning progress of fouled tube heat exchangers" (Vortrag), 5th Internat. Technical Symposium on Food Processing, Monitoring Technology in Bioprocesses and Food Quality Management, Potsdam, 2009

E. Wallhäußer, M.A. Úbeda-Trillo, M.A. Hussein, T. Becker
"Using acoustic parameters for determining presence and cleaning success of dairy fouling" (Vortrag), Fouling and Cleaning in Food Processing 2010, Cambridge, UK, 2010

E. Wallhäußer, M.A. Hussein, T. Becker
"Usage of ultrasound in detecting fouling presence on stainless steel" (Vortrag), 14. Deutsche Physikerinnentagung, München, 2010

E. Wallhäußer, W.B. Hussein, M.A. Hussein, T. Becker
"Usage of ultrasound in detecting dairy fouling on stainless steel" (Poster), International Workshop: Online sensors for fouling monitoring, Frankfurt, 2010

E. Wallhäußer, W.B. Hussein, M.A. Hussein, J. Hinrichs, T. Becker
"On the usage of acoustic properties combined with and artificial neural network – a new approach of determining presence of dairy fouling", Journal of Food Engineering, 103, 2011

E. Wallhäußer, W.B. Hussein, M.A. Hussein, T. Becker
"Detection methods of fouling in heat exchangers in the food industry", Food Control, 27, 2012

E. Wallhäußer, M.A. Hussein, T. Becker
"How to detect protein fouling and cleaning in heat exchangers using ultrasonic based measurements and classification methods" (Vortrag), DPG-Frühjahrstagung, Berlin, 2012

E. Wallhäußer, M.A. Hussein, T. Becker
"Probing and understanding fouling in a planar setup using ultrasonic methods", Review of Scientific Instruments, 2012 (akzeptiert)

E. Wallhäußer, W.B. Hussein, M.A. Hussein, J. Hinrichs, T. Becker
"Determination of fouling presence and absence using a combined method of ultrasonic measurements and classification methods", Engineering of Life Science, 2012 (akzeptiert)

E. Wallhäußer, S. Nöbel, A. Sayed, M.A. Hussein, J. Hinrichs, T. Becker
"Kontinuierliche Detektion von Milchfouling mittels einer Kombination von Ultraschall und Klassifizierungsmethoden", Chemie-Ingenieur-Technik, 2012 (akzeptiert)

E. Wallhäußer, A. Sayed, S. Nöbel, M.A. Hussein, J. Hinrichs, T. Becker
"Monitoring fouling presence and absence by an online measuring method of combined ultrasonic measurements and classification methods", Food and Bioprocess Technology, 2012 (akzeptiert)

E. Wallhäußer, M.A. Hussein, J. Hinrichs, T. Becker
"Detecting fouling using different methods", (Vortrag) AMA conference 2013, Nürnberg, 2013

Sonstiges

Ehrenamtliche Tätigkeiten

1998-2001	Teilnahme am SAK (Sozialer Arbeitskreis) „Schüler unterrichten Senioren": Unterricht im Fach Astronomie
Interessen	Musik (Viola, Klavier, Chor), Reisen (archäologische und historische Stätten), Lesen, Astronomie, Sport

Datum
31.12.2013